DYNAMIC FOOT MODEL

QILONG FENG

M.Phil

The Hong Kong Polytechnic University

2015

The Hong Kong Polytechnic University

Institute of Textile and Clothing

Dynamic Foot Model

Qilong FENG

A thesis submitted in partial fulfilment of the requirements for the degree of Master of Philosophy

NOV 2014

CERTIFICATE OF ORIGINALITY

I hereby declare that this thesis is my own work and that, to the best of my knowledge and belief, it reproduces no material previously published or written, nor material that has been accepted for the award of any other degree or diploma, except where due acknowledge has been made in the text.

_________________ (Signed)

Qilong FENG (Name of student)

To my dear family.

And to the future me.

ABSTRACT

The development of footwear design is influenced by fit and comfort requirements. This involves judging a pair of shoes not only based on esthetic, but based on support, material and the matching between shoe shape and foot shape. As one of the most complicated and the most essential structure of the human body, foot shape varies widely. Hence, the foundation of making the proper shoes is to obtain enough knowledge of foot shape and its deformations. Moreover, the foot shape varies widely in dynamic situations and due to the complexity of obtaining dynamic foot shape it is mostly neglected in the footwear industry. A model of the dynamic foot shape with detailed information about deformation and range of motion could provide essential information for footwear design.

The aim of this research is to develop a dynamic foot model with foot deformation to complement the footwear design and production. To obtain the relevant information two experiments are designed and conducted. First, a trial experiment with three participants each 10 trials was to observe the gait cycle was conducted. The individual trajectory for nine landmarks were presented and compared. The average motion in 2D coordinate system was also generated. Results show differences in motion pattern between foot joints while walking. The hind foot and the forefoot would rotate at different time in the swing phase. Moreover, from one heel strike to another heel strike,

there is lateral medial swing in the foot as previous researchers have mentioned. Furthermore, the change in several angles was calculated while walking. Also a high-speed camera recorded the profile in the stance phase. This provides basic information for the foot shape changes. The main experiment was then conducted to find detailed foot deformation in static and simulated dynamic settings.

In the second experiment, the 3D foot shape was scanned at different settings (heel height, plantarflexion-dorsiflexion, inversion-eversion, simulated walking position). The Kinect scanner was used to obtain 3D foot shape together with texture information. Fifty subjects were recruited to participate in the experiment. The analyzed parameters include the surface created by triangulated landmarks, distance between landmarks, and angles created based on landmark locations. In total 37 landmarks were extracted, and 56 triangular faces created to represent the 3D foot surface. 93 edges (line between landmarks) were calculated to obtain the lengths, and 11 angles were selected to represent the foot shape in 3D.

Results indicate that the inversion and eversion settings have small changes in foot shape. On the other hand, heel height, plantarflexion-dorsiflexion, and simulated walking settings all showed significant influence on foot surface deformation. Based on landmark distance analysis, the most deformed areas include the foot dorsal, the lateral of ankle and the back of Achilles tendon. Relatively, the medial side had less variation.

In the simulated walking most of the surface region changed at different setting. As for the 16 angles representing the plantarflexion and dorsiflexion at the ankle joint, instep position, and forefoot position, and eversion and inversion at the ankle joint, instep position, and forefoot position were considered. For the angle change, inversion and eversion postures had less shape deformation. While the heel height elevation and the plantarflexion-dorsiflexion postures had significant influence in the angle changes and were represented by regression equations with high R^2 value. The simulated walking analysis showed significant changes in angles, implying the need for dynamic shape analysis of the gait cycle.

In this study the investigation on the dynamic foot was carried out. Results indicate changes in distances between landmarks and angles at different settings. Regression equation were developed to create prediction model of foot deformation. Several improvement and limitations of the study has also been discussed. In conclusion, foot shape deformation is important for design of better fitting footwear, especially for high heel shoes and sports shoes, and further research is needed to develop accurate 3D shape prediction models for dynamic foot.

PUBLICATIONS

Papers in Conference Proceedings

Feng Q.L., Luximon A., Chan A.C.K., (2013). Outsole form 2D to 3D. Paper presented at the the Proceedings of the 12th Asian Textile Conference, 2013.

FENG Q.L., Luximong A., Ganesan B., Chan C.K., (2014). Foot dynamic model for investigate foot motion during walking. Paper presented at the Proceedings of the 5th International Conference on Applied Human Factors and Ergonomics AHFE 2014, Krakow, Poland, 2014, pp.7451-7458.

ACKNOWLEDGEMENT

Firstly, I would like to show my deepest gratitude to my chief supervisor, Dr. Ameersing Luximon, who set a respectable, responsible, and friendly environment and acted as a genuine mentor. As the first guide leading me to do the research, Dr. Luximon used all his effort in teaching me the logic, research thinking, research attitude, ethics, and dedication in achieving a result. His effort laid the foundation not only in my research work, but also in my life. It will cast a long-lasting impact on my future career. Without his tolerance and constant improvement, I could never withstand till today. From the moment he patiently explained to me the basic knowledge, or spent spare time just for working out tough problems, I see a selfless teacher, who sacrifices his own time on training the younger generation. He simply hopes the best from the young researchers. I cannot help appreciate the fortune I have been endowed, to meet such a nice supervisor who supported me to achieve a high level of education.

I would like to deeply thank my co-supervisor, Dr. Alan Chan, who kindly introduced me to study here at the Hong Kong Polytechnic University. It is precious and important to have someone offer an opportunity when one is just in desperate need to have a new beginning. To me, Dr. Chan is the essential person who changed the life path. It is still clearly the first moment I got the email from Dr. Chan. Without his help in the start, I would never step forward and learn how to do research.

With all my appreciation, I thank everyone in Dr. Luximon's team: Matthew, Yifan

Zhang, Bala, Jack, Sheila, Yani, and many other colleagues. Their suggestions and comments enlightened me to think differently. Their tacit cooperation in the experiment ensured the good result. Without the support from the whole team, I will not be able to finish the tough work in time. I have many thanks to Mr. Chung Ho LAU, for the great effort to help me process the data.

For those who accompanied me all the time, my parents, my former director, my friends, and my student hall roommates, I appreciate the understanding and support all the time. I want to express my eternal gratitude to my parents, for the endless love and constant communications. Their consolation in the ‘dark’ time, encourage me to overcome the difficulties, and build firm confidence in me. It built my strong will to work hard all the time. I cannot forget my former director, Dr. Li LIU, for the suggestion on my future career. And my sincere thanks are to my intimate friends, Michelle FENG, Peng XUE, Yijia TANG, for every memorable moment we spent together sharing our thoughts and experiences. My special appreciation is to Jennifer BIAN, and Jessie GANG, for the same aspiration we have and the care for each other. In addition I thank all my friends in Hong Kong and in Beijing, for the roller coaster emotional ride during the time of my study. I want to share my joy and excitement with everyone.

At last, I want to thank those who asked questions at conferences and casual talks. The different views and attitude stimulated me to think and work harder. In addition, a lot thanks to my boyfriend who provided me a silent and ‘lack of presence’ situation for me to fully concentrate on my work and study.

TABLE OF CONTENTS

LIST OF FIGURES

LIST OF TABLES

CHAPTER 1 INTRODUCTION

1.1 Background

The development of footwear is always based on the foot shape. As part of both decoration and protection, consideration of the foot surface is an essential aspect regarding the fitting quality of shoes. As the cover of the complex structure of the human foot, footwear enhances and constrains the foot motion. Researches have been conducted to identify the negative influence of footwear (Freychat, 1996; Cong, 2011; Morio et al., 2009). Among the large amount of researches, heel height influence is significant (Speksnijder et al., 2005; Gu et al., 2011). Effect and distribution of plantar foot pressure have also been considered in footwear design (Cong, 2011). Besides the footwear constrain on normal foot motion, there are also cases reporting foot problems caused by improper footwear. Daily wear of shoes involves static foot postures and dynamic foot motion. Dynamic situations influence more foot pressure and hence more foot problems. Nowadays the public appreciation on foot health and environment calls for better fitting shoes; and thus foot shape evaluation in static and dynamic situation becomes key role for footwear design and development. Due to the complex foot surface and inner structure of the foot, the investigation of foot shape representation and modeling is a challenge.

The foot structure is composed of 26 bones, 33 joints, accompanied with muscles, tendons, ligaments. It is divided into three parts: the forefoot, the mid-foot, and the hind foot, with each part contains totally different bone structure (Rose and Martorana, 2011). As an important “functional unit” working to both support the body in static postures and to help the body forward as a lever in dynamic situations, the foot requires enough in-shoe space while requires the proper bounding support for protection. In dynamic situation, joints rotate and adapt to various situations. The motion range varies between individuals, but the directions are classified as dorsiflexion and plantar-flexion, pronation and supination, and eversion and inversion. In these categories, the rotation ranges are obtained based on joint movement and rotations (Dawe & Davis, 2011; Klenerman, 1991). While walking, joint rotations are complex, given that the motion axis sometimes swing between two directions, or move up and down, to keep the body balanced. Then current research knowledge of dynamic is limited.

Modern research technology enables to scan the foot to obtain digital foot shape. In this way it can be visually displayed and the foot shape represented by points or multiple curves. 3D scanning technique is able to record the actual surface of the objects. The result in the form of three-dimensional points and surface models makes it possible to illustrate the slight deformation on the foot surface under different situations. From the early static scanner which enable the recording of flat-standing foot (Witana, 2006; Yu & Tu, 2008), to the current research on dynamic 3D scanners, there are strong need for the foot deformation data in time sequence (Blenkinsopp et al., 2012; Herrewegen et al., 2012). There are needs to report the significant foot shape changes in dynamic state to improve footwear design. The awareness of the foot rolled-over deformation during motion requires a prediction model, so that the model could offer enough information about foot parameters. In a way the geometry and biomechanical knowledge could be obtained (Herrewegen, 2012), together with new requirement and expectations on footwear design.

Not limited within the description of foot dimensions only, nowadays researchers are seeking various methods to provide an efficient foot model for foot shape representation. Rough observation of the dynamic foot was to record the walking trajectories based on few landmarks. By displaying the general motion in space, a conventional gait model (Kadaba et al., 1990; Davis et al., 1991) with the information of foot movement in the sagittal plane can be obtained. The motion model was applied in clinical field, combined with the movement of upper parts above human feet. Later the detailed simulation of human foot joints rotation (Jenkyn & Nicol, 2007) was brought up for ergonomic purposes. Although rotation angles gave some reference for the foot-motion ranges. The dynamic foot shape prediction are still regarded as the most effective way to calculate the changes in dynamic situation. Luximon and Goonetilleke (2004) generated a "standard" foot by collecting scanned feet, and by modifying the "standard" foot a method to predict customized foot shape became possible. Similar techniques may be developed for dynamic foot modeling. The method is intended to be used in the footwear design, and later more ideas on the fast approach to foot simulation and its interaction with footwear have been developed (Tang & Hui, 2011). Now there are different approaches to present foot shape for modeling: to collect the mass data for a general shape, and to form the multi-segment model for detailed analysis. The modeling for prediction is still at its infancy and required more research.

1.2 Aims and objectives

The main goal of the research is to develop a foot dynamic model with foot shape deformation in static and semi dynamic state in order to improve footwear design from the ergonomic aspect. In order to achieve this aim, foot movement within one gait cycle during walking was recorded, and foot shapes under different settings were scanned. The detailed objectives are summarized as follows:

(1) To obtain representative research of foot motion.

(2) To collect gait cycle data and give general observation for one gait cycle.

(3) To calculate foot shape changes in different static setting (different heel heights, plantar flexion and dorsiflexion, eversion and inversions)

(4) To calculate foot shape changes in different simulated walking cycle

(5) To build a dynamic foot model

1.3 Significance and contribution

Footwear fit has long been an unsolved problem. The relationship between footwear and the human foot requires a thorough understanding on the foot shape deformation. However, current researches are limited to foot shape representation under static situations. Furthermore, the motion researches are mainly focused on whole body gait analysis with limited focus on the 3D foot shape. This research has attempted to obtain a complete set of information about 3D foot surface deformation under various circumstances, so that the change in dimensions could be applied to footwear improvement. It also provide visualized results of the foot deformation during walking, and standing, which will enhance the general understanding of the human foot in static and dynamic phase.

1.4 Organization

This thesis is in the following structure. For a brief understanding of the current research field, chapter 2 provides a literature review of all the relative researches conducted before. In this part, the knowledge includes foot basic information, inner structure, and the function of footwear influencing the foot. Followed up a general review of the research related to foot motion is presented, for the former result supports the current study. Chapter 3 illustrates the methodology of the research, as well as the detailed experiment adopted in this study. Two parts of experiment was conducted to fully complete the foot model. In Chapter 4 and 5, results from experiment 1 and 2 were analyzed and compared separately. Chapter 4 focuses on the continuous change in landmark position during walking, with the assistance of data obtained from motion capture system. In chapter 5 the deformation on the foot surface was carefully observed, for the shape varies related to the standing conditions. In this part both the distance and angle changes are investigated for a thorough understanding of changes in dynamic foot. Chapter 6 discussed the implications of the result and its possible uses. The conclusion and discussion section summarizes the main result and discusses the usefulness and limitation of the study. Future work on the development and refinement of dynamic foot model are also discussed. At last, appendices and references are listed in attachment for further reading.

CHAPTER 2 LITERATURE REVIEW

2.1 Foot structure and anatomy

2.1.1 Skeleton structure

Human foot is a small but complex unit. This unit consists of 26 bones, 33 joints, ligaments, muscles, nerves, blood vessels, and other tissues, all covered with skin (Tremaine & Awad, 1998). All the parts in the foot works together, as well as integrating with other parts of body to facilitate human perform the movements and weight bearing chores (Tremaine & Awad, 1998).

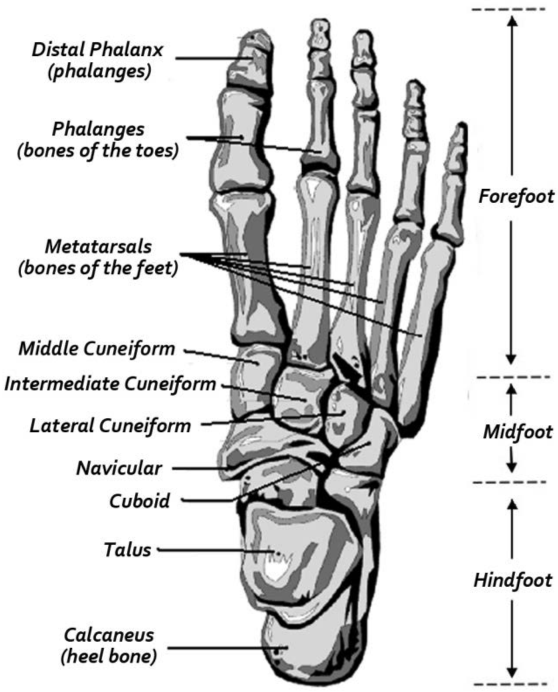

Figure 2-1 Bone structure of foot

Mostly a foot is divided into three parts (Figure 2-1): the forefoot, the midfoot, and the hindfoot (Rose & Martorana, 2011).

The forefoot includes phalanges (two in the hallux and three in each of the other four toes) and metatarsals. The joints between the toes and metatarsals are called the metatarsophalangeal joints, which are at the ball of foot. While under the head of first metatarsal there are two small bones, sesamoids (Rose & Martorana, 2011).

In the midfoot there are five bones, three cuneiforms, a navicular, and a cuboid. Here in the midfoot bones form the arch, mainly acting to stabilize and support body weight, as well as absorb stress and shock (Tremaine & Awad, 1998). This part is linked to the forefoot and the hindfoot with small muscles and significant arch ligaments called plantar fascia.

The heel used to be a separate category but Jonathan introduced the ankle bone, and the heel bone together in the hindfoot part. There are talus and calcaneus with three joints within this part. The talus is linked to two bones in the lower leg, forming the ankle joint; and is also beside the heel bone, calcaneus, forming the subtalar joint (Rose & Martorana, 2011). These two joints plus the midtarsal joint are called the triple joint (Tremaine & Awad, 1998).

2.1.2 Muscles, tendons, ligaments

The motion of foot is controlled by the part between bones, namely joints, and muscles (Figure 2-2). Muscles conduct movement by pulling or pushing the tendons that are linked to the muscles. The largest and strongest tendon is the Achilles tendon (Figure 2-3), connecting the calf muscles and the back of heel. It elevates the heel and controls the downward motion of the front foot. The anterior tibial and posterior tibial muscle help the foot move up and down; and the tibial tendons and peroneal tendons enable the foot to rotate inward and outward relative to the body central line. In addition, the flexor and extensor muscles allow foot to bend and straight the toes.

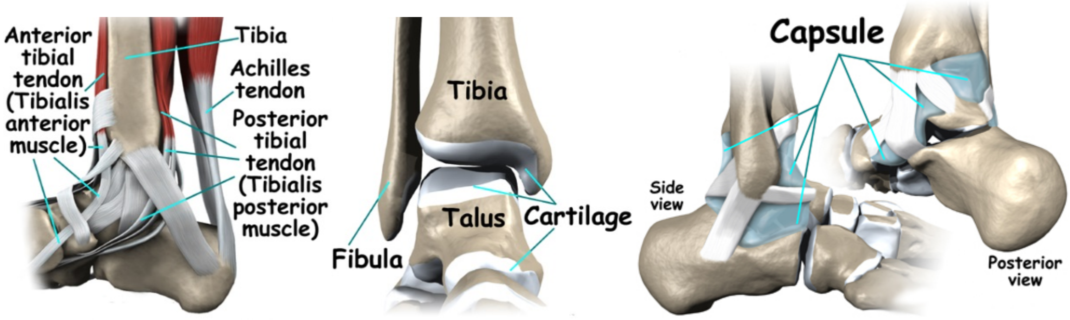

Figure 2-2 Soft tissue in foot bones

Ligaments also connect bones to stabilize joints (Tremaine & Awad, 1998). The most common is the plantar fascia (Figure 2-3), the longest fiber tissue through the sole of foot arch (Tremaine & Awad, 1998; Klenerman, 1991). It stretches and tightens as the arch curvature changes, so as to provides balance and comfort during walking, also a strength for pushing off (Tremaine & Awad, 1998). Cartilage is the part between bones for protection and cushioning during joints movement, with its smooth surface allowing glides in minimum friction; Capsule is the soft tissue that forms the space to support joints (Rose & Martorana, 2011).

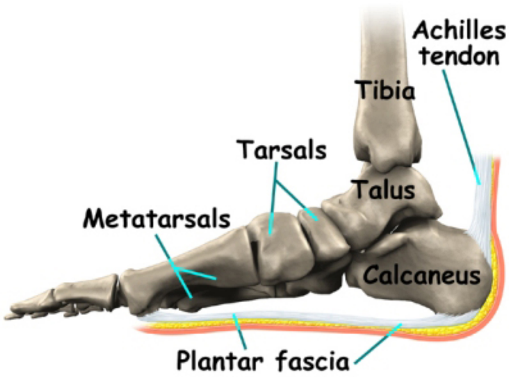

(http://www.eorthopod.com/content/plantar-fasciitis)

Figure 2-3 Achilles tendon and Plantar fascia

2.2 Foot Structure

From the view of biomechanical field, the foot is considered as a “functional unit” in terms of two aims: one is to support the body weight (when static) and the other one is to propel the body forward in motion in the form of a lever (when dynamic) (Wright et al., 2011).

The overall shape of a foot is a bony arch (Figure 2-4). Foot arches can be divided into a longitudinal arch and a transverse arch (Mann, 1988). In detail the longitudinal arch contains a medial structure and a lateral one. In the same way the transverse arch includes a proximal transverse arch and a distal transverse arch (Mann, 1988). This arch structure can be either flexible or rigid, for it could be easily adapted to the surface of different types of ground. A foot has the passive and active mechanisms for individual movements (Nitin & Stephen, 2011). The active ones means arising from the action of muscles, on the contrary the passive ones are more obscure, of which there are functions of four structures (Figure 2-5): The subtalar joint, the transverse tarsal joint, the tarsometatarsal joints, and the plantar fascia (Nitin & Stephen, 2011).

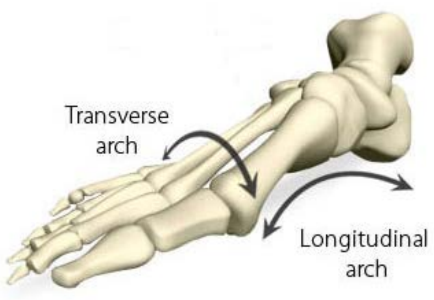

Figure 2-4 The arch structure within foot

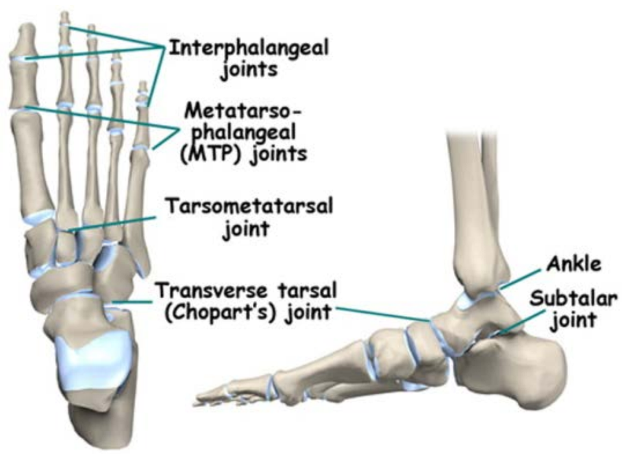

Figure 2-5 Significant joints in foot

The subtalar joint motion involves inversion and eversion and its motion principle is like an

Archimedes screw or spiral when viewed at the facets. This joint can explain the arch shape changes but is not able to show the foot deformation from being compliant to be rigid as the variation of the ground. The transverse tarsal joints, also known as Chopart's joint, is made up with the calcaneocuboid and talonavicular joints (Mann, 1988). Except for these joints, there are interphalangeal joints between two phalange bones, and also metatarso-phalangeal joints between phalanges and metatarsal bones.

2.3 Foot variations

In general the foot is defined as a functioned unit. Based on the assumption that an 'ideal foot' keeps the minimal risk of injury in subtalar neutral, Astrom & Arvidson (1995) gathered over 120 subjects (59 men and 62 women) in Sweden to investigate the normative goniometric data.

Cavanagh (1997) has reviewed the relationship of static structure to dynamic function in the way of radiographic measurements. By selecting 27 measurements, which are mostly reliable, two models were presented. Three and four variables showed the significance as predictors. In the static researches on foot, bone orientation or joints motion allowance are mostly discussed.

2.3.1 Gender influence

From the aspect of gender, foot and leg shape presents differences in former researches. Generally, men feet were larger than women feet. In the research of Fessler et al. (2005), foot length proportionate to stature was confirmed to relate closely with sexual differentiate. All male foot length to stature ratio was larger than female. It is also related to the populations. When comparing with variables in detail, with the same foot lengths, women feet have larger calf and ankle circumference, lower ankle and medial malleolus height. Also, female arch is higher, and the first toe shallower. All the data was at a certainty of 93%, which showed the characteristics between male and female foot dimensions (Wunderlich & Cavanagh, 2000). Krauss et al. (2008) had the experiment with foot scanner to investigate the different variations influenced by gender. Compared to former studies of Anil et al. (1997). Krauss et al. (2008) showed larger value (up to 1cm) at ball width. By using the average value of foot measurements, a general result showed that female toe height and ankle length were smaller. On the contrary to the result of lower toe height in women group, medial ball length showed larger values.

2.3.2. Foot load influence

In research and experiment, foot plantar load is an essential factor influencing comfort. Above researches related to foot shape between genders provided limited information of foot load during data collection. Most frequently set weight loads include: non-weight bearing, semi-weight, and full-weight. As the load increase, the shape of foot arches, especially the longitudinal arch, will adjust the shape to support the body. The plantar will also deform as the bone structure changes. In the quantitative research of Tsung et al. (2003), findings showed that as load increases, parameters such as contact area, foot length, foot width all increased, and at the same time the height parameters such as arch height, arch angle decreased. Some directly and significantly changed parameters, for example, contact area, would increase by up to 60.4% during full-weight bearing than non-weight bearing. Arch height would decrease by 20%, with arch angle becoming 41.2% smaller than before. To observe more information of foot deformation influenced by weight bearing, an experiment was conducted by Xiong et al. (2009) using nine dimensions (foot length, arch length, foot width, midfoot width, heel width, midfoot height, medial malleolus height, lateral malleolus height, ball girth). By collecting measurement data at specially set conditions, results showed the relationships between weight bearing effects and foot dimensions and rotations, and the relationship between foot size, weight and stature (Xiong et al., 2009). The basic dimensions changed as the weight increases. From no weight to full weight load, male foot length increased by 1.3% on average, the same as arch length; width increased by 3.0%, and midfoot width by 4.5%; all foot height decreased, with most significantly midfoot height by 6.3%, as the same result of former researches. Female foot showed similar results. As the load increases, Female foot length increased by 1.5%, while the arch length extended by 1.3%; foot width enlarged by 2.1% and the midfoot width by 1.3%; the midfoot height also changed by 6.0%. With the influence of weight increase, foot rotation angles tend to be reduced. The angle was set crossing the section of midfoot, showing the direction of major principal axis. For the extension of foot arches, male foot angle turned out to reduce 9.6% to 21.9%, and female foot angle would reduce by 5.5% to 28.3%. The researchers also investigated the relative changes between foot size, weight and stature. As with former researches, there was significant correlation between foot length and statures under any load settings for both genders. Their new findings was that male foot width tend to closely related to weight, however, female foot width did not show the relationship. The research was considering the foot from general shape changes. The detailed investigations into the differed shape of part of the foot also gave sufficient information. Midfoot shape was the most significantly changed part during weight load increases, and it is also an important part for footwear design. Xiong and Goonetilleke (2006) has scanned female feet and collected the data of height of midfoot. By using a linear regression of the form, a statistical result describing the height distribution of midfoot was given by $BH=1.079*NBL+0.314$, where BH stands for ball-to-strip height, and NBL stands for the ball-to-strip length after normalization of all the participants. The conclusion suggested a strong correlation between the height and length, and it can be applied to modify current footwear inner space.

2.3.3. Cultural variation

Foot shape could show some variation between different cultures. The inner factor such as the origin of race and outside factor such as living condition or traditional habit would all shed light on the deformation of foot shape. In the early research of foot morphology between Philippino and Japanese women, Kusumoto et al. (1996) compared the foot size, dimensions, and shapes to identify the foot difference caused by daily footwear. By comparing components of the foot size, position of foot axis, and the angle between foot axis and ball axis, an inverse pattern was reported between Philippines and Japanese. This is deduced due to the dramatically change in Japanese footwear since World War II. The most significant phenomenon is the hallux valgus deformity found in the Japanese group, which is presumed being caused by the Japanese traditional footwear, geta and zori. In other countries there are also reports on the external foot morphology. Hawes et al. (1994) collected the foot dimensional data with a population of 1197 North American. The result showed the close relationship between the metatarsal and the fibular length, which would influence the angle and position of metatarsal phalangeal joint axis. Also the height of hallux, the MPJ joints, and the arch varies independently from other dimensions. In 2007, Hawes et al. compared the ethnic difference at the forefoot between groups composed of Caucasian and American (NA), versus Japanese and Korean (JK) people. The study suggested no significant difference in foot breadth. However, the height of hallux, the MPJ axis, and the anterior margin shapes differed significantly. This result showed the necessity of shoe last modification between groups of people. Mauch et al. (2008) researched into the structure difference between German and Australian children. In the result the German children showed much longer and flatter feet, whereas the Australian children have a square forefoot shape. In addition, the German children have longer and straighter toes. These differences were deduced as being influenced by the mix percentage of ethnic groups in the two areas, for that the German population was mostly Caucasian with 8% population from outside Europe, while the Australian was mixed with 24% Asian-born immigrants after World War II.

2.4. Dynamic foot

2.4.1 Gait cycle

To understand the dynamic foot, firstly the general movement is by understanding the gait cycle. A 'gait cycle' is the period from the time one of the feet strikes the ground until the same foot makes contact with the ground again (Figure 2-6). A single walking cycle on an horizental surface consists of 60% stance phase and 40% swing phase (Klenerman, 1991).

The foot is a rather remarkable structure in that it is both flexible and rigid. As a flexible structure the foot can adapt to its environment. Once the foot is fixed to the ground, it is converted into a rigid structure that supports the weight of the body as we rise up onto our toes during the last half of the walking cycle in preparation for toe-off. Though the period of time during one gait cycle is short to observation, there is still an official break down of the overall process. Considering the whole gait cycle involves both of the feet, the steps are listed as terminal swing, heel strike, foot flat, opposite toe-off, heel rise, opposite heel strike, toe-off, and swing phase (Klenerman, 1991).

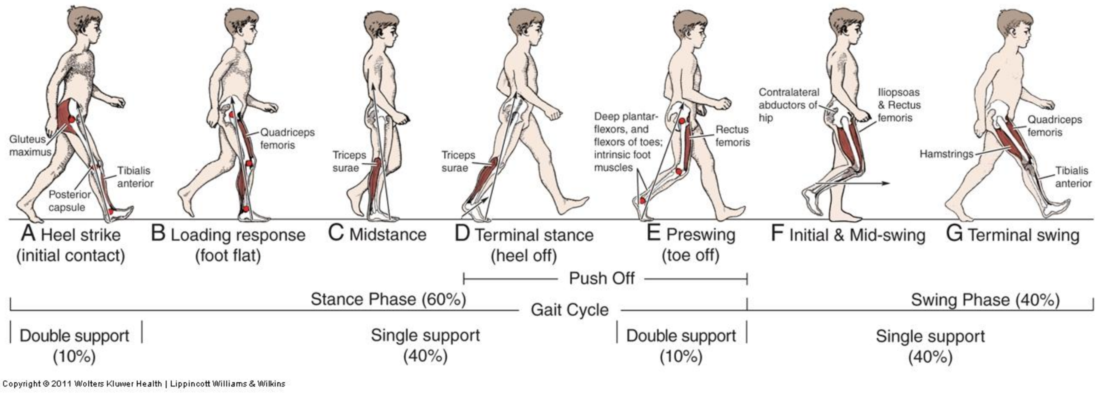

Figure 2-6 The division of a gait cycle

The calculation of gait is by walking cycle, which starts when the heel strikes the ground as 0% and ends when the same heel again strikes the ground as 100% (Mann, 1988). Of the two periods in walking cycle, the first, stance phase, occupies approximately 62% of the whole process; and the other, swing phase, takes up 38% of the cycle.

In convention the stance part of the cycle is divided into three phases (Figure 2-7): first interval, second interval, and third interval. Other period is referred to as “intervals” or “rockers” (Nitin & Stephen, 2011). In the first interval the heel makes contact with the ground and the foot flexes to be flat (contact phase). The movement is a passive process when the foot is loaded and the heel changes into eversion. In this phase the focus is the absorption of the forces by heel strike. The second interval is the time that the body’s center of gravity is passing over the foot (midstance phase). During this phase, the foot changes from a flexible one to a rigid structure, and the subtalar joint forms the external rotation in order to make the midtarsal joins more stable. In the third interval (propulsive phase) the ankle starts plantarflexion, and foot muscles becomes active to stabilize the longitudinal arch, while the stabilizer in the foot is the plantar fascia. The subtalar joint continue to invert till toe-off, and this inversion is driven by the plantar fascia as well as other factors such as the obliquity of the axis of the ankle joint and the orientation of the lesser metatarsophalangeal joints.

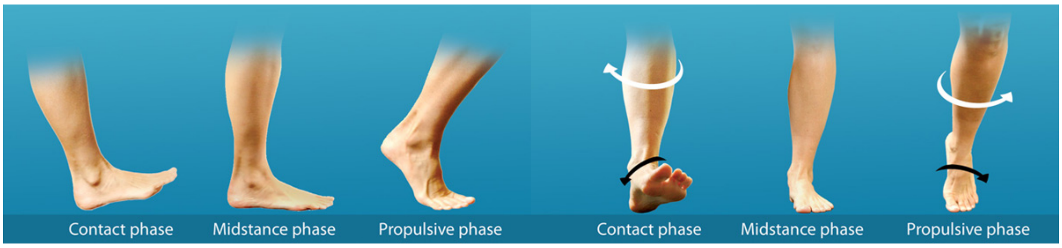

(http://www.footlogics-medical.ca/lower-limb-biomechanics.html)

Figure 2-7 Division and rotation during stance phase

In continuous observation, body parts show displacement as well. Trunk will rise at toe-off and lower at heel strike; the pelvis, hip and knee also have vertical movement. Meanwhile, the shoulders and pelvis will rotate during gait cycle, and femur and tibiae also showed similar changes. For example, the tibiae rotate differently: in the swing phase and the early part of stance phase they rotate internally, while in the later part of the stance phase they rotate externally. During walking the whole body will oscillates, which is thought to be keeping the center of gravity over the weight bearing foot (Nitin & Stephen, 2011).

The measurement of gait cycle has been long investigated by different researchers in different fields. Helwig et al. (2011) has conducted several known methods and made comparison. Nowadays the temporal alignment of gait cycle including the early one by converting the data to percentages of the gait cycle (Winter, 1991; Perry, 1992), also the later ones by dividing trajectories into subphases and adjusting with other corresponding subphases (Forner-

Cordero et al., 2006; Sadeghi et al., 2003) and ones by utilizing variations of dynamic time warping in computer science (Boulgouris et al., 2004; Kale et al., 2003). In the evaluation and comparison researcher chose point of interest as a parameter. The alignment techniques have diverse advantages based on various applications. While piecewise linear length normalization and piecewise dynamic time warping are more suitable for biomechanical and clinical application aiming to obtain the aligning subphase in the trajectories (Helwig et al., 2011). With the overall knowledge of gait cycle and the achieved result of the subphases, the detailed sections of the foot movement can be further illustrated.

2.4.2 Foot rotation and its angles

<u>General researched rotation angles</u>

With the foot in shape of a vaulted configuration for equilibrium maintenance, the body inclinations may be 1-1.5° relative to the vertical. This occurs with both the deformed ankle joint and the plantar surface skin compression (Wright et al., 2011). Around the ankle joint there is a range of 10-12° in motion. The ankle joint rotation up and down is called dorsiflexion and plantar flexion. The subtalar joint is able to invert by 20° and evert by 50°. In addition, it has the motion range of 42° above the coronal plane and 16° medial to the sagittal plane in midline of human body (Figure 2-8).

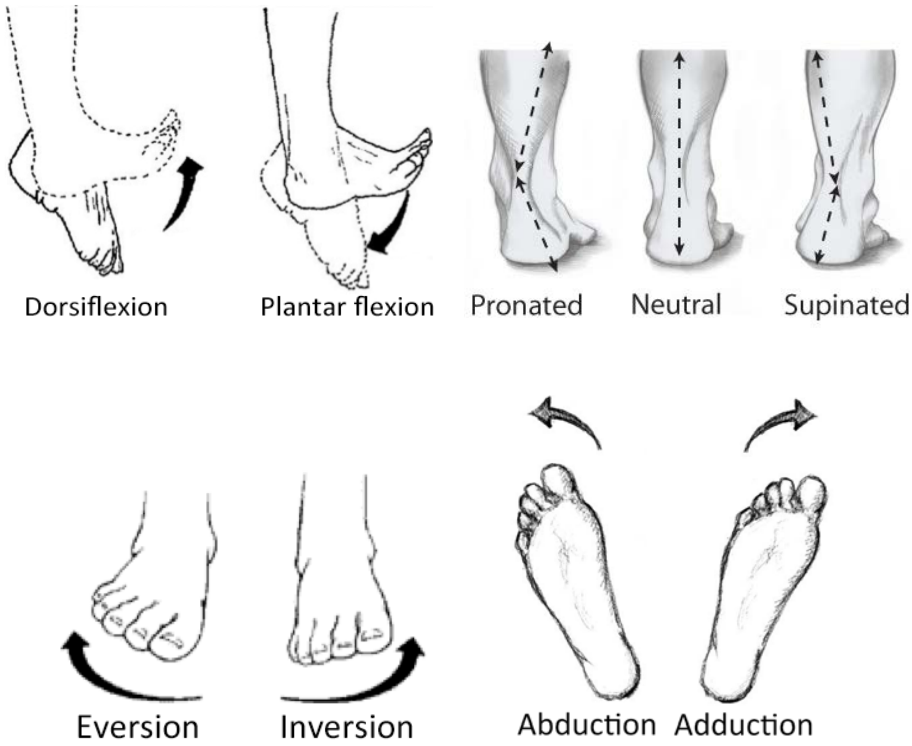

Figure 2-8 Foot rotation towards different directions

For other direction of rotation, the joints rotation in mid-foot can be more detailed. The tarsometatarsal joint varies as the joint position. The first tarsometatarsal joint can rotate 3.5° in flexion and extension and 1.5° in pronation and supination; while the fifth tarsometatarsal has the range of 9° in flexion and extension and the same 9° in pronation and supination.

Metatarsalphalangeal joints vary the same way as above. For detailed information, it can rotate 30° for plantar flexion and even 90° for dorsiflexion, but usually it keep the range between 50° -70°.

Also, when there is load with limb, the height of the longitudinal foot arch would decrease. Mcpoil et al estimated an average change in dorsal arch height between non-weight bearing and weight bearing to be as much as 10mm (McPoil et al., 2008).

Without weight bearing

The static foot rotation is referred to reports mainly related to the categories of plantar flexion/dorsiflexion, inversion/eversion, abduction/adduction, and pronation/supination.

For the plantar flexion/dorsiflexion, Oatis (1988) stated the ‘normal’ ranges of motion researches rarely described the population for observation. Reported results of normal plantar flexion varied 40 to 65 degree, and normal dorsiflexion varied between 10 to 30 degrees. However, in the overview of the study on dynamic foot model, the motion range was reported as 49.9 to 62.1 degree for plantar flexion, and 8.6 to 17.4 degree for dorsiflexion (Luximon & Luximon, 2011). Dawe and Davis (2011) introduced the ankle joint motion, stating a primary axis of rotation at 10 degree to the frontal plane. Along this axis the normal range of movement was 10 to 20 degree for dorsiflexion, and 25 to 30 degree for plantarflexion. Abboud (2002) gave the conclusion of the minimum range of ankle joint motion as necessary for normal locomotion was 10°of dorsiflexion and 20°of plantar flexion.

For the inversion/eversion motion range, Oatis (1988) reported the motion values of inversion excursion range from 5 to 50 degree, and eversion vary from 5 to 26 degree. As the same with plantarflexion/dorsiflexion report, the population in the observation was not stated. However, the total subtalar joint range varied from 10 to 65 degrees, with the average of 40 degree. Luximon (2011) also gave the motion range of inversion and eversion in the general summary. The inversion range was 32.5 to 41.5 degree, and the eversion range was from 16 to 26 degree (Luximon & Luximon, 2011). At the same time, Dawe and Davis (2011) stated that the subtalar joint was able to invert by 20°and evert by 5°in the normal foot.

Table 2-1 A summary of the foot rotation angles

No.	Posture	Referencing range		Researchers	Year
		Min	Max		
(A)	Plantar flexion	40°	65°	Oatis	1988
		49.9°	62.1°	Luximon & Luximon	2011
		25°	30°	Dawe and Davis	2011
		20°		Abboud	2002
	Dorsiflexion	10°	30°	Oatis	1988
		8.6°	17.4°	Luximon & Luximon	2011
		10°	20°	Dawe and Davis	2011
		10°		Abboud	2002
(B)	Inversion	5°	50°	Oatis	1988
		32.5°	41.5°	Luximon & Luximon	2011
		20°		Dawe and Davis	2011
	Eversion	5°	26°	Oatis	1988
		16°	26°	Luximon & Luximon	2011
		5°		Dawe and Davis	2011
(C)	Abduction	21.1°	34.9°	Luximon & Luximon	2011
	Adduction	23.2°	32.8°	Luximon & Luximon	2011

For other rotation angle ranges there is also report on abduction range from 21.1°to 34.9°, and adduction range from 23.2°to 32.8°(Luximon & Luximon, 2011). For the limitation of reference on abduction/adduction motion, the existing information will be considered as the selected one in experiment. Still, in the stance phase some angles at significant postures were reported. At the moment when heel strike happens, the calcaneus is inverted about 2°. This is the time foot begins to pronate. Then in the midstance phase the foot continues to reach 4°of pronation, in total 6° of pronation. This time is hard to keep in static posture, so the information is for reference in the motion capture experiment. In the next period at toe off the foot is at a 2°supinated position. As a summary of the information above, the Table 2-1 shows the referencing rotation angles.

<u>With weight bearing</u>

The early investigation of foot motion tried to collect data of foot ankle rotation ranges. The result turned out to vary a lot between different individuals. The ankle dorsiflexion range was from 5 to 40 degrees, plantar flexion from 10 to 55 degrees, and valgus motion from 15 to 50 degrees, varus motion from 15 to 50 degrees. This result differed from former research, partly because of the difficulty in measuring the angles of motion, and inter-individual variation (Roaas & Andersson, 1982). This early investigation was just to record the angle degrees under static rotations. Later researches try to record the foot movement in walking or running to seek for the range of motion. Most focused parts are the hind foot and the fore foot. At the hind foot, ankle rotation is the most significant for it will rotate to many directions. McPoil (1996) recorded the motion during foot walking through a 6-meter-long path with retro-reflective markers. And later it was compared with the walking movement to full-weight load standing states. First the result showed that the mean stance phase duration in walking took around 0.653 seconds, the relaxed standing foot rotated 3.7 degree while single leg standing foot would rotate up to 7.2 degree to keep balance. In stance phase, the maximum rearfoot eversion could be 6.3 degree. By data analysis and statistical analysis, the data illustrated the motion of rearfoot from the back angle, roughly described the movement of foot ankle. And the result was found that normal rearfoot path would not pass through subtalar joint neutral position, yet it would intersect the relaxed standing position. This result repeated former conclusions, showed the reliability of the experiment. This research was conducted to suggest foot orthoses for normal function. However, the limitation of the result showed that only the angles from the back view of the foot in movement. The stance phase was the most focused part when observing the degrees of angle changes. Hunt et al. (2001) investigated the foot motion of male during stance phase. The rotation change varied between forefoot and rearfoot over the stance phase. In the three dimensional coordinate, the forefoot changed 12°on the sagittal plane, 4°on the frontal plane, and 10°on the transverse plane. By contrary, the rearfoot rotated 22°on the sagittal plane, 8°on the frontal plane, and 10°on the transverse plane. The arch height would decrease when heel contact happened, and increase from the heel rise till toe-off, when the height showed the maximum value. By attaching more landmarks on the foot, Gatt et al. (2011) recorded the foot walking and try to observe the foot rotation in sagittal plane. The main focus was during passive ankle dorsiflexion, with comparing the hindfoot and forefoot position, to obtain the movement and angle changes. Obtained mean maximum foot dorsiflexion angle during pronation, neutral, and supination phase showed the significantly reduced trend, during which period the general maximum degree appeared at pronated posture. In the free moment during walking, foot will go through two stages of shape change: inward at the first half and outward at the other half (Almosnino et al., 2009).

2.4.3 Foot surface variation

In the motion analysis, foot rotation angles can only provide the part of its motion range. The shape changes during different stages of walking were observed, mainly for modifying the inner shape of footwear design. The prominent method to obtain foot surface shape is to draw the cross-sectional shape and to further measure the significant deformation (Kimura et al., 2005; Kouchi et al., 2009). With the use of multiple cameras (Kimura et al., 2005), multiple video cameras (Kouchi et al., 2009), stereo camera system (Blenkinsopp et al., 2012), or even dynamic scan (Samson et al., 2014), an accurate 3D shape of the dorsal foot surface can be rebuilt and cut into sections for later evaluation. Kimura et al. (2005) measured the surface over foot walking during stance phase. With two marker lines and two landmarks showing the sections painted on the surface, the superimposed frames were obtained for observation.

Result showed that there was a similarity between individuals of the cross-section shape changes and dimensions. The arch lengths (medial and lateral), and breadth changes (ball breadth and heel breadth) can be drawn to see the deformation, among which the medial length and ball breadth showed the similarity with former research results measured by electric arch gauge (Yang et al., 1985). The changes of the sections (ball and heel) turned out to be influenced by tendons during joint flexion.

Later in the further research the amount of cross-sections added up to four positions (forefoot, instep, navicular, and heel), the number of landmarks was increased to eight, and at the same time the recording system was improved to be 4D measurement system with twelve high-speed video cameras (Kouchi et al., 2009). The general result showed no significant differences between genders. In the analysis, dimensions of length and breadth were compared, with the result that from the first peak moment to the minimum ground force moment, the ball breadth became larger and the heel breadth became smaller. The instep breadth varied significantly between individuals, while the navicular breadth showed no variation at all. Arch heights were selected as a single change. Except for the result that only dorsal arch height decreased from the first peak moment to the mid-stance valley moment, no more significant difference was found. The cross-sectional shapes were the main topics for describing the foot deformation. At the earlier stage of walking, more subjects showed that the instep would supinate more during walking than standing. The heel and the navicular tended to incline more laterally than the standing posture. The degree of lateral inclination was calculated to be around 6°. Setting for the angle was between the midline of medial and lateral in reference of heel cross-section, in which situation the medial inclination was defined as positive.

This similar idea later inspired the measurement of dynamic foot surface and deformation of running foot (Blenkinsopp et al., 2012). In the research the shape was obtained six cameras and modified with digital image correlation. The 3D shape changes were analyzed together with ground reaction force. Measurement of foot breadth showed that compared to the breadth of 96mm at reference stage, the length could increase to the maximum of 8mm during midstance. This was because the foot transverse arch would flatten to reduce the average bearing and to support the body to move. Strain maps could provide the information of surface deformation. As the figure demonstrated, the first metatarsal-phalange joint and the achilles tendon would deform the most among all surface parts, as up to 3mm. The medial side would deform more than the lateral side relatively, and the lateral side of midfoot and hind foot showed the least tendency to deform.

2.4.4 Pressure and force analysis

Companied with the shape deformation, the results of foot plantar pressure vertical ground reaction force were also recorded for evaluation by Hunt et al. (2001). In the stance phase the major vertical peak pressure happened at two occasions: the beginning (20% of stance) and end (78% of stance) approaching to push-off (Hunt et al., 2001). Close to the two peaks, there was a posterior force peak at 15% of stance, and an anterior force peak at 86% of stance. The latter one was happened at the foot push-off. In the moment of push-off there is also a complex pressure distribution at the bottom of foot. During the push-off, the ground force was loaded mostly on the first and second metatarsal heads and the toe, with 64% of the total forefoot load. The load under the toe and the first metatarsal head showed a negative correlation with the other metatarsal heads. This indicated that the lateral and the medial ground reaction force also had a negative correlation (Hayafune et al., 1999).

2.5 Footwear and foot

2.5.1 Footwear function

Footwear has long been a part of the decoration for human fashion. As known to all, one of the functions for footwear is to offer protection, avoiding “the hot and cold environment, unstable terrain and excessive impact from surfaces (Cong, 2011)”. Evaluation criteria of a proper shoe include shock absorption, motion control, and slip prevention. Footwear bear the bilateral influence of both enhancing the foot motion and also injuring the foot itself. Knowing foot shape is essential to footwear research.

2.5.2 Foot problems related to footwear

Researchers tried in numerous ways to describe that wearing footwear could constrain the barefoot motion. Stacoff et al. (1991) concluded the relation between shoe and foot as the degree of natural foot motion was modified as the stiffness of the shoe increases. Freychat et al. (1996) also found that the natural motion of forefoot turned out to decrease compared to rear foot shod locomotion. Cong (2011) summarized foot problem related to footwear, mainly ankle sprain, hallux valgus, corns and calluses, pointing that current shoes are driven by fashion but not foot comfort.

Morio et al. (2009) compared the walking and running motion between barefoot and foot wearing identical sandals, the footwear motion at forefoot and rear foot, the quantitative result was presented with a multi-segment foot model. They found that foot adduction amplitude increased significantly from soft to hard sandals, eversion slope increase from shod foot to barefoot, the spreading for the foot metatarsal bases and metatarsal heads became smaller during shod condition. These key variables confirmed that sandals constrained the natural foot motion. Furthermore, the authors concluded that the restriction caused by the sandals showed diminution compared to walking. The overall result presented differences in foot motion of barefoot and shod condition, and the changes were caused from the sole and the strap. However, because of the experiment with sandals, the midsole influence was not clear, and the interaction between foot and footwear is not representative for formal shoes.

Heel height has a great influence on foot shape and pressure changes, especially during high heel shoes condition. It has been verified that foot load distribution will change with the elevated height of heel, and thus modified the structure of foot shape. When heel height lifted, the contact area index at mid-foot, lateral foot decreased; while the maximum peak pressure increase under the metatarsal and forefoot showed high correlation with heel height (Speksnijder et al., 2005). During walking in high heel shoes, the pressure distribution concentrated at the heel and forefoot regions, yet the mid-foot pressure decreased to none, which is supposed to be one of the reasons for foot damages on heel structure (Gu et al., 2011).

Cong (2011) tested the in-shoe plantar pressure and shear stress simultaneously. The shear stress over the hallux increased much larger than plantar pressure, and its spatial difference appeared compared to peak pressure. This indicates that shear stress could be responsible for foot injuries relate to soft tissue. From the aspect of resisting slip and falls in high-heel shoes, Blanchette et al. (2011) determined that the heel height and utilized friction would increase together during walking. The resultant shear force turned out to add 14.5% more during high heel trial than low heel trial. The kinematic results showed that the ankle plantarflexion angle increased when the heel height elevated.

2.6 Foot scanner

Foot scanning technology is applied to foot measurement and shape examination. Compared to manually measured result, the scanning technique is tested for its validity. The accuracy of the scanned result could vary between objects or the applied methods for scanning (Witana et al., 2006). Generally the human foot can be obtained with “slices” of scanned data together with the length (Luximon and Goonetilleke, 2004). The early attempt with 3D foot scanner was to document the foot shape for measurement without the appearance of the real subject. Later the investigation on different foot postures appeared in the research of foot deformation. The static foot scan can only save the shapes of standing foot. Later the development of dynamic foot scan enabled the analysis on foot in motion, most frequently about the foot during walking, some about foot running (Kimura et al., 2008; Sturmer et al., 2011; Blenkinsopp et al., 2012).

2.6.1 Static 3D foot model

The relatively early trial with foot scanner and 3 foot shape was conducted by Witana (2006) to compare the simulated measurement and the manual measurements. The method of scanning technique was based on the “repeated measures” design (Montgomery, 2001). The determination of dimensions included foot lengths, widths, heights, and girths. By testing the inter- and intra- operator reliabilities, comparing the measurement, and forming linear regression model, the result of the new method showed that the former adopted measuring method need development in order to be more accuracy.

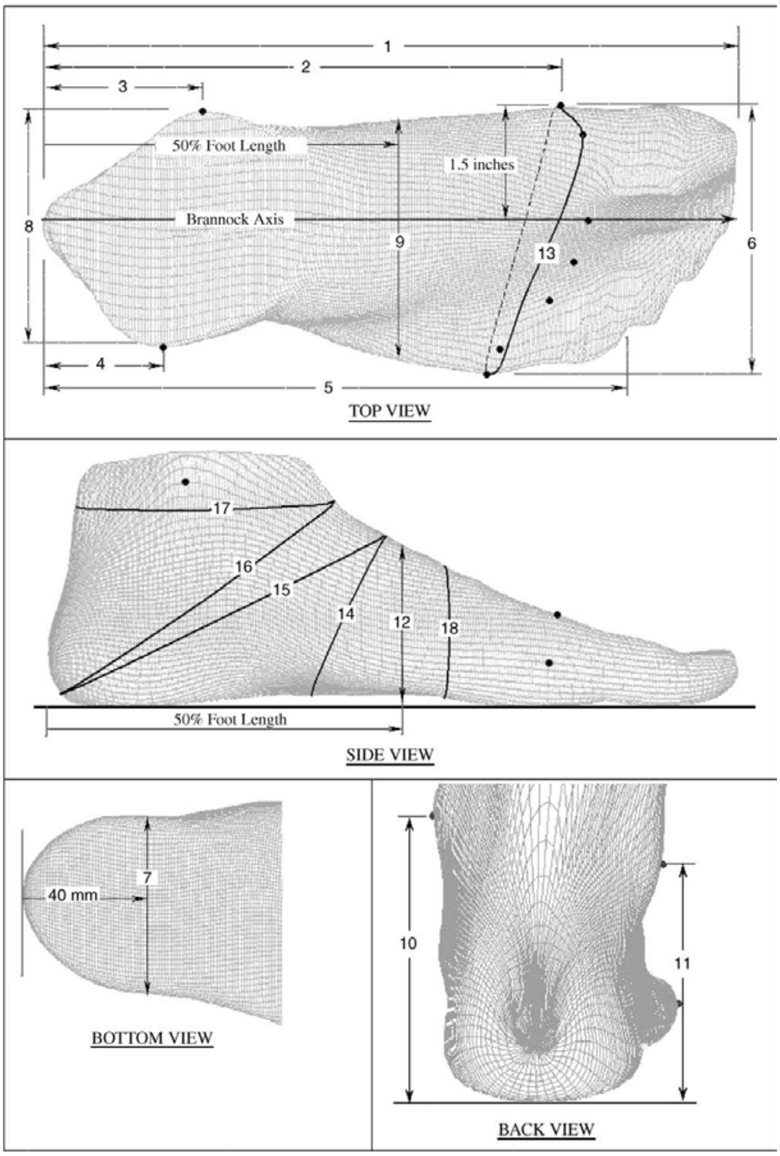

Figure 2-9 The foot determination dimensions (length, width, and girth) applied in research.

(Witana et al., 2006)

With the validity of 3D foot scan result, the application of the 3D shapes spread to the evaluation of the foot surface and estimation. Yu and Tu (2009) established a foot surface area (FSA) database and gave an estimation formula with the data from 3D scanner. Based on the equation: FSA=on1.04*foot length*(ball girth + ankle girth), results showed that FSA of the male had a mean of 650.78 cm2 and the FSA of a female had the mean of 591.19 cm2. The estimated surface area turned out to be larger than before, with the difference of 4.06%. To estimate the amount of the surface area, foot length and ball girth were selected as estimators for that they showed high correlation with each other, and less tend to differ in predicting the FSA. The study gave an advanced formula to estimate the foot surface area in the static situation. It surpasses the former researches with three parameter measurements and confirmed foot length and ball girth to be effective as estimators. However, the formula could not provide the change of value during when foot posture changes. Considering the skin extension and reduction even a slight movement, the surface area needs the expression of the dynamic situation. Still, the formula is for estimating the overall area of foot surface, rather than describing the change of particular part. Figure 2-10 shows the comparison of the newly invented scan method with former result.

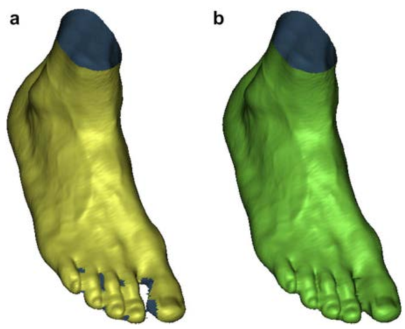

Figure 2-10 (a) Foot scanned from the 3-D foot scanner with areas hiding between toes missing. (b) Foot scanned in newly applied method with areas hiding between toes measured. (Yu and Tu, 2009)

Tu and Yu (2008) earlier have investigated on the foot surface area estimation formula with 3D scan technique. The study modified their earlier formula, and concluded that foot length-ball girth pair relation to be the better predictor of the surface database. Meanwhile the parameter of foot ankle girth to be implied not important predictor. With the refinement of formula, a more accuracy shape and faster time can be provided. The general formula turned out to be FSA=1.051×foot length × ball girth, while for male the regression model was FSA_{Male}=1.050 × foot length × ball girth, and for female the regression model was FSA_{Female}=1.052 × foot length × ball girth.

As the limitation of foot surface estimation, the parameters need to be listed in detail as required in both foot research and footwear design. The application of 3D foot scan in foot measurements were reviewed by Telfer and Woodburn (2010). As the scanners include commercial and non-commercial, foot shape presenting or foot features description, dynamic and static, various functions were adopted in different scanners, but all of them aimed at automatically capturing the measurements surpassing the manual measurements. Generally the foot linear measurements include foot length, width, and girth. By collecting data feet and categorizing into voluminous, flat pointed and slender. The scanned result was also taken into research for assessing the differences between male and female feet. The results confirmed the fact that a male foot tends to be longer and wider than a female one (Luo et al., 2009). Girths are more connected with the footwear design, for a better fit. Compared to traditional manufacturing with tape to obtain girth measurement, the scanned results can be used for investigating the fit between footwear and foot. Many researchers look for the method to qualify the shoe fit (Nacher et al., 2006; Witana et al., 2004; Wang, 2010). Witana et al. (2004) compared the shoes and the foot scans, and pointed out the significance differences; Nacher et al. (2006) gave a model to predict the fitting lever with an accuracy of 65.7%; Wang (2010) suggested developing a process which was able to choose the most suitable last for an individual’s ball girth, waist girth and instep girth.

Besides foot liner measurements only, the anthropometric changes during weight bearing were investigated. The changes of foot length and breadth showed greater changes from unloaded to half loaded states than the changes from half load to full load states. Variations were also found when different studies involved different amount of subjects. Before most of the studies were for medical use. Until recent years the scanners started to appear in shoe manufactures. By scanning the positive and negative cast or a foot directly, the shape would facilitate the footwear development. Rout et al. (2010) have developed the system with 3D foot scan and customized shoe last machine. The scanning of the foot was formed with 99 sections, and 360 surface points with 2 extra points indicating the front and back. The scanned shape later was used to modify the shoe last. And finally both the casts were used for estimation of comfort and quantification of footwear fit.

2.6.2 Dynamic 3D foot model

Almost at the same time as the researches on the foot static shapes, dynamic foot scans were developed to investigate the deformation of foot surface during motion. Early attempts to observer the foot shape change was brought up by Kimura et al. (2005). They used the cross-section to generate the flow of changes to see the deformation of foot girths in time sequence. Though the amount of sections was not big, the result did shed light on the foot motion principles. The breadths and arch length were the most significant changed parameters, and the shapes of cross-sections at the ball and the heel deformed due to the tendon movement during joint flexes. Based on the same method they improved the experiment by adopting motion capture and coded structured lights. The result was categorized into the shapes of foot side and the foot sole. The curves of the surface can be acquired by the display of the points (Kimura et al., 2008). The latter was able to record the surface shape of the whole foot, and also was able to provide the plantar deformation due to weight bearing changes during walking. However, the profile was not given in the same experiment, and the parameters were not fixed as the former research. For the limitation of the light points on the surface, the output result would turn grey a hardly record the landmarks on the foot surface, so that the shape could give the general change rather than specific landmark movement for comparison during walking. Another method to obtain foot surface deformation was designed by Couder et al. (2006), with cameras taking photos from different angles and later the 3D reconstruction with them. Also, there was a method using multiple time-of-flight 3D cameras for aligning the foot shapes in walking (Sturmer et al., 2011).

To improve the former dynamic foot scan and eliminate the limitation that most of the system can only capture foot shape from one or two view, Jezersek et al. (2011) developed a multi-laser-plane triangulation technique to obtain the human foot shape as in many modules simultaneously. All the modules later would be transferred into a two- or three-dimensional shape based on the points of the detected line segment. The application was still to measure the cross-sections and to compare the deformation of the profile as time sequence. Blenkinsopp et al. (2012) reported a methodology with 3D digital image correlation system to measure foot surface change during walking. Except for the commonly analyzed parameters such as foot length, breadth change, and the cross-sections comparison, the result was combined with strain map to provide the degree of deformation. Together with the recorded ground reaction force, the foot shape deformation can be concluded as a sequenced change.

As the advance of Japan research, the dynamic foot scan was developed from 3D to a 4D measurement system. It was composed of one video camera and one projector. The reflected pattern on the foot surface was formed with in 2*2 pixels made up of 9 colors. In the research they found a method in the sequence of ‘acquiring the homologous model-form activated shape of foot-postural change-model fitting’. In this way the foot shape deformation could be modified based on a homologous model, and the problems in measurement could be solved with the template by fitting. The inspiration was still in refinement (Yoshida et al., 2012).

At almost the same time, German researchers brought up a new approach to obtain the foot shape during walking. They used a set of scan system to output the 3D geometric point cloud of the foot and to present the surface as time sequence. For the parameters they predefined several foot segments for recognition. With the scan of foot while walking, an automatically constructed virtual foot shape, based on the predefined segments, gave the vector direction and rotation axes. Thus the highly related joints would also be recorded with the changes in angle (Herrewegen et al., 2012). However, it still needs improvement, since the result would be highly dependent on the predefined segments. The size and amount of the segments were not stored to facilitate the segments, which may cause the misconstruction of the real foot shape.

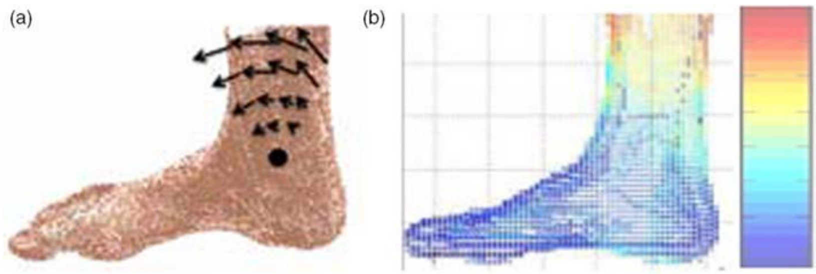

Figure 2-11 Simplified example of a vector field, (a) direction and (b) norm with color bar. Segments and rotation axes can be extracted from these vectors. (Herrewegen et al., 2012)

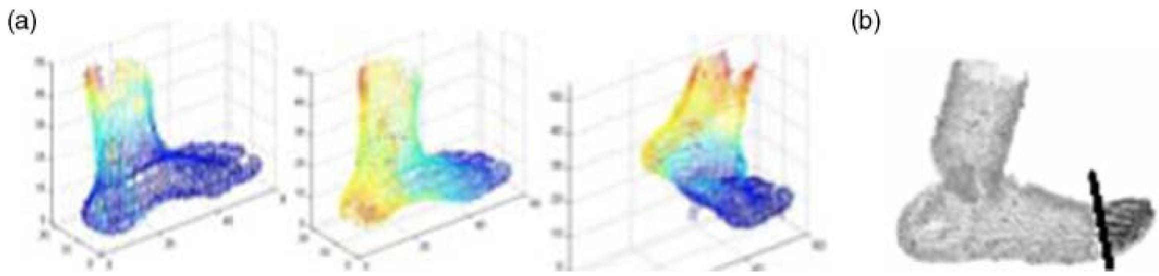

Figure 2-12 (a) Foot motion vector fields (norm) during midstance, heel off and toe off. (b) Artificial foot with detected toe rotation axis and toe segment. (Herrewegen et al., 2012)

The real application with the 3D dynamic foot scan was in the research of Samson et al. (2014). The dynamic foot scan was also composed of three time-of-flight cameras, which was referred to Japanese researchers' theory (Mochimaru and Kouchi, 2011). The foot shapes was captured frame by frame, and the foot sole pictures were specially picked out as 2D analysis for foot roll-over evaluation. As the analysis was focused on the footprint-shaped sole projection, and its relation with foot height, this research was to simplify the 3D shape changes into a 2D image.

2.7 Motion research

2.7.1 Motion capture system introduction

Researchers have long been trying different ways to construct the human body movement. Among them the representative one is the motion capture technique. Bishop (2012) integrated former models reflecting body motion, including variability found biomechanical model parameters, methodological design, and model reliability. Bishop et al. (2012) have given recommendations for the reporting of foot and ankle models. They searched and assessed reports involving different methods of motion model.

The motion capture research into human body motion was started since the 19th century. Being in use in many fields such as medicine, sports, entertainment, law, engineering, and of course ergonomic environment, the various types include optical motion capture systems, radio frequency position systems, electromagnetic trackers, electromechanical performance capture suits, digital armatures, and facial motion capture systems (Menache, 2011). They can be more generally categorized into three groups: optical systems, magnetic systems, and mechanical systems (Kitagawa et al., 2008).

As early as the classical antiquity, human motion patterns were studied in relation to motion of animals, and mathematics was used for describing human poses or motions. But most of such studies were only presented by means of static artworks (Klette et al. 2008). Later in the 19th century technology of locomotion allowed the recording of several phases of motion in the same time (Klette & Tee, 2008). Marey presented pictures with the technique of chronophotograph in his book in the year 1894. The pictures included both a striding man dressed partially in white, and partially in black, and also white lines in a chronophotograph of a runner (Marey, 1894).

In research of the human motion, experts in biomechanics, computer graphics, and computer vision are all searching for solutions to present the dynamic model. In the latter half of 19th century Christian Wilhelm Braune (1831-1892) and Otto Fischer (1861-1917) started experimental studies of human gait, and till 20th century biomechanics developed into a specific field of science. The research method supported by marker-based pose tracking systems spread widely into many topics. This system was oriented from the work of Johannsson (2011), and now most frequently used in animation industry, clinical research specifically for body motion model and facial expression simulation.

Recent researches using motion capture have been exploring into whole human body motion (Tranberg, 2010; Ceseracciu, 2011). Some experiments have been designed on the gait analysis (Stone & Skubic, 2013; Nielsen & Daugaard, 2008). From the perspective of detailed methodology of data collection, those researches can be categorized into ones with motion capture based on optical markers (Tranberg, 2010; Nielsen & Daugaard, 2008; Jenkyn & Nicol, 2007), and ones with markless motion captures (Corazza et al., 2006; Stone & Skubic, 2013; De Vries et al., 2009).

Tranberg evaluated the influence of soft-tissue artifacts on analyses of body motions based on optical markers, and also tried new application with instrumented gait analysis into clinical situations (Tranberg, 2010). He tested former result between bone motion and skin detection, finding out that there was slight incompatibility of conclusion in different methods. Also in additional gait analysis, which is a part of the whole experiment, landmark setting covered the body lower extremity. 15 reflective skin markers were divided into 5 groups in a form of 3 points within one group representing one body part or joint.

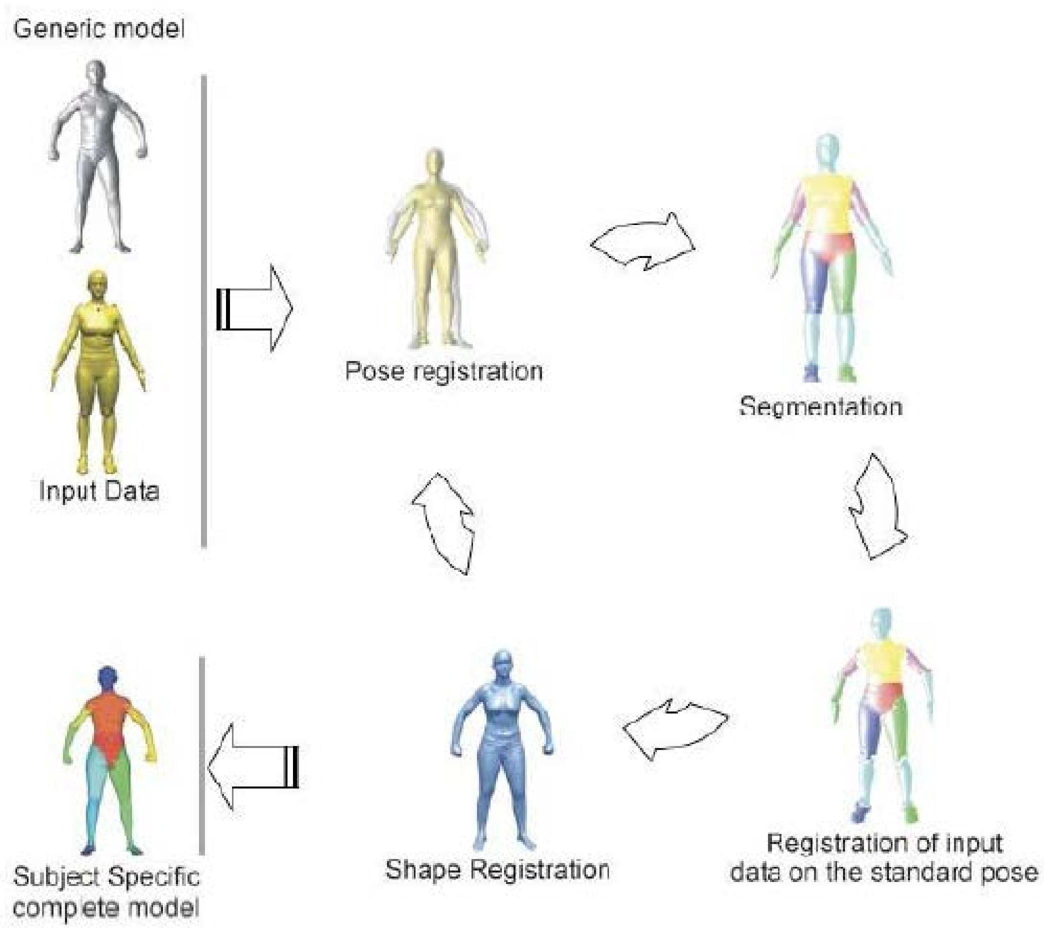

Figure 2-13 The pipeline of method with markerless motion capture for swimming. (Ceseracciu, 2011)

Ceseracciu （2011） used a method with markerless motion capture to evaluate the swimming biomechanics and gait analysis. The pipeline is as follows (Figure 2-13). The new method combines triangle mesh, kinematics and automatic model generation to obtain a subject specific complete model. Segments are divided based on standard model and sports biomechanics basics. With the modification of each part based on the standard model, a new set of components can be assembled together to form the specified 3D model.

Livne and Sigal (2012) also researched into a simple proof-of-concept model for human attributes inference. The main research range is within walking motion, a generic 3D pose tracker, the simple motion features, and a basic set of attributes. With the use of low-dimensional representation of joint trajectories in a body-centric coordinate frame, the result can reach the rate of 90% in gender classification from video-based tracking data (Livne et al., 2012).

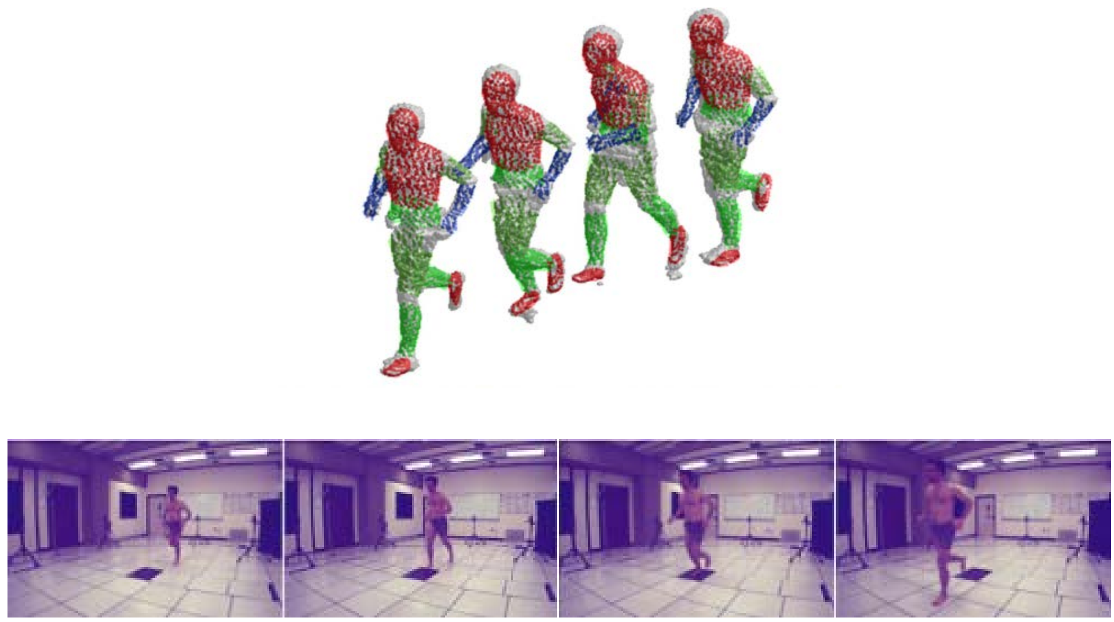

Figure 2-14 The result of the matching algorithm applied to experimental data sequence.

(Corazza et al., 2006)

Corazza and Mundermann et al. (2006) set a markerless motion capture system to study musculoskeletal biomechanics of human body. The method is based on visual hull reconstruction and a priori model of the subject. 16 cameras in the virtual environment and eight cameras in the experimental setup were used to obtain the subject's 3D representation. Using the 3D representation and a matching algorithm it can provide the extraction of the subject's kinematics. The result of the matching algorithm applied to experimental data sequence is shown as follow (Corazza et al., 2006) (Figure 2-14).

2.7.2 Gait analysis with motion capture system

Many researchers tend to simulate the motion of human walking with the help of motion capture. In the gait analysis, motion capture is taken into the experiment for acquiring the joint movement. Contemporary advances in computer technology and data analysis techniques contribute significantly to the progress. In this field the experimental methods include not only motion capture systems, but also contain force plates, electromyography, and equipment integration. The data analysis techniques include kinematics, joint angles, kinetics, and inverse dynamics (Chester et al., 2005). Lundberg overviewed the technical consideration of methods, summarized them as optical methods, radiographic methods, optoelectronic (or photogrammetric) methods, Rontgen stereophotogrammetric analysis (RSA), magnetic tracking, sonic and ultrasonic tracking, and strain gauge methods (Lundberg, 1996). The movements of bone segments were also reviewed in Lundberg's work. Among the many regional aspects of human body, pelvis, hip, knee and ankle and foot are main divisions at lower extremity for research.

Collins et al. evaluated the performance of a six degrees-of-freedom marker set for gait analysis, through comparison with a conventional set and assessment of repeatability (Collins et al., 2009). 16 landmarks representing body lower extremity structure based on definitions of 6 degrees-of-freedom set system and 14 landmarks based on anatomical sets representing body lower extremity structure were combined into experiments respectively and were compared for repeatability (Figure 2-15). The landmark settings include body positions such as pelvis, hip, knee, and ankle, as previously mentioned in Lundberg’s work. The data were calculated in values of CMC (mean and SD) and the results showed both sets have generally high repeatability compared to previous studies.

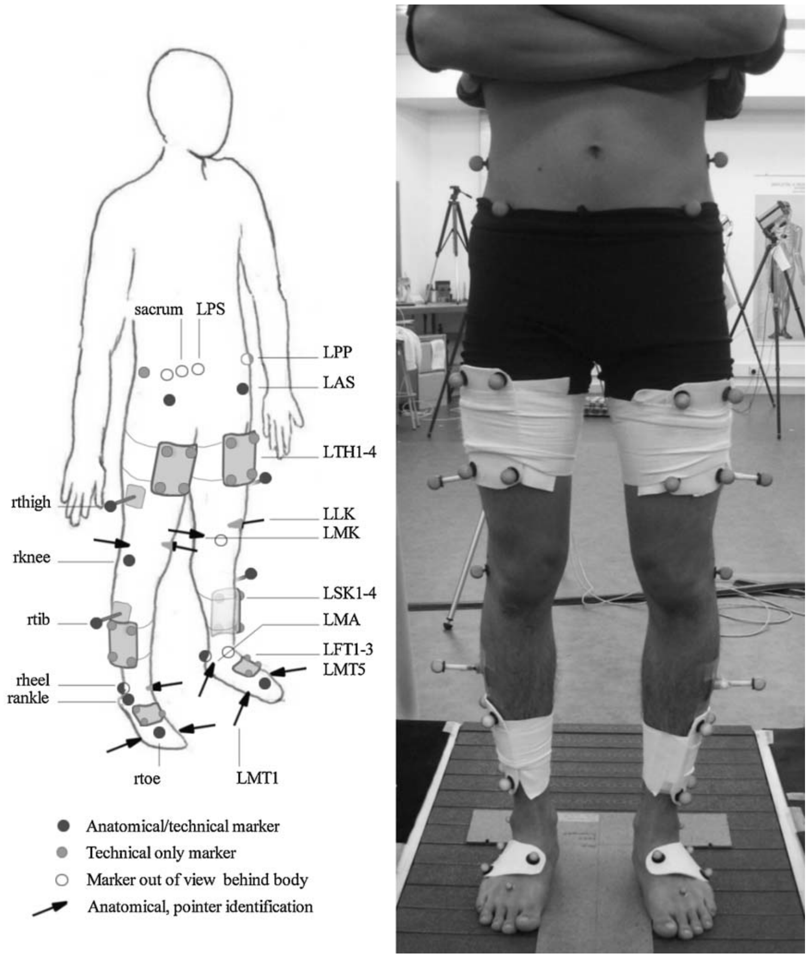

Figure 2-15 Landmark setting in experiment. (Collins et al., 2009)

The lower-extremity skeletal kinematics research with optical markers is not a new topic. Comparisons have been tested to identify the repeatability of surface mounted markers and other analysis methods (Fuller et al., 1997; Manal er al., 2000; Nester et al., 2007).

Fuller et al. (1997) had conducted experiment to evaluate the validity of using skin-mounted markers to measure the three-dimensional kinematics of the underlying bone. Analysis centered on the kinematics of the femur and the tibia, and reported on the validity of skin-mounted markers for the estimation of skeletal kinematics. Results showed the skin-mounted marker data were inappropriate for representing the motion of underlying bones. The patterns of motion in any of the experiment were task dependent.

Manal et al. (2000) analyzed gait in order to understand how the bones of the lower extremity move during locomotion. It is the first time for a new proposal of optimal surface tracking marker array for motion capture to be suggested with combination of high-speed video. The locations for 11 markers were set based on foot physical characteristics and angular kinematics (Figure 2-16). In the result rotation deviations were found in different experiments and this situation cannot be thoroughly avoided by observation of each individual subject data.

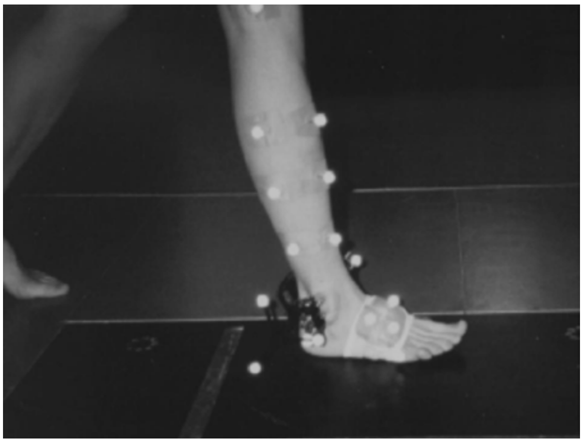

Figure 2-16 Landmark setting in Manal experiment. (Manal et al., 2000)

Nester et al. (2007) have compared kinematic data from an experimental foot model comprising four segments, including heel, navicular, cuboid, and medial forefoot, and the kinematics of the individual bones comprising each segment. By recording the markers pinned to skin, plate, and bones respectively, the data showed small differences between the stance phases while statistically significant differences in the tibial kinematics.

Leardini et al. (2007) suggested a protocol for gait analysis for children. With the aim to provide a complete description of 3D segment and joint motion protocol, and to report the quantities in accordance with the recent recommendation, the method was set with attachment of 22 skin markers, the calibration by a pointer of 6 anatomical landmarks, and the identification of the hip joint center by a prediction approach.

Carson et al. (2001) analyzed the repeatability of a method used in clinical kinematic research. With stereophotography and motion capture they developed a protocol of evaluation of foot kinematics based on a multi-segment foot model. The foot model is divided into four part, including hindfoot, forefoot, hallux, and tibial segment. 14 landmarks were settled and the data of both static and walking trials were collected and analyzed in the way of component variability. Results showed good consistency between trials and confirmed that artifacts from skin movement are repeatable and systematic.

Stone and Skubic (2013) raised an inexpensive depth camera evaluation for in-home gait assessment of older people. In the method two Kinect cameras and two web cameras were applied in positions on the edge of a squared area for walking path. The kinect cameras were on the point and the normal cameras were in the middle of edges, respectively. An existing algorithm was used to extract gait data. A 3D point cloud data from the Kinect camera is for shaping the model of a single person.

Due to the high performance of Vicon system in capturing human body motion, researches involving multi-aspects were proposed for further exploration. The first is to convert 2D pictures into 3D model. Luximon gave a prediction model of 3D static foot shape with simple anthropometric measures including foot length, foot width, foot height, and foot curvatures

(Luximon & Goonetilleke, 2004). 11 landmarks were applied on foot covered with sock and the scanned curvatures, especially metatarsal-phalangeal joint curve, were transformed into equations and the foot shape data were generated into a “standard” foot shape prediction model. This model has been refined in later published paper, with its variation of two models using foot outline and foot height, and foot outline and foot profile respectively (Luximon et al., 2007). By comparison the second method displayed higher accuracy but need as many as 99 images of the foot sections. Another practical and economical methodology for foot shape prediction was proposed in Kwong’s thesis in 2007. The result of the study was a 3D point cloud which was able to represent the foot shape. Also a method to correct the linear perspective distortion of captured foot images was demonstrated (Tang, 2007). The methods mentioned above are all about extracting the foot shape in an inexpensive way, and all of them are to form the static standing foot shape. The 3D transformation technique could be applied into the forming of dynamic foot model, and to provide the walking process.

The dynamic model of foot walking is also researched during last few years. Ren et al. (2007) proposed an inverse dynamic multi-segment model with optimization techniques of human walking. All segmental motions and ground reactions were predicted from three representative gait descriptors, walking velocity, cycle period, and double stance duration.

2.8 Foot Modeling

To research into the movement of foot, a way of presenting it varied with the development of technology. In the early period of research, 2D trajectories were drawn to display the motion range of foot in both walking and running states. However, the 2D display can only present the view from a single angle, not the motion in a real space. With the application of motion capture, the movement of landmarks can be recorded and the tridimensional models in various methods are developed. Oxford foot model and Heidelburg model are two representative ones (Pratt, 2012). While along with the attempts to obtaining a visible model, mathematical models are also under modification for thoroughly describing the movement principles. Finite element modeling is in development for the imitation of more accurate foot shape model.

2.8.1 Trajectory findings

By recordings the movement of landmarks on foot, trajectories can be matched into a whole line. The lines reflect the general motion range during human walking or running, giving the basic reference of range of study. The use of conventional gait models (Kadaba et al., 1990; Davis et al., 1991) and the Cleveland Clinic Model (Cappozzo et al., 1995) were notable and widespread in the clinical field. However, those models share the shortcoming in that the single-segment representation of the foot is unable to clearly display the deformities on particular foot part (Long et al., 2011). Milwaukee Foot Model incorporated in the anatomy-based indexing methods allowing tracked anatomical markers to show bone orientation (Kidder et al., 1996; Myers et al., 2004). Jenkyn and Nicol (2007) researched into former six studies of Carson et al. (2001), Hunt et al. (2001), Moseley et al. (1996), Rattanaprasert et al. (1999), Kidder et al. (1996), and Leardini et al. (1999), but found no consensus on segment or joint motion definition.

Long (2011) developed a model for analyzing the lower extremity motion by estimating hip joint center location and tracked the motion of six segments during stance and swing periods. The study was based on the referencing of Milwaukee Foot Model. Meanwhile, a multisegmental model was formed to explore the foot and ankle motion. Divided segments included pelvis, bilateral thigh, tibia, hindfoot, forefoot, and hallux. Based on the settings that the time period was from 0% to 100% of a gait cycle, the tracking results were calculated with correlation analysis and showed good correlation between the new integrated model and the former standard one (Figure 2-17).

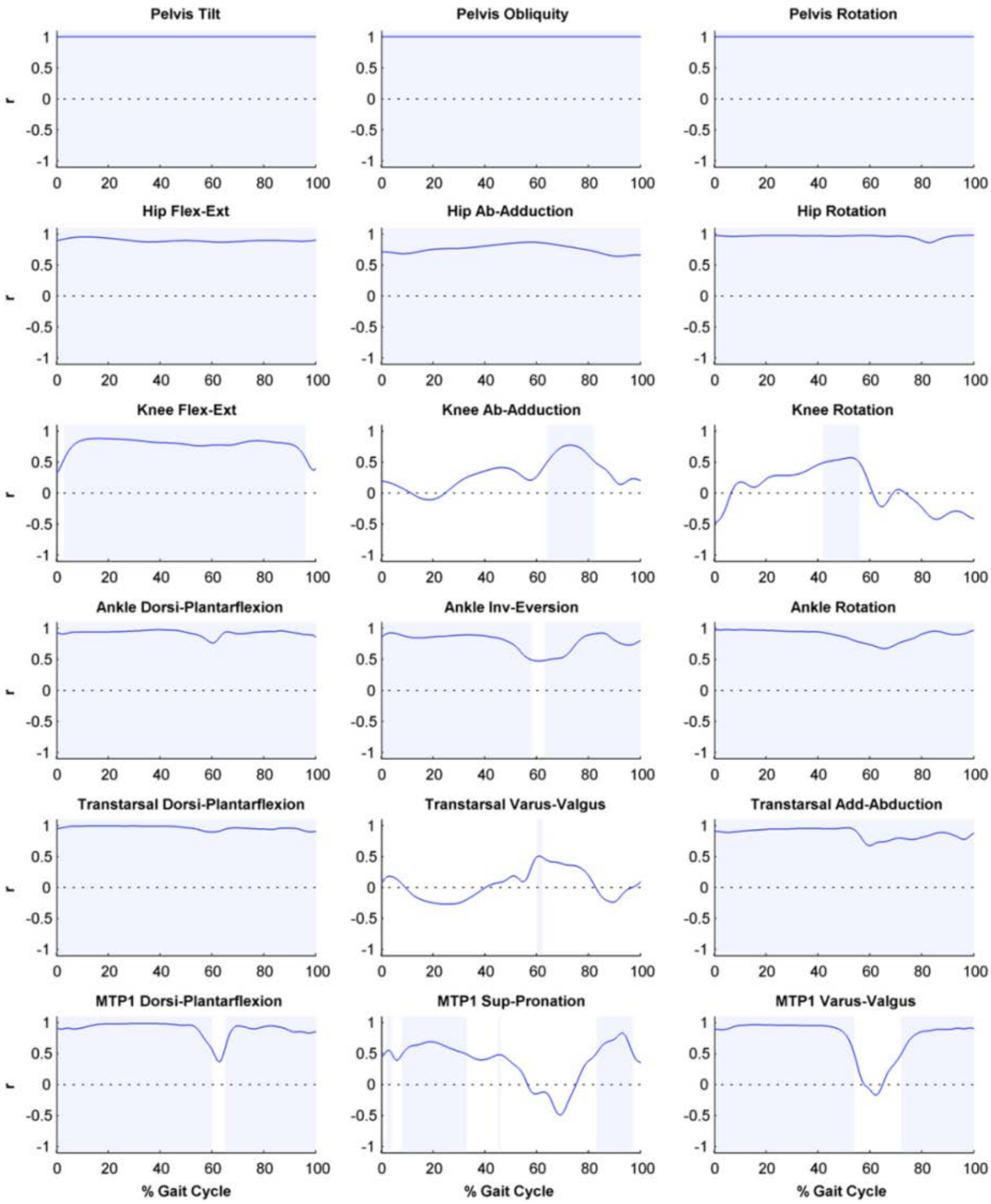

Figure 2-17 Pooled point wise correlation results from all participants. Data are plotted from 0% to 100% gait cycle; shaded regions indicate significant nonzero correlation. (Long, 2011)

Though the new integrated model exceeded previous established values for clinical use, the research focus was set at the hip joint center and the result could only reflect the overall lower extremity movement. With the limitation of output, the model needs more modification in the long run.

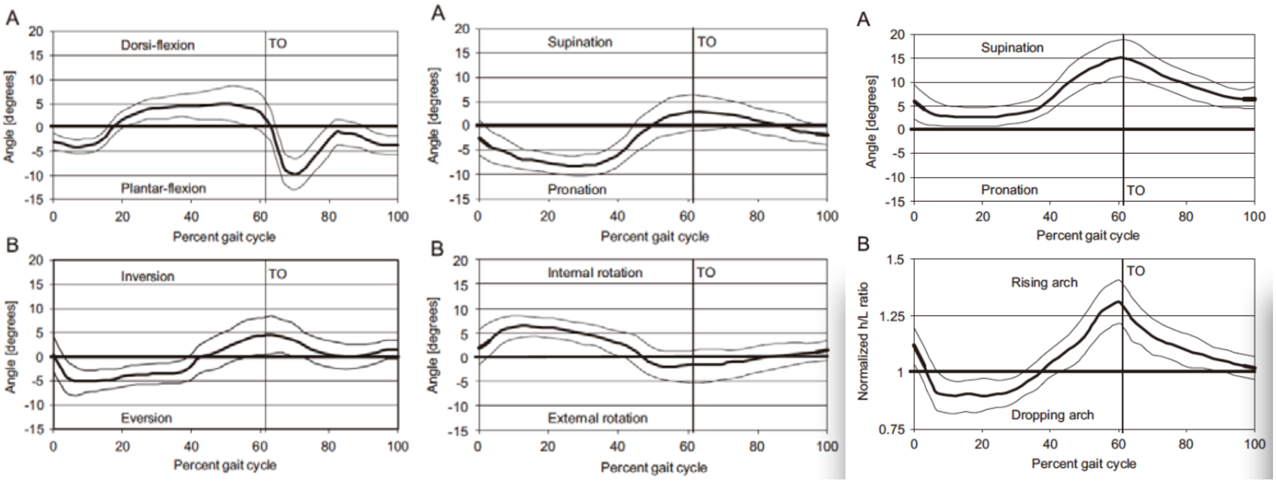

Figure 2-18 (A) Ankle joint motion and (B) Subtalar joint motion averaged over all subjects (bold line) showing the positive and negative standard deviation (solid lines).

Figure 2-19 Hindfoot segment motion with respect to the midfoot in (A) the frontal plane and (B) transverse plane.

Figure 2-20 (A) Twisting motion of the forefoot segments with respect to the midfoot. (B) Height-to-length ratio of the medial longitudinal arch normalized to 1.0 in quiet standing. (Jenkyn and Nicol, 2007)

Jenkyn and Nicol (2007) reported their research into the motion range during a gait cycle. With the division of five segments (hindfoot, talus, midfoot, midial and lateral forefoot) and six functional joints (ankle and subtalar joint, frontal and transverse plane motion of the hindfoot relative to midfoot, supination and pronation twist of the forefoot relative to midfoot and medial longitudinal arch height-to-length ratio), segment-fixed axes were defined for the forming of vectors. Based on the setting of relative motion, a three-vector system was designed for calculating the movement of functional joints. By integrating the rotation angle, foot motion range could be displayed in respect to the angle change in particular timing within a gait cycle (Figure 2-18, Figure 2-19, Figure 2-20). Studied motion included dorsiflexion and plantar flexion, inversion and eversion, supination and pronation, internal rotation and external rotation, and together with rising arch and dropping arch degree. The former four calculations were compared with angle, and the last one was with normalized height and length ratio.

2.8.2 Shape visualization

The visual model displaying the foot shape is not a new idea in modeling research. Bruderlin and Calvert (1989) suggested their hybrid approach to the animation of human motion combining a goal-directed and dynamic motion control. The KLAW (Keyframe-Less Animation of Walking) system was developed for the animation of dynamic movement.

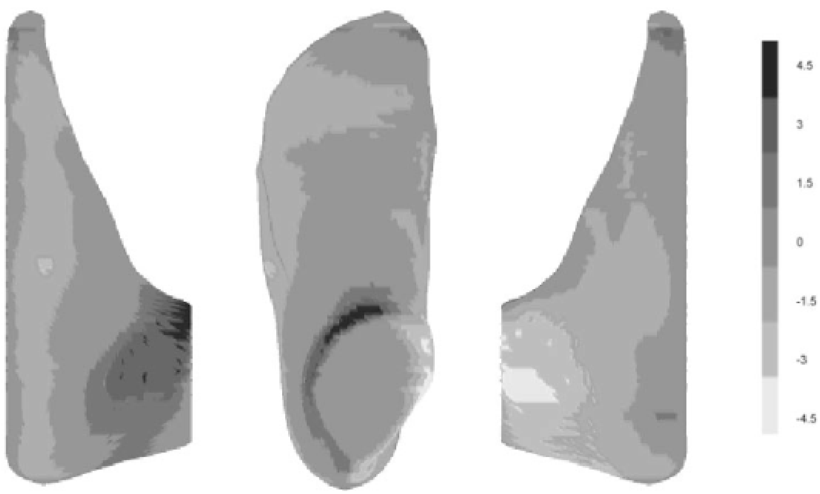

Figure 2-21 Predicted shape of foot with gray-scale-coded error. Scale values are in millimeters. (Luximon and Goonetilleke, 2004)

Luximon and Goonetilleke (2004) studied into a “standard” foot and the prediction with foot length, width, height and measure of foot curvature based on the standard foot. With the attached 11 landmarks indicating the metatarsal phalangeal joints, dorsal surface and plantar side of the foot, and also chosen 4 points for ensuring the scanned foot shape. 3D point cloud data were for analyzing and 99 sections set with 1% of foot length apart were abstracted for forming the shape of foot. A local coordinate system surpassed the global coordinate system in comparing among individuals. Landmark coordinate axis was transformed and normalized, as well as a polynomial regression was used to determine the metatarsal-phalangeal joint curve. Following a integrated "standard" foot model, prediction with particular foot parameters can be formed based on modifying the standard foot model. The new model and its modification method can be applied into developing custom lasts for the manufacture without actually scanning a person's feet (Figure 2-21).

The model was later improved with the comparison of two methods. The first one used foot outline and foot height, and the second one used foot outline and the foot profile (Luximon et al., 2005). Both two methods were incorporated with the standard foot model and the latter one showed better accuracy in presenting the foot shape.

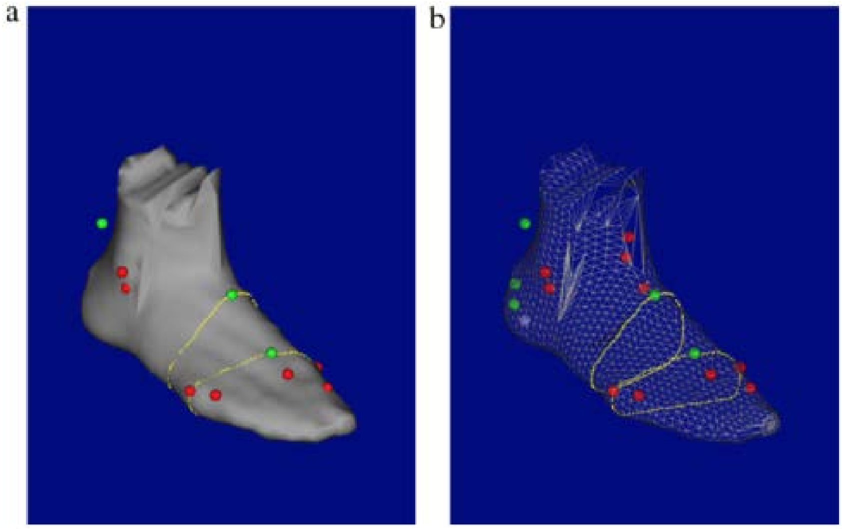

Figure 2-22 Initial human foot: (a) surface; (b) polygon models. (Tang and Hui, 2011)

Tang and Hui (2011) proposed a fast approach to modeling foot deformation and simulating the interaction between foot and footwear toward footwear design. The workflow started from an initial foot model and combined with captured foot motion, so a human foot animation could be created. A footwear model was developed fitted to the foot model in order to analysis the deformation and stress in the footwear. The initial foot model was obtained with 3D foot scanner, and then transformed into a surface polygon mesh (Figure 2-22). The motion data was captured with optical motion analysis system. The template foot model is adjusted to fit with markers tracks so that the number of markers will determine the accuracy of the deformed foot model. Boundary element method was applied in the research of simulating the foot model and its motion. As the results turned out, the method is effective to animate human foot with different motions and subjects.

2.8.3 Computational model

For the requirement of detailed foot model which is able to present the slight deformation, boundary element method is not the only method of obtaining the surface shape. Researchers tried finite element model to present the foot as well.

Ledoux et al. (2000) generated an anatomically accurate finite element model of the human foot and ankle to predict the response of the foot to tibial forces. The geometry of the model was based upon the foot of a 67 year old male. A triangulated surface mesh was created from each tissue’s contour set, and reconstructed as a mesh surface shell elements. As an anatomy model, the limitation included the ignorence of muscle and cartilage. Meanwhile the approach to further modifying the experimental conditions were taken into consideration.

The finite element analysis method was applied into shoe shape forming, and mainly for calculating the effect of material selection for the outsole (Lewis, 2003). The model was for a therapeutic shoe on the stresses and displacements. With the drawing of the shoe shape, a finite element mesh of the model could be generated (Figure 2-23). To simulate the material response, a relevent elastic properties for all the materials were supplied, so that the constraint conditions could be continued to be applied to the model. The model was tested to well displayed the interface between the bottom of the foot and the top layer of the insole, and the differences in responses were potential for translating into perceived comfort level. The limitation lies in the fact that the model was still in 2D form and a more accurate 3D model was expected to come out.

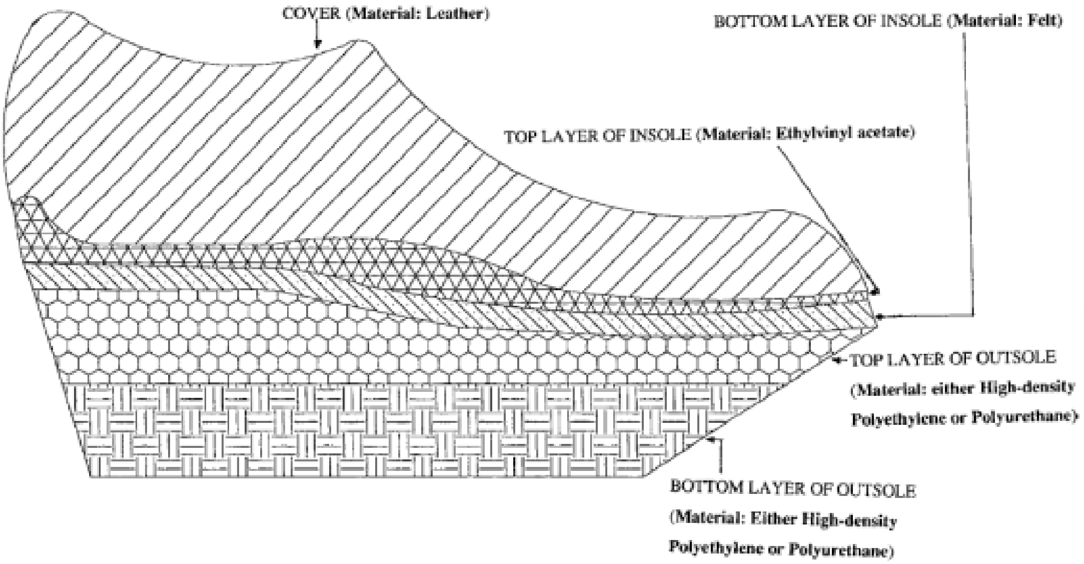

Figure 2-23 Parts of and typical materials for a “solid rocker-bottom” type therapeutic shoe.

(Lewis, 2003)

Another finite element model for analysis integrated foot and shoe was introduced by Yu et al. (2008). A model of female foot for high-heeled shoe design was developed and applied for evaluating the biomechanical effects of high-heeled support on the ankle foot complex (Figure 2-24). The 3D anatomical model a balanced standing position was simulated and the result presented peak plantar pressure changes in metatarsal-phalangeal joint. Arch height was also found to be decreased compared to horizontal support. For the development of model was for anatomical use, a more practical foot model for life and customized footwear design is still in need.

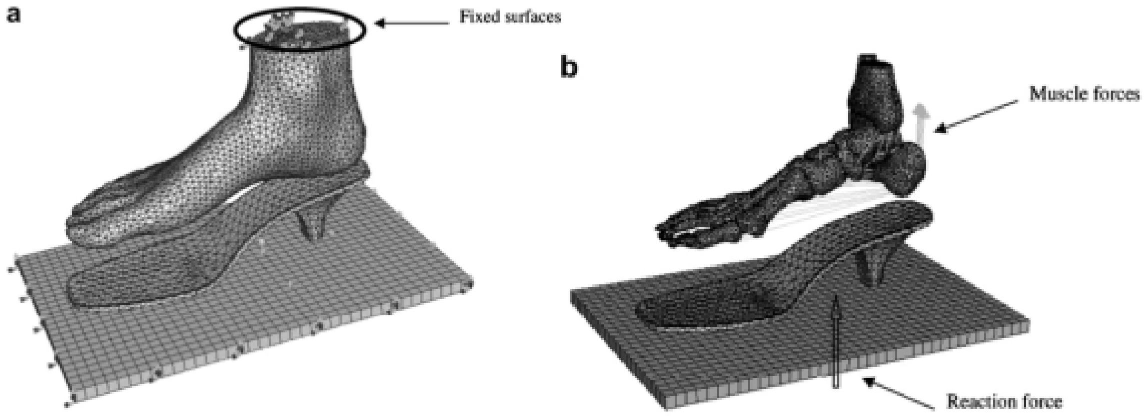

Figure 2-24 The FE mesh of the bulk soft tissue, foot bones, ligamentous structures, and support showing (a) boundary and (b) loading conditions for simulating balanced standing with a high-heeled shoe. (Yu et al., 2008)

There are also researches into modeling of human walking movement. Roos et al. (2011) published study in influence of neuromuscular noise to fall risk in method of 3D dynamic walking model in 2011 and 2013, respectively. Firstly the simulation study was correlated (Roos & Dingwell, 2010), with the replication of former dynamic model (Kuo, 1999). Then the motion orientation was prescribed by four angles: (1) splay angle, (2) stance angle, (3) roll angle, and (4) swing angle.

2.9 Summary

Current research on dynamic foot can be divided into two directions. One direction is focus on the general foot-leg motion, in ways of gait analysis and walking trajectories. To obtain this paths motion capture is adopted widely for its convenience in recording joints motion with time. The other direction is to record the foot shape in 3D space, and in this way the shape can be calculated and compared for long-time researches. In the latter 3D foot scan is applied to facilitate the measurement, shape presenting, and building up the general foot shape database. The two methods have different benefit. The motion capture could provide the consistent movement of the landmarks attached on the object in time sequence; the 3D foot scanner could provide the shape in details without the attendance of the subject for further analysis. To combine the shape with time factor, current research is trying to develop and improve the dynamic 3D foot scan system. Results showed good accuracy and shape changes with time, however, it can hardly provide a general prediction of foot dimension.

Nowadays the foot natural shape is more considered in footwear design and production. Footwear fit is based on the foot shape recognition. In lots of former researches reports static foot shape can be obtained instantly and saved, but the dynamic shapes in walking or running needs more clear understanding for the reason that foot shape will deform dramatically compared to static situation. Foot in motion requires the knowledge in both joints angle and the dimension value changes. To form a thorough and detailed map of foot shape in movement, the methods of both motion capture and the foot scanner are essential for the research. The model of dynamic foot is able to contain both general foot motion and detailed parameter reference with the support of multiple methods.

So based on the former literature, the future of the research could be in one direction: to combine both methods and to develop a model of dynamic foot. In the model, foot information in walking, in various movements will be described. Furthermore a prediction model is potential for the footwear design.

CHAPTER 3 METHODOLOGY AND EXPERIMENT

3.1 General methodology

The foot in dynamic status presents a more complex shape to adjust to various situations. To keep the body balanced, some specific parts may deform to a larger degree than when it is standing still. For the presenting of the dynamic posture, both 3D shape and time factors should not be neglected. In addition, the foot may rotate, twist, or fold to different directions under different circumstances. Therefore, this study adopted methods that can record the foot shapes, while also keep time with foot movement. One of the approaches is by using the 3D foot scan to obtain a complete foot surface with relatively high resolution. Another way is to adopt motion capture system into the dynamic research of body movement. Both methods were tested in this study to collect a whole set of foot motion information. Also, a high-speed camera was set at the side during walking to acquire the profile information.

This research mainly aims at developing a dynamic foot model, which is able to provide the changes in foot deformed area, rotation angles, and other representative references. In order to acquire sufficient data, three experiments were designed to document the deformed data from different viewpoints. The framework of the study is as in Figure 3-1.

This research covers four steps: first, an experiment to observe the movement of foot joints and landmark trajectories was conducted based on the application of motion capture system. In this experiment, a series of time-dependent landmarks and time combined to provide the foot walking trajectories and variation of rotation angles during walking. At the same time the high-speed camera recorded the time-dependent profiles for reference. With the time-dependent information a general look into the foot shapes was settled within one gait cycle.

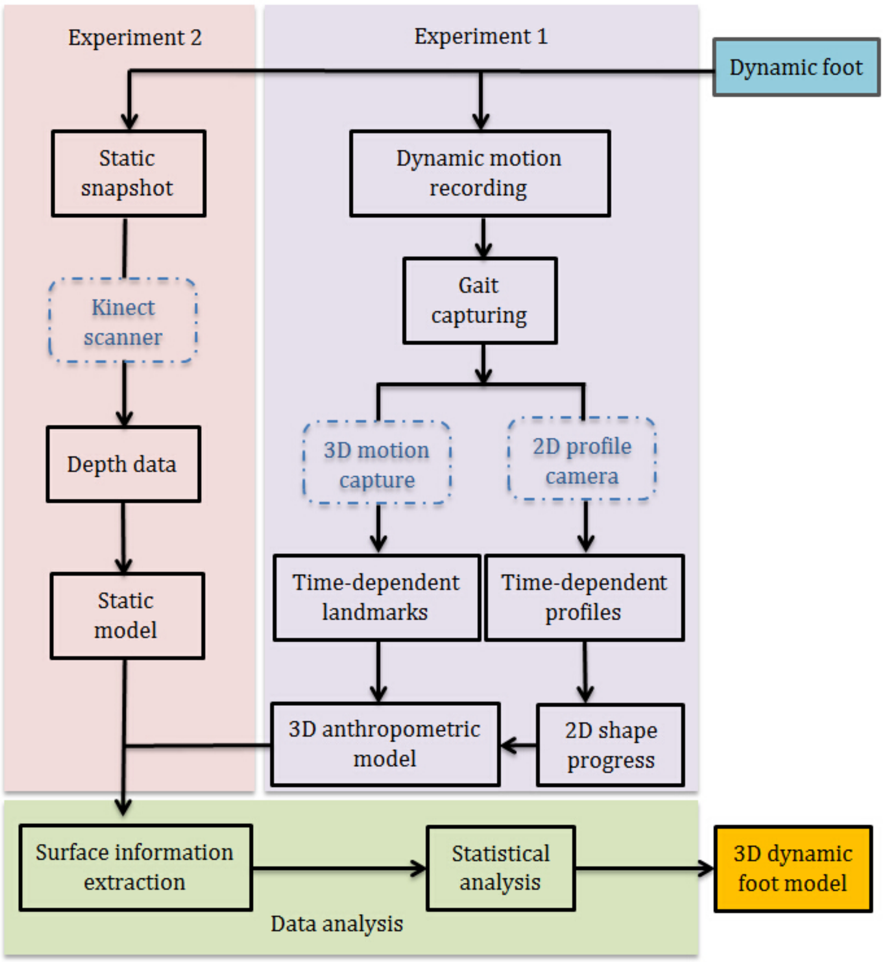

Figure 3-1 Framework of the development of dynamic foot model

The second part of the research is the main experiment, with the support of a 3D scanner. The scanned result was formed with integrated depth data of the object and its surroundings. From the scanned result (static model) the landmark locations in the three dimensional coordinate system are extracted for further analysis. The static model provides both the surface information and the landmark for measurements under different situations. To observe the changes and the regulation of foot parameters, data of all the lengths and angles are extracted for statistical analysis.

In the analysis of obtained data, landmark triangulation was developed for simulating the 3D foot motion. Landmark distances and the main angle for representing foot rotation were calculated separately and compared. The overall results suggest the trend and range of foot movement. In the statistical analysis, ANOVA test and comparison of means were applied to the data. After the basic analysis, a simplified model simulating the foot surface and movement was proposed.

3.2 Experiment 1—Motion capture for gait analysis

3.2.1 Introduction

The application of the motion capture is to obtain the trajectories of characteristic positions on foot. Retro-reflective landmarks are applied to the skin so that the camera can catch and record their regular movement pattern.

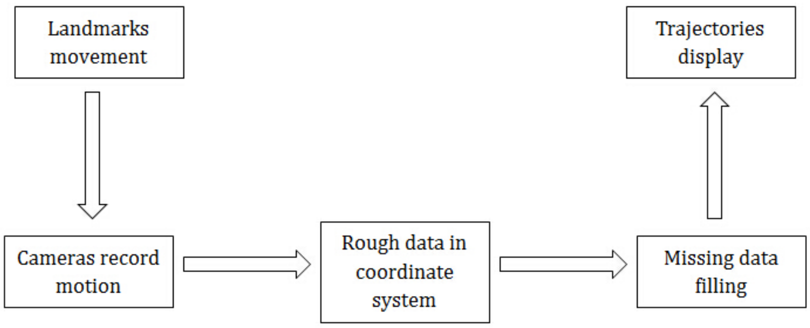

Figure 3-2 Flowchart of motion capture recording process

During the walking movement the cameras may possibly fail to detect the retro-reflective balls; some missing area is considered acceptable in the results. To reduce the missing area, multiple trials were recorded for each subject. The average movement in the three dimensional coordinate system will be integrated to form a regular pattern of the gait. A flowchart of the motion capture recording process is shown in Figure 3-2.

3.2.2 Participants

In this experiment thirty female Chinese participants were recruited and documented in the database. Each participant was required to repeat the same procedure 5 times for accuracy of results. So in total there are 150 data recordings. All the participants were examined to be normal and without any foot problems. In addition, individual information including height, weight, and foot length and width, ball girth were recorded for later reference.

3.2.3 Procedure and equipment

Two documents were included before the real experiment. After signing a consent form, each participant was instructed to fill in a basic information form including their age, height, and weight, foot length and width, foot ball girth. After drying the feet, the foot length and foot width of participants were measured using the Brannock device (Brannock, 2004). Also their foot girths were measured with flexible measuring tape. While the equipment of the Vicon system was preparing, 21 landmarks were attached to the surface of the foot.

Landmarks are set based on basic knowledge of anatomy and former researches. In the existing researches numbers of landmarks vary from four points (Nielsen and Daugaard, 2008) to as many as 17 points (Heidelberg measurement, 2006). In terms of the specific area on the foot, there was no clear landmark setting that could reflect the overall foot movement. In this experiment, twenty-one spherical markers with a diameter of 5mm will be attached to the surface of the foot and the lower calf with double-adhesive tape, covering a relatively thorough range from the heel to the toe. Table 3-1 shows the detailed landmark design and Figure 3-3 gives the distribution of points.

The design of the platform is based on the requirement of the experiment. The base is the length of general six steps long, among which there can be at least two gait cycles. From multiple tests for the needed space, the final platform is set at the size of 200cm long and 60cm wide.

Table 3-1 Details of landmark design and description

No.	Abbreviation	Description
1	TP2	Toe point 2
2-4	MPJ 1, 2, 5	Metatarsal-phalangy joint 1, 2, 5
5-7	TML, MML, LML	Top, medial, lateral side point on the line vertical to the middle foot length
8	LTIB	The anterior border of the lower tibia
9-10	MMAL, LMAL	Medial and lateral malleolus
11-12	MCAL, LCAL	Medial and lateral calcaneus
13	TENCAL	Tendo calcaneus
14-17	F/M/B/L VS1	Horizontal calf section at 25cm above the ground
18-21	F/M/B/L VS2	Horizontal calf section at 30cm above the ground

Figure 3-3 Distribution of landmarks on foot surface

The motion capture (Vicon-612) for recording foot walking is a six-camera system. It is utilized for the recording of human gait movement. Besides the walking platform, a high-speed camera (Miro-4M 8156) was set for recording the motion change. Figure 3-4 shows the high-speed camera and the Vicon system used in the experiment.

The total recording time is counted from the moment subject raises the heel and starts walking, over five heel strikes and finally the other foot swings back. Though the walking pattern varies based on personal habit, in this experiment subjects are required to start walking with the right foot, so as to unify the collected data results.

Figure 3-4 The Miro high-speed camera

And Figure 3-5 shows the whole course of the walking requirement. Figure 3-6 shows the walking procedure in real experiment.

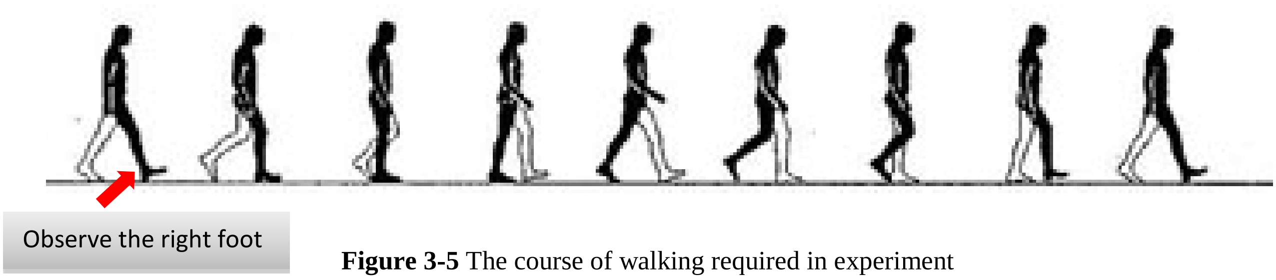

Figure 3-5 The course of walking required in experiment

On hearing the instruction to start walking, the participant would step out along the path platform. The recording starts from one foot of the subject stepping out and switching to the other foot and then stepping to the original foot again. The whole course records at least three steps, covering a complete gait cycle. The whole process repeated for 5 samples, so that the final mean result error could be decreased.

Figure 3-6 The walking period in real experiment

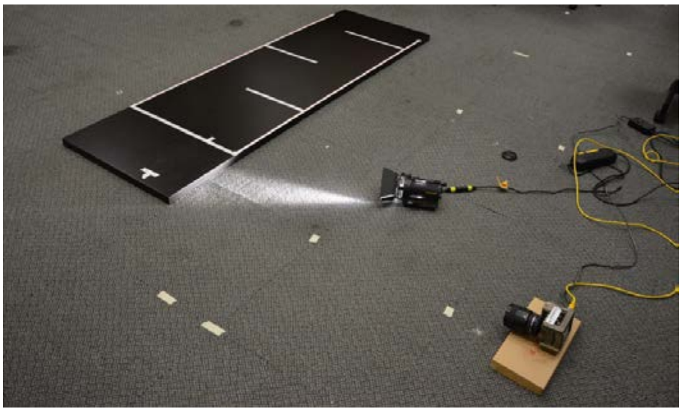

Figure 3-7 The platform design for experiment

To record the outline change of foot as clearly as possible, the time selection for high-speed camera shooting is decided at the starting point and the heel strike point. Camera position was set at the best lens distance. At these two time periods, foot bottom shapes change to the most extreme state and the outlines of these two positions are the most significant. For each motion there are five recordings, to collect a sufficient database for later analysis.

The recording of the movement started at the same time with the motion capture one, and a series of photos at the frequency of 20 slides per second are documented. The amount of photographs per second has currently surpassed the existing research method.

3.2.4 Data processing

The observation of the foot motion is based on the extraction of proper landmarks. When the foot moves, landmarks were recognized by the reflection of light. So it can be identified in the screen covering the whole period of a gait cycle. Before output the final result, processing of the selection of the landmarks was conducted for setting the clean data.

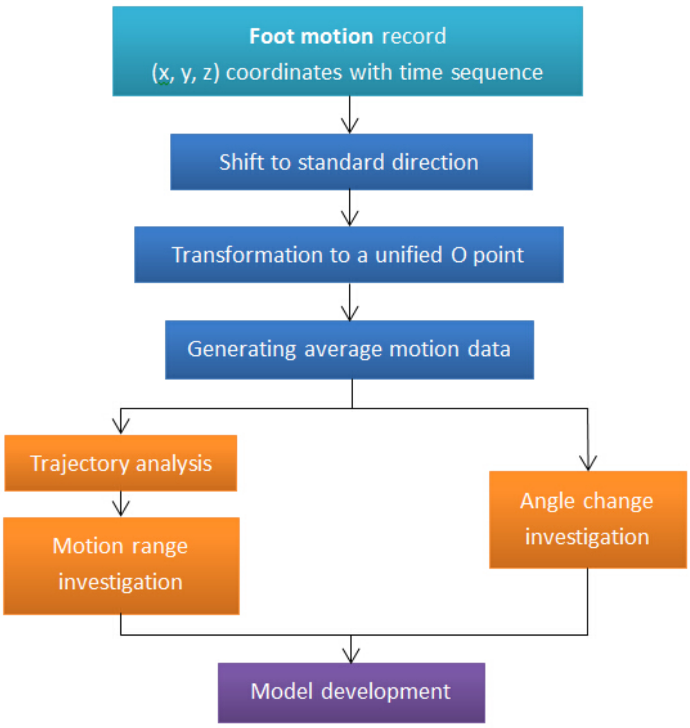

Figure 3-8 The flowchart of investigation of foot motion

The multiple trials of the recording were in different directions (Figure 3-8). To align all the trial data together, the first procedure is to shift all the points into the parallel direction. After the data was shifted, the translation was applied to the parallel trajectories so that all the trajectories at the same position corresponding to the foot landmarks could overlap with each other. Thus all the data are transformed into a unified coordinate system.

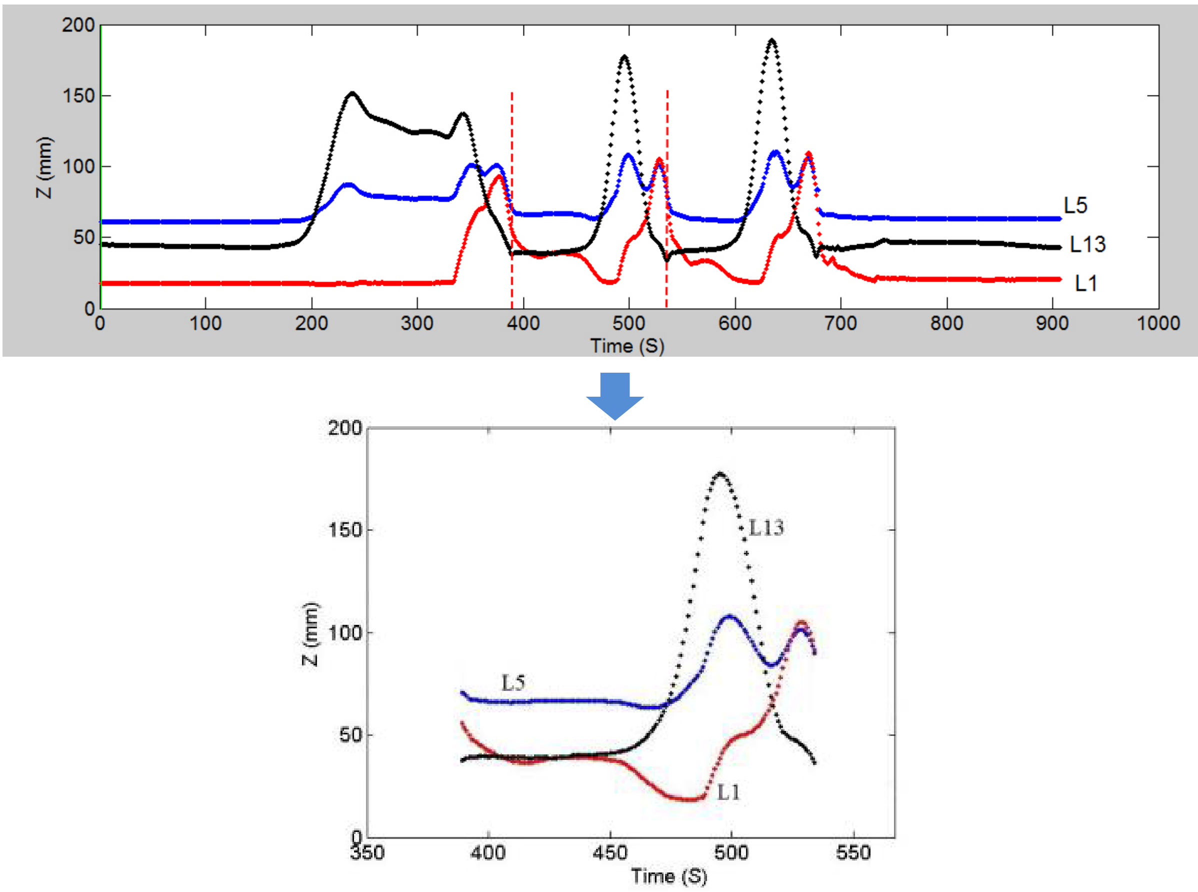

Figure 3-9 The selection of data presenting one gait cycle (starting from heel strike)

By displaying all the captured landmark positions, especially the height above the ground in time sequence, the rough trajectory (Figure 3-9) of the point shows the curve as the value of coordinate repeats with time. Take the landmark 13, which is at the back of the heel as example, of each repeated unit circle, the lowest point indicates the time of the heel goes down to the ground. Based on the definition of one gait cycle, the lowest moment is defined as the heel strike, the starting moment of one gait cycle. So the two points of two conjoint heel strikes were set as the start point and the end point of one gait cycle. Once the whole set of clean data covering one gait cycle was selected, further analysis could be achieved.

3.3 Experiment 2—3D foot scan for foot shape evaluation

3.3.1 Introduction and framework

The main aim for using the 3D scanner is to obtain the foot shape under different settings and compare the deformation of the surface points. For the complex structure of foot, the adjustment to adapt to different situations is accompanied with the deformation. The deformation would suggest the footwear design for improvement. Thus the 3D foot shapes could be recorded for further evaluation. The framework of the experiment and analysis is demonstrated below in Figure 3-10. From the raw data of foot shape, a series of data can be extracted and applied into investigations for different purposes. Then all the results would be combined together to form a thorough foot model for dynamic shape prediction.

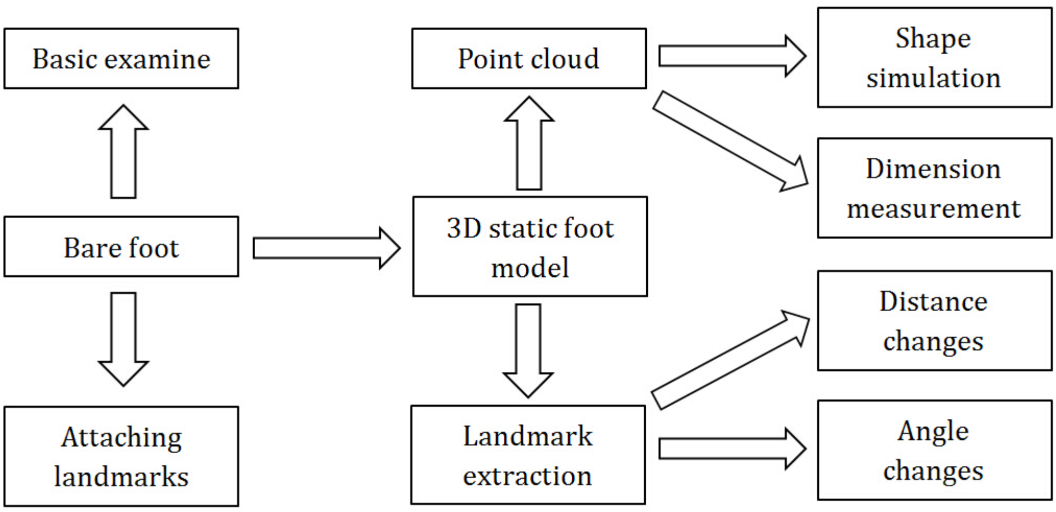

Figure 3-10 The framework of the 3D foot scanning experiment and analysis

3.3.2 Platform and equipment

The design of the supporting platform was based on the foot rotation directions and angles. Mainly the foot rotation is divided into plantar-flexion and dorsiflexion, supination and pronation, inversion and eversion. To observe the foot rotation only, the platforms toward four directions were designed and produced. The angles were described before as in the literature review. In this experiment, considering the standing situation with body load on the platform, the rotation angles were tested before settled. With six subjects standing with a foot rotated to their extremity to keep balance, the final result of angles was confirmed as in Table 3-2.

Table 3-2 The setting of the platform directions and angles

Setting 1	Setting 2	Setting 3	Setting 4
10° invertion	25° plantar-flexion	Foot flat standing	0% of gait cycle
5° invertion	12.5° plantar-flexion	Heel height at 10mm	25% of gait cycle
5° evertion	10° dorsiflexion	Heel height at 40mm	50% of gait cycle
2.5° evertion	20° dorsiflexion	Heel height at 70mm	62% of gait cycle

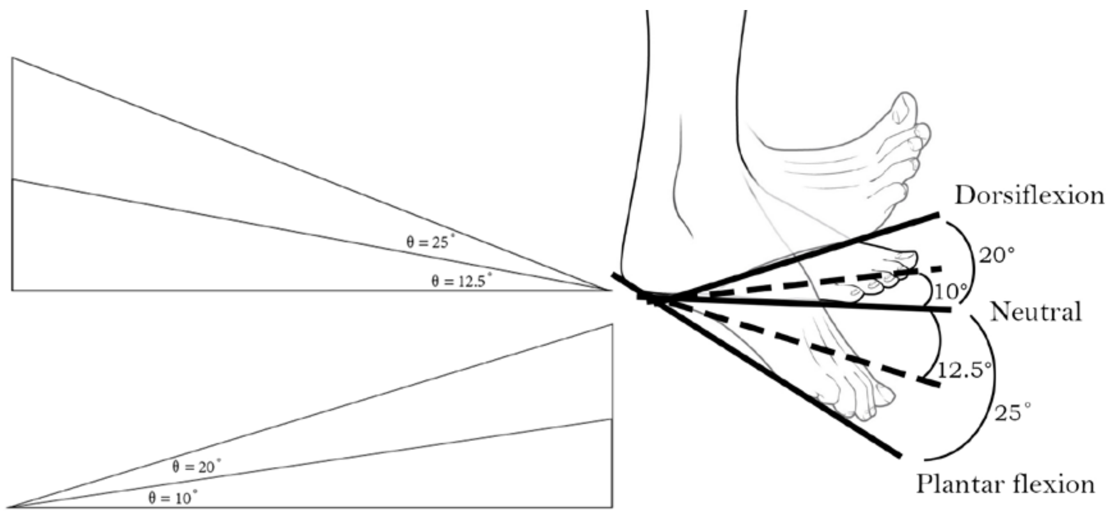

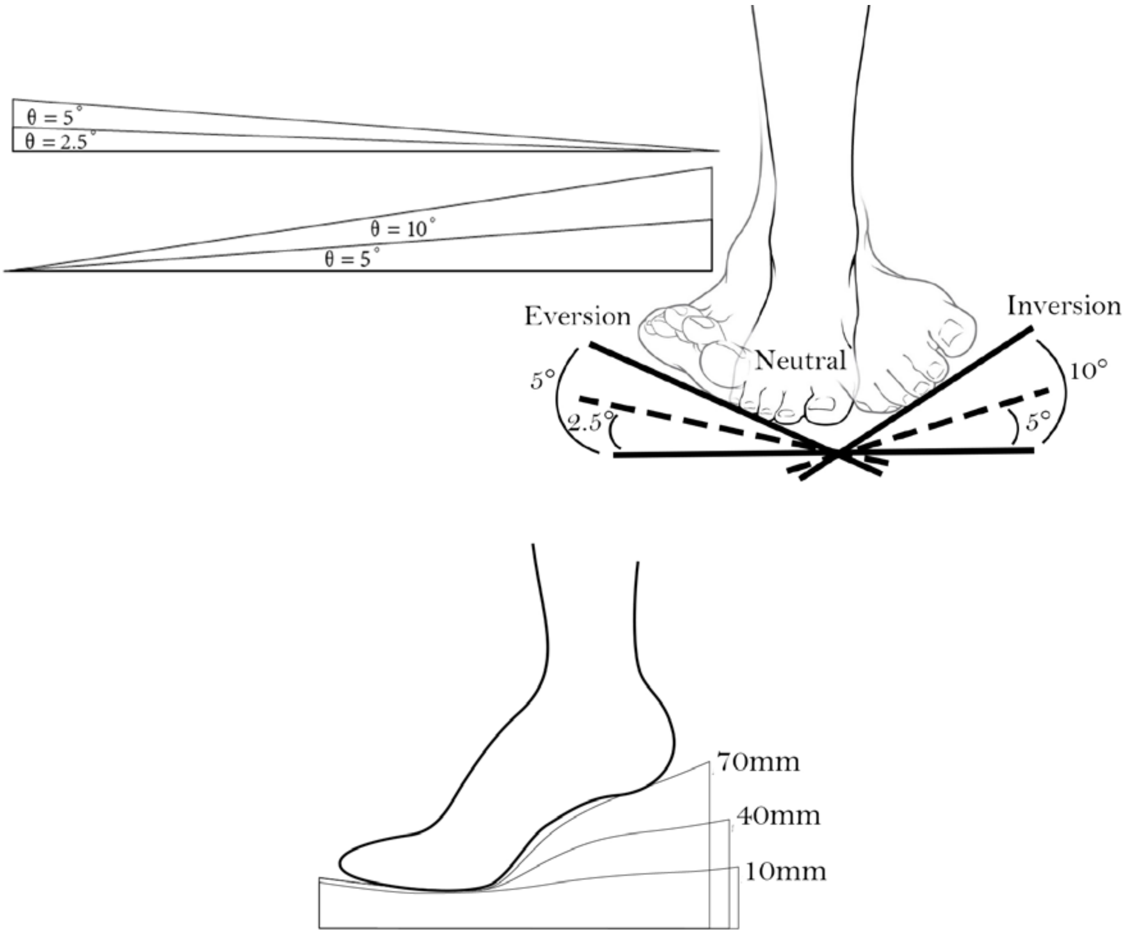

Figure 3-11 The platform settings in the experiment and the foot standing positions

The supports with angles were made of high-density compressed paper, which is as the same quality as wood board. For purposes of portability, the platforms were made into two identical pairs. This platform setting requires the subject to stand symmetrically on the platform so that it keeps the standing load divided average on both sides. Based on the angle settings, there are in total eight pairs of platforms with slopes plus a flat pair for comparison. Together with the slope platforms there are high-heel settings at three heel levels: 10mm, 40mm, and 70mm (Figure 3-11). The curved contacting plane provides same the situation as wearing high heel shoes. Finally a plane board is used in the walking record.

The Microsoft Kinect scanner for Windows was used as the main equipment for recording the foot shapes. Artec studio professional software was used for raw data processing. The further processing of the data adopted Rapidform to obtain the detailed foot shape and landmark.

3.3.3 Participants

A group of 50 participants was recruited in the experiment. All of the 50 participants were females ages 20 to 40. No foot problem was identified on the subjects, and their foot size was limited within 36 to 37 (5.5 to 6 in U.S standard). Before the experiment, individual basic information was recorded with their permission. The information included age, height, weight, foot length, width, and girth dimensions. During the experiment, nobody left, so all the data were taken at one time.

3.3.4 Procedure

Before the experiment was started, the participant was required to fill in a consent form for approval. Two parts were in the consent form. The first part is the introduction of experiment purposes and the detailed procedure. The second part is the content of approval from the subject and her basic information (Appendices A and B). The basic information page includes the height, weight, foot size and width, and foot ball-girth for both left and right sides. While measuring the basic foot dimensions, some significant landmark positions were marked with black marker pen on the surface of foot. While measuring the foot length, a set of points indicating the middle of foot was marked; while measuring the ball-girth, markers on the first and fifth metatarsal-phalangeal joints were marked.

Figure 3-12 The distribution of landmarks in the foot scanning experiment

Table 3-3 The landmark setting in the foot scanning experiment

No.	Abbreviation	Description
1-5	Toes 1-5	At the tip of toe nail 1-5
6-10	MPJ joints 1-5	The upper part of the MPJ joints
11-12	Side MPJ joint	The medial side and the lateral side of MPJ joints
13-15	Middle line	On the 50% vertical line of foot length across the foot dorsal
16	Cun-Met Joint	Joint between medial cuneiform and the first metatarsal
17	Cub-Met Joint	Joint between the cuboid and the fifth metatarsal
18	Nav-Tal Joint	Joint between the navicular and the talus
19-20	Ankle	Medial and lateral ankle
21-22	Heel	Medial and lateral calcaneus
23-25	Back heel	Along the vertical line of the back of heel
26-37	Shank	Along the vertical line of front, medial, back, lateral of the shank

After recording the basic information, landmarks were attached to the non-load bearing foot. In order to obtain the surface information of the foot, as many landmarks were set as needed to provide the shape. In this experiment 37 points with a diameter of 2.5mm were attached, covering the foot toes, MPJ, middle line and the heel. For obtaining the ankle information and ankle rotation, more landmarks were attached around the shank. Table 3-3 shows the detailed landmark setting and Figure 3-12 gives the distribution of points.

Microsoft Kinect was used for scanning the foot shapes. When the participant was standing steadily with feet shoulder width apart on the platform (Figure 3-13), the Kinect scanner was manually moved by the researcher around the participant for one circle while recording the time-sequenced frames. Artec Studio software was used to record the raw data and adjust the information into a whole shape. After each scanning were taken to record the temporal foot situation and landmark positions for later reference.

Figure 3-13 The standing postures of the subject in scanning procedure

The scan was repeated 12 times for various slope angles and heel heights. Then there were four scans for foot walking. The subject was asked to walk as usual and stop and fix at selected times. Four time points were: the moment when the heel made contact with the ground (0% of gait cycle), the moment when foot plantar was all laying on the ground (25% of gait cycle), the moment when the heel was raised while the MPJ were still touching the ground (50% of gait cycle), the moment the whole plantar was lifted and when the toe was about to lifted (62% of gait cycle). The motion trends were to be calculated for the gait cycle.

3.3.5 Data processing

The output data for the foot shape is in form of point cloud in XYZ coordinate system. Modification was conducted to delete the unused part of the shape for reducing the time in later processing. The exported data include information of the point cloud of foot shape in coordinate system, the landmark positions visually distinguished by color, and the reference platforms. The flowchart in Figure 3-14 shows the extraction of results from the raw data for different analysis purposes. The application of the results will be explained in the following chapters.

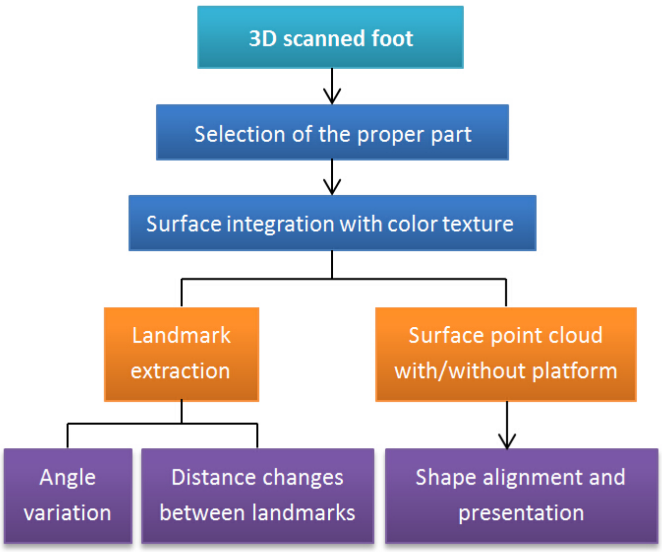

Figure 3-14 The data cleaning and extraction from the scanned foot

In the experiment all the right feet only were applied in later analysis, so only the right feet of subjects were selected. To obtain the position of landmarks, the surface texture was applied on the 3D scan model and exported altogether in the clean data.

3.4 Data analysis

3.4.1. Point extraction from the motion capture system

The XYZ value indicates the landmark position. After the data processing, a set of reference points can be used for calculation. In the processed data, landmarks on all the subjects are listed in the same sequence. For any point, the position is in the form of P_i (x_i, y_i, z_i), where i=1, 2, …, 9. In this way, the whole set of point information is grouped as P_1 to P_9. So the landmark could be calculated as function

$$f(Pi)=(x_i, y_i, z_i), \text{ where } i = 1, 2, 3, \ldots, 9$$

Besides the coordinate value showing the positions, in the data time was kept with the foot movement. Based on the time T, there are different sets of points at t_1, t_2, t_3, …, t_n. To present the dynamic foot within one gait cycle, the above equation is influenced by time factor. At time t_n (n = 5%, 10%, 15%, …, 100% of gait cycle), the foot shape can be expressed as equation:

$$F(Pi, ti) = f\,(x_i, y_i, z_i, t_n), where\ i = 1,2, \ldots ,9;\ t = 5\%, 10\%, \ldots ,100\%\ of\ gait\ cycle$$

In the experiment of motion capture and high-speed camera, the landmarks were output together with time reference.

3.4.2. Angle evaluation of foot walking in one gait cycle

For each three points (P_a, P_b, P_c), there would be an included angle between the two connection lines. The angle was set to obtain foot joint motion and the following figure gives an example of the analysis with the data.

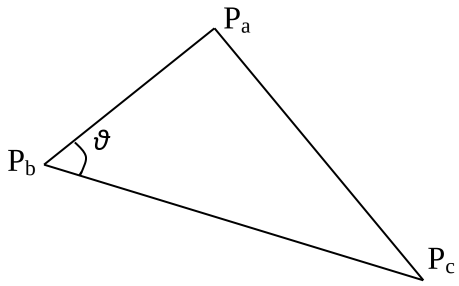

Based on Trigonometric functions, the original function is as follows:

$$P_aP_b{}^2 + P_bP_c{}^2 + 2P_aP_b \cdot P_bP_c \cos\theta = P_aP_c{}^2$$

So that the target angle of joint could be calculated with the transformed function

$$\cos\theta = \frac{P_aP_c{}^2 - (P_aP_b{}^2 + P_bP_c{}^2)}{2P_aP_b \cdot P_bP_c}$$

Meanwhile, the distance between two points can be obtained with the formula of distance

$$D_{P_aP_b} = \sqrt{(x_a - x_b)^2 + (y_a - y_b)^2 + (z_a - z_b)^2}$$

Then the function of the angle can be obtained with each group of points

$$\theta_i = f(P_i, P_j, P_k),\ \textit{where } i = 1, 2, 3, \ldots, 9;\ j = 1, 2, 3, \ldots, 9;\ \textit{and } k = 1, 2, 3, \ldots, 9$$

With the above angle calculation, the angle change during walking could be counted and figured out. The angle of two landmarks connected line could be

$$\alpha_i = f(M_i, M_j),\quad \textit{where i =1, 2, 3,...,9; j = 1, 2, 3,...,9;}$$

And the change of this angle relative to the vertical plated could be presented as

$$\Delta\alpha_i = f(M_i, M_j, \mathrm{t}),\quad \textit{where i =1, 2, 3,...,9; j = 1, 2, 3,...,9;}$$

3.4.3. Distances between surface landmarks

The length between two points provides the general distances on the foot surface, and the changes would describe the deformation. For the significantly changed points, results show that the foot would need a flexible space during its dynamic state. On the contrary, the less significantly deformed parts suggest stable posture. In experiment 2 the distances between surface landmarks will be calculated in detail.

As mentioned above, for each foot landmark, there is a point at position (x, y, z). As in Figure 3-15, on the whole foot there are 37 points listed in sequence. Assuming on the foot surface there are points $P_i= (x_i, y_i, z_i)$, $P_j=(x_j, y_j, z_j)$, $P_k=(x_k, y_k, z_k)$, where i, j, k=1, 2, …, 37, then the triangle area can be in the form of an equation:

$$F(\triangle P_{\mathrm{ijk}}) = f(P_i, P_j, P_k)\ (\textit{i=1,2,...,37; j=1,2,...,37; k=1,2,...,37})$$

Point Pi, Pj, Pk is in form of X-Y-Z value, so there is the equation:

$$F(\triangle P_{\mathrm{ijk}}) = f(x, y, z)$$

The distance between P_i and P_j (Figure xxx), it can be calculated with the distance equation

$$\mathrm{D_{ij}}=\sqrt{(\mathrm{x_i}-\mathrm{x_j})^2+(\mathrm{y_i}-\mathrm{y_j})^2+(\mathrm{z_i}-\mathrm{z_j})^2},\ \textit{where i=1,2,...,37 and j=1,2,...,37.}$$

For the selected n landmarks, only the distances of two neighboring points are for calculation. In total there are 93 edges composed with all the 37 landmarks. Figure 3-16 illustrates the triangular structure for further calculation. For all the 50 participants, there is an average distance of selected landmarks:

$$\text{Mean } \mathrm{D_{ij}} = \frac{\sum_{\mathrm{n}=1}^{50} \mathrm{D_{ijn}}}{50}$$

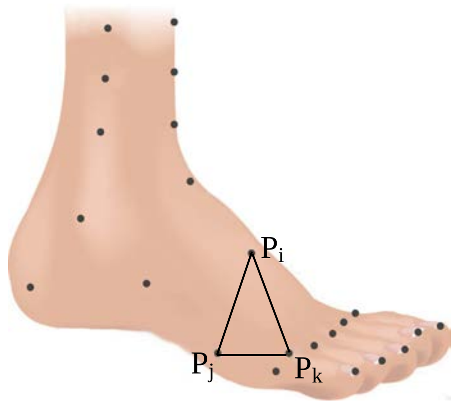

Figure 3-15 The connection of landmarks to form a triangle

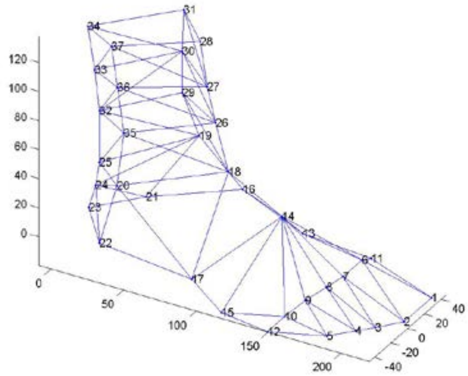

Figure 3-16 The Triangular structure for simulation

3.4.4. Angle variation of the foot rotation

To obtain the angle with landmarks is based on the formula of the angle between lines in three-dimensional space. For each two points P_i (xi, yi, zi) and P_j (xj, yj, zj), there is a vector representing the line P_iP_j=(xi-xj, yi-yj, zi-zj). With another two points P_m and P_n, there is another vector P_mP_n. Then the angle A between the two lines can be calculated with formula

$$\cos A = \frac{P_iP_j{*}P_mP_n}{/P_iP_j/{*}/P_mP_n/}, \; where\ i, j, m, n \; = 1,2, \ldots, 37; \; and \ \mathrm{i} \neq j \neq m \neq n$$

Then the angle A can be obtained with the landmarks.

CHAPTER 4 MOTION CAPTURE AND SPEED CAMERA FOR FOOT WALKING INVESTIGATION

4.1 Foot profile observation with high-speed camera

In the trial observation experiment, a high-speed camera was adopted to restore the foot motion during heel strike. Pictures of the outline showed the foot shape changes. It was captured at the frequency of 50HZ, storing 20 slides per second. And the significant shapes variations are for evaluation.

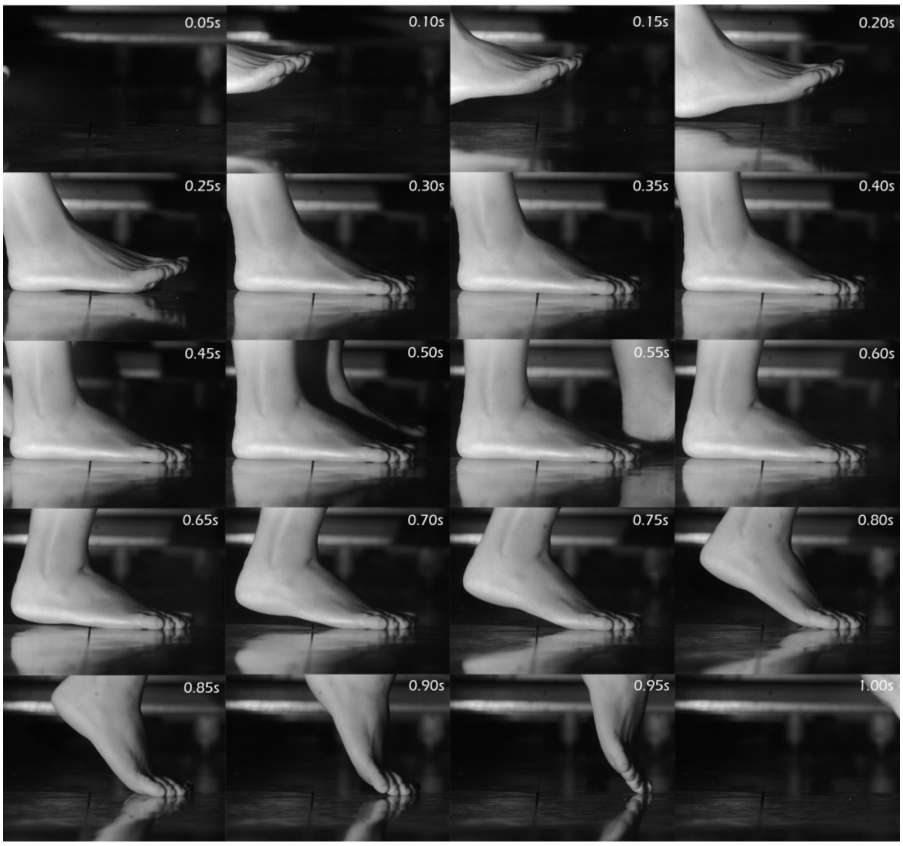

Figure 4-1 The course presenting the start of foot walk from high-speed camera

Figure 4-1 shows the obtained photo of the starting point of foot walk. The frequency of taking the photos is 0.05 sec per frame, with 20 frames in total. The outline can be distinguished clearly by the highly contract image color. The focus of the observed period of time is from the heel strike to the toe off, when most of the foot bottom makes contact with the ground and thus causing the main deformation.

Foot profile was extracted from the picture for further comparison and alignment. From the picture with light and shade contract, the outline of the foot shape can be extracted as in Figure 4-2. Adobe Photoshop CS6 was applied in obtaining the profile.

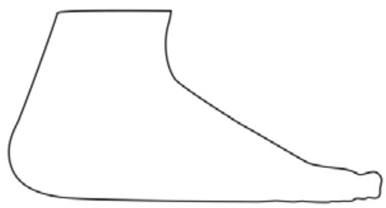

Figure 4-2 The extracted profile from the high-speed camera image

Each single profile represents the separate moment when foot walks through the heel strike to toe off. And for the reason that pictures were taken at a stable speed, the observed information provides a relatively actual time distribution.

By attaching the profiles of the images in time sequence, the movement change can be calculated. The shape change with its displacement can help the refinement of the foot model. The first step of observation was to combine all the profiles as the real positions. The integrated picture contains all the outlines of foot when any part of the foot bottom contacting the ground.

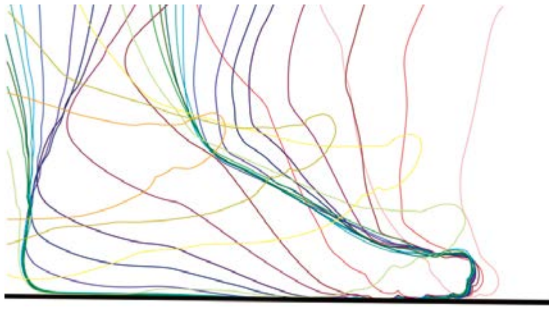

Figure 4-3 The integrated picture of all profiles during walking

By distinguished colors a series of foot profile deformation was shown that not only the angle between foot bottom and the ground increased, but the shape of foot dorsal and bottom itself presents significant variations.

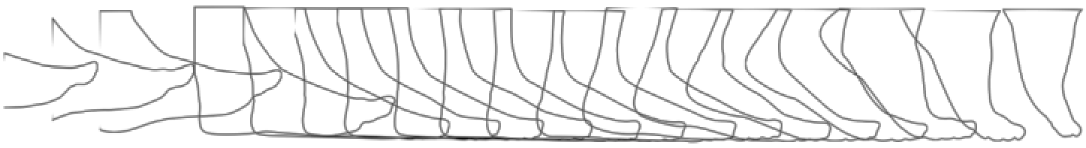

Figure 4-4 The integrated picture of all profiles based on time intervals

The second step of profile alignment was to display the outlines based on time intervals (Figure 4-4). The extended overlapping profiles explain the angle variation relative to the time of the walking. Most significantly at the nearly end of the stance phase, when the foot heel lifted and foot dorsal was elevated to the moment of toe off, the angle increased at a high speed from 0 to over 45° . The displaying profile stated the essential part of the walking period and gave a reference for the following further experiment and investigation.

4.2 Trajectory analysis

4.2.1 First calculation: individual gait data analysis

After the extraction of one gait data from a general recorded landmark path, the individual gait trajectory can be tracked down for further observation. The trajectories of each landmark could be presented in XYZ axis coordinates. An average of the gait trajectory was presented for normalization, at the same time standard deviation result was also calculated for evaluating the range variation. Figure 4-5 provides the average trajectories of landmark 1, landmark 5, and landmark 13 as examples. The trajectories were presented in X, Y, and Z axis directions separately.

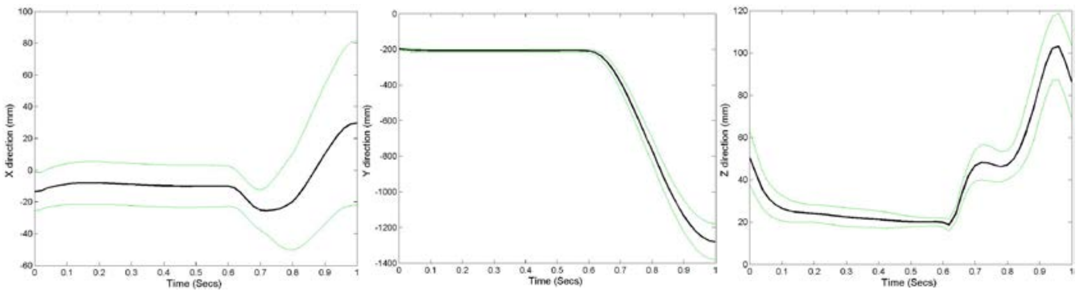

(Trajectory of landmark 1 in X, Y, Z axis)

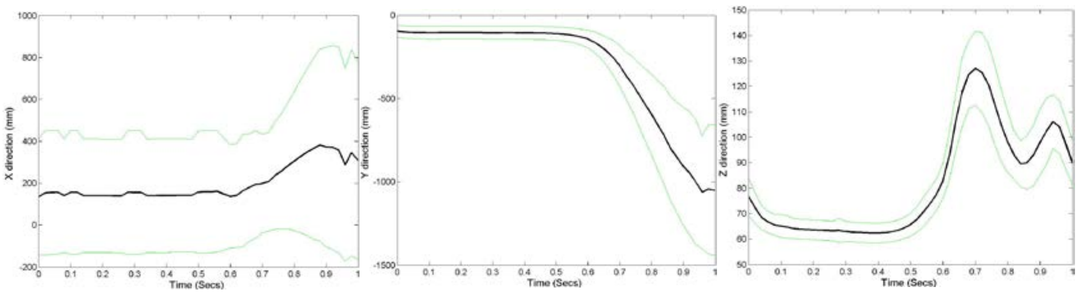

(Trajectory of landmark 5 in X, Y, Z axis)

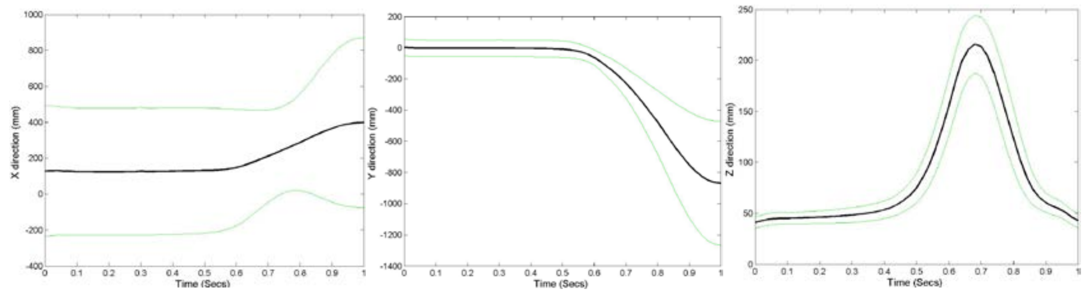

(Trajectory of landmark 13 in X, Y, Z axis)

Figure 4-5 The individual trajectories of the retro-reflective landmarks

In observation of the obtained graphs and compared with former researches, the foot motion trajectories are in good correlation with other researches with tracking methods and X-ray graph techniques. Though the landmarks were located differently all over the foot and lower calf, the motion trajectories were in the similar direction, and in a stable curve. The result reflects the general area of the foot movement within one gait cycle. Along X axis is the area of foot swing between the left and the right direction; along the Y axis is the increase of the walking direction; and the Z axis represents the height of the landmark above the ground. The variation of the motion range was not significant.

From the curve it is obvious that the foot started swing phase at the approximately 60% of the whole gait cycle. Compare to the toe and the heel part, the middle of the foot (landmark 5) will rotate between the left and the right more. The left and right swing movement among the three landmarks described the variation of the forefoot, midfoot, and the hindfoot part. Landmark 1 would go through a fluctuation, which means that the forefoot tend to adjust across a larger area, on the other hand, landmark 13 kept in a relatively static movement without much fluctuation. The Z values differed among three landmarks. The distinct peak and lowest points shows the moment when the landmarks conducted relative movement. Among the trajectories of all the landmarks, those of the heel showed a longer and more noticeable curve at the first half of swing phase; those for the toes went through a mild and lower curve at first, and slightly rose at the very end of the swing phase. Relatively, the hind foot moves to a higher position and then swings back first to the ground. The forefoot showed stable movement over a gait cycle.

4.2.2 Second calculation: multiple gait data integration

The rough observation of the gait data was integrated in one coordinate system for correction. As Figure 4-6 shows, all the landmarks on one foot are displayed together. The paths of different landmarks show the foot movement and also provide the motion range throughout the walking period. The hind foot raised rapidly at first, while keeping steadily downward till the end of one gait cycle. When at the very last of the gait cycle, the forefoot raises when the foot is ready for another heel strike.

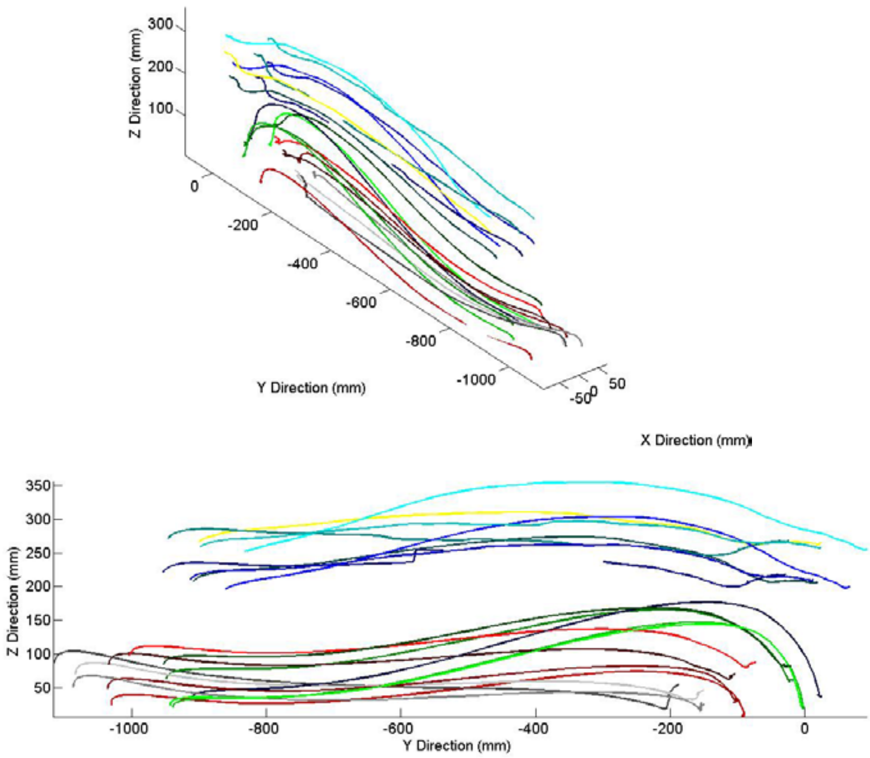

Figure 4-6 All the landmark trajectories are in one coordinate system

The trajectories indicated that foot movement was in one general direction except for the point on the lower calf. With the data showing foot motion of one gait cycle, an overlapped graph combining all different trials together illustrates the general direction of the average path.

As in Figure 4-7, the path of all landmarks was displayed in the 2D coordinate system for evaluation. The value was separated in X-time, Y-time, and Z-time, respectively. The graph suggests a foot motion observed in the angle of view at the side. As the similar curve with the average individual trajectories, the overall integrated landmarks paths reflect the fluctuation and the swing movement during one gait cycle. Most significantly is that at the swing phase when the foot prepares for another heel strike, the hind foot raised higher to a more fluctuated curve than the lower calf.

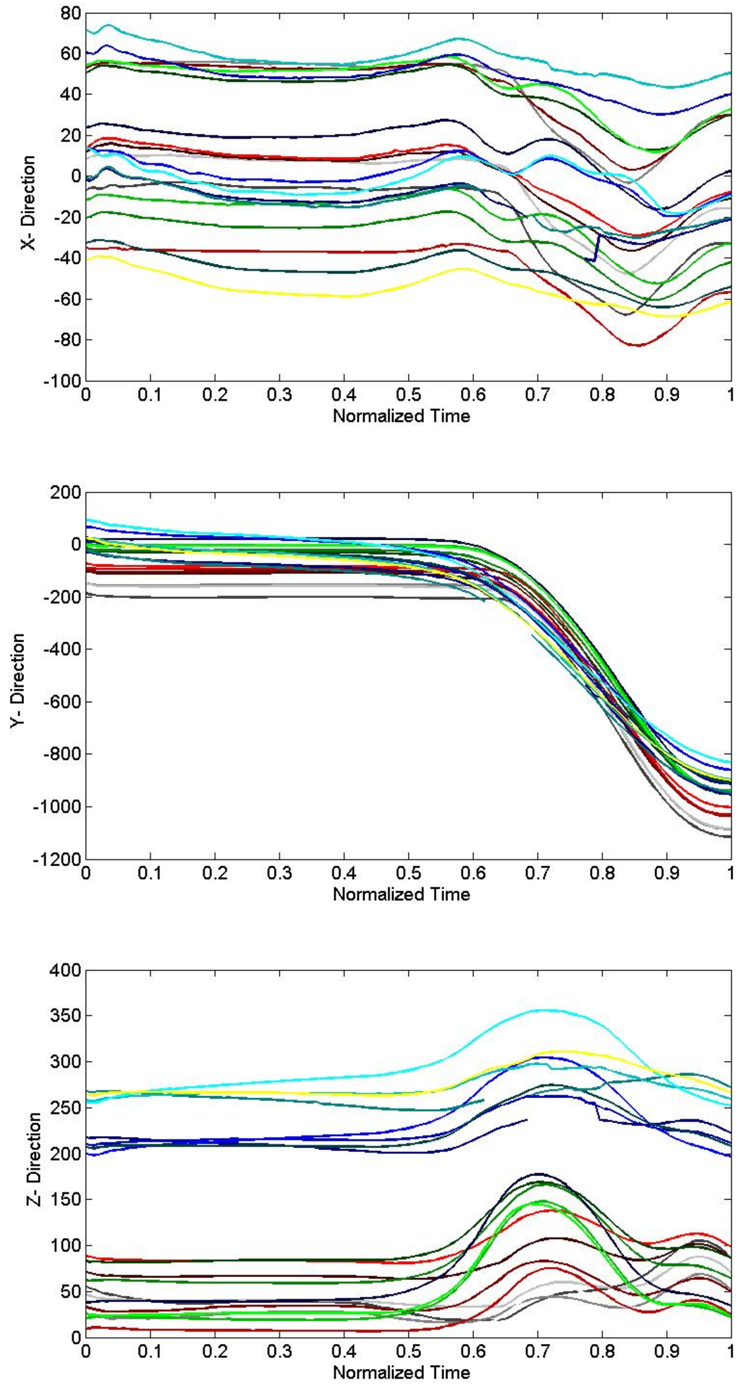

Figure 4-7 Paths of multiple trials are in the 2D coordinate system

To observe the motion range over time, the 2D display of trajectories provides the ranges more clearly. During the swing phase, foot movement, not only the height and the width of the gait, but the path also differed. Some may fluctuate a little before the foot is going down for heel strike (as the Y value shows). And the moment between stance phase and swing phase still differed between individuals.

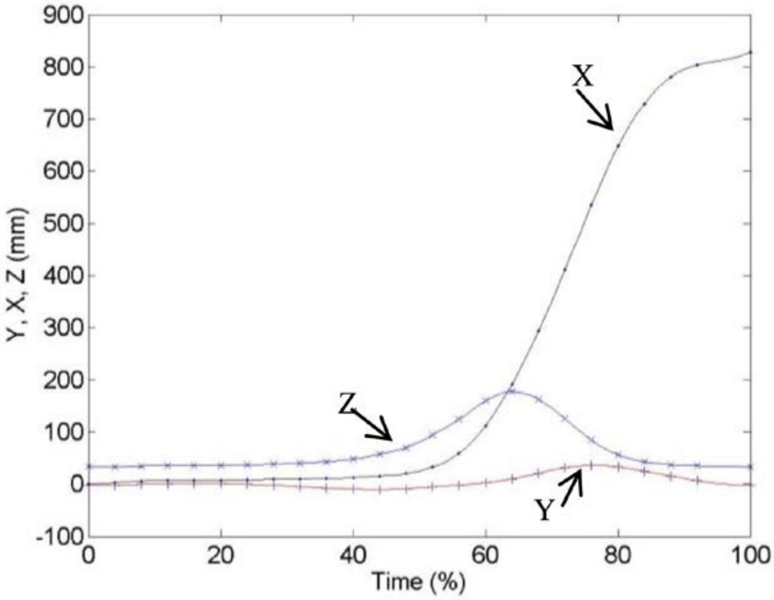

Figure 4-8 The average values in X-Y-Z axis are in one coordinate system

In the average motion changes with time, the 2D graph provides the average foot motion in all three plates in the 3D space (Figure 4-8). From 0% to 100% of a gait cycle, the X value keeps increasing, which means the foot moves forward and in the second half moves faster. The Y value is relatively steady and gentle. The line shows the foot motion between the lateral side and the medial side. At around 75% of the gait cycle, the foot goes inward slightly, indicating that the foot would rotate rather than stepping out straight. Furthermore, the Z value suggests the foot rising up after around 50% of the gait cycle. In walking, the human foot would move forward, inward, and upward at the same time.

4.3 Changes in angle during walking

Surface landmarks on the foot are connected to form representative angles for further calculation about the angle of joints. The relative landmark position given by the output could show the angle of segments. In further analysis landmarks were linked up and referencing plates were used for angle extraction. With the total 21 landmarks, a series of angles were set in category of dorsiflexion-plantar flexion angles, inversion-eversion angles, and pronation-supination angles. At the same time, a series of foot rotation relative to the ground was also plotted to present the regulation. For convenience in the following part angles were grouped as within foot angles an foot rotation angles to the ground.

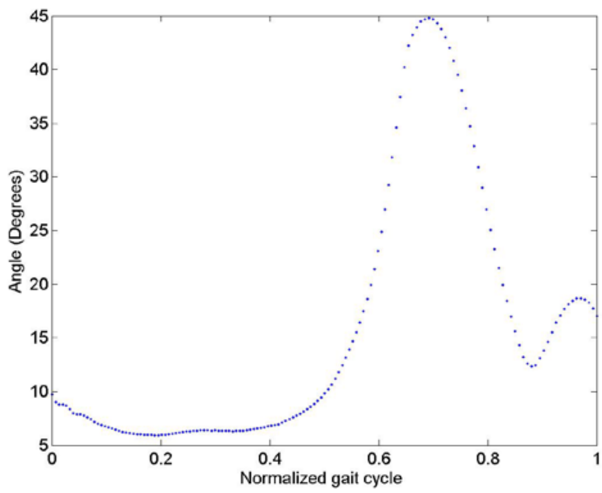

Figure 4-9 The rotation angle showing connection of landmark 1 and 13 relative to the ground

To observe the foot rotation angles to the ground, landmark 1 and 13 are connected to represent the foot front and back rotation. This angle is similar to the foot dorsiflexion and plantar flexion. By plotting the angle degree versus time, the graph provides the rotation of foot during walking. Figure 4-9 shows the plot of the degree variation. It shows that at the swing phase the foot would rotation significantly and then the angle reversed. This part is in correspondence with the moment when the forefoot lifted and adjusted itself to move forward.

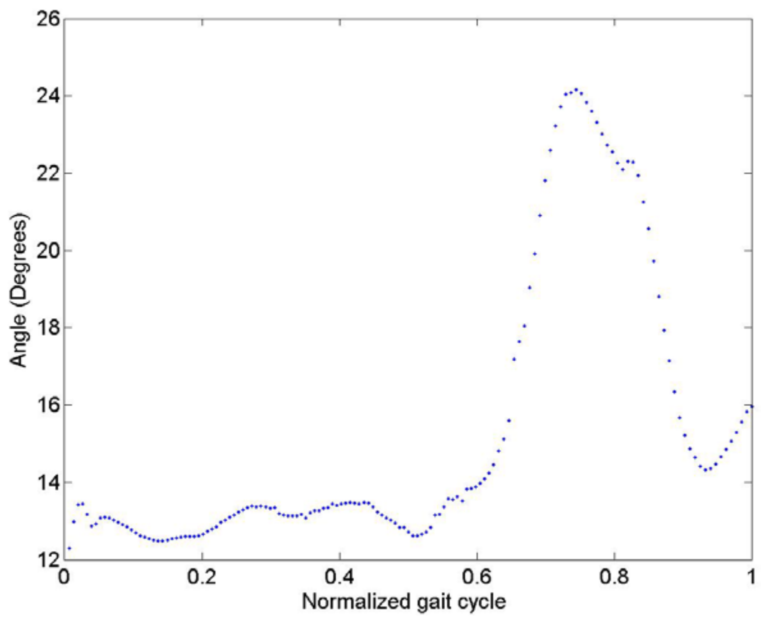

Figure 4-10 The rotation angle showing connection of landmark 2 and 4 relative to the ground

In the same way more connections of landmarks were observed. Landmark 2 and 4 were connected to observe the foot inversion and eversion (Figure 4-10). Similarly, landmark 9 and 10 (Figure 4-11), landmark 11 and 12 (Figure 4-12) were also connected to plot the joint rotation degree to the left and right side. The angles showed slightly difference, but generally in the similar direction. The difference of degree between the angles reflects the foot inner joint rotations.

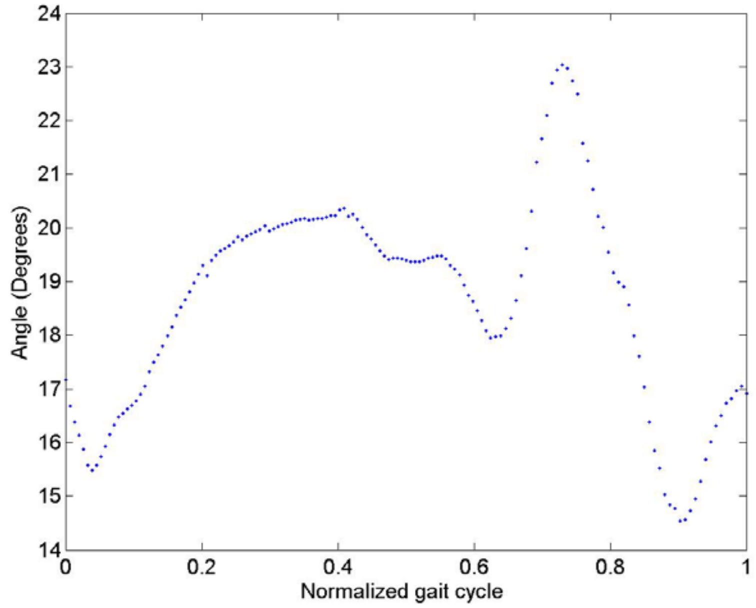

Figure 4-11 The rotation angle showing connection of landmark 9 and 10 relative to the ground

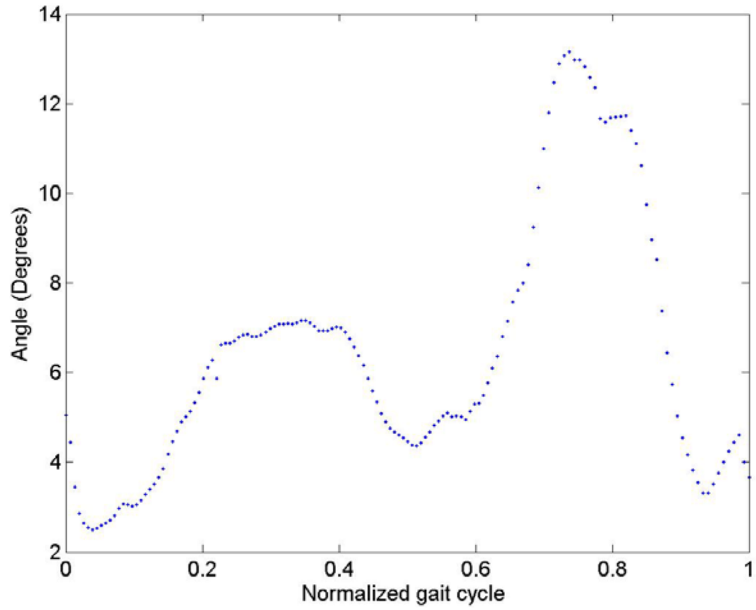

Figure 4-12 The rotation angle showing connection of landmark 11 and 12 relative to the ground

The angle variation was plotted for displaying the changes. With the angle rotation during walking, a picture of how the foot rotates and works in dynamic state is more consistent. A series of inner foot rotation angle exploration was tested, to observer the relative rotation between landmarks. Landmark 1, 3, and 5 were connected to simulate the forefoot movement (Figure 4-13). In the same way, landmark 5, 8, and 14 were linked to calculate the dorsiflexion influence on the front surface (Figure 4-14).

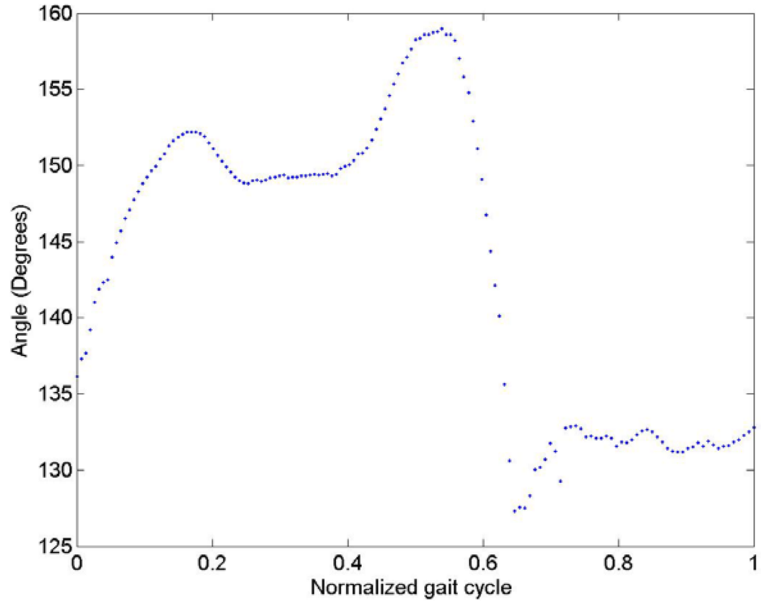

Figure 4-13 The rotation angle showing connection of landmark 1, 3, and 5

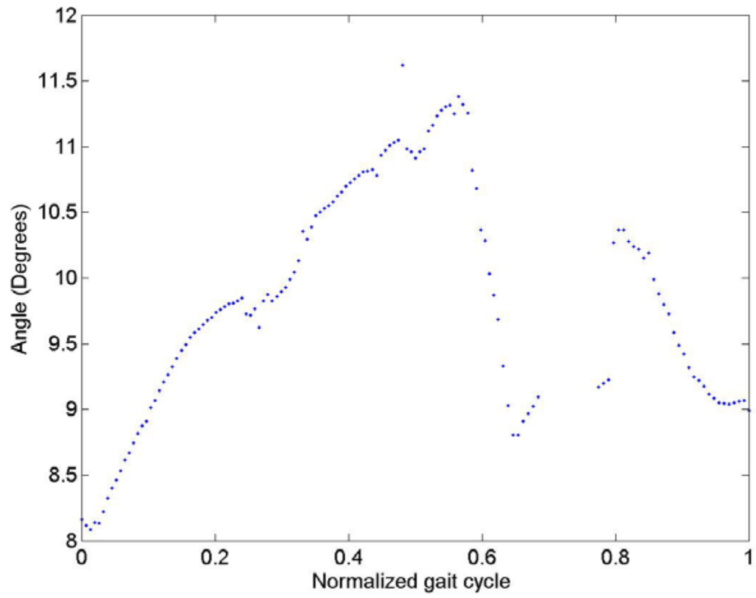

Figure 4-14 The rotation angle showing connection of landmark 5, 8, and 14

As in Figure 4-13, the graph shows the angle formed by the forefoot in one gait cycle. At the first 60% of the gait cycle the angle stays at a relatively stable range of degree, until nearly 60% of the gait cycle the value dropped significantly to the lowest point.

The value is in correspondence with when the heel lifted and the foot started the swing phase. This is the moment when the forefoot leave the ground and step forward for another heel strike. When at the near end of the gait cycle the forefoot angle recovered and kept stable again.

For the influence of the swing phase the dorsiflexion on the front side showed similar drop at the 58% of the gait cycle. Following was a rapid increase of the angle and the value recovered almost the same as the original state. The front part rotates significantly due to the foot movement adjustment. After the recovery of the degree the foot prepared to another heel strike.

The connection of all the landmarks could provide a triangulation model movement with time to simulate the foot shape deformation during one gait cycle. Based on the three dimensional coordinate values of the landmarks, the movement speed and distance are tracked down to provide information of the normal walking regulations. Figure 4-15 gives the sequenced change of the foot during one gait cycle. The linking lines between points can display the angles.

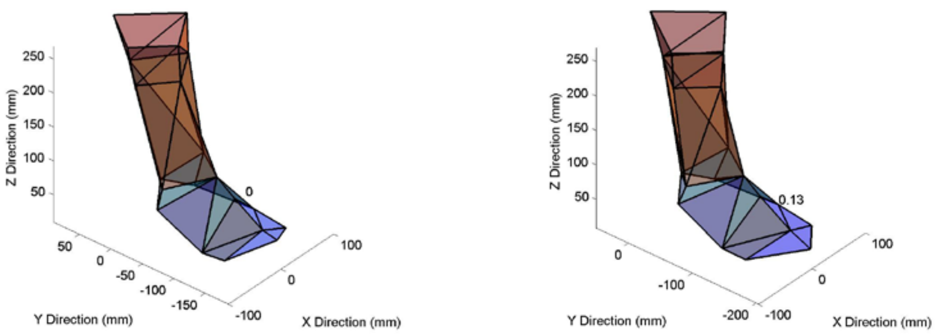

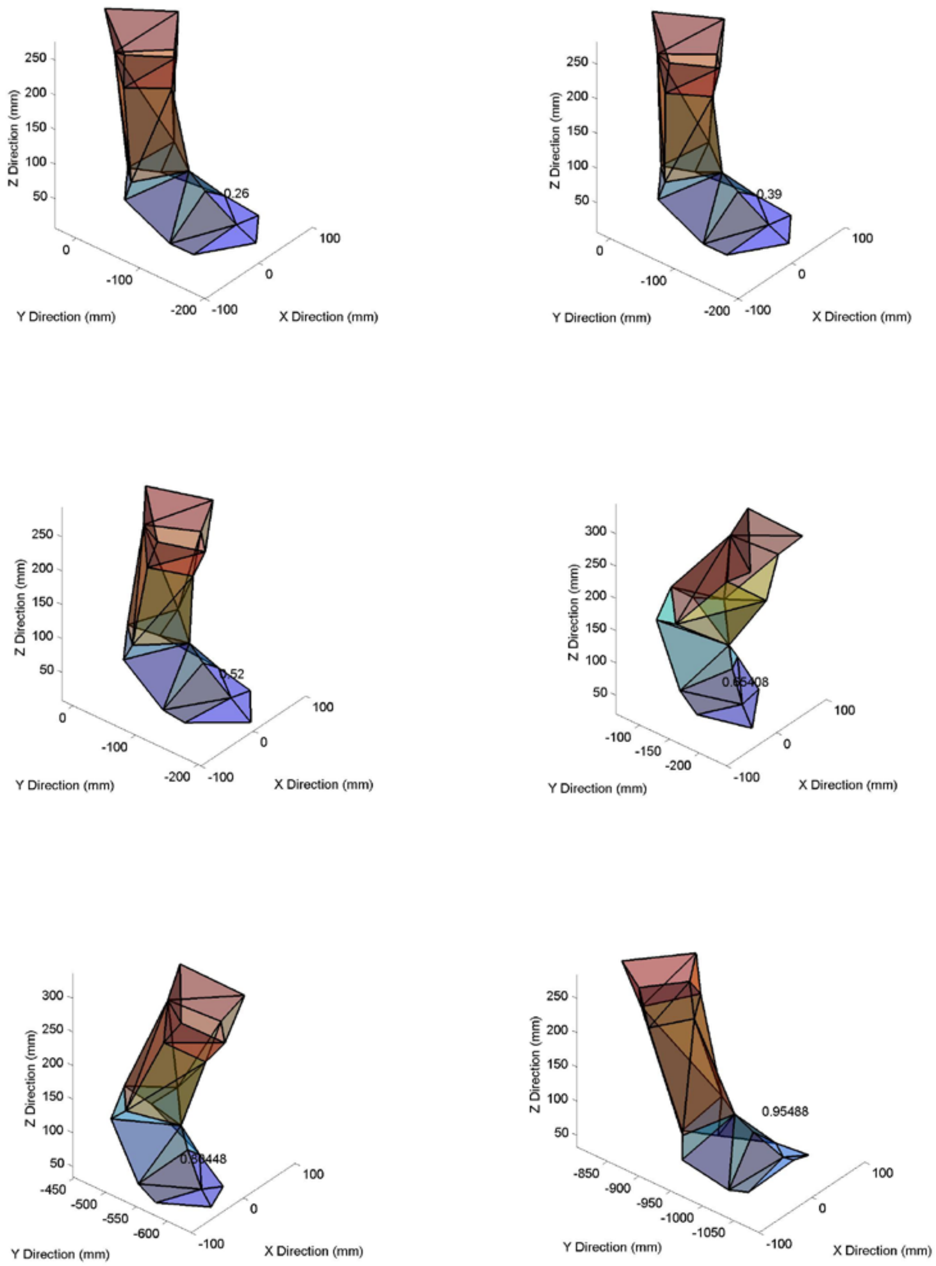

Figure 4-15 The foot triangulation model in time sequence during walking

4.4 Summary

In this part of the experiment, motion capture system was applied to obtain the foot motion path and rotation during normal walking. The main observation was set within one gait cycle, focusing on the walking trajectories and rotation angle changes. Results showed that the foot motion tends to be a curve rather than a straight line in the oriental plane. The curve suggested that foot motion is in a multiple range in a complex three-dimensional direction, rather than a simple straight line from the first heel strike to the next one. In the angle investigation, the rotation and fluctuation of the forefoot was significant. The rolled-over motion and the waving period indicated the rapid but dramatic shaking motion in the swing phase. The profile obtained from the high-speed camera photos supplement the deformation of the foot shape.

CHAPTER 5 3D SCANNED FOOT ANALYSIS

5.1 Subject information

In this part of the experiment, 50 subjects were recruited to step on the platform when the 3D scanner recorded the standing foot postures. Before the experiment started all the subjects were examined to ensure no foot problem situations, and all signed the consent form. In the recording of the foot information, content includes the age, the height, the weight, the foot lengths of both right and left foot, the foot width of both feet, and the ball girths of both feet. At the time of measuring, the position at 50% of foot length was marked on the surface of the right foot, for the use of the landmarks. The description is in Table 5-1 below:

Table 5-1 The information of subjects recruited in the experiment

Items	Minimum	Maximum	Mean	Std. Deviation
Age	23	33	26.34	2.327
Height (mm)	156.0	170.0	161.510	3.2047
Weight (kg)	45.0	73.0	52.668	5.5598
Right foot length (mm)	22.5	23.6	23.114	.3511
Left foot length (mm)	22.5	24.2	23.232	.3760
Right ball girth (mm)	19.9	23.0	21.233	.8295
Left ball girth (mm)	19.8	22.8	21.259	.7311

5.2 Landmark extraction

The output data of the scanned foot is in the form of a point cloud. In this file the points provide the exact positions in XYZ coordinates. With the XYZ coordinate points covering the whole surface of foot, the dimensions in relative distance between landmarks can be calculated and compared.

The scanned result was output in the form of a ply document and prepared for landmark selection. The selection of the landmarks is shown in Figure 5-1. The color difference between the surface and the landmarks indicated the landmark positions.

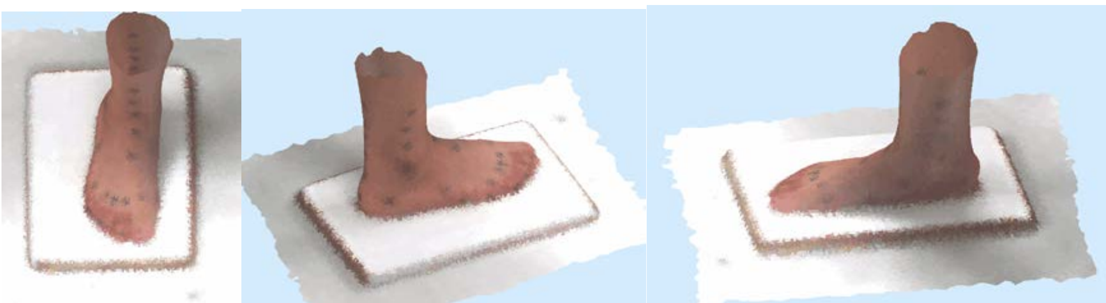

Figure 5-1 The landmarks selection on the surface of foot

5.3 Triangular face presentation

As mentioned in the methodology chapter, by grouping each three points together and connecting them, there will be a triangle representing the area. For the combination of three-point groups for the triangles, only the neighboring points are selected.

Table 5-2 The defined triangles to simulate the foot movement

Notation	P1	P2	P3	Notation	P1	P2	P3	Notation	P1	P2	P3
T1	11	1	6	T20	18	16	14	T39	18	19	29
T2	1	2	6	T21	17	14	15	T40	29	18	26
T3	2	7	6	T22	18	14	17	T41	26	29	30
T4	2	3	7	T23	18	20	17	T42	26	30	27
T5	3	8	7	T24	17	22	20	T43	27	30	31
T6	3	4	8	T25	18	19	16	T44	27	31	28
T7	4	9	8	T26	16	19	21	T45	20	25	35
T8	4	5	9	T27	21	23	24	T46	25	35	32
T9	5	10	9	T28	22	23	24	T47	32	35	36
T10	5	12	10	T29	20	22	24	T48	32	36	33
T11	13	11	6	T30	19	21	24	T49	33	36	37
T12	6	14	13	T31	20	24	25	T50	33	37	34
T13	14	6	7	T32	19	24	25	T51	19	25	32
T14	7	8	14	T33	18	20	35	T52	19	32	29
T15	14	8	9	T34	18	35	26	T53	32	29	30
T16	9	10	14	T35	26	35	36	T54	32	30	33
T17	14	10	15	T36	36	26	27	T55	30	33	34
T18	15	10	12	T37	27	36	37	T56	30	34	31
T19	16	13	14	T38	37	27	28				

On the surface of the scanned foot, in total 56 triangles simulate the foot movement and deformation in general. Table 5-2 provides the combination of points for the triangle structure. In the later result, triangles are named Ti (i=1,2,...,56) for substitution. In Figure 5-2 the triangle distribution on the foot is displayed, and the connecting lines show the combination of landmarks.

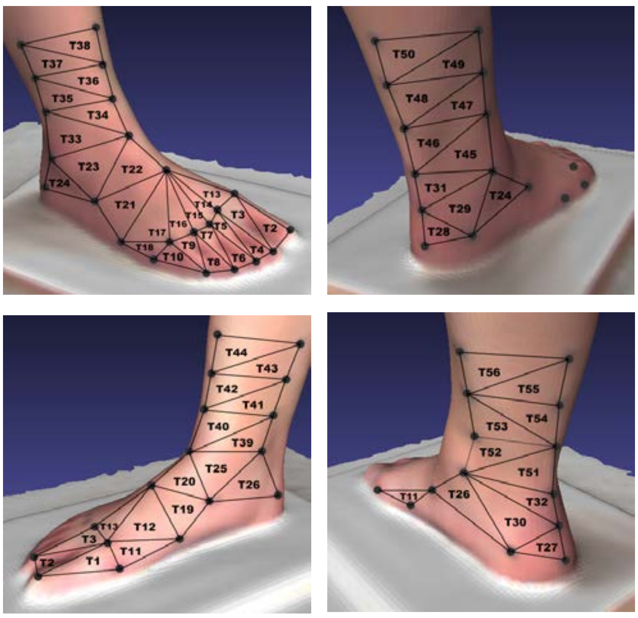

Figure 5-2 The distribution of triangles (T1-T56) based on the surface landmarks

The development of triangles covering the foot provides a method to obtain foot shape simulation. First a rough structure could suggest the relative movement of each landmark, which stands for the significant joints on foot.

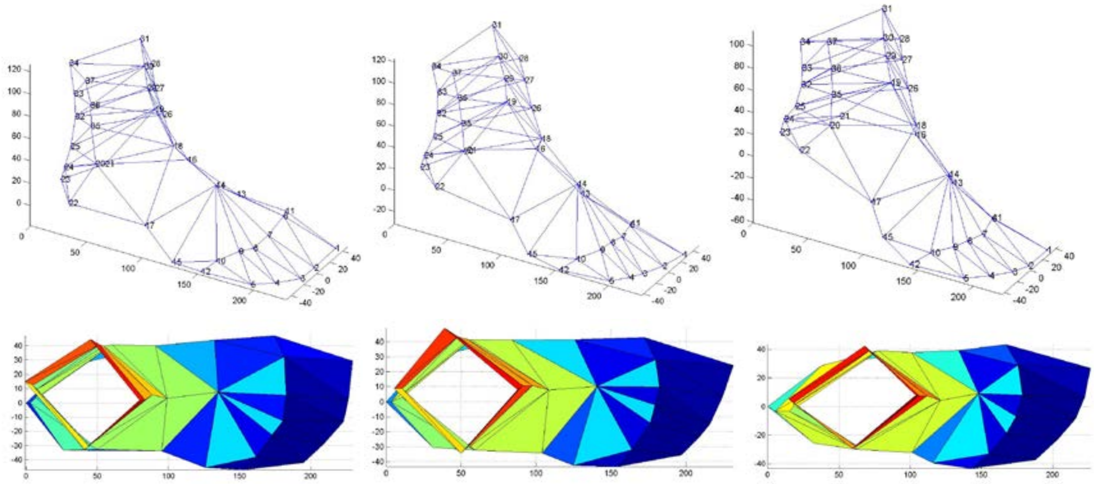

Figure 5-3 The triangle structure developed with landmarks

The triangle structure will be applied into the foot measurement and angle evaluation for further research. Figure 5-3 shows the result of developing the triangle structure with landmarks. By adding up the referencing points in the middle of each triangle and connecting the center point with other three corner points, the smaller but thicker triangle groups will form the overall foot shape. The refinement can be obtained multiple times, so the more modification, the more accurate the shape will be. It will be described in later chapters.

5.4 Distances between landmarks

In this research only the neighboring two landmarks are linked up; in other words, the edges of the triangles are adopted in the evaluation. The distance between landmarks could indicate the surface extension during movement. By connecting 37 landmarks, there are 93 edges in the list for analysis. Table 5-3 shows the edges extracted from the triangles, and the related landmarks.

Table 5-3 The list of edges extracted from triangle structure

Notation	P1	P2	Notation	P1	P2	Notation	P1	P2	Notation	P1	P2
E1	11	1	E25	14	13	E49	23	24	E73	29	30
E2	1	6	E26	7	14	E50	24	21	E74	30	26
E3	6	11	E27	8	14	E51	22	23	E75	30	27
E4	1	2	E28	9	14	E52	24	22	E76	30	31
E5	2	6	E29	10	14	E53	24	20	E77	31	27
E6	2	7	E30	10	15	E54	24	19	E78	31	28
E7	7	6	E31	15	14	E55	24	25	E79	25	35
E8	2	3	E32	12	15	E56	25	20	E80	35	32
E9	3	7	E33	16	13	E57	25	19	E81	32	25
E10	3	8	E34	14	16	E58	20	35	E82	36	32
E11	8	7	E35	18	16	E59	35	18	E83	36	33
E12	3	4	E36	14	18	E60	35	26	E84	33	32
E13	4	8	E37	17	14	E61	26	18	E85	37	33
E14	4	9	E38	15	17	E62	35	36	E86	37	34
E15	9	8	E39	17	18	E63	36	26	E87	34	33
E16	4	5	E40	18	20	E64	26	27	E88	32	19
E17	5	9	E41	20	17	E65	27	36	E89	32	29
E18	5	10	E42	17	22	E66	36	37	E90	30	32
E19	10	9	E43	22	20	E67	37	27	E91	30	33
E20	5	12	E44	18	19	E68	27	28	E92	34	30
E21	12	10	E45	19	16	E69	28	37	E93	34	31
E22	13	11	E46	19	21	E70	19	29			
E23	6	13	E47	21	16	E71	29	18			
E24	6	14	E48	21	23	E72	26	29			

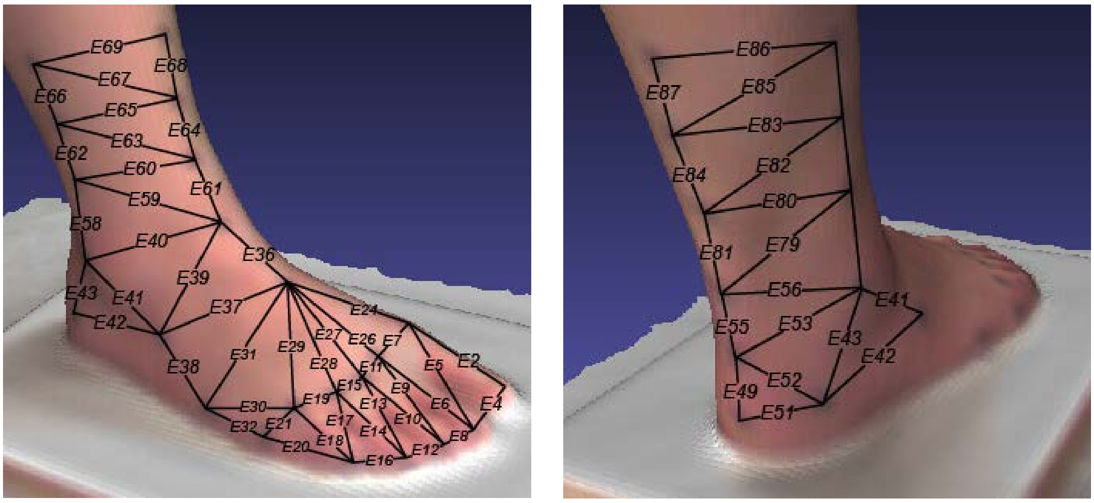

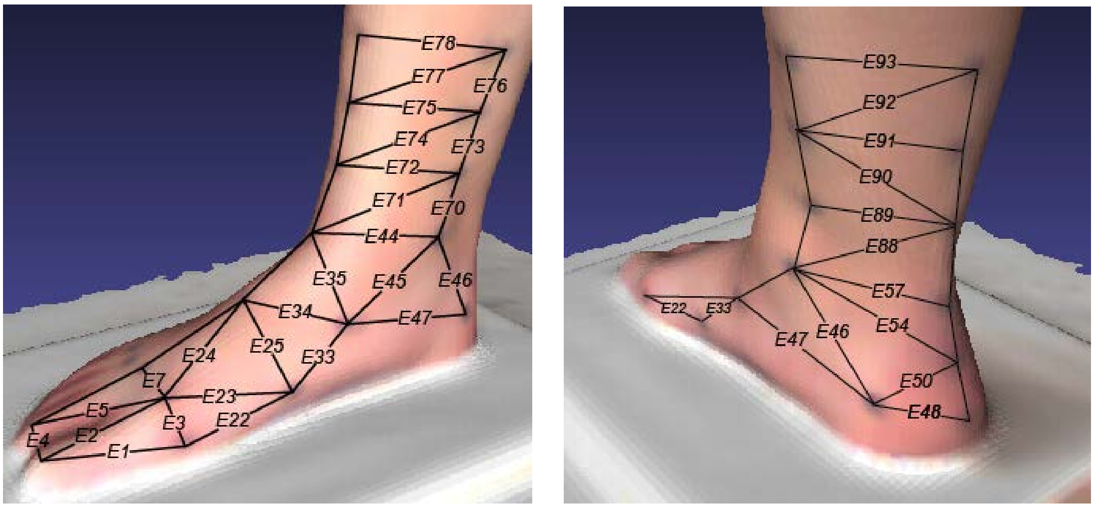

Figure 5-4 The distribution of edges for evaluating lengths

5.5 Statistical analysis

The length of edges in the developed structure will be used in the statistical analysis. The analysis includes descriptions of the general data, the ANOVA test to distinguish the significance of factors, and a comparison of means. First, with the distance data, the descriptive results showed the distribution and the variation. For the total 16 postures adopted in the experiment, all data are evaluated by category. Some of the descriptive statistics are displayed below. The full set of the tables showing the descriptive statistics is in Appendix C. Next, the ANOVA test was conducted with the data to observe the significance and the relationship between landmarks.

For the general description of all the data, average of the distance was calculated to form a representative foot information model. The whole set of data was based on the 50 subjects' information, and the results can be further applied to a standard foot on the dimensions of a foot model.

5.5.1 The influence of heel height

Table 5-4 The descriptive of edges lengths with standing height at 0

(Heel=0)

Distance	Mean	Std. Deviation	Distance	Mean	Std. Deviation	Distance	Mean	Std. Deviation
D_11_1	58.1	4.82	D_12_15	34.9	6.26	D_36_26	63.1	6.60
D_1_6	52.7	4.47	D_16_13	42.0	7.25	D_26_27	28.7	5.12
D_6_11	21.4	3.22	D_14_16	54.1	6.39	D_27_36	54.9	6.28
D_1_2	25.1	3.79	D_18_16	47.8	4.38	D_36_37	29.0	6.73
D_2_6	56.2	5.35	D_14_18	35.3	6.63	D_37_27	64.4	7.60
D_2_7	46.5	3.42	D_17_14	64.1	5.15	D_27_28	28.2	4.73
D_7_6	23.6	3.71	D_15_17	32.4	9.69	D_28_37	58.8	7.90
D_2_3	19.0	2.37	D_17_18	65.8	7.19	D_19_29	33.9	8.26
D_3_7	43.3	3.78	D_18_20	66.8	4.63	D_29_18	68.0	5.85
D_3_8	40.8	4.14	D_20_17	62.8	10.65	D_26_29	51.9	5.93
D_8_7	15.2	2.12	D_17_22	67.5	6.71	D_29_30	28.5	5.81
D_3_4	16.5	2.45	D_22_20	48.6	3.55	D_30_26	62.3	5.26
D_4_8	35.9	3.66	D_18_19	58.0	5.19	D_30_27	55.5	5.21
D_4_9	37.1	3.95	D_19_16	48.0	5.93	D_30_31	28.5	6.53
D_9_8	14.3	1.90	D_19_21	61.6	3.89	D_31_27	66.6	6.25
D_4_5	18.0	2.82	D_21_16	71.3	7.28	D_31_28	61.9	6.41
D_5_9	29.8	3.32	D_21_23	35.2	4.38	D_25_35	61.6	6.09
D_5_10	34.6	3.90	D_23_24	23.0	4.17	D_35_32	49.8	4.78
D_10_9	19.5	2.34	D_24_21	37.1	4.28	D_32_25	37.6	7.31
D_5_12	38.2	3.89	D_22_23	38.0	4.99	D_36_32	58.9	5.91
D_12_10	14.2	2.62	D_24_22	42.5	4.98	D_36_33	53.7	5.62
D_13_11	50.8	6.99	D_24_20	54.9	5.62	D_33_32	30.3	5.79
D_6_13	57.7	6.23	D_24_19	68.9	6.36	D_37_33	62.5	6.20
D_6_14	59.6	5.33	D_24_25	23.7	4.04	D_37_34	58.9	5.92
D_14_13	47.4	4.33	D_25_20	50.7	5.40	D_34_33	29.8	6.17
D_7_14	59.4	5.47	D_25_19	57.0	5.91	D_32_19	61.1	5.76
D_8_14	60.1	5.77	D_20_35	39.1	7.33	D_32_29	51.3	5.17
D_9_14	60.3	5.91	D_35_18	70.9	6.75	D_30_32	61.1	5.77
D_10_14	63.1	5.89	D_35_26	55.1	5.67	D_30_33	52.5	5.30
D_10_15	41.7	6.04	D_26_18	35.7	11.35	D_34_30	60.6	5.12
D_15_14	68.1	4.03	D_35_36	29.8	6.19	D_34_31	56.7	5.78

Table 5-5 The ANOVA result and compare means of edges lengths 1

Edge	P-value	H0	H10	H40	H70	Edge	P-value	H0	H10	H40	H70
E1	0	0	0	0	0	E10	0.003	0	-0.8	-1.0	-2.4
E2	0	0	-2.8	-3.5	-6.2	E19	0.003	0	-0.9	-1.0	-2.1
E5	0	0	-3.1	-4.2	-5.2	E30	0.003	0	-0.7	-1.8	-2.6
E6	0	0	-1.6	-2.0	-3.8	E84	0.005	0	0.7	-2.6	-2.9
E9	0	0	-2.0	-2.2	-3.5	E13	0.006	0	-1.1	-0.9	-2.0
E23	0	0	-0.5	-3.5	-4.7	E71	0.006	0	-0.5	3.1	4.8
E36	0	0	1.4	4.2	6.3	E26	0.011	0	0.1	-0.8	-1.5
E39	0	0	0.4	1.9	3.4	E31	0.011	0	-1.1	-0.1	1.1
E41	0	0	-0.4	2.1	2.5	E18	0.012	0	0.3	0.4	-1.7
E43	0	0	-1.6	-2.5	-4.0	E59	0.012	0	1.8	3.1	4.5
E46	0	0	-1.8	-3.5	-8.5	E27	0.013	0	-0.2	-1.1	-1.6
E49	0	0	-1.4	-2.1	-3.6	E22	0.018	0	0.4	-1.7	-2.0
E55	0	0	-0.8	-3.5	-5.5	E64	0.018	0	0.0	1.0	1.7
E79	0	0	-0.2	-3.1	-4.1	E52	0.025	0	1.3	0.1	-1.0
E81	0	0	0.1	-5.8	-8.9	E32	0.028	0	-0.7	-0.9	-2.3
E54	0.001	0	-1.9	-1.6	-4.3	E3	0.039	0	0.1	0.4	1.7
E61	0.002	0	0.3	4.5	7.4	E69	0.042	0	-2.5	-2.2	-3.1

In the exploration of the influence of heel height on foot surface deformation, the result was tested first for the general description. In the ANOVA test, results showed that a great proportion of the foot surface was influenced by the lifted heel height. Foot dorsal and the back of heel was greatly deformed; however, the medial part of foot showed the least changes.

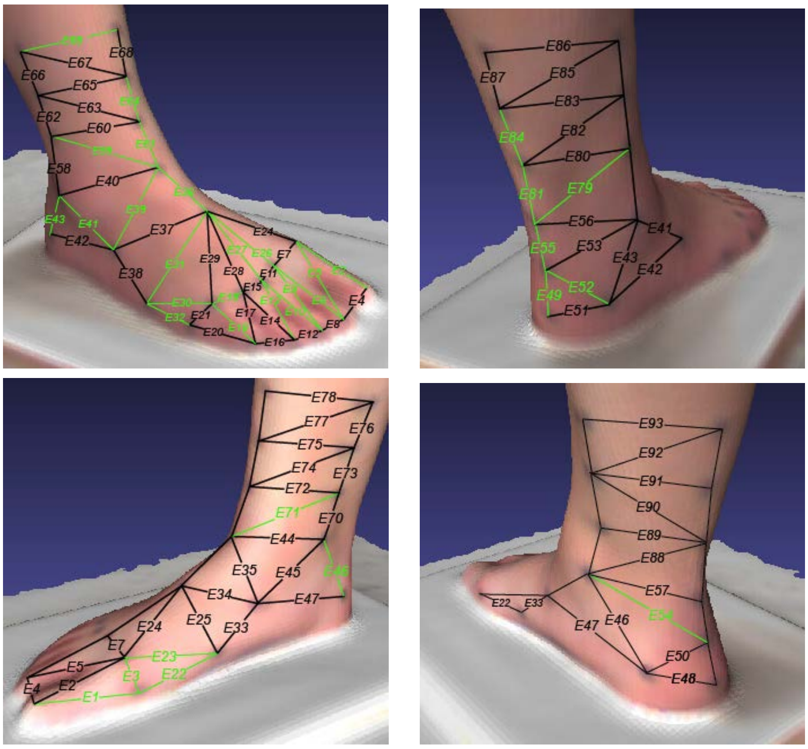

Figure 5-5 The significantly relevant edges to heel height

From the figures, results were clearly displayed that as the heel height lifted up, almost the whole forefoot part was changed due to the heel condition. The back of the heel also formed a totally new curve to adjust to the standing posture. Compared to the area around the ankle, edges at the forefoot showed more significant relation to heel height, with the P value even at 0. There was no severe deformation at the medial side, at either the plantar or the shank.

5.5.2 Changes due to dorsiflexion and plantar flexion

The tables below show the description of the edges during foot dorsiflexion and plantar flexion. In these foot rotation settings the ANOVA test resulted in the most edges influenced by the vertical rotation.

Table 5-6 The ANOVA result and compare means of edges lengths 2

Edge	P-value	25	12.5	0	-10	-20	Edge	P-value	25	12.5	0	-10	-20
E1	0	0.0	0.0	0.0	0.0	0.0	E76	0	-1.5	-0.5	0.0	-3.5	-3.8
E2	0	1.0	2.0	0.0	3.0	4.0	E81	0	-4.7	-3.7	0.0	0.0	0.7
E26	0	3.3	3.2	0.0	-0.4	0.9	E82	0	0.4	-0.7	0.0	-2.0	-4.3
E28	0	3.4	2.2	0.0	-1.1	-1.3	E83	0	-7.8	-4.9	0.0	2.8	5.0
E29	0	3.3	2.2	0.0	-1.9	-1.8	E23	0.001	-0.8	-0.7	0.0	0.4	1.2
E30	0	3.6	2.7	0.0	-1.8	-1.5	E88	0.001	-1.5	-1.5	0.0	-1.3	-3.4
E31	0	2.8	1.4	0.0	-1.9	-1.1	E90	0.001	1.5	1.1	0.0	-0.7	-2.1
E38	0	6.1	3.0	0.0	-3.1	-8.7	E9	0.002	1.0	1.0	0.0	-0.9	-0.6
E41	0	1.4	0.1	0.0	-1.2	-1.1	E71	0.002	-3.7	-3.8	0.0	-2.1	-0.8
E42	0	-2.4	-2.3	0.0	-0.3	1.9	E85	0.005	-0.4	-0.9	0.0	-1.2	-3.7
E43	0	0.4	0.4	0.0	-2.0	-4.1	E62	0.01	-2.1	-2.9	0.0	-1.2	0.8
E45	0	-5.2	-3.4	0.0	0.9	1.4	E77	0.012	-3.2	-1.7	0.0	-2.3	-1.4
E47	0	-1.0	-0.5	0.0	-4.2	-6.0	E17	0.013	0.3	0.8	0.0	-0.1	-0.7
E48	0	-7.4	-2.4	0.0	1.7	3.0	E22	0.014	1.0	-0.3	0.0	-1.2	-1.6
E51	0	-4.1	-1.8	0.0	2.3	2.9	E21	0.017	0.0	-0.6	0.0	-1.5	-1.0
E52	0	-1.0	0.2	0.0	1.3	2.7	E20	0.019	0.8	0.3	0.0	-0.8	-1.4
E55	0	-3.0	-3.2	0.0	-0.2	0.3	E33	0.019	-0.6	-1.3	0.0	-0.9	0.4
E56	0	-1.7	-0.8	0.0	1.8	2.7	E49	0.02	-3.6	-2.3	0.0	-2.6	-2.0
E57	0	-5.4	-3.0	0.0	2.4	3.1	E86	0.02	-1.9	-1.8	0.0	0.1	1.1
E58	0	0.5	-0.6	0.0	-2.4	-3.8	E18	0.028	0.1	0.1	0.0	-1.5	-0.7
E61	0	3.5	1.0	0.0	-4.3	-6.2	E39	0.034	-1.7	-1.9	0.0	-1.3	-0.2
E63	0	6.2	2.6	0.0	-6.5	-12.1	E87	0.034	-1.1	-1.3	0.0	-1.6	-2.5
E66	0	1.9	1.3	0.0	-2.4	-4.8	E7	0.035	-0.2	-0.6	0.0	-1.3	-2.1
E67	0	-3.0	-3.2	0.0	-1.3	0.5	E65	0.035	-2.1	-2.0	0.0	-2.2	-3.1
E73	0	6.2	0.9	0.0	-5.3	-8.1							

Similar to the heel height changing, in the dorsiflexion and plantar flexion rotation settings, the forefoot part changes most significantly and almost the overall area was deformed due to the various angle settings. For the rotation involving both upward and downward directions, almost all the parts on the surface, including the forefoot, the hind foot, and the lateral side of shank, cannot keep the original position.

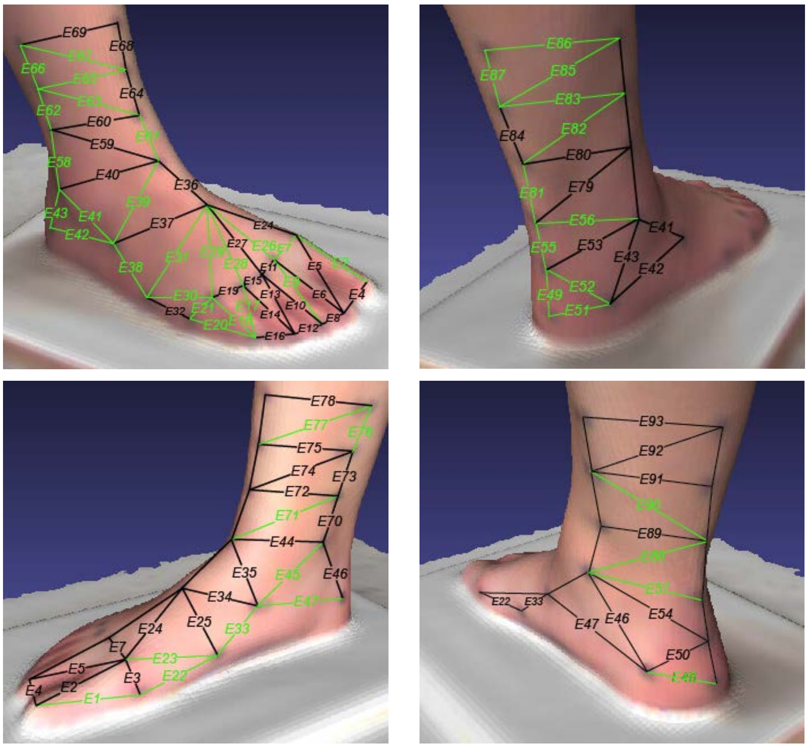

Figure 5-6 The significantly relevant edges to plantar flexion and dorsiflexion

5.5.3 Changes due to inversion and eversion

The length of edges in the developed structure will be used in the statistical analysis. The analysis includes descriptions of the general data, the ANOVA test to distinguish the significance of factors, and a comparison of means. In the following tables and figures, only the results in the high level of settings are listed in the context.

In the inversion-eversion investigation, the ANOVA test suggested less edges influenced by the rotation angle. The lateral side and the medial side of the ankle deformed more than the other positions, and on the first toe the change is more significant. On the contrary, the dorsal, except for the middle line, turned out to be stable under inversion and eversion situations. In addition, the back of the ankle proved to be less influenced by the rotation angle.

Table 5-7 The ANOVA result and compare means of edges lengths 3

Edge	P	10.0	5.0	0.0	-2.5	-5.0	Edge	P	10.0	5.0	0.0	-2.5	-5.0
E1	0	0.0	0.0	0.0	0.0	0.0	E5	0.005	1.3	1.2	0.0	0.2	-0.6
E2	0	1.0	2.0	0.0	3.0	4.0	E39	0.007	-0.2	-1.8	0.0	-1.4	-1.4
E43	0	3.3	1.9	0.0	-0.6	-1.6	E87	0.007	-2.6	-0.8	0.0	-0.5	-0.2
E45	0	1.0	0.7	0.0	-1.5	-2.0	E72	0.009	-3.5	-1.0	0.0	-1.5	-1.3
E47	0	-4.0	-2.5	0.0	-0.2	0.4	E55	0.012	-2.5	-1.1	0.0	-0.8	-0.5
E58	0	-3.1	-1.6	0.0	-0.9	-0.7	E26	0.018	-0.3	0.8	0.0	1.2	1.2
E60	0	2.7	1.5	0.0	0.7	-0.6	E59	0.034	2.2	2.2	0.0	1.0	-0.1
E82	0	-3.3	-1.4	0.0	-1.1	-0.6	E76	0.038	-2.6	-1.2	0.0	-2.2	-2.7
E84	0	-2.9	-1.5	0.0	-1.3	-0.5	E27	0.04	1.2	1.6	0.0	0.5	-0.2
E85	0	-3.1	-1.3	0.0	-1.1	-0.6	E73	0.042	-2.1	-1.6	0.0	-1.9	-3.1
E88	0	-2.9	-1.1	0.0	-0.5	-0.3	E56	0.044	2.5	2.2	0.0	1.1	-0.1
E48	0.001	-1.6	-1.1	0.0	1.2	1.3	E65	0.045	-0.5	-2.5	0.0	-1.7	-1.1
E41	0.003	1.0	-0.2	0.0	-0.8	-1.0							

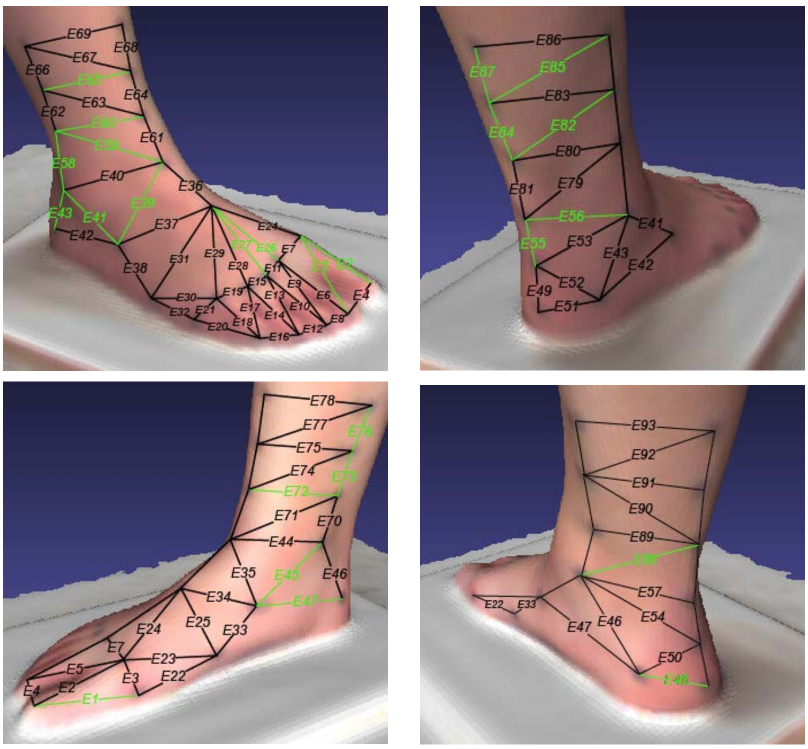

Figure 5-7 The significantly relevant edges to inversion and eversion

5.5.4 Changes during walking

In the walking comparison four representative stages are selected: heel strike, foot flat, heel rise, and toe lifted. The four stages altogether provide the foot deformation during stance phase, and the surface measurement of the edges can show the most significant change.

Table 5-8 The descriptive of edges lengths of four stages during walking

(Walk=0% of gait cycle)

Distance	Mean	Std. Deviation	Distance	Mean	Std. Deviation	Distance	Mean	Std. Deviation
D_11_1	57.1	6.58	D_12_15	31.8	6.20	D_36_26	62.1	5.70
D_1_6	51.0	5.90	D_16_13	42.8	7.87	D_26_27	28.3	4.25
D_6_11	21.4	3.66	D_14_16	51.1	6.72	D_27_36	53.9	5.62
D_1_2	21.8	4.75	D_18_16	46.6	3.97	D_36_37	28.5	5.71
D_2_6	51.8	6.23	D_14_18	36.8	7.37	D_37_27	63.1	7.03
D_2_7	46.0	4.07	D_17_14	62.2	4.91	D_27_28	27.4	4.42
D_7_6	19.3	3.38	D_15_17	33.5	11.98	D_28_37	56.4	6.60
D_2_3	15.3	3.34	D_17_18	66.3	7.68	D_19_29	32.0	5.29
D_3_7	42.0	4.23	D_18_20	65.4	5.23	D_29_18	66.4	4.64
D_3_8	41.5	4.83	D_20_17	61.5	12.07	D_26_29	50.0	4.76
D_8_7	13.4	1.97	D_17_22	66.3	6.81	D_29_30	28.2	5.35
D_3_4	15.6	3.77	D_22_20	47.1	3.73	D_30_26	59.9	4.85
D_4_8	35.6	4.42	D_18_19	55.0	4.70	D_30_27	53.1	5.08
D_4_9	37.4	5.44	D_19_16	45.5	5.47	D_30_31	28.0	4.78
D_9_8	13.5	1.80	D_19_21	59.2	5.16	D_31_27	63.7	6.14
D_4_5	17.1	3.29	D_21_16	68.3	5.73	D_31_28	58.8	5.91
D_5_9	29.5	4.61	D_21_23	35.8	4.97	D_25_35	61.5	6.02
D_5_10	35.0	6.19	D_23_24	22.2	4.60	D_35_32	52.3	6.61
D_10_9	17.1	2.81	D_24_21	38.5	4.84	D_32_25	35.0	8.83
D_5_12	38.7	6.50	D_22_23	38.1	5.23	D_36_32	59.4	7.76
D_12_10	13.7	3.03	D_24_22	42.6	5.59	D_36_33	56.0	7.85
D_13_11	49.5	8.05	D_24_20	56.0	4.89	D_33_32	28.9	4.99
D_6_13	54.0	7.22	D_24_19	66.2	6.77	D_37_33	63.3	8.30
D_6_14	58.5	6.50	D_24_25	21.5	4.50	D_37_34	60.4	7.59
D_14_13	45.0	4.30	D_25_20	53.3	5.58	D_34_33	28.1	4.90
D_7_14	56.5	5.80	D_25_19	57.1	6.65	D_32_19	63.8	6.96
D_8_14	55.8	6.38	D_20_35	40.0	6.89	D_32_29	50.5	6.69
D_9_14	56.4	6.00	D_35_18	70.8	6.27	D_30_32	57.9	5.92
D_10_14	58.8	5.69	D_35_26	54.1	4.72	D_30_33	52.7	6.39
D_10_15	36.9	6.30	D_26_18	35.1	7.25	D_34_30	62.3	7.73
D_15_14	65.7	4.83	D_35_36	27.9	6.30	D_34_31	56.9	6.87

(Walk=25% of gait cycle : foot flat)

Distance	Mean	Std. Deviation	Distance	Mean	Std. Deviation	Distance	Mean	Std. Deviation
D_11_1	62.2	4.65	D_12_15	35.3	5.69	D_36_26	61.2	4.92
D_1_6	55.9	4.33	D_16_13	43.3	6.65	D_26_27	29.3	4.87
D_6_11	22.2	3.15	D_14_16	54.0	6.23	D_27_36	52.8	4.74
D_1_2	23.7	4.10	D_18_16	49.3	4.01	D_36_37	29.2	5.64
D_2_6	57.1	4.80	D_14_18	36.4	6.67	D_37_27	62.2	6.49
D_2_7	47.5	3.85	D_17_14	62.4	4.33	D_27_28	28.0	4.19
D_7_6	22.7	3.83	D_15_17	30.9	8.56	D_28_37	55.7	6.22
D_2_3	18.6	2.72	D_17_18	63.5	6.59	D_19_29	34.1	6.62
D_3_7	44.3	3.51	D_18_20	65.6	3.98	D_29_18	65.9	5.29
D_3_8	42.1	3.52	D_20_17	57.9	9.80	D_26_29	50.5	5.26
D_8_7	15.2	2.02	D_17_22	67.6	6.10	D_29_30	29.6	5.38
D_3_4	17.8	2.67	D_22_20	45.5	3.41	D_30_26	60.0	5.17
D_4_8	37.6	3.95	D_18_19	56.6	5.41	D_30_27	53.6	5.19
D_4_9	38.5	4.16	D_19_16	49.5	4.53	D_30_31	28.6	6.31
D_9_8	14.5	1.97	D_19_21	60.6	5.57	D_31_27	63.2	6.97
D_4_5	17.6	3.07	D_21_16	68.6	5.62	D_31_28	59.0	6.90
D_5_9	31.9	4.21	D_21_23	34.3	4.25	D_25_35	62.9	6.58
D_5_10	36.3	4.56	D_23_24	21.9	4.46	D_35_32	51.7	6.13
D_10_9	19.1	2.61	D_24_21	37.1	4.88	D_32_25	35.6	8.87
D_5_12	39.4	4.00	D_22_23	37.1	4.24	D_36_32	61.2	6.36
D_12_10	15.1	2.71	D_24_22	40.8	4.30	D_36_33	55.2	6.68
D_13_11	52.6	6.21	D_24_20	54.8	5.86	D_33_32	30.3	5.45
D_6_13	59.8	5.72	D_24_19	65.8	6.60	D_37_33	64.1	7.00
D_6_14	61.3	6.08	D_24_25	22.7	4.28	D_37_34	59.7	6.70
D_14_13	47.1	3.21	D_25_20	50.8	5.76	D_34_33	28.7	5.32
D_7_14	61.2	6.12	D_25_19	55.7	6.16	D_32_19	62.0	6.40
D_8_14	61.3	6.31	D_20_35	38.8	7.01	D_32_29	48.6	6.03

Distance	Mean	Std. Deviation	Distance	Mean	Std. Deviation	Distance	Mean	Std. Deviation
D_9_14	60.8	6.08	D_35_18	70.0	6.23	D_30_32	57.9	6.14
D_10_14	62.5	5.60	D_35_26	53.3	3.76	D_30_33	50.6	7.14
D_10_15	42.4	5.45	D_26_18	34.9	6.97	D_34_30	59.9	7.61
D_15_14	67.0	4.00	D_35_36	28.8	5.48	D_34_31	55.2	8.48

(Walk=50% of gait cycle)

Distance	Mean	Std. Deviation	Distance	Mean	Std. Deviation	Distance	Mean	Std. Deviation
D_11_1	60.6	5.25	D_12_15	33.8	6.47	D_36_26	61.4	7.04
D_1_6	51.8	3.36	D_16_13	41.1	6.65	D_26_27	28.9	4.52
D_6_11	22.7	3.79	D_14_16	51.0	6.40	D_27_36	55.0	5.97
D_1_2	23.8	3.76	D_18_16	47.1	4.68	D_36_37	29.3	6.20
D_2_6	51.3	4.22	D_14_18	36.1	6.57	D_37_27	62.2	8.39
D_2_7	43.7	3.68	D_17_14	64.6	5.22	D_27_28	28.1	5.33
D_7_6	22.6	3.72	D_15_17	33.4	10.84	D_28_37	57.9	7.36
D_2_3	20.1	2.37	D_17_18	67.5	7.15	D_19_29	33.2	7.23
D_3_7	40.2	3.55	D_18_20	67.3	4.48	D_29_18	64.8	4.33
D_3_8	39.5	4.11	D_20_17	64.9	11.13	D_26_29	49.4	4.82
D_8_7	15.6	2.19	D_17_22	67.7	6.83	D_29_30	29.7	5.69
D_3_4	18.1	2.65	D_22_20	47.4	3.75	D_30_26	59.3	6.34
D_4_8	34.3	3.15	D_18_19	55.0	4.15	D_30_27	52.7	4.60
D_4_9	35.6	3.36	D_19_16	44.7	5.41	D_30_31	28.8	5.77
D_9_8	14.5	1.93	D_19_21	59.5	5.24	D_31_27	63.4	7.19
D_4_5	19.1	2.49	D_21_16	68.0	6.57	D_31_28	58.6	6.01
D_5_9	28.4	3.30	D_21_23	35.0	3.94	D_25_35	59.9	7.49
D_5_10	33.5	3.78	D_23_24	23.0	4.46	D_35_32	47.7	5.41
D_10_9	19.1	2.94	D_24_21	36.6	3.94	D_32_25	37.2	8.35
D_5_12	38.4	3.93	D_22_23	37.2	5.09	D_36_32	56.6	6.26
D_12_10	15.5	3.05	D_24_22	41.6	5.69	D_36_33	51.4	5.44
D_13_11	49.8	6.59	D_24_20	53.6	6.17	D_33_32	30.4	5.66
D_6_13	55.0	5.88	D_24_19	68.6	7.19	D_37_33	60.6	6.46
D_6_14	59.0	5.71	D_24_25	23.0	4.42	D_37_34	57.1	5.68
D_14_13	47.9	4.00	D_25_20	49.3	5.07	D_34_33	29.2	5.51
D_7_14	55.9	5.48	D_25_19	57.3	6.19	D_32_19	60.2	6.46
D_8_14	55.2	5.58	D_20_35	41.2	6.79	D_32_29	50.1	5.43
D_9_14	56.4	5.29	D_35_18	70.1	5.70	D_30_32	62.3	6.62
D_10_14	60.6	5.13	D_35_26	55.0	4.82	D_30_33	52.8	6.18
D_10_15	39.8	5.96	D_26_18	35.1	8.52	D_34_30	59.6	6.16
D_15_14	68.5	3.77	D_35_36	29.3	5.43	D_34_31	57.5	6.91

(Walk=62% of gait cycle: toe lift)

Distance	Mean	Std. Deviation	Distance	Mean	Std. Deviation	Distance	Mean	Std. Deviation
D_11_1	58.7	4.52	D_12_15	32.2	6.22	D_36_26	61.0	5.65
D_1_6	44.5	5.24	D_16_13	42.5	7.04	D_26_27	32.3	6.40
D_6_11	26.9	4.78	D_14_16	50.0	6.26	D_27_36	53.7	5.53
D_1_2	22.4	4.39	D_18_16	49.7	5.00	D_36_37	28.8	4.94
D_2_6	47.5	5.45	D_14_18	42.9	8.49	D_37_27	60.5	6.34
D_2_7	38.2	5.32	D_17_14	64.2	4.64	D_27_28	28.1	5.28
D_7_6	21.1	3.76	D_15_17	33.2	10.12	D_28_37	56.3	7.24
D_2_3	17.2	2.56	D_17_18	72.6	7.79	D_19_29	31.2	6.62
D_3_7	38.1	4.38	D_18_20	66.2	4.66	D_29_18	68.6	4.15
D_3_8	35.8	4.96	D_20_17	64.9	11.69	D_26_29	51.0	5.13
D_8_7	14.8	2.03	D_17_22	66.5	5.61	D_29_30	28.9	6.50
D_3_4	16.7	2.80	D_22_20	44.3	2.97	D_30_26	63.1	6.40
D_4_8	34.1	4.08	D_18_19	54.6	4.90	D_30_27	55.1	6.76
D_4_9	34.2	4.32	D_19_16	45.1	4.67	D_30_31	28.6	4.86
D_9_8	14.4	2.38	D_19_21	54.1	7.13	D_31_27	66.1	7.01
D_4_5	16.4	2.73	D_21_16	65.1	6.42	D_31_28	61.5	8.66
D_5_9	30.4	4.63	D_21_23	34.1	3.91	D_25_35	54.4	6.16
D_5_10	32.9	4.41	D_23_24	20.0	4.42	D_35_32	49.8	4.80
D_10_9	14.8	2.36	D_24_21	34.7	3.29	D_32_25	27.6	7.79
D_5_12	38.4	4.89	D_22_23	38.2	4.12	D_36_32	54.7	6.82
D_12_10	16.5	3.43	D_24_22	42.3	4.66	D_36_33	53.2	5.03
D_13_11	45.5	6.86	D_24_20	52.5	5.40	D_33_32	27.2	5.32
D_6_13	47.1	5.52	D_24_19	65.9	8.36	D_37_33	59.8	6.69
D_6_14	53.6	7.59	D_24_25	20.2	4.94	D_37_34	58.3	5.44
D_14_13	50.7	5.30	D_25_20	51.0	5.47	D_34_33	27.3	5.72
D_7_14	50.7	6.63	D_25_19	56.2	5.75	D_32_19	59.5	5.34
D_8_14	53.0	6.90	D_20_35	38.8	7.41	D_32_29	49.0	5.20
D_9_14	57.2	6.33	D_35_18	70.5	5.90	D_30_32	58.4	7.60
D_10_14	63.7	6.67	D_35_26	53.2	5.47	D_30_33	50.5	6.67
D_10_15	38.3	5.53	D_26_18	39.4	6.78	D_34_30	57.0	7.14
D_15_14	71.9	5.16	D_35_36	28.9	6.00	D_34_31	54.1	7.65

During walking, most parts on the surface of the foot are activated in the motion. To keep balance and move forward, the lateral side of the dorsal and the posterior of the shank are mostly applied to adjust the foot motion. Relatively, the anterior of the medial shank is not as active as the other parts. The large amount of involved edges showed the complexity of the walking stage.

Table 5-9 The ANOVA result and compare means of edges lengths 4

Edge	P-value	0%	25%	50%	62%	Edge	P-value	0%	25%	50%	62%
E1	0	0.0	0.0	0.0	0.0	E57	0	-2.1	-0.4	-0.7	-3.3
E2	0	1.0	2.0	3.0	4.0	E66	0	0.2	0.2	-0.1	4.0
E3	0	-0.6	4.9	3.1	0.7	E81	0	-1.6	0.3	-3.3	-7.9
E4	0	-0.9	3.8	0.0	-7.4	E82	0	0.8	1.0	-3.9	-1.5
E5	0	-0.6	0.6	1.2	4.4	E83	0	-3.0	-3.3	-1.2	-9.6
E7	0	-3.0	1.6	-4.5	-7.8	E84	0	-0.1	1.8	-3.2	-5.5
E8	0	-0.4	1.5	-2.7	-7.7	E85	0	0.6	0.8	-3.6	-2.1
E9	0	-4.3	-0.5	-1.4	-2.4	E86	0	-1.1	-0.7	-0.1	-3.2
E10	0	-3.3	0.4	0.8	-1.6	E87	0	-0.2	1.5	-2.7	-4.1
E11	0	-1.8	1.0	-2.9	-5.0	E92	0	-3.6	-4.2	0.1	-3.4
E12	0	0.2	1.4	-1.1	-4.9	E15	0.001	-0.8	1.7	-1.2	-1.7
E16	0	0.0	1.4	-1.4	-2.5	E88	0.001	0.1	0.3	-3.0	-2.1
E21	0	-3.2	-0.6	-0.1	-4.7	E19	0.002	-0.2	2.2	-0.9	0.9
E23	0	-0.6	1.2	1.3	2.3	E51	0.002	0.1	-0.5	0.1	-2.8
E24	0	-0.7	1.4	-0.7	-5.6	E36	0.003	-2.4	0.1	-3.1	-3.9
E25	0	-3.2	2.4	-2.5	-10.8	E58	0.003	0.8	-0.8	-3.1	-0.8
E26	0	-0.4	1.2	-0.3	-6.3	E39	0.006	-1.9	-0.7	0.1	0.8
E27	0	-2.1	-0.4	0.3	2.8	E40	0.007	0.2	-0.6	1.0	1.5
E28	0	-1.4	1.5	-2.8	-8.9	E46	0.007	-3.0	-1.6	-3.5	-3.7
E29	0	-3.2	0.7	-4.6	-7.6	E55	0.008	-0.7	-0.9	-3.2	-3.2
E30	0	-3.1	0.3	-3.7	-3.5	E60	0.013	0.7	-0.9	2.0	0.1
E31	0	-3.8	-0.6	-2.3	0.5	E52	0.015	1.3	0.6	-0.1	-2.4
E32	0	-3.7	0.5	-2.5	-3.1	E93	0.015	-0.7	-3.2	-0.8	-2.9
E33	0	-2.7	-0.8	0.2	4.0	E14	0.016	-1.2	1.3	1.5	-0.3
E38	0	0.1	0.5	-0.5	7.1	E73	0.02	-1.1	-1.8	-3.7	0.9
E41	0	0.7	-2.2	1.2	7.0	E18	0.021	-1.5	-0.4	0.9	-1.9
E43	0	-0.2	-4.8	2.8	2.7	E69	0.034	-0.8	-1.8	-2.0	-3.2
E45	0	-1.3	-3.1	-1.7	-4.0	E79	0.036	-2.3	-3.0	-3.7	-0.4
E47	0	-3.5	0.8	-4.0	-3.3	E13	0.041	-1.6	0.0	0.3	-0.2
E48	0	-2.2	-0.6	-2.2	-7.2	E34	0.043	-1.7	0.3	-1.1	-1.9
E49	0	-4.0	-2.7	-4.0	-6.5						

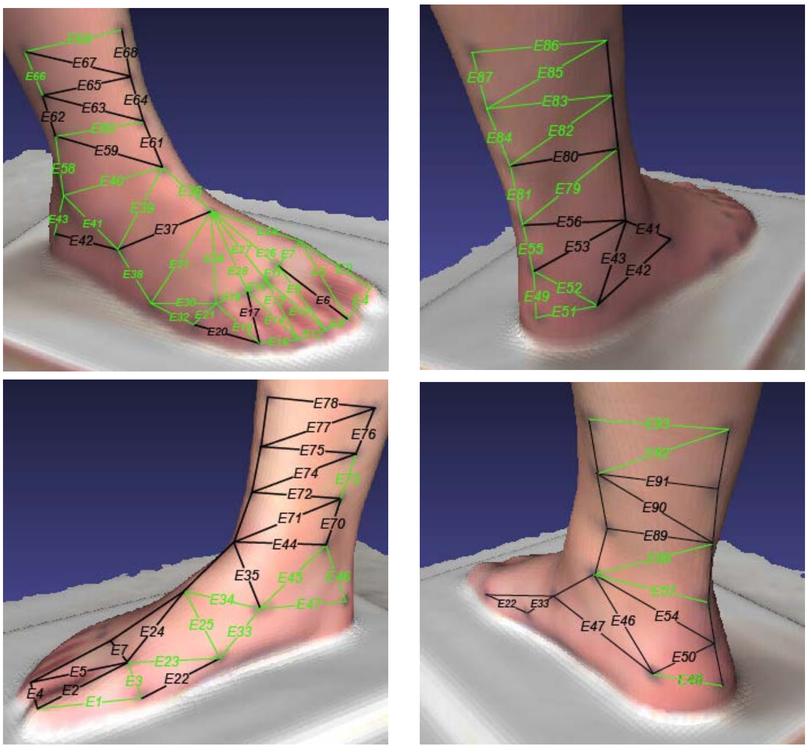

Figure 5-8 The significantly relevant edges to four stages during walking

5.6 Angle change

To further illustrate the changes of the surface, representative angles were selected and analyzed to investigate the regulation. Based on the settings of plantar flexion and dorsiflexion, inversion and eversion, the angles were chosen to simulate the foot folding and twisting. In Table 5-10 the details of the angle edges are presented, and in Figure 5-9 the reference landmarks and relative positions of the angle edges are drawn in the foot shapes.

Table 5-10 The composition of the investigated angles

Notation	Line1		Line2	
	P1	**P2**	**P3**	**P4**
A1	Middle of 16-17	Middle of 19-20	Middle of 26-32	Middle of 28-34
A2	Middle of 13-15	Middle of 19-20	Middle of 26-32	Middle of 28-34
A3	Middle of 11-12	Middle of 19-20	Middle of 26-32	Middle of 28-34
A4	Middle of 1-5	Middle of 19-20	Middle of 26-32	Middle of 28-34
Notation	**Line1**		**Line2**	
	P1	**P2**	**P3**	**P4**
A5	14	18	26	28
A6	7	14	14	18
A7	2	7	7	14
Notation	**Line1**		**Line2**	
	P1	**P2**	**P3**	**P4**
A8	Middle of 29-35	Middle of 31-37	19	20
A9	Middle of 29-35	Middle of 31-37	16	17
A10	Middle of 29-35	Middle of 31-37	13	15
A11	Middle of 29-35	Middle of 31-37	11	12
A12	Middle of 29-35	Middle of 31-37	1	5
Notation	**Line1**		**Line2**	
	P1	**P2**	**P3**	**P4**
A13	16	17	19	20
A14	13	15	19	20
A15	11	12	19	20
A16	1	5	19	20

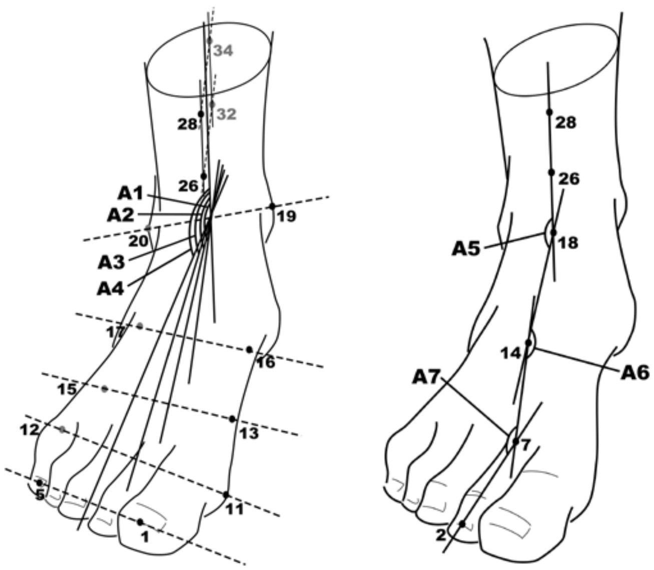

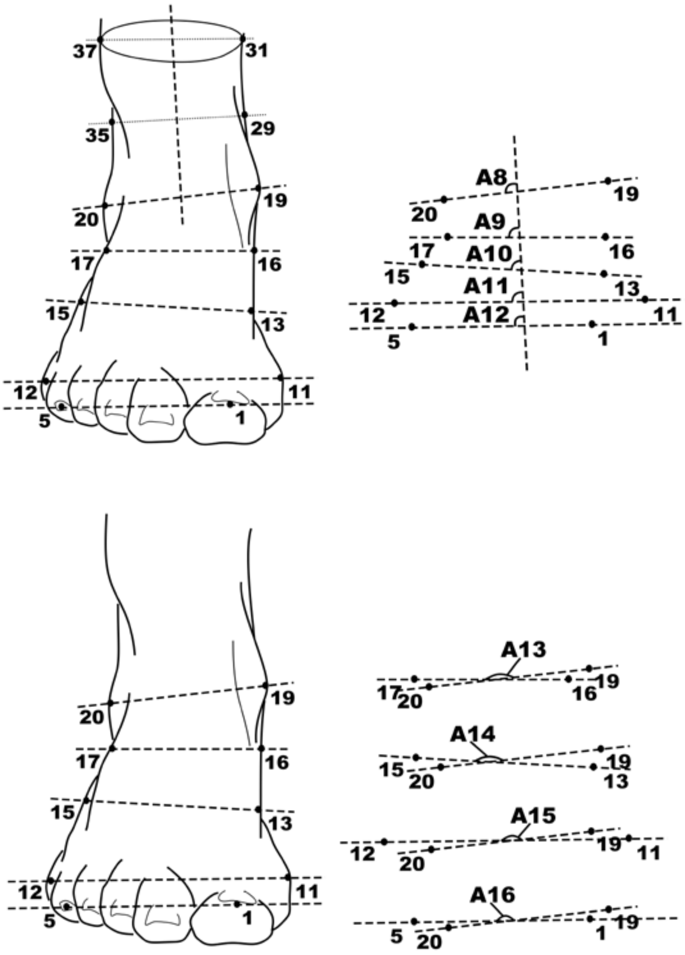

Figure 5-9 The relative position of edges composing the angles

As the figure shows, there are three groups of angles for exploration. The first group is to test the foot folding regulations with the center of the ankle. The second group is to observe the dorsal surface deformation. And the third group is for comparing the foot twisting in dynamic situations. The angle settings are based on the landmarks, with the middle point of two-landmark connections as the central line.

To test the data obtained from the experiment, the angle values were also examined to observe the description and the ANOVA test results. As a hypothesis, the angle changes should show the relation with the standing postures. In other words, the slope of the platforms is expected to influence the foot rotation angles. The results of the description are listed in Appendix E. Following is an example of the standing position with heel height at 0.

Table 5-11 The descriptive of the angle change at standing position

Notation	Minimum	Maximum	Mean	Std. Deviation
A1	2.2	120.9	15.118	16.8431
A2	1.4	127.2	9.872	17.5762
A3	1.1	120.8	12.239	16.5432
A4	3.1	107.6	26.277	13.9726
A5	51.1	136.3	124.630	12.1138
A6	158.1	177.3	168.082	5.1867
A7	165.0	179.0	172.265	3.7081
A8	86.6	108.5	99.068	4.6975
A9	89.2	123.9	105.874	7.4253
A10	89.0	115.3	100.624	4.4391
A11	86.7	108.4	97.832	4.5705
A12	85.2	102.6	93.510	4.0761
A13	73.9	145.3	131.806	12.7530
A14	69.9	138.3	127.562	12.2135
A15	78.2	128.5	117.242	8.9004
A16	79.9	122.1	112.410	7.3658

For further comparison, a series of ANOVA tests and comparisons of means were conducted on the data for finding the influence from slope angles. The following paragraphs will explain the results in detail.

5.6.1 The influence of heel height

In the ANOVA test of the heel height, angles of the midfoot folding, the forefoot folding, and the whole foot twisting relative to the oriental plane showed great deformation influenced by the heel height (Table 5-12).

Table 5-12 The result of the foot angle influenced by heel height

Angle	P-value	Mean value			
		H0	H10	H40	H70
A1	.000	132.9491	135.9107	142.5866	149.3642
A2	.000	128.7624	132.1396	141.5204	149.9929
A3	.000	118.0553	122.4045	132.9859	142.1250
A4	.000	113.0879	115.9347	123.9261	131.5060
A5	.000	124.5057	131.8903	139.7274	148.7929
A6	.561	168.2907	169.3170	168.6735	170.7248
A7	.000	172.2494	164.5901	154.6065	145.3045
A8	.868	99.0681	98.5349	98.0028	98.4635
A9	.220	105.8735	105.0590	107.3389	109.2583
A10	.001	100.6238	98.7463	101.7798	103.6304
A11	.015	97.8319	94.6047	95.5661	94.5828
A12	.019	93.5100	93.3390	95.2165	96.1874
A13	.120	12.9147	13.0816	15.7793	15.7227
A14	.133	7.4268	8.4775	8.2953	9.5123
A15	.321	9.9780	10.1712	8.4611	9.5462
A16	.140	24.5821	23.4864	21.3012	22.4427

The results suggested that the heel height would change the foot's normal deformation when it raises level. On the contrary, the ankle rotation did not show relatively regular change. In the dorsal surface deformation, the angle A6 with the center of middle line showed no significant influence under the heel height changing condition.

5.6.2 The influence of plantar flexion and dorsiflexion

In the exploration of foot rotation during plantar flexion and dorsiflexion, the result showed opposite results between groups. The result is shown as follows. As the above table suggests, the rotation with the center of the ankle showed no great change under the influence of plantar flexion and dorsiflexion postures. However, the dorsal shape changes with the foot folding up and down. The inward and outward twisting angles change with the foot moves.

Table 5-13 The result of the foot angle during plantar flexion and dorsiflexion

Angle	P-value	Mean value				
		-25	-12.5	0	10	20
A1	.000	150.1037	144.1031	132.9491	125.4774	117.6202
A2	.000	148.3989	140.7495	128.7624	119.3850	110.3312
A3	.000	139.6641	130.8327	118.0553	107.6086	98.3403
A4	.000	135.6246	126.3356	113.0879	102.1908	92.4430
A5	.000	145.9368	138.4921	124.5057	113.9777	106.7270
A6	.001	170.7943	171.2522	168.2907	167.0106	165.0937
A7	.020	172.2224	171.2207	172.2494	170.2658	170.2438
A8	.780	98.3479	99.6463	99.0681	100.0618	99.1014
A9	.027	107.1385	108.2573	105.8735	103.5806	101.8724
A10	.826	101.0462	101.6900	100.6238	102.3660	101.4380
A11	.000	93.9083	96.6316	97.8319	101.2288	101.9480
A12	.000	83.5051	88.7098	93.5100	100.7950	104.4863
A13	.284	14.4419	14.7793	12.9147	16.1684	15.3083
A14	.001	6.8976	7.6980	7.4268	9.0682	10.0468
A15	.183	9.5084	8.4933	9.9780	7.9278	8.4466
A16	.363	24.3737	23.1250	24.5821	22.1673	22.6251

The result indicates that the foot motion in the vertical direction would also influence the shape of the medial and lateral sides. It can be inferred that the midfoot surface and the forefoot surface would also deform on a large scale due to the plantar flexion and dorsiflexion.

5.6.3 The influence of inversion and eversion

The result of the ANOVA test for foot angle change based on inversion and eversion was not as expected. Only the angle A4 was significantly affected by the foot motion. The result is that it is possible that either the foot angle is not related to inversion and eversion movement, or that the deformation is related to other angle settings. For further information, there need to be more tests on the movement.

Table 5-14 The result of the foot angle during inversion and eversion

Angle	P-value	Mean value				
		10.0	5.0	0.0	-2.5	-5.0
A1	.668	134.9910	133.9689	132.9491	134.3270	133.3379
A2	.710	130.1831	129.6216	128.7624	129.9070	128.7165
A3	.835	118.8903	118.5857	118.0553	118.6876	117.8772
A4	.712	113.8001	113.8101	113.0879	113.6202	112.7820
A5	.784	126.3240	124.8848	124.5057	126.4528	124.5571
A6	.749	169.4382	168.3561	168.2907	168.1478	168.5227
A7	.821	171.7587	171.5650	172.2494	171.3047	171.4541
A8	.000	103.6262	100.9835	99.0681	99.9146	98.3982
A9	.000	115.6886	111.2115	105.8735	104.7688	102.7522
A10	.000	111.9554	107.0835	100.6238	99.9783	97.4686
A11	.000	109.7252	104.3515	97.8319	96.8269	94.9118
A12	.000	103.9034	99.4048	93.5100	92.8740	91.1269
A13	.000	18.9439	16.8098	12.9147	15.2139	13.1636
A14	.000	12.5213	10.8442	7.4268	8.0684	7.9048
A15	.413	9.2326	8.4661	9.9780	8.8727	9.8491
A16	.000	19.0547	20.9276	24.5821	23.2610	24.2535

5.6.4 The influence of foot walking

The results of the relation between foot angle changes and foot walking postures provide a great amount of information. Most of the angles have been influenced significantly, except for the angle between the vertical line in the shank and the line across the middle slice of the foot shape. This explains that during the walking period, almost all over the foot would change with the movement, and all the changes could be predicted based on time and motion stages. The result of the angle response to walking postures can be regarded as the same as hypothesized. Further evaluation is still needed to form the prediction model.

Table 5-15 The result of the foot angle during walking

Angle	P-value	Mean value			
		0%	25%	50%	62%
A1	.000	140.8909	134.9243	134.3612	152.1356
A2	.000	136.9647	130.5065	131.6009	153.9487
A3	.000	127.0938	120.2621	120.7095	146.1606
A4	.000	118.6358	114.6736	109.7011	132.5244
A5	.000	135.8883	129.3440	127.9784	153.1374
A6	.002	169.2656	166.4647	167.8858	170.1298
A7	.000	153.3656	171.2467	152.7166	127.3718
A8	.000	98.8235	94.7368	103.1079	104.1032
A9	.000	108.4110	94.8690	113.1019	116.2292
A10	.000	103.4800	87.2078	107.3683	108.7576
A11	.000	95.8633	82.2774	100.0867	97.7086
A12	.000	88.4565	78.6136	101.8615	109.8381
A13	.000	15.1074	10.9913	17.5740	16.7602
A14	.091	9.2209	10.3047	11.9100	11.5025
A15	.000	12.1851	16.9968	8.0860	11.2699
A16	.000	30.2546	33.0223	19.7160	17.2806

5.6.5 The regression equations of angles

To further find out the relation between the foot rotation angles and the platform settings, regression analysis was tested with the significantly influenced angles in the above ANOVA test and the value of comparison of means results. After selecting the angles with P values smaller than 0.05 in the ANOVA test, linear regression was applied to obtain the regression model. Tables 5-16 to 5-19 show the regression equation for each angle and platform setting. The plot of the regression equations are listed in Appendix F.

As the tables indicate, generally it is clear that the first three tables mostly conform with the linear regulation. The angle notations suggest the parts on the foot that respond significantly to the settings. For the heel height factor, the ankle folds together with the height increases. And there are changes in the dorsal surface, meaning that the foot dorsal will deform based on the bottom of the high heel shoes. To deduce the deformation of the foot, it can be inferred that the arch structure will rotate to a more curved shape, in order to adapt to the high heel situation. Another group of angles located at the forefoot relative to the shank was significantly influenced by heel height; however, the equation is not matched with linear regulation. This result suggests that the angle deformation may have some other relation with the heel height at the forefoot part.

Table 5-16 The regression equations of selected angles-Heel elevation

Notation	P-value	Regression equation	R^2
A1	.000	y = 0.2312x + 133.27	0.9986
A2	.000	y = 0.3031x + 129.01	0.999
A3	.000	y = 0.3417x + 118.64	0.9968
A4	.000	y = 0.2627x + 113.23	0.9996
A5	.000	y = 0.3253x + 126.47	0.973
A7	.000	y = -0.367x + 170.2	0.9772
A10	.001	y = 0.0565x + 99.501	0.7592
A11	.015	y = -0.0294x + 96.527	0.3695
A12	.019	y = 0.0425x + 93.287	0.9564

In table 5-17, the result show the regression model between the plantar flexion-dorsiflexion angles and the foot inner angles deformation. As with the heel height increasing settings, when the foot is in plantar flexion and dorsiflexion, the ankle folding movement shows great significance to the degree of rotation angles. In the heel part, most of the possible angles changed to the platform settings. In addition, unlike in the high heel test, the dorsal curve at the lower tibia and the relative angle between the toes and the shank were also reported to deform with the foot folding postures. The difference in the results between high heel standing test and the plantar flexion-dorsiflexion test is possibly due to the heel shape. This may because when standing on the high heel shoes, the foot heel contacting the bottom is still in oriental direction, while in the simple plantar flexion posture, the heel presents a downward direction, pointing to the ground. The difference in the supporting situations can lead to a variation of the response angles.

Table 5-17 The regression equations of selected angles-Plantar flexion and dorsiflexion

Notation	P-value	Regression equation	R^2
A1	.000	y = -0.7412x + 132.94	0.9919
A2	.000	y = -0.8641x + 128.23	0.994
A3	.000	y = -0.9389x + 117.49	0.9956
A4	.000	y = -0.9799x + 112.47	0.9957
A5	.000	y = -0.914x + 124.56	0.99
A6	.001	y = -0.1377x + 168.28	0.9017
A7	.020	y = -0.0425x + 171.18	0.5845
A9	.027	y = -0.1326x + 105.15	0.8219
A11	.000	y = 0.1834x + 98.585	0.9674
A12	.000	y = 0.4785x + 94.919	0.988
A14	.000	y = 0.0667x + 8.3275	0.8415

For inversion and eversion postures, foot angles did not show many differences in the sagittal plane. As the most obvious response to the rotation, lines used to parallel to the transverse plane showed the linear regulation compared to the vertical line based on shank. The angles at the midfoot also reported great changes. The result indicates that the foot will not only rotate to the direction when inversion and eversion posture happens, it will also twist to some degree. Relative to the twisting changes, the foot rotation inward and outward is still more significant. The twisting postures may not be in linear regulation, for the results showed no strong correlation to the linear equation.

Table 5-18 The regression equations of selected angles-Inversion and eversion

Notation	P-value	Regression equation	R^2
A8	.000	y = 0.3201x + 99.918	0.8862
A9	.000	y = 0.8746x + 106.75	0.9911
A10	.000	y = 0.9794x + 101.95	0.984
A11	.000	y = 1.0132x + 99.21	0.9824
A12	.000	y = 0.8759x + 94.85	0.979
A13	.000	y = 0.3729x + 14.85	0.7826
A14	.000	y = 0.342x + 8.8401	0.8601
A16	.000	y = -0.3611x + 22.957	0.8478

In the analysis of the data in the walking stages, results showed great significance between the foot movement and the time in a gait cycle. Though the result suggests that almost every part on the foot would respond to the walking postures, the linear equation did not provide a satisfying answer. Considering that in the walking situation, there is also pronation and supination happening in a human foot, the result is supposed not in the linear relation.

Table 5-19 The regression equations of selected angles-Walking

Notation	P-value	Regression equation	R^2
A1	.000	y = 11.613x + 136.6	0.1503
A2	.000	y = 19.614x + 131.54	0.2486
A3	.000	y = 21.599x + 121.16	0.2401
A4	.000	y = 12.357x + 114.65	0.1206
A5	.000	y = 18.211x + 130.35	0.1883
A6	.002	y = 1.2368x + 168.01	0.045
A7	.000	y = -39.396x + 164.67	0.3618
A8	.000	y = 11.059x + 96.405	0.5024
A9	.000	y = 18.276x + 101.89	0.2856
A10	.000	y = 15.733x + 96.315	0.191
A11	.000	y = 10.69x + 90.323	0.1357

A12	.000	y = 39.333x + 81.221	0.6092
A13	.000	y = 5.3931x + 13.261	0.2571
A15	.000	y = -5.906x + 14.157	0.1947
A16	.000	y = -24.228x + 33.366	0.7447

5.7 Summary

In the exploration with 3D foot scanner a series of information including foot landmarks, surface point cloud and settings of standing postures were required. The main focus of the evaluation was based on the landmarks and the value in the coordinate system. With the XYZ value and the relative position between landmarks, results of the landmark triangulation, the lengths of edges, and the angles between representative joints were obtained separately.

For the calculation of the triangular edges on the surface of the foot model, the lengths stand for the extension and constriction during dynamic motions. Results of the lengths indicate that among all the four groups of settings, inversion and eversion motions have the least effect on the surface changes of foot. The other three settings (heel height elevation, plantar flexion and dorsiflexion, walking) all have significant influence on the edges' changes. By observing the surface areas, the results illustrate that the dorsal part, the lateral part of the ankle and the back of the heel are the main areas to deform with the outside conditions. By contrast, the medial of the shank and heel are relatively stable, with not as much deformation. The most changes happen during the walking stage, with almost

66% of the surface edges deformed dramatically and reporting regular changes with time. Among all the 93 edges, E1, E2, E26, E39, E41, E43, and E55 were influenced in all four groups of settings. These edges are located at the toe, the lateral side of the ankle starting from the lower tibia across the lower fibula, to the very back of Achilles' Tendon. It indicates that the lateral ankle and foot would deform more in dynamic situations to adjust to the various environments.

In the angle analysis, the foot showed great changes based on the platform settings. In the heel height elevation setting and the plantar flexion-dorsiflexion setting, both of the results suggested that the foot will rotate in a linear regulation matching the folding angles. However, in the inversion-eversion setting, no significant response happened in the forefoot, but the midfoot part has the linear relationship to the angles for prediction. Unlike the static settings, in the walking test most of the foot dimensions reported great significance influence during one gait cycle, but the result of linear equation evaluation was not strong. More possible changes are to be further explored for a proper prediction model.

CHAPTER 6 DISCUSSION AND CONCLUSION

In this study, the main goal was to develop a dynamic foot model for footwear design. The dynamic model is expected to provide foot motion pattern and information on the surface deformation under various situations. To achieve this goal, two experiments were conducted to obtain foot information, and the experiment settings were generalized into rotated situations and high heel situations and the shape during normal walking. First, a trial exploration of trajectories and angle gradual change during foot walking in a gait cycle was proposed. By applying the motion capture system to record the landmarks on the surface of the walking foot, data of the XYZ value in the coordinate system and the time within one gait cycle were extracted for calculation.

Second, a series of foot standing postures were stored in the form of a 3D model. From the 3D model, the foot measurement, landmark position, and surface point cloud can be obtained for the general simulation model. The landmarks can be used for triangulation, to provide the lengths of edges in surface extension and contraction. By connecting the main landmarks, the angles reflecting foot rotation are calculated. Finally, the integrated foot model with all the analyzed results provides knowledge of the dynamic foot.

6.1 Foot walking analysis in one gait cycle with motion capture

In this part of research, foot movement during normal walking was captured with retro-reflective landmarks. Trajectories and continuous angle changes in coordinate systems were drawn with landmark paths. Results of the individual walking trajectories illustrate mainly the swing phase of one gait cycle. The relative motion between the hind foot and the forefoot is obvious: the hind foot moves higher and more rapidly at the first half of swing phase, while the forefoot keeps steady at first but is raised slightly at the end of swing phase. This motion difference is the same as the definition of a gait cycle, claiming that the heel raises first during supination, and the forefoot rolls higher before the heel strike for pronation. Next the overall motion pattern combining results of all the trials is shown in 2D display with X, Y, and Z values changing with time. The graphs suggested the foot motion in the swing phase is toward multiple directions, rather than on one plane. From 50% of a gait cycle, the foot starts to move rapidly, and at 75% of the gait cycle, it goes inward, away from the original position and also upward slightly. The trajectories in the 3D coordinates supplement the former 2D research of gait cycle, showing not only the side view of the foot motion, but also finding the curve around the body on the oriental plan. The curve is suggested to be the connection of supination of the last step and the pronation of the following one. And the motion supports and balances the body wave in the left and right directions.

The angle analysis focuses on the forefoot motion relative to the ground. The figure of the angles turned out to fluctuate during the second half of the gait cycle, among which the rotation of the 1st and the 5th MPJ shows severe ups and downs. The fluctuation indicates that the foot would shake and wave during the swing phase, and this may be due to the instinct of keeping balance when the body is moving. In the continuous pictures with all landmarks linked up, the rotation of the forefoot and the midfoot are more obviously displayed to change with time. Finally a series of pictures captured by the high-speed camera in the frequency of 0.05 second per frame provide the side view of foot motion in stance phase. The profile extracted from the picture illustrated the foot heel strikes and turns to foot flat stage, with the ankle part still moving forward, and later the heel lift stage shows the heel deformation with strength to support the step.

6.2 Foot surface analysis for rotation situations and heel height influence

The foot shapes were scanned and stored with a portable Kinect scanner. The result was categorized as landmark information and surface point cloud data. The landmark triangulation provides the triangles to represent the areas, edges for the distance analysis between foot joints. In total there are 56 triangles and 93 edges selected. As in the foot normal walking analysis, the forefoot was the most significantly influenced by all the settings. This suggested that the forefoot would rotate or deform in order to keep the body balance, and also to adjust foot plantar in fitting non-flat platforms. Generally the medial side of the shank stays steady, without much significant deformation influenced by foot rotations. The areas around the foot arches report more severe deformation to adjust to various situations. To select the edges reacting to all the rotation settings and heel heights, Edge 1, Edge 2, Edge 26, Edge 39, Edge 41, Edge 43, and Edge 55 are the most significantly influenced. These notations represent the first toe, the middle line on the sagittal plane, the lateral side of the ankle from the lower tibia to the cuboid, then passing the fibula and on to the very back of the Achilles' tendon. The ankle rotates more than the other part in the mid-foot and hind foot area. The role of the ankle as a location of multiple joints connecting together would be one of the reasons for the obvious deformation.

In the evaluation and comparison of selected angles folding, foot ankle, dorsal surface curve deformation, and the plantar in the mid-foot and forefoot were taken into consideration. Among all the settings, the inversion and eversion postures showed the least influence on the angle change. In the settings only the relative angles located in the midfoot turned out to deform with the rotation angles. However, a slight twisting posture happened in the inversion and eversion tests. The twisting is inferred to keep the body balanced, and the foot will move the force area apart in response to the friction from the side.

Relatively, the forefoot will respond more to the plantar flexion and dorsiflexion settings. Compared to the simple slope, the high heel shoes platforms restricted the foot heel rotation. Mostly the dorsal curve and the plantar would respond to the rotation angles, which was more obvious on the high heel platforms. This may due to the bottom keeping flat to support the body, and in response to the flat heel support the ankle will not deform to a large scale.

Especially in the walking postures, almost every part on the foot turned out to deform all the time in one gait cycle. Fifteen angles out of 16 reported to be significantly affected by the time in the stance phase. The complex angle changes were not in the linear regulation, but the deformed results are deduced to happen together with pronation and supination. The regression equations of the angles are still in exploration; for future research the foot is expected to be predicted in the model.

6.3 Limitation and future work

In this study a series of foot motions in dynamic situation were investigated. The result showed obvious changes in the foot surface shape, the distances between attached landmarks, and the angle extracted from the inner structure. Exploration to illustrate the foot dynamic movement was tested, and current result is able to provide knowledge on foot surface deformation. However, the current results can only provide the changes in distance and angle. To obtain a complete shape of the foot motion, more programming and analysis are needed. The development of the foot model is now in the early stages, which also means the potential for future achievement.

In the future research is possible to obtain a consistent prediction of foot significant joints, to calculate the overall ranges taken during dynamic situations for footwear design, and to form a visual foot shape prediction with the surface point cloud. The expected results are able to direct the design of footwear, especially high heel shoes and sports footwear. The dynamic foot will attract increasing attention to fulfill the knowledge of the ergonomic field.

APPENDICES

APPENDIX A CONSENT FORM

Subject No.	

DYNAMIC FOOT MODELING

Aim and objectives

- To investigate the joint motion changes that influence or be influenced during walking movement;
- To observe the shape deformation of foot surface when rotation angles change to different directions.
- To analyze the motion regulation during walking period, and to find the rule of angle change in significant joints.
- To form the foot dynamic model, to present foot deformation and motion range during walking.

Procedure

- Pointing 37 landmarks (Marker pen) on the surface of foot. (There will be direct contact on the foot surface.)
- Subject step on the platform in different directions and angles (9 of slopes with angles, 3 of high-heel platforms). The static shapes in standing position will be scanned and saved as 3D pictures. The whole surface will be recorded.
- Subject fix posture at 4 selected time during walking. The shape will be recorded within 30 seconds with 3D scanner.
- The landmarks can be removed with antiseptic wet tissue.

Notice

- The personal image or figure of any body part (except the right foot) **will not** be presented in the final work. Nor will the image be made for commercial use.
- The whole procedure **may** be finished in a two-time experiment.

Subject No.	

CONSENT TO PARTICIPATE IN RESEARCH

I _______________ hereby consent to participate in the captioned research conducted by the Hong Kong Polytechnic University.

I understand that information obtained from this research may be used in future research and publishes. However, my right to privacy will be retained, i.e. my personal details will not be revealed.

The procedure as set out in the attached information sheet has been fully explained. I understand the benefit and risks involved. My participation in the project is voluntary.

I acknowledge that I have the right to question any part of the procedure and can withdraw at any time.

Name of participant:	Signature of participant:
__________________	______________________
Name of researcher:	**Signature of researcher:**
__________________	______________________
	Date:
	______________________

APPENDIX B

PERSONAL INFORMATION FORM

Subject No.	

PERSONAL INFORMATION

Age		
Height (cm)		
Weight (kg)		
Foot Length (cm)	Right	Left
Foot Width (Brannock)	Right	Left
Ball Girth (cm)	Right	Left

Telephone Num. ____

Email Address: ____

APPENDIX C

THE SHIFTED PATH OF ONE SAME LANDMARK DISPLAYED IN THE 2D COORDINATE SYSTEM

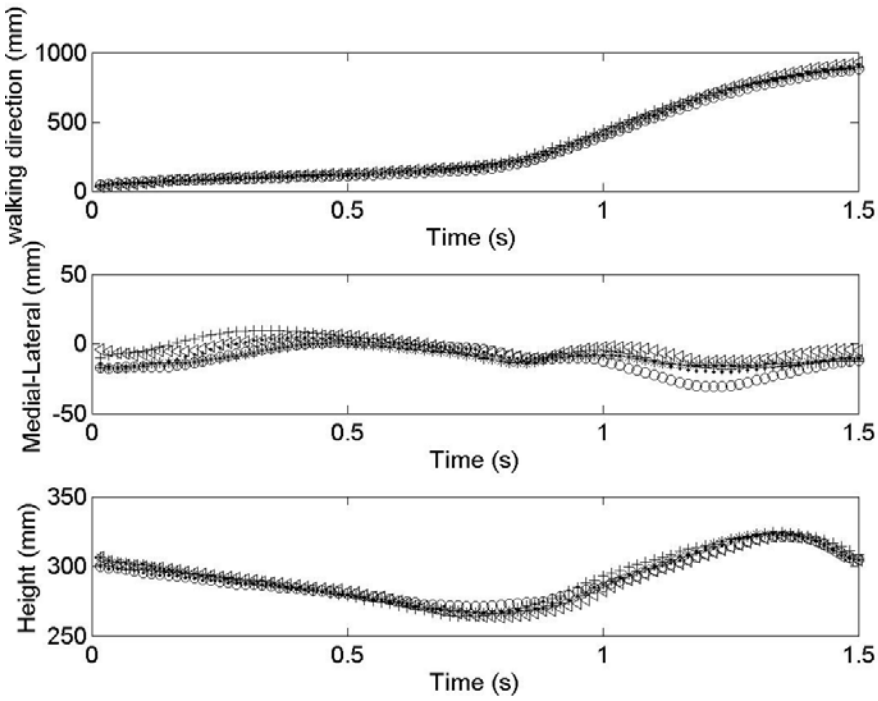

(1) The three dimensions trajectories of MIDTIB

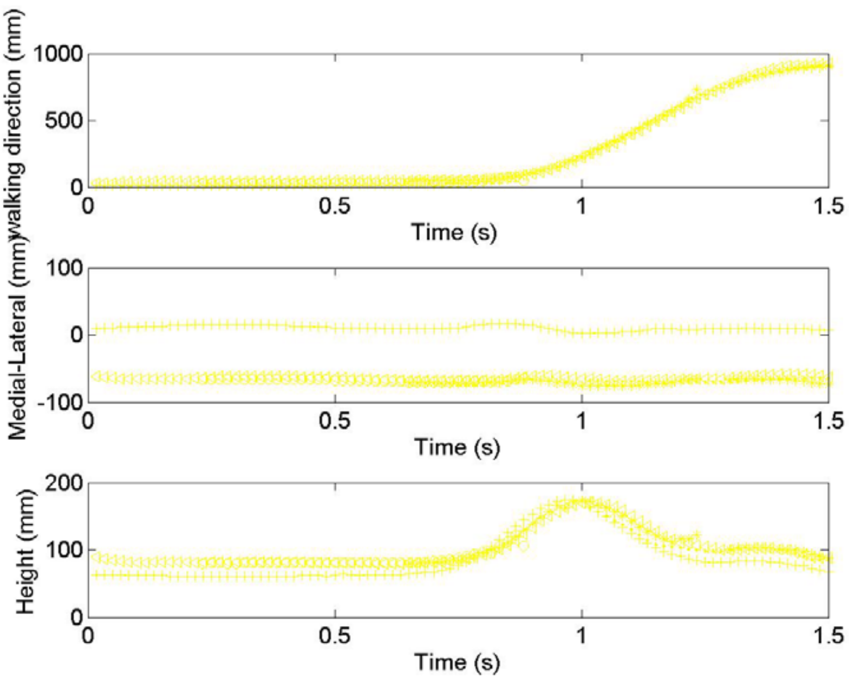

(2) The three dimensions trajectories of TENCAL

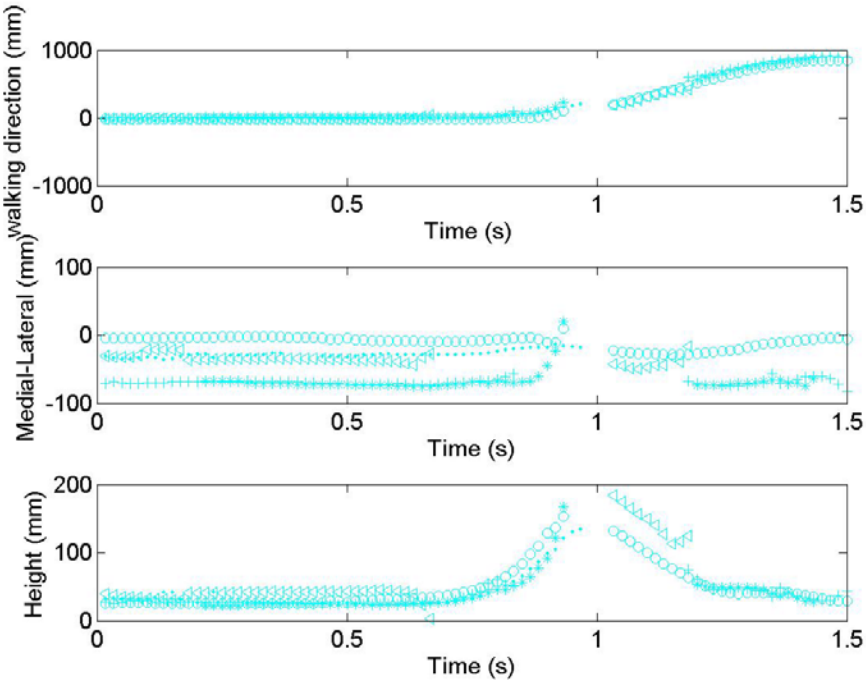

(3) The three dimensions trajectories of LATMAL

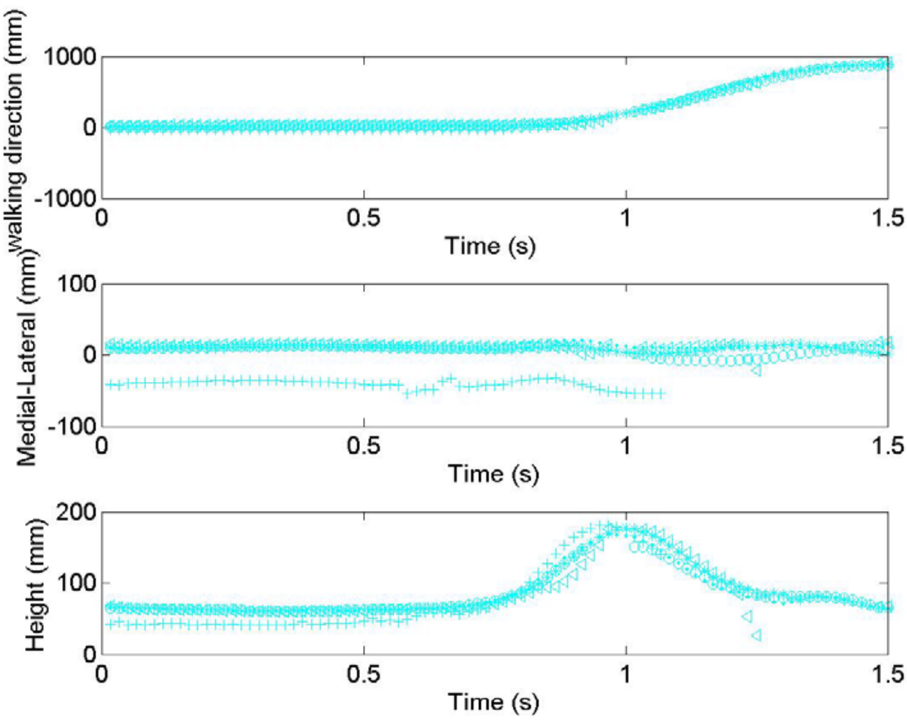

(4) The three dimensions trajectories of MEDMAL

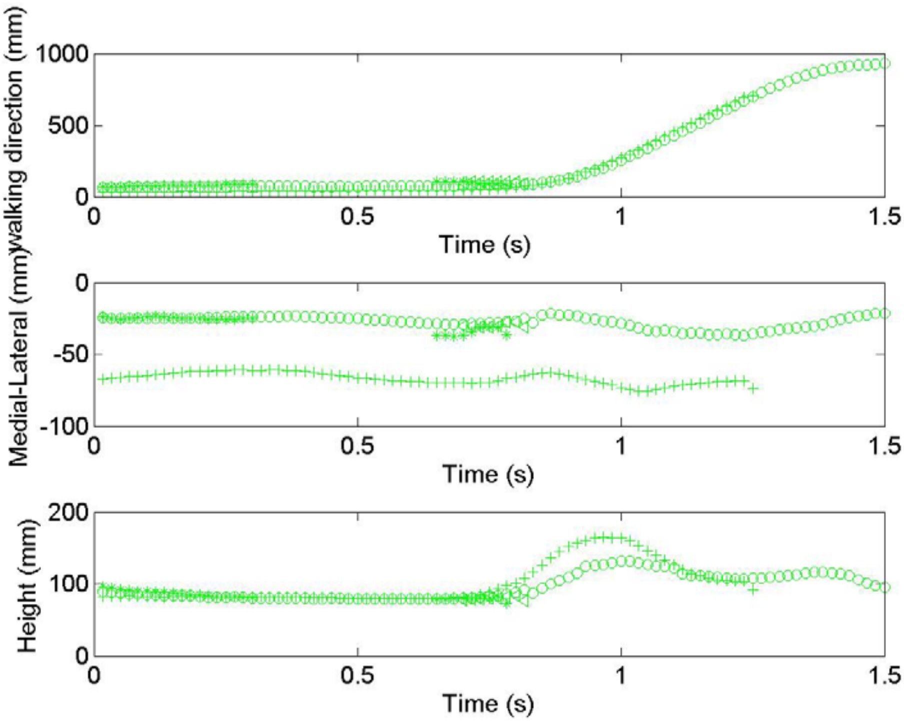

(5) The three dimensions trajectories of ANTLOWTIB

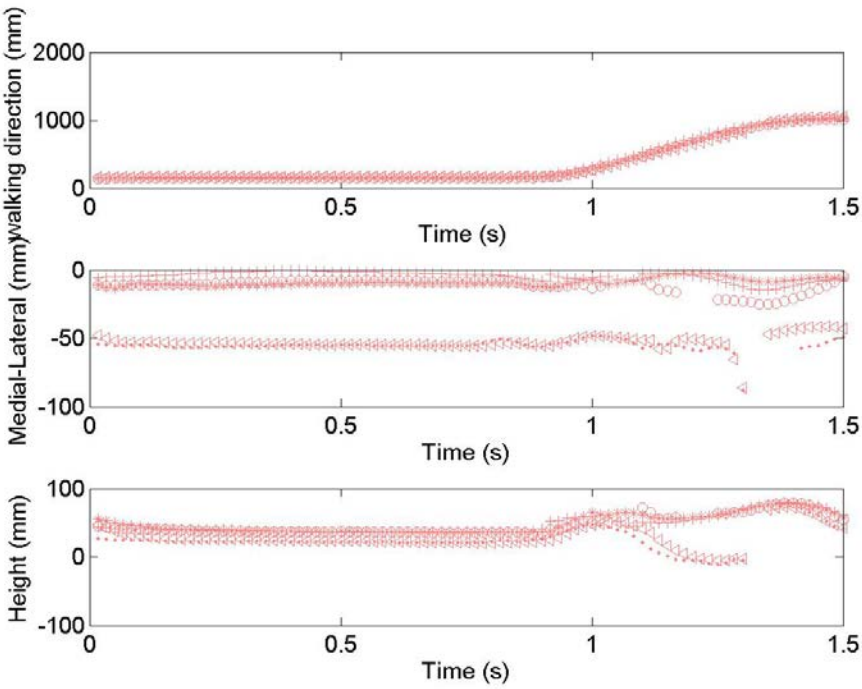

(6) The three dimensions trajectories of MPJ1

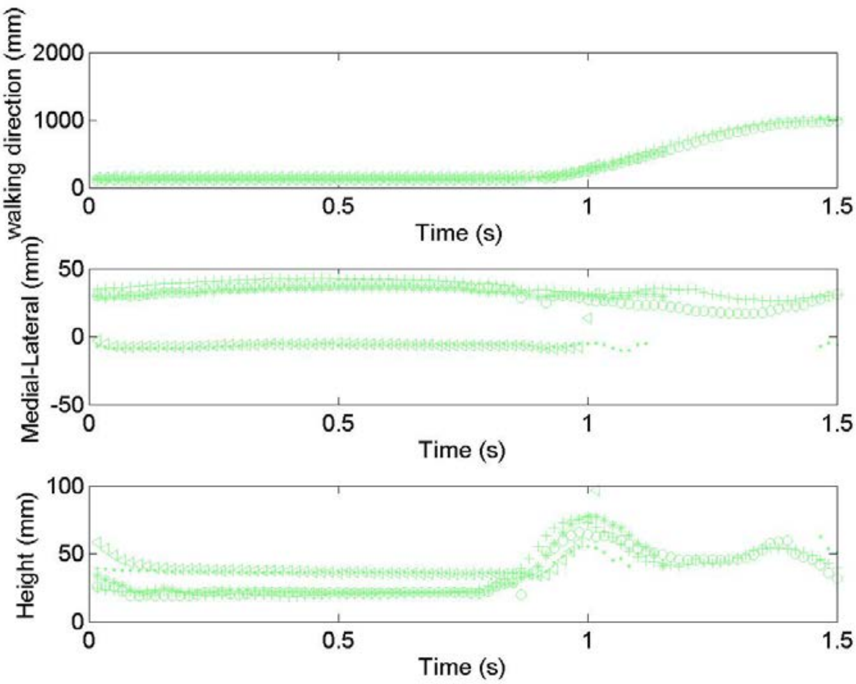

(7) The three dimensions trajectories of MPJ2

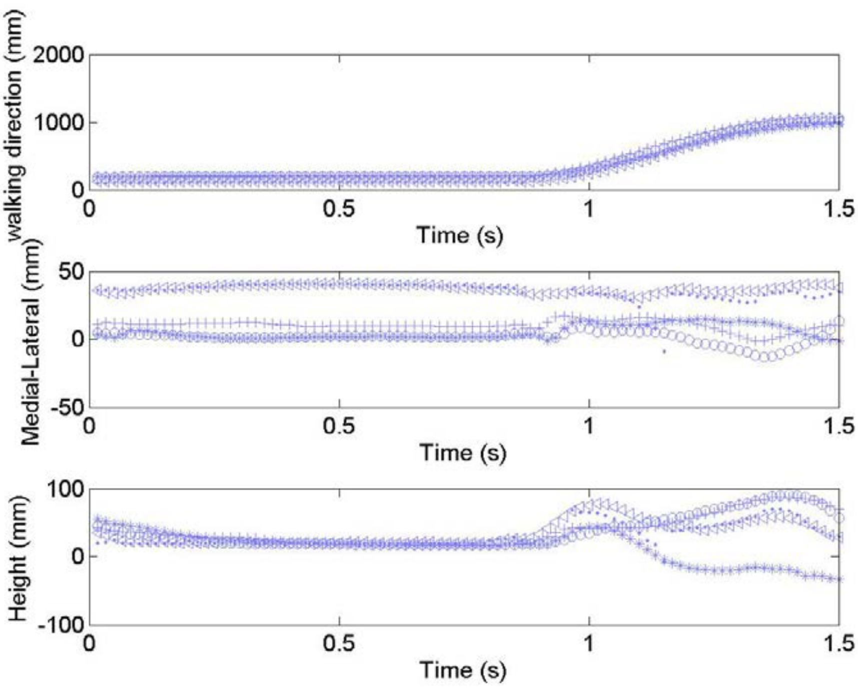

(8) The three dimensions trajectories of MPJ5

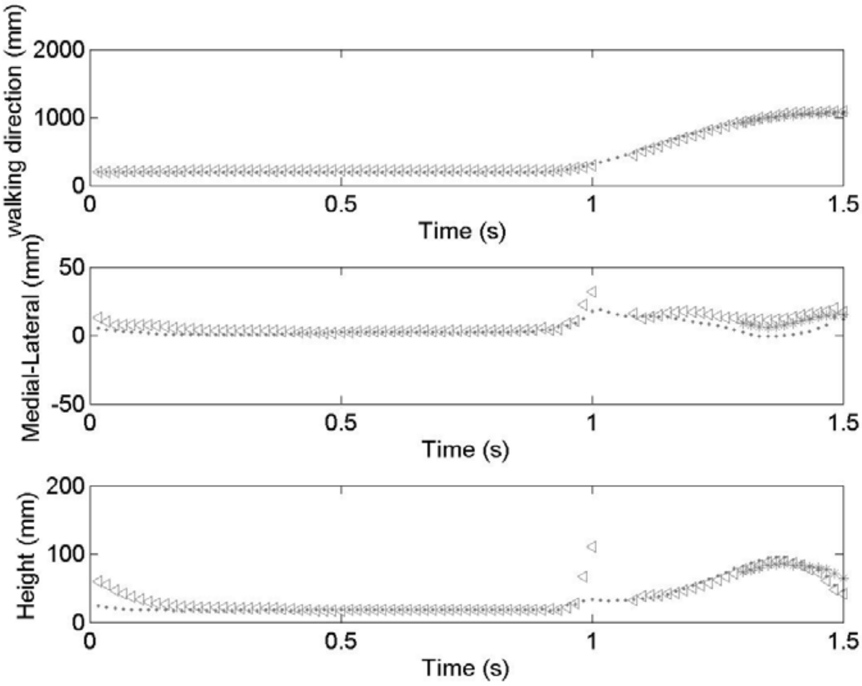

(9) The three dimensions trajectories of TP2

APPENDIX D

THE DESCRIPTIVE OF DISTANCES BETWEEN LANDMARKS

(Heel=0)

Distance	Mean	Std. Deviation	Distance	Mean	Std. Deviation	Distance	Mean	Std. Deviation
D_11_1	58.1	4.82	D_12_15	34.9	6.26	D_36_26	63.1	6.60
D_1_6	52.7	4.47	D_16_13	42.0	7.25	D_26_27	28.7	5.12
D_6_11	21.4	3.22	D_14_16	54.1	6.39	D_27_36	54.9	6.28
D_1_2	25.1	3.79	D_18_16	47.8	4.38	D_36_37	29.0	6.73
D_2_6	56.2	5.35	D_14_18	35.3	6.63	D_37_27	64.4	7.60
D_2_7	46.5	3.42	D_17_14	64.1	5.15	D_27_28	28.2	4.73
D_7_6	23.6	3.71	D_15_17	32.4	9.69	D_28_37	58.8	7.90
D_2_3	19.0	2.37	D_17_18	65.8	7.19	D_19_29	33.9	8.26
D_3_7	43.3	3.78	D_18_20	66.8	4.63	D_29_18	68.0	5.85
D_3_8	40.8	4.14	D_20_17	62.8	10.65	D_26_29	51.9	5.93
D_8_7	15.2	2.12	D_17_22	67.5	6.71	D_29_30	28.5	5.81
D_3_4	16.5	2.45	D_22_20	48.6	3.55	D_30_26	62.3	5.26
D_4_8	35.9	3.66	D_18_19	58.0	5.19	D_30_27	55.5	5.21
D_4_9	37.1	3.95	D_19_16	48.0	5.93	D_30_31	28.5	6.53
D_9_8	14.3	1.90	D_19_21	61.6	3.89	D_31_27	66.6	6.25
D_4_5	18.0	2.82	D_21_16	71.3	7.28	D_31_28	61.9	6.41
D_5_9	29.8	3.32	D_21_23	35.2	4.38	D_25_35	61.6	6.09
D_5_10	34.6	3.90	D_23_24	23.0	4.17	D_35_32	49.8	4.78
D_10_9	19.5	2.34	D_24_21	37.1	4.28	D_32_25	37.6	7.31
D_5_12	38.2	3.89	D_22_23	38.0	4.99	D_36_32	58.9	5.91
D_12_10	14.2	2.62	D_24_22	42.5	4.98	D_36_33	53.7	5.62
D_13_11	50.8	6.99	D_24_20	54.9	5.62	D_33_32	30.3	5.79
D_6_13	57.7	6.23	D_24_19	68.9	6.36	D_37_33	62.5	6.20
D_6_14	59.6	5.33	D_24_25	23.7	4.04	D_37_34	58.9	5.92
D_14_13	47.4	4.33	D_25_20	50.7	5.40	D_34_33	29.8	6.17
D_7_14	59.4	5.47	D_25_19	57.0	5.91	D_32_19	61.1	5.76
D_8_14	60.1	5.77	D_20_35	39.1	7.33	D_32_29	51.3	5.17
D_9_14	60.3	5.91	D_35_18	70.9	6.75	D_30_32	61.1	5.77
D_10_14	63.1	5.89	D_35_26	55.1	5.67	D_30_33	52.5	5.30
D_10_15	41.7	6.04	D_26_18	35.7	11.35	D_34_30	60.6	5.12
D_15_14	68.1	4.03	D_35_36	29.8	6.19	D_34_31	56.7	5.78

(Heel=70mm)

Distance	Mean	Std. Deviation	Distance	Mean	Std. Deviation	Distance	Mean	Std. Deviation
D_11_1	55.9	5.37	D_12_15	32.6	7.01	D_36_26	62.2	4.59
D_1_6	46.5	4.65	D_16_13	43.4	6.73	D_26_27	30.6	4.26
D_6_11	23.1	3.02	D_14_16	52.4	5.69	D_27_36	52.4	4.46
D_1_2	24.0	3.60	D_18_16	49.4	7.44	D_36_37	29.6	6.84
D_2_6	51.3	4.48	D_14_18	42.0	8.21	D_37_27	62.5	6.59
D_2_7	42.8	3.73	D_17_14	63.4	5.22	D_27_28	28.3	4.54
D_7_6	22.5	3.21	D_15_17	35.7	14.69	D_28_37	55.3	5.67
D_2_3	17.9	2.17	D_17_18	68.9	7.40	D_19_29	31.3	6.81
D_3_7	39.7	3.50	D_18_20	66.4	4.61	D_29_18	72.5	11.26
D_3_8	38.4	3.76	D_20_17	65.0	10.32	D_26_29	50.8	5.45
D_8_7	14.6	2.00	D_17_22	68.4	7.70	D_29_30	28.7	5.64
D_3_4	16.8	2.13	D_22_20	44.8	3.96	D_30_26	62.2	5.43
D_4_8	33.5	3.33	D_18_19	59.7	9.11	D_30_27	54.0	5.28
D_4_9	35.1	3.90	D_19_16	49.5	7.99	D_30_31	28.3	6.01
D_9_8	14.1	1.84	D_19_21	52.7	5.32	D_31_27	64.8	6.80
D_4_5	17.3	3.27	D_21_16	69.8	9.49	D_31_28	59.3	6.10
D_5_9	28.1	3.29	D_21_23	36.7	4.25	D_25_35	57.8	5.01
D_5_10	32.7	3.54	D_23_24	19.4	2.87	D_35_32	50.6	4.87
D_10_9	17.5	2.41	D_24_21	36.4	4.05	D_32_25	28.8	6.53
D_5_12	38.8	3.60	D_22_23	37.5	4.96	D_36_32	57.5	5.53
D_12_10	14.4	2.90	D_24_22	41.2	5.07	D_36_33	53.3	5.15
D_13_11	48.9	6.42	D_24_20	53.2	5.65	D_33_32	27.2	5.45
D_6_13	52.7	5.67	D_24_19	64.4	6.91	D_37_33	61.1	5.93
D_6_14	59.0	5.26	D_24_25	17.9	2.78	D_37_34	57.3	5.74
D_14_13	48.6	4.01	D_25_20	51.3	5.19	D_34_33	28.4	5.71
D_7_14	57.9	5.54	D_25_19	57.0	6.47	D_32_19	61.7	6.22
D_8_14	58.7	5.52	D_20_35	38.0	6.96	D_32_29	52.2	6.58
D_9_14	60.2	5.98	D_35_18	75.1	9.01	D_30_32	59.6	6.14
D_10_14	64.6	5.63	D_35_26	53.2	4.79	D_30_33	52.9	6.18
D_10_15	39.0	6.46	D_26_18	43.1	14.60	D_34_30	60.9	5.61
D_15_14	69.4	4.44	D_35_36	28.4	5.81	D_34_31	56.5	6.87

(Heel=40mm)

Distance	Mean	Std. Deviation	Distance	Mean	Std. Deviation	Distance	Mean	Std. Deviation
D_11_1	56.7	4.01	D_12_15	34.2	6.13	D_36_26	63.5	5.47
D_1_6	49.2	3.48	D_16_13	42.8	6.98	D_26_27	29.7	4.36
D_6_11	21.9	2.97	D_14_16	52.3	6.19	D_27_36	54.1	4.97
D_1_2	23.9	4.41	D_18_16	48.4	6.32	D_36_37	29.0	6.37
D_2_6	52.3	3.95	D_14_18	39.9	6.99	D_37_27	63.9	6.67
D_2_7	44.4	3.50	D_17_14	63.3	7.31	D_27_28	28.2	5.01
D_7_6	22.5	3.55	D_15_17	34.5	13.35	D_28_37	56.9	6.51
D_2_3	18.1	2.67	D_17_18	67.6	7.55	D_19_29	32.9	6.83
D_3_7	40.8	3.37	D_18_20	66.7	4.84	D_29_18	71.2	8.93
D_3_8	39.6	3.37	D_20_17	65.2	11.51	D_26_29	51.0	5.41
D_8_7	14.3	2.27	D_17_22	68.3	7.86	D_29_30	28.8	5.27
D_3_4	16.4	2.76	D_22_20	46.1	3.75	D_30_26	62.2	5.79
D_4_8	34.5	2.61	D_18_19	58.0	7.83	D_30_27	54.9	6.62
D_4_9	35.8	2.60	D_19_16	47.9	5.57	D_30_31	28.2	6.76
D_9_8	14.1	2.16	D_19_21	58.1	5.32	D_31_27	66.2	7.78
D_4_5	17.1	2.26	D_21_16	70.8	6.91	D_31_28	61.1	7.96
D_5_9	28.4	3.35	D_21_23	36.0	4.43	D_25_35	58.4	6.58
D_5_10	34.5	3.74	D_23_24	20.6	3.23	D_35_32	49.4	5.22
D_10_9	18.7	2.93	D_24_21	37.6	3.68	D_32_25	32.4	6.18
D_5_12	39.4	3.34	D_22_23	38.1	5.70	D_36_32	57.6	6.29
D_12_10	14.3	2.44	D_24_22	42.1	5.79	D_36_33	52.4	6.27
D_13_11	49.3	6.49	D_24_20	52.9	5.84	D_33_32	28.1	5.29
D_6_13	54.3	6.32	D_24_19	67.4	7.42	D_37_33	61.2	7.44
D_6_14	59.9	5.78	D_24_25	20.00	3.14	D_37_34	57.1	7.60
D_14_13	47.7	4.46	D_25_20	50.5	5.00	D_34_33	29.5	5.48
D_7_14	58.7	5.40	D_25_19	58.6	6.47	D_32_19	62.8	6.98
D_8_14	59.2	5.01	D_20_35	38.0	6.67	D_32_29	52.4	6.79
D_9_14	60.5	5.28	D_35_18	74.3	7.29	D_30_32	61.1	6.08
D_10_14	63.5	5.48	D_35_26	54.7	4.79	D_30_33	53.4	6.54
D_10_15	40.0	5.59	D_26_18	40.6	10.69	D_34_30	61.0	7.02
D_15_14	68.0	4.20	D_35_36	29.4	5.51	D_34_31	56.6	7.08

(Heel=10mm)

Distance	Mean	Std. Deviation	Distance	Mean	Std. Deviation	Distance	Mean	Std. Deviation
D_11_1	56.5	4.85	D_12_15	34.3	6.45	D_36_26	62.0	6.03
D_1_6	49.8	3.95	D_16_13	41.3	6.78	D_26_27	28.8	4.76
D_6_11	21.5	2.59	D_14_16	53.2	5.81	D_27_36	53.9	6.00
D_1_2	22.9	4.93	D_18_16	48.2	4.06	D_36_37	28.1	6.50
D_2_6	53.4	4.31	D_14_18	37.0	7.12	D_37_27	62.7	7.40
D_2_7	44.8	4.23	D_17_14	63.9	4.83	D_27_28	27.8	4.22
D_7_6	23.2	3.37	D_15_17	33.0	10.80	D_28_37	56.7	7.33
D_2_3	17.7	2.20	D_17_18	66.4	7.11	D_19_29	32.4	7.30
D_3_7	41.3	4.17	D_18_20	66.5	4.89	D_29_18	67.6	5.01
D_3_8	39.9	3.94	D_20_17	62.9	11.40	D_26_29	50.7	4.82
D_8_7	14.8	2.12	D_17_22	67.3	6.83	D_29_30	28.6	5.52
D_3_4	16.2	2.33	D_22_20	47.2	4.00	D_30_26	61.1	5.45
D_4_8	34.6	3.57	D_18_19	57.4	5.07	D_30_27	54.3	5.55
D_4_9	36.2	4.00	D_19_16	48.9	5.83	D_30_31	31.6	22.43
D_9_8	14.0	1.60	D_19_21	60.2	5.09	D_31_27	67.5	17.89
D_4_5	17.6	2.68	D_21_16	70.7	7.02	D_31_28	63.3	22.02
D_5_9	29.0	4.18	D_21_23	35.8	5.04	D_25_35	61.7	7.13
D_5_10	34.5	4.87	D_23_24	21.5	4.04	D_35_32	51.0	6.05
D_10_9	19.0	2.84	D_24_21	37.3	4.70	D_32_25	37.5	16.40
D_5_12	39.3	4.14	D_22_23	38.8	4.85	D_36_32	59.9	8.13
D_12_10	14.1	2.42	D_24_22	43.4	5.07	D_36_33	53.7	6.17
D_13_11	51.6	6.99	D_24_20	54.6	5.41	D_33_32	30.9	9.71
D_6_13	57.5	6.53	D_24_19	67.5	7.12	D_37_33	61.8	6.71
D_6_14	60.3	5.36	D_24_25	22.3	3.67	D_37_34	58.7	7.28
D_14_13	47.9	3.92	D_25_20	51.3	5.75	D_34_33	28.7	5.70
D_7_14	59.6	5.92	D_25_19	56.9	6.79	D_32_19	62.9	10.72
D_8_14	59.9	5.57	D_20_35	41.3	12.76	D_32_29	52.7	7.72
D_9_14	60.5	5.38	D_35_18	72.9	12.70	D_30_32	60.8	6.80
D_10_14	63.3	4.75	D_35_26	55.1	9.77	D_30_33	53.4	6.84
D_10_15	41.1	6.49	D_26_18	36.5	6.84	D_34_30	60.6	7.79
D_15_14	67.3	4.00	D_35_36	30.3	10.30	D_34_31	59.7	17.81

(Dorsiflexion=25°)

Distance	Mean	Std. Deviation	Distance	Mean	Std. Deviation	Distance	Mean	Std. Deviation
D_11_1	59.6	4.85	D_12_15	34.9	5.74	D_36_26	60.9	5.69
D_1_6	52.2	4.28	D_16_13	42.9	6.83	D_26_27	30.5	4.08
D_6_11	22.3	3.00	D_14_16	54.4	6.49	D_27_36	51.7	5.04
D_1_2	24.3	4.40	D_18_16	48.9	5.44	D_36_37	29.6	6.13
D_2_6	56.3	5.28	D_14_18	41.7	8.63	D_37_27	61.9	6.87
D_2_7	46.2	4.29	D_17_14	62.5	6.15	D_27_28	28.7	4.42
D_7_6	24.6	2.914	D_15_17	34.1	13.94	D_28_37	55.1	6.60
D_2_3	18.8	2.32	D_17_18	67.2	8.13	D_19_29	35.5	27.79
D_3_7	42.7	4.22	D_18_20	64.2	5.01	D_29_18	73.8	19.96
D_3_8	40.4	4.07	D_20_17	62.7	10.40	D_26_29	53.1	25.19
D_8_7	15.3	1.96	D_17_22	66.5	7.32	D_29_30	32.9	30.12
D_3_4	17.2	2.24	D_22_20	43.5	3.41	D_30_26	60.9	4.80
D_4_8	35.8	4.20	D_18_19	57.1	5.87	D_30_27	52.4	4.47
D_4_9	36.6	4.02	D_19_16	47.1	5.40	D_30_31	28.2	6.67
D_9_8	14.8	1.72	D_19_21	54.1	5.46	D_31_27	64.0	5.87
D_4_5	18.1	2.53	D_21_16	67.7	6.25	D_31_28	58.5	5.10
D_5_9	30.4	3.52	D_21_23	37.2	4.87	D_25_35	57.1	5.54
D_5_10	35.3	3.96	D_23_24	18.7	3.50	D_35_32	50.7	4.94
D_10_9	19.7	2.64	D_24_21	35.9	4.28	D_32_25	29.2	11.66
D_5_12	39.1	3.47	D_22_23	36.9	4.83	D_36_32	58.0	6.43
D_12_10	13.6	3.07	D_24_22	41.4	5.58	D_36_33	53.4	5.23
D_13_11	50.5	7.12	D_24_20	52.1	5.05	D_33_32	28.2	7.62
D_6_13	58.2	6.10	D_24_19	67.1	7.05	D_37_33	61.6	6.40
D_6_14	62.8	6.26	D_24_25	18.1	2.96	D_37_34	57.5	5.64
D_14_13	48.2	4.22	D_25_20	51.4	5.22	D_34_33	28.6	5.89
D_7_14	62.7	6.38	D_25_19	57.0	6.45	D_32_19	62.5	6.33
D_8_14	63.2	6.32	D_20_35	38.3	9.93	D_32_29	56.7	31.94
D_9_14	63.8	6.42	D_35_18	73.8	9.14	D_30_32	59.8	7.16
D_10_14	65.8	6.01	D_35_26	52.7	7.62	D_30_33	53.2	6.60
D_10_15	41.7	6.04	D_26_18	41.9	10.11	D_34_30	61.0	6.40
D_15_14	67.5	3.52	D_35_36	29.4	7.92	D_34_31	56.3	7.12

(Dorsiflexion=12.5°)

Distance	Mean	Std. Deviation	Distance	Mean	Std. Deviation	Distance	Mean	Std. Deviation
D_11_1	58.0	4.85	D_12_15	34.4	6.75	D_36_26	61.0	6.17
D_1_6	51.6	4.60	D_16_13	42.4	6.97	D_26_27	30.0	4.65
D_6_11	21.3	2.74	D_14_16	53.3	5.27	D_27_36	51.7	5.58
D_1_2	25.3	4.10	D_18_16	48.1	4.12	D_36_37	30.1	5.61
D_2_6	55.9	5.24	D_14_18	38.6	7.32	D_37_27	62.1	7.07
D_2_7	46.5	3.72	D_17_14	62.2	5.14	D_27_28	28.0	4.13
D_7_6	24.40	3.13	D_15_17	33.0	10.78	D_28_37	55.0	6.86
D_2_3	18.6	2.65	D_17_18	66.0	7.91	D_19_29	31.8	6.68
D_3_7	43.1	3.52	D_18_20	64.4	4.87	D_29_18	68.8	4.63
D_3_8	40.4	3.34	D_20_17	63.0	11.14	D_26_29	50.1	3.98
D_8_7	14.8	2.19	D_17_22	66.2	6.67	D_29_30	28.9	4.99
D_3_4	17.0	2.11	D_22_20	45.3	3.36	D_30_26	61.8	4.52
D_4_8	35.8	3.57	D_18_19	56.2	4.12	D_30_27	53.8	4.75
D_4_9	36.5	3.90	D_19_16	47.7	7.39	D_30_31	28.4	5.92
D_9_8	15.3	1.89	D_19_21	59.2	4.87	D_31_27	65.8	5.95
D_4_5	18.2	2.09	D_21_16	69.1	6.66	D_31_28	60.2	5.46
D_5_9	29.6	3.67	D_21_23	36.0	4.76	D_25_35	58.2	6.07
D_5_10	34.7	4.12	D_23_24	21.0	3.61	D_35_32	49.1	5.32
D_10_9	19.3	2.57	D_24_21	37.3	4.01	D_32_25	32.7	7.29
D_5_12	37.8	4.25	D_22_23	36.6	5.00	D_36_32	57.0	5.89
D_12_10	13.6	2.16	D_24_22	41.2	5.56	D_36_33	52.5	5.43
D_13_11	49.9	6.91	D_24_20	51.9	5.66	D_33_32	28.4	5.63
D_6_13	57.1	6.65	D_24_19	68.1	6.56	D_37_33	61.1	6.07
D_6_14	62.4	5.14	D_24_25	20.6	3.46	D_37_34	57.1	5.54
D_14_13	48.2	3.66	D_25_20	50.1	5.29	D_34_33	28.8	5.19
D_7_14	61.3	5.29	D_25_19	58.6	5.49	D_32_19	62.2	6.21
D_8_14	62.0	5.48	D_20_35	39.1	6.70	D_32_29	51.4	5.77
D_9_14	62.6	5.54	D_35_18	71.5	6.36	D_30_32	60.2	5.97
D_10_14	64.3	4.96	D_35_26	52.2	4.22	D_30_33	52.6	5.74
D_10_15	40.9	6.50	D_26_18	38.2	6.76	D_34_30	60.3	7.04
D_15_14	66.9	3.76	D_35_36	28.2	5.93	D_34_31	56.5	7.07

(Plantar flexion=10°)

Distance	Mean	Std. Deviation	Distance	Mean	Std. Deviation	Distance	Mean	Std. Deviation
D_11_1	57.5	4.74	D_12_15	34.1	6.31	D_36_26	60.7	5.94
D_1_6	53.0	4.42	D_16_13	41.1	6.97	D_26_27	26.7	5.05
D_6_11	21.71	2.66	D_14_16	53.5	5.98	D_27_36	53.5	5.62
D_1_2	26.45	3.92	D_18_16	48.6	5.99	D_36_37	29.0	6.15
D_2_6	55.2	4.69	D_14_18	32.4	7.75	D_37_27	62.1	7.45
D_2_7	46.0	4.53	D_17_14	62.8	6.43	D_27_28	27.6	4.18
D_7_6	22.72	3.78	D_15_17	34.4	12.46	D_28_37	56.6	7.53
D_2_3	18.6	2.33	D_17_18	64.7	6.74	D_19_29	32.1	6.99
D_3_7	42.6	4.33	D_18_20	66.2	4.64	D_29_18	62.3	9.54
D_3_8	40.4	4.22	D_20_17	60.8	10.89	D_26_29	49.4	4.59
D_8_7	14.4	1.89	D_17_22	67.4	7.85	D_29_30	28.8	5.24
D_3_4	17.1	2.20	D_22_20	49.6	3.48	D_30_26	58.6	4.32
D_4_8	36.4	3.63	D_18_19	56.0	7.82	D_30_27	53.2	4.79
D_4_9	36.6	3.99	D_19_16	43.9	5.44	D_30_31	28.3	5.10
D_9_8	14.3	1.59	D_19_21	62.8	5.56	D_31_27	63.7	5.77
D_4_5	16.6	2.36	D_21_16	68.6	6.13	D_31_28	58.8	5.96
D_5_9	30.2	3.53	D_21_23	35.6	4.50	D_25_35	61.8	7.29
D_5_10	33.5	4.04	D_23_24	25.0	4.57	D_35_32	47.8	5.43
D_10_9	18.0	2.78	D_24_21	38.4	3.90	D_32_25	40.4	7.65
D_5_12	36.8	4.23	D_22_23	37.3	4.38	D_36_32	58.2	9.85
D_12_10	14.8	2.51	D_24_22	42.3	5.06	D_36_33	52.1	7.41
D_13_11	50.0	6.73	D_24_20	54.7	5.54	D_33_32	30.4	5.27
D_6_13	56.2	5.72	D_24_19	70.2	7.07	D_37_33	60.7	7.49
D_6_14	59.0	5.20	D_24_25	25.9	4.39	D_37_34	57.2	6.85
D_14_13	47.3	3.38	D_25_20	48.3	4.57	D_34_33	29.8	5.68
D_7_14	58.2	5.36	D_25_19	56.7	6.55	D_32_19	60.3	5.97
D_8_14	58.1	5.26	D_20_35	39.9	7.73	D_32_29	49.6	5.58
D_9_14	58.5	5.10	D_35_18	66.2	7.06	D_30_32	60.3	7.43
D_10_14	61.1	4.61	D_35_26	53.8	4.27	D_30_33	52.0	6.08
D_10_15	41.2	6.02	D_26_18	29.1	10.58	D_34_30	59.7	5.97
D_15_14	67.1	3.65	D_35_36	30.0	7.70	D_34_31	56.1	7.32

(Plantar flexion=20°)

Distance	Mean	Std. Deviation	Distance	Mean	Std. Deviation	Distance	Mean	Std. Deviation
D_11_1	58.3	4.91	D_12_15	33.6	5.81	D_36_26	28.8	6.23
D_1_6	52.6	4.15	D_16_13	40.5	6.99	D_26_27	63.1	7.16
D_6_11	22.4	2.98	D_14_16	53.4	5.43	D_27_36	27.0	5.21
D_1_2	26.3	4.48	D_18_16	48.6	4.75	D_36_37	57.7	6.92
D_2_6	54.3	4.61	D_14_18	27.0	6.51	D_37_27	32.1	6.40
D_2_7	46.3	4.82	D_17_14	63.9	5.05	D_27_28	59.1	4.27
D_7_6	22.7	3.38	D_15_17	33.7	10.42	D_28_37	50.4	4.52
D_2_3	18.4	2.97	D_17_18	64.7	6.09	D_19_29	28.8	4.46
D_3_7	43.7	5.09	D_18_20	68.2	4.98	D_29_18	58.4	4.77
D_3_8	41.3	4.86	D_20_17	58.6	11.61	D_26_29	53.9	5.12
D_8_7	14.6	2.19	D_17_22	66.5	6.24	D_29_30	29.9	18.12
D_3_4	17.4	3.05	D_22_20	49.8	3.97	D_30_26	65.3	11.36
D_4_8	37.1	3.89	D_18_19	56.4	4.27	D_30_27	61.6	14.82
D_4_9	36.8	4.29	D_19_16	41.1	6.11	D_30_31	62.8	7.57
D_9_8	13.8	1.74	D_19_21	64.2	5.83	D_31_27	46.0	4.27
D_4_5	17.7	2.48	D_21_16	69.2	7.23	D_31_28	42.6	8.51
D_5_9	30.7	3.69	D_21_23	35.7	4.15	D_25_35	56.8	6.64
D_5_10	33.0	4.71	D_23_24	26.0	5.48	D_35_32	50.1	5.21
D_10_9	18.3	2.99	D_24_21	39.7	3.91	D_32_25	31.6	5.36
D_5_12	36.4	5.21	D_22_23	37.0	4.13	D_36_32	60.0	6.74
D_12_10	15.7	3.17	D_24_22	41.6	5.30	D_36_33	55.6	5.98
D_13_11	49.9	6.73	D_24_20	55.6	4.52	D_33_32	29.7	5.37
D_6_13	56.8	6.16	D_24_19	71.5	8.23	D_37_33	59.1	5.62
D_6_14	60.2	4.57	D_24_25	26.4	5.24	D_37_34	49.3	7.11
D_14_13	47.7	3.41	D_25_20	47.4	4.34	D_34_33	61.4	7.51
D_7_14	57.8	4.88	D_25_19	57.3	7.50	D_32_19	51.9	6.07
D_8_14	57.9	5.02	D_20_35	39.6	6.91	D_32_29	58.7	6.09
D_9_14	58.5	5.29	D_35_18	63.7	5.39	D_30_32	58.6	18.42
D_10_14	61.5	5.25	D_35_26	55.5	4.63	D_30_33	28.8	6.23
D_10_15	41.1	5.18	D_26_18	23.2	5.33	D_34_30	63.1	7.16
D_15_14	68.3	4.05	D_35_36	28.5	5.63	D_34_31	27.0	5.21

(Inversion=10°)

Distance	Mean	Std. Deviation	Distance	Mean	Std. Deviation	Distance	Mean	Std. Deviation
D_11_1	58.0	4.90	D_12_15	35.2	5.98	D_36_26	62.0	6.45
D_1_6	52.9	4.50	D_16_13	41.6	6.96	D_26_27	28.2	4.83
D_6_11	21.9	2.87	D_14_16	53.8	5.78	D_27_36	54.3	5.65
D_1_2	25.5	4.06	D_18_16	48.0	4.45	D_36_37	29.1	5.94
D_2_6	56.1	4.79	D_14_18	34.9	6.67	D_37_27	63.4	7.34
D_2_7	46.3	3.79	D_17_14	63.4	5.01	D_27_28	27.8	4.64
D_7_6	23.7	3.40	D_15_17	32.9	10.42	D_28_37	57.6	7.26
D_2_3	18.6	2.30	D_17_18	66.0	7.21	D_19_29	32.7	7.21
D_3_7	43.0	3.95	D_18_20	66.5	4.44	D_29_18	66.4	4.83
D_3_8	40.6	3.87	D_20_17	63.6	11.15	D_26_29	50.6	5.79
D_8_7	14.9	2.03	D_17_22	67.5	6.44	D_29_30	28.7	5.71
D_3_4	17.0	2.45	D_22_20	48.3	4.01	D_30_26	60.8	5.08
D_4_8	35.8	3.44	D_18_19	56.8	4.85	D_30_27	54.4	5.35
D_4_9	36.7	3.77	D_19_16	46.6	6.14	D_30_31	28.4	6.23
D_9_8	14.5	1.83	D_19_21	61.8	5.43	D_31_27	65.5	6.13
D_4_5	17.7	2.51	D_21_16	70.4	7.11	D_31_28	60.8	6.58
D_5_9	29.7	3.45	D_21_23	35.7	4.60	D_25_35	60.9	6.15
D_5_10	34.1	3.93	D_23_24	22.9	4.19	D_35_32	48.6	4.61
D_10_9	19.2	2.71	D_24_21	37.5	4.02	D_32_25	38.0	7.36
D_5_12	37.5	4.10	D_22_23	37.2	4.85	D_36_32	57.7	6.18
D_12_10	14.4	2.55	D_24_22	41.9	5.15	D_36_33	52.4	5.53
D_13_11	50.3	6.74	D_24_20	53.9	6.15	D_33_32	30.1	5.13
D_6_13	56.9	6.21	D_24_19	70.0	7.84	D_37_33	61.4	6.83
D_6_14	60.1	5.56	D_24_25	23.3	3.98	D_37_34	57.8	6.23
D_14_13	48.2	3.76	D_25_20	49.4	5.26	D_34_33	29.4	5.88
D_7_14	59.8	5.45	D_25_19	58.2	7.15	D_32_19	61.7	6.10
D_8_14	60.4	5.59	D_20_35	40.2	6.99	D_32_29	51.9	6.72
D_9_14	60.5	5.61	D_35_18	70.4	6.49	D_30_32	61.8	6.52
D_10_14	63.1	5.27	D_35_26	54.5	5.22	D_30_33	53.5	6.52
D_10_15	41.9	5.61	D_26_18	35.3	9.17	D_34_30	61.2	6.65
D_15_14	67.8	4.01	D_35_36	29.2	6.12	D_34_31	57.6	6.86

(Inversion=5°)

Distance	Mean	Std. Deviation	Distance	Mean	Std. Deviation	Distance	Mean	Std. Deviation
D_11_1	58.2	4.70	D_12_15	35.5	5.91	D_36_26	61.0	6.38
D_1_6	53.5	4.21	D_16_13	40.6	7.07	D_26_27	28.4	4.80
D_6_11	22.6	2.63	D_14_16	53.7	5.10	D_27_36	53.4	5.79
D_1_2	26.2	4.83	D_18_16	48.3	4.18	D_36_37	29.5	5.96
D_2_6	56.6	4.80	D_14_18	34.7	6.60	D_37_27	63.0	7.57
D_2_7	46.8	3.79	D_17_14	62.8	4.85	D_27_28	27.6	5.54
D_7_6	23.6	3.53	D_15_17	33.3	11.13	D_28_37	57.3	7.77
D_2_3	18.4	2.08	D_17_18	66.2	7.90	D_19_29	33.3	8.15
D_3_7	43.4	4.01	D_18_20	65.8	4.73	D_29_18	66.5	5.41
D_3_8	41.0	4.19	D_20_17	65.1	11.47	D_26_29	50.9	6.98
D_8_7	14.8	1.70	D_17_22	67.6	6.49	D_29_30	28.8	5.40
D_3_4	17.1	2.29	D_22_20	49.6	4.53	D_30_26	61.3	5.23
D_4_8	36.0	3.46	D_18_19	57.1	4.60	D_30_27	54.4	5.74
D_4_9	36.6	3.75	D_19_16	45.7	5.87	D_30_31	27.8	6.30
D_9_8	14.6	1.59	D_19_21	60.9	6.01	D_31_27	65.4	6.52
D_4_5	17.7	2.13	D_21_16	70.4	7.15	D_31_28	60.9	7.31
D_5_9	29.3	3.81	D_21_23	36.7	5.56	D_25_35	61.0	5.99
D_5_10	33.9	3.87	D_23_24	23.0	3.89	D_35_32	48.1	4.47
D_10_9	19.3	3.03	D_24_21	38.2	3.99	D_32_25	38.8	6.97
D_5_12	37.1	4.17	D_22_23	36.9	4.29	D_36_32	57.3	5.85
D_12_10	13.8	2.38	D_24_22	42.0	5.05	D_36_33	52.2	5.65
D_13_11	50.6	7.18	D_24_20	53.7	6.22	D_33_32	30.5	5.04
D_6_13	56.9	6.65	D_24_19	70.9	9.24	D_37_33	61.0	7.23
D_6_14	60.5	5.26	D_24_25	23.2	3.95	D_37_34	57.4	6.49
D_14_13	49.3	3.52	D_25_20	48.9	5.00	D_34_33	29.6	6.01
D_7_14	60.2	5.09	D_25_19	59.1	8.62	D_32_19	62.3	6.40
D_8_14	60.8	5.52	D_20_35	41.1	6.80	D_32_29	53.1	7.94
D_9_14	61.2	5.44	D_35_18	70.0	6.81	D_30_32	63.4	7.16
D_10_14	63.6	4.95	D_35_26	53.7	6.20	D_30_33	54.8	7.39
D_10_15	41.8	5.59	D_26_18	36.0	9.90	D_34_30	62.5	7.40
D_15_14	67.4	4.08	D_35_36	29.0	6.07	D_34_31	58.9	8.05

(Eversion=2.5°)

Distance	Mean	Std. Deviation	Distance	Mean	Std. Deviation	Distance	Mean	Std. Deviation
D_11_1	58.0	4.90	D_12_15	35.2	5.98	D_36_26	62.0	6.45
D_1_6	52.9	4.50	D_16_13	41.6	6.96	D_26_27	28.2	4.83
D_6_11	21.9	2.87	D_14_16	53.8	5.78	D_27_36	54.3	5.65
D_1_2	25.5	4.06	D_18_16	48.0	4.45	D_36_37	29.1	5.94
D_2_6	56.1	4.79	D_14_18	34.9	6.67	D_37_27	63.4	7.34
D_2_7	46.3	3.79	D_17_14	63.4	5.01	D_27_28	27.8	4.64
D_7_6	23.7	3.40	D_15_17	32.9	10.42	D_28_37	57.6	7.26
D_2_3	18.6	2.30	D_17_18	66.0	7.21	D_19_29	32.7	7.21
D_3_7	43.0	3.95	D_18_20	66.5	4.44	D_29_18	66.4	4.83
D_3_8	40.6	3.87	D_20_17	63.6	11.15	D_26_29	50.6	5.79
D_8_7	14.9	2.03	D_17_22	67.5	6.44	D_29_30	28.7	5.71
D_3_4	17.0	2.45	D_22_20	48.3	4.01	D_30_26	60.8	5.08
D_4_8	35.8	3.44	D_18_19	56.8	4.85	D_30_27	54.4	5.35
D_4_9	36.7	3.77	D_19_16	46.6	6.14	D_30_31	28.4	6.23
D_9_8	14.5	1.83	D_19_21	61.8	5.43	D_31_27	65.5	6.13
D_4_5	17.7	2.51	D_21_16	70.4	7.11	D_31_28	60.8	6.58
D_5_9	29.7	3.45	D_21_23	35.7	4.60	D_25_35	60.9	6.15
D_5_10	34.1	3.93	D_23_24	22.9	4.19	D_35_32	48.6	4.61
D_10_9	19.2	2.71	D_24_21	37.5	4.02	D_32_25	38.0	7.36
D_5_12	37.5	4.10	D_22_23	37.2	4.85	D_36_32	57.7	6.18
D_12_10	14.4	2.55	D_24_22	41.9	5.15	D_36_33	52.4	5.53
D_13_11	50.3	6.74	D_24_20	53.9	6.15	D_33_32	30.1	5.13
D_6_13	56.9	6.21	D_24_19	70.0	7.84	D_37_33	61.4	6.83
D_6_14	60.1	5.56	D_24_25	23.3	3.98	D_37_34	57.8	6.23
D_14_13	48.2	3.76	D_25_20	49.4	5.26	D_34_33	29.4	5.88
D_7_14	59.8	5.45	D_25_19	58.2	7.15	D_32_19	61.7	6.10
D_8_14	60.4	5.59	D_20_35	40.2	6.99	D_32_29	51.9	6.72
D_9_14	60.5	5.61	D_35_18	70.4	6.49	D_30_32	61.8	6.52
D_10_14	63.1	5.27	D_35_26	54.5	5.22	D_30_33	53.5	6.52
D_10_15	41.9	5.61	D_26_18	35.3	9.17	D_34_30	61.2	6.65
D_15_14	67.8	4.01	D_35_36	29.2	6.12	D_34_31	57.6	6.86

(Eversion=5°)

Distance	Mean	Std. Deviation	Distance	Mean	Std. Deviation	Distance	Mean	Std. Deviation
D_11_1	57.7	5.16	D_12_15	35.1	5.93	D_36_26	28.9	6.20
D_1_6	52.1	4.64	D_16_13	42.6	6.91	D_26_27	61.8	6.70
D_6_11	20.9	2.63	D_14_16	53.6	5.81	D_27_36	27.7	4.67
D_1_2	25.2	3.26	D_18_16	47.8	5.16	D_36_37	54.4	5.34
D_2_6	56.0	4.92	D_14_18	34.9	6.90	D_37_27	28.9	5.60
D_2_7	46.1	4.19	D_17_14	63.0	5.09	D_27_28	63.3	6.84
D_7_6	24.4	3.54	D_15_17	32.9	10.72	D_28_37	28.0	3.87
D_2_3	18.6	2.20	D_17_18	65.3	6.77	D_19_29	57.7	6.99
D_3_7	42.5	4.02	D_18_20	66.5	4.10	D_29_18	33.2	6.88
D_3_8	40.2	3.94	D_20_17	61.3	10.49	D_26_29	65.5	3.70
D_8_7	14.6	2.00	D_17_22	67.0	6.49	D_29_30	50.1	6.09
D_3_4	17.2	2.62	D_22_20	46.7	3.79	D_30_26	29.0	6.27
D_4_8	36.0	3.73	D_18_19	56.2	4.06	D_30_27	60.1	4.87
D_4_9	36.9	4.03	D_19_16	48.1	5.05	D_30_31	53.8	5.70
D_9_8	15.1	1.92	D_19_21	62.9	5.14	D_31_27	28.2	5.61
D_4_5	17.6	2.60	D_21_16	70.4	5.88	D_31_28	64.6	6.28
D_5_9	30.1	3.58	D_21_23	35.2	4.12	D_25_35	59.9	7.05
D_5_10	33.8	4.29	D_23_24	23.3	4.42	D_35_32	61.1	5.87
D_10_9	18.3	2.81	D_24_21	37.9	4.02	D_32_25	49.3	4.41
D_5_12	37.6	4.85	D_22_23	37.2	4.95	D_36_32	37.2	7.81
D_12_10	14.9	2.65	D_24_22	41.4	5.16	D_36_33	58.4	6.33
D_13_11	50.0	6.64	D_24_20	54.2	6.07	D_33_32	53.2	5.51
D_6_13	56.6	5.95	D_24_19	68.9	7.65	D_37_33	29.7	4.58
D_6_14	60.6	5.65	D_24_25	23.5	4.06	D_37_34	62.1	6.97
D_14_13	47.7	3.52	D_25_20	50.0	5.29	D_34_33	58.5	6.47
D_7_14	59.8	5.54	D_25_19	57.2	6.89	D_32_19	29.3	5.89
D_8_14	60.2	5.68	D_20_35	38.9	7.37	D_32_29	61.5	6.26
D_9_14	60.3	5.63	D_35_18	70.4	5.76	D_30_32	51.3	6.65
D_10_14	63.0	5.14	D_35_26	54.9	5.17	D_30_33	61.3	5.93
D_10_15	42.5	5.40	D_26_18	35.6	10.58	D_34_30	53.1	6.47
D_15_14	67.7	4.01	D_35_36	35.1	5.93	D_34_31	60.6	6.76

(Walk=0% of gait cycle)

Distance	Mean	Std. Deviation	Distance	Mean	Std. Deviation	Distance	Mean	Std. Deviation
D_11_1	57.1	6.58	D_12_15	31.8	6.20	D_36_26	62.1	5.70
D_1_6	51.0	5.90	D_16_13	42.8	7.87	D_26_27	28.3	4.25
D_6_11	21.4	3.66	D_14_16	51.1	6.72	D_27_36	53.9	5.62
D_1_2	21.8	4.75	D_18_16	46.6	3.97	D_36_37	28.5	5.71
D_2_6	51.8	6.23	D_14_18	36.8	7.37	D_37_27	63.1	7.03
D_2_7	46.0	4.07	D_17_14	62.2	4.91	D_27_28	27.4	4.42
D_7_6	19.3	3.38	D_15_17	33.5	11.98	D_28_37	56.4	6.60
D_2_3	15.3	3.34	D_17_18	66.3	7.68	D_19_29	32.0	5.29
D_3_7	42.0	4.23	D_18_20	65.4	5.23	D_29_18	66.4	4.64
D_3_8	41.5	4.83	D_20_17	61.5	12.07	D_26_29	50.0	4.76
D_8_7	13.4	1.97	D_17_22	66.3	6.81	D_29_30	28.2	5.35
D_3_4	15.6	3.77	D_22_20	47.1	3.73	D_30_26	59.9	4.85
D_4_8	35.6	4.42	D_18_19	55.0	4.70	D_30_27	53.1	5.08
D_4_9	37.4	5.44	D_19_16	45.5	5.47	D_30_31	28.0	4.78
D_9_8	13.5	1.80	D_19_21	59.2	5.16	D_31_27	63.7	6.14
D_4_5	17.1	3.29	D_21_16	68.3	5.73	D_31_28	58.8	5.91
D_5_9	29.5	4.61	D_21_23	35.8	4.97	D_25_35	61.5	6.02
D_5_10	35.0	6.19	D_23_24	22.2	4.60	D_35_32	52.3	6.61
D_10_9	17.1	2.81	D_24_21	38.5	4.84	D_32_25	35.0	8.83
D_5_12	38.7	6.50	D_22_23	38.1	5.23	D_36_32	59.4	7.76
D_12_10	13.7	3.03	D_24_22	42.6	5.59	D_36_33	56.0	7.85
D_13_11	49.5	8.05	D_24_20	56.0	4.89	D_33_32	28.9	4.99
D_6_13	54.0	7.22	D_24_19	66.2	6.77	D_37_33	63.3	8.30
D_6_14	58.5	6.50	D_24_25	21.5	4.50	D_37_34	60.4	7.59
D_14_13	45.0	4.30	D_25_20	53.3	5.58	D_34_33	28.1	4.90
D_7_14	56.5	5.80	D_25_19	57.1	6.65	D_32_19	63.8	6.96
D_8_14	55.8	6.38	D_20_35	40.0	6.89	D_32_29	50.5	6.69
D_9_14	56.4	6.00	D_35_18	70.8	6.27	D_30_32	57.9	5.92
D_10_14	58.8	5.69	D_35_26	54.1	4.72	D_30_33	52.7	6.39
D_10_15	36.9	6.30	D_26_18	35.1	7.25	D_34_30	62.3	7.73
D_15_14	65.7	4.83	D_35_36	27.9	6.30	D_34_31	56.9	6.87

(Walk=25% of gait cycle)

Distance	Mean	Std. Deviation	Distance	Mean	Std. Deviation	Distance	Mean	Std. Deviation
D_11_1	62.2	4.65	D_12_15	35.3	5.69	D_36_26	61.2	4.92
D_1_6	55.9	4.33	D_16_13	43.3	6.65	D_26_27	29.3	4.87
D_6_11	22.2	3.15	D_14_16	54.0	6.23	D_27_36	52.8	4.74
D_1_2	23.7	4.10	D_18_16	49.3	4.01	D_36_37	29.2	5.64
D_2_6	57.1	4.80	D_14_18	36.4	6.67	D_37_27	62.2	6.49
D_2_7	47.5	3.85	D_17_14	62.4	4.33	D_27_28	28.0	4.19
D_7_6	22.7	3.83	D_15_17	30.9	8.56	D_28_37	55.7	6.22
D_2_3	18.6	2.72	D_17_18	63.5	6.59	D_19_29	34.1	6.62
D_3_7	44.3	3.51	D_18_20	65.6	3.98	D_29_18	65.9	5.29
D_3_8	42.1	3.52	D_20_17	57.9	9.80	D_26_29	50.5	5.26
D_8_7	15.2	2.02	D_17_22	67.6	6.10	D_29_30	29.6	5.38
D_3_4	17.8	2.67	D_22_20	45.5	3.41	D_30_26	60.0	5.17
D_4_8	37.6	3.95	D_18_19	56.6	5.41	D_30_27	53.6	5.19
D_4_9	38.5	4.16	D_19_16	49.5	4.53	D_30_31	28.6	6.31
D_9_8	14.5	1.97	D_19_21	60.6	5.57	D_31_27	63.2	6.97
D_4_5	17.6	3.07	D_21_16	68.6	5.62	D_31_28	59.0	6.90
D_5_9	31.9	4.21	D_21_23	34.3	4.25	D_25_35	62.9	6.58
D_5_10	36.3	4.56	D_23_24	21.9	4.46	D_35_32	51.7	6.13
D_10_9	19.1	2.61	D_24_21	37.1	4.88	D_32_25	35.6	8.87
D_5_12	39.4	4.00	D_22_23	37.1	4.24	D_36_32	61.2	6.36
D_12_10	15.1	2.71	D_24_22	40.8	4.30	D_36_33	55.2	6.68
D_13_11	52.6	6.21	D_24_20	54.8	5.86	D_33_32	30.3	5.45
D_6_13	59.8	5.72	D_24_19	65.8	6.60	D_37_33	64.1	7.00
D_6_14	61.3	6.08	D_24_25	22.7	4.28	D_37_34	59.7	6.70
D_14_13	47.1	3.21	D_25_20	50.8	5.76	D_34_33	28.7	5.32
D_7_14	61.2	6.12	D_25_19	55.7	6.16	D_32_19	62.0	6.40
D_8_14	61.3	6.31	D_20_35	38.8	7.01	D_32_29	48.6	6.03
D_9_14	60.8	6.08	D_35_18	70.0	6.23	D_30_32	57.9	6.14
D_10_14	62.5	5.60	D_35_26	53.3	3.76	D_30_33	50.6	7.14
D_10_15	42.4	5.45	D_26_18	34.9	6.97	D_34_30	59.9	7.61
D_15_14	67.0	4.00	D_35_36	28.8	5.48	D_34_31	55.2	8.48

(Walk=50% of gait cycle)

Distance	Mean	Std. Deviation	Distance	Mean	Std. Deviation	Distance	Mean	Std. Deviation
D_11_1	60.6	5.25	D_12_15	33.8	6.47	D_36_26	61.4	7.04
D_1_6	51.8	3.36	D_16_13	41.1	6.65	D_26_27	28.9	4.52
D_6_11	22.7	3.79	D_14_16	51.0	6.40	D_27_36	55.0	5.97
D_1_2	23.8	3.76	D_18_16	47.1	4.68	D_36_37	29.3	6.20
D_2_6	51.3	4.22	D_14_18	36.1	6.57	D_37_27	62.2	8.39
D_2_7	43.7	3.68	D_17_14	64.6	5.22	D_27_28	28.1	5.33
D_7_6	22.6	3.72	D_15_17	33.4	10.84	D_28_37	57.9	7.36
D_2_3	20.1	2.37	D_17_18	67.5	7.15	D_19_29	33.2	7.23
D_3_7	40.2	3.55	D_18_20	67.3	4.48	D_29_18	64.8	4.33
D_3_8	39.5	4.11	D_20_17	64.9	11.13	D_26_29	49.4	4.82
D_8_7	15.6	2.19	D_17_22	67.7	6.83	D_29_30	29.7	5.69
D_3_4	18.1	2.65	D_22_20	47.4	3.75	D_30_26	59.3	6.34
D_4_8	34.3	3.15	D_18_19	55.0	4.15	D_30_27	52.7	4.60
D_4_9	35.6	3.36	D_19_16	44.7	5.41	D_30_31	28.8	5.77
D_9_8	14.5	1.93	D_19_21	59.5	5.24	D_31_27	63.4	7.19
D_4_5	19.1	2.49	D_21_16	68.0	6.57	D_31_28	58.6	6.01
D_5_9	28.4	3.30	D_21_23	35.0	3.94	D_25_35	59.9	7.49
D_5_10	33.5	3.78	D_23_24	23.0	4.46	D_35_32	47.7	5.41
D_10_9	19.1	2.94	D_24_21	36.6	3.94	D_32_25	37.2	8.35
D_5_12	38.4	3.93	D_22_23	37.2	5.09	D_36_32	56.6	6.26
D_12_10	15.5	3.05	D_24_22	41.6	5.69	D_36_33	51.4	5.44
D_13_11	49.8	6.59	D_24_20	53.6	6.17	D_33_32	30.4	5.66
D_6_13	55.0	5.88	D_24_19	68.6	7.19	D_37_33	60.6	6.46
D_6_14	59.0	5.71	D_24_25	23.0	4.42	D_37_34	57.1	5.68
D_14_13	47.9	4.00	D_25_20	49.3	5.07	D_34_33	29.2	5.51
D_7_14	55.9	5.48	D_25_19	57.3	6.19	D_32_19	60.2	6.46
D_8_14	55.2	5.58	D_20_35	41.2	6.79	D_32_29	50.1	5.43
D_9_14	56.4	5.29	D_35_18	70.1	5.70	D_30_32	62.3	6.62
D_10_14	60.6	5.13	D_35_26	55.0	4.82	D_30_33	52.8	6.18
D_10_15	39.8	5.96	D_26_18	35.1	8.52	D_34_30	59.6	6.16
D_15_14	68.5	3.77	D_35_36	29.3	5.43	D_34_31	57.5	6.91

(Walk=62% of gait cycle)

Distance	Mean	Std. Deviation	Distance	Mean	Std. Deviation	Distance	Mean	Std. Deviation
D_11_1	58.7	4.52	D_12_15	32.2	6.22	D_36_26	61.0	5.65
D_1_6	44.5	5.24	D_16_13	42.5	7.04	D_26_27	32.3	6.40
D_6_11	26.9	4.78	D_14_16	50.0	6.26	D_27_36	53.7	5.53
D_1_2	22.4	4.39	D_18_16	49.7	5.00	D_36_37	28.8	4.94
D_2_6	47.5	5.45	D_14_18	42.9	8.49	D_37_27	60.5	6.34
D_2_7	38.2	5.32	D_17_14	64.2	4.64	D_27_28	28.1	5.28
D_7_6	21.1	3.76	D_15_17	33.2	10.12	D_28_37	56.3	7.24
D_2_3	17.2	2.56	D_17_18	72.6	7.79	D_19_29	31.2	6.62
D_3_7	38.1	4.38	D_18_20	66.2	4.66	D_29_18	68.6	4.15
D_3_8	35.8	4.96	D_20_17	64.9	11.69	D_26_29	51.0	5.13
D_8_7	14.8	2.03	D_17_22	66.5	5.61	D_29_30	28.9	6.50
D_3_4	16.7	2.80	D_22_20	44.3	2.97	D_30_26	63.1	6.40
D_4_8	34.1	4.08	D_18_19	54.6	4.90	D_30_27	55.1	6.76
D_4_9	34.2	4.32	D_19_16	45.1	4.67	D_30_31	28.6	4.86
D_9_8	14.4	2.38	D_19_21	54.1	7.13	D_31_27	66.1	7.01
D_4_5	16.4	2.73	D_21_16	65.1	6.42	D_31_28	61.5	8.66
D_5_9	30.4	4.63	D_21_23	34.1	3.91	D_25_35	54.4	6.16
D_5_10	32.9	4.41	D_23_24	20.0	4.42	D_35_32	49.8	4.80
D_10_9	14.8	2.36	D_24_21	34.7	3.29	D_32_25	27.6	7.79
D_5_12	38.4	4.89	D_22_23	38.2	4.12	D_36_32	54.7	6.82
D_12_10	16.5	3.43	D_24_22	42.3	4.66	D_36_33	53.2	5.03
D_13_11	45.5	6.86	D_24_20	52.5	5.40	D_33_32	27.2	5.32
D_6_13	47.1	5.52	D_24_19	65.9	8.36	D_37_33	59.8	6.69
D_6_14	53.6	7.59	D_24_25	20.2	4.94	D_37_34	58.3	5.44
D_14_13	50.7	5.30	D_25_20	51.0	5.47	D_34_33	27.3	5.72
D_7_14	50.7	6.63	D_25_19	56.2	5.75	D_32_19	59.5	5.34
D_8_14	53.0	6.90	D_20_35	38.8	7.41	D_32_29	49.0	5.20
D_9_14	57.2	6.33	D_35_18	70.5	5.90	D_30_32	58.4	7.60
D_10_14	63.7	6.67	D_35_26	53.2	5.47	D_30_33	50.5	6.67
D_10_15	38.3	5.53	D_26_18	39.4	6.78	D_34_30	57.0	7.14
D_15_14	71.9	5.16	D_35_36	28.9	6.00	D_34_31	54.1	7.65

APPENDIX E

THE DESCRIPTIVE OF ANGLES EXTRACTED FROM STATIC FOOT MODEL

（Heel=0）

	Minimum	Maximum	Mean	Std. Deviation
A1	2.2	120.9	15.118	16.8431
A2	1.4	127.2	9.872	17.5762
A3	1.1	120.8	12.239	16.5432
A4	3.1	107.6	26.277	13.9726
A5	51.1	136.3	124.630	12.1138
A6	158.1	177.3	168.082	5.1867
A7	165.0	179.0	172.265	3.7081
A8	73.9	145.3	131.806	12.7530
A9	69.9	138.3	127.562	12.2135
A10	78.2	128.5	117.242	8.9004
A11	79.9	122.1	112.410	7.3658

(Heel=10mm)

	Minimum	Maximum	Mean	Std. Deviation
A1	1.4	31.5	13.082	7.4157
A2	1.0	19.9	8.477	3.9995
A3	1.9	24.7	10.171	5.1932
A4	6.1	38.9	23.486	7.2948
A5	114.7	147.3	131.890	6.0185
A6	156.8	179.2	169.317	4.3136
A7	152.8	170.9	164.590	4.1369
A8	67.6	150.7	135.911	11.3818
A9	60.1	149.6	132.140	11.5500
A10	52.7	138.5	122.404	11.3480
A11	47.7	136.4	115.935	11.2003

(Heel=40mm)

	Minimum	Maximum	Mean	Std. Deviation
A1	.9	50.3	15.629	8.7058
A2	1.7	20.0	8.234	4.3650
A3	1.8	16.1	8.574	3.8455
A4	1.2	36.5	21.406	7.1409
A5	70.9	150.8	139.790	11.4482
A6	100.2	177.5	168.684	11.2021
A7	146.9	162.0	154.653	3.9094
A8	115.0	153.0	142.590	6.1195
A9	133.5	153.3	141.461	4.1687
A10	126.0	144.2	132.939	3.7748
A11	116.3	133.5	123.874	3.7139

(Heel=70mm)

	Minimum	Maximum	Mean	Std. Deviation
A1	2.8	41.7	15.723	8.0647
A2	.8	21.6	9.512	4.6371
A3	.9	24.6	9.546	5.2779
A4	8.2	40.2	22.443	6.3537
A5	82.6	158.3	148.793	10.9592
A6	96.2	178.4	170.725	12.0054
A7	135.5	152.4	145.305	4.3069
A8	120.4	162.7	149.364	6.6732
A9	136.6	161.1	149.993	4.2597
A10	129.8	152.6	142.125	3.9720
A11	120.6	139.6	131.506	3.5141

(Plantar=25°)

	Minimum	Maximum	Mean	Std. Deviation
A1	.3	50.5	14.442	8.5487
A2	1.2	17.4	6.898	3.4896
A3	1.4	20.5	9.508	4.9737
A4	7.9	34.6	24.374	6.3147
A5	75.8	154.3	145.937	11.1515
A6	107.4	178.3	170.794	10.0087
A7	166.2	177.7	172.222	3.1569
A8	102.9	162.7	150.104	8.5646
A9	131.0	157.4	148.399	4.8641
A10	128.5	149.8	139.664	4.0157
A11	124.3	144.0	135.625	3.7558

(Plantar=12.5°)

	Minimum	Maximum	Mean	Std. Deviation
A1	3.2	26.9	14.779	6.1178
A2	1.9	16.9	7.698	3.6963
A3	.8	21.5	8.493	4.5035
A4	7.6	39.5	23.125	7.3828
A5	124.7	149.1	138.492	4.6667
A6	157.0	178.3	171.252	4.7788
A7	162.4	178.1	171.221	3.8782
A8	135.1	154.1	144.103	4.1661
A9	132.9	148.0	140.750	3.6988
A10	119.9	140.4	130.833	3.7857
A11	116.5	135.3	126.336	3.6916

(Dorsiflexion=10°)

	Minimum	Maximum	Mean	Std. Deviation
A1	3.5	49.0	16.168	7.7351
A2	1.4	19.2	9.068	4.6616
A3	1.6	17.3	7.928	4.3832
A4	1.8	39.7	22.167	7.1629
A5	72.0	130.0	113.978	8.6677
A6	98.5	177.5	167.011	11.1261
A7	162.6	176.4	170.266	3.9048
A8	104.7	136.8	125.477	5.7603
A9	110.2	132.3	119.385	4.6625
A10	98.8	116.6	107.609	4.2039
A11	93.0	110.5	102.191	4.1110

(Dorsiflexion=20°)

	Minimum	Maximum	Mean	Std. Deviation
A1	.1	131.2	17.626	18.1483
A2	3.0	129.3	12.432	17.5612
A3	.7	127.4	10.825	17.4569
A4	2.4	114.4	24.461	14.7880
A5	84.3	149.4	107.580	10.0454
A6	132.5	174.6	165.082	7.4564
A7	158.2	179.1	170.288	5.0009
A8	104.8	130.6	117.500	5.5283
A9	100.0	122.8	110.295	4.9527
A10	87.5	115.7	98.687	4.8781
A11	81.0	118.3	92.959	5.4316

(Inversion=10°)

	Minimum	Maximum	Mean	Std. Deviation
A1	3.3	34.0	18.944	7.4410
A2	2.0	27.7	12.521	6.0352
A3	1.4	17.1	9.233	3.6274
A4	3.3	35.9	19.055	7.2667
A5	112.9	138.1	126.324	5.3615
A6	154.4	178.3	169.438	5.1154
A7	157.9	177.2	171.759	3.7013
A8	124.7	150.7	134.991	5.2871
A9	123.1	142.2	130.183	4.1714
A10	110.0	127.6	118.890	3.3450
A11	105.8	121.9	113.800	3.3359

(Inversion=5°)

	Minimum	Maximum	Mean	Std. Deviation
A1	3.3	33.9	16.810	7.9285
A2	2.8	23.1	10.844	5.5860
A3	1.6	20.9	8.466	4.1238
A4	6.2	35.7	20.928	6.1173
A5	48.4	137.9	124.885	12.6148
A6	151.7	177.9	168.356	5.9732
A7	158.3	179.9	171.565	4.4835
A8	91.2	141.1	133.969	7.9443
A9	92.5	142.4	129.622	6.9885
A10	95.9	125.4	118.586	4.7935
A11	99.5	120.0	113.810	4.1737

(Eversion=5°)

	Minimum	Maximum	Mean	Std. Deviation
A1	4.1	29.5	15.303	6.2431
A2	1.4	20.0	8.025	4.4424
A3	.7	20.5	8.793	4.6762
A4	6.8	41.4	23.271	7.1162
A5	107.6	136.4	126.067	6.0582
A6	153.8	176.8	168.111	5.0163
A7	161.4	178.4	171.396	3.9046
A8	50.0	144.9	132.606	12.9530
A9	55.7	138.7	128.392	11.4466
A10	67.0	127.6	117.634	8.4669
A11	72.1	121.7	112.772	7.1998

(Eversion=2.5°)

	Minimum	Maximum	Mean	Std. Deviation
A1	3.1	30.3	13.164	6.8017
A2	1.7	20.3	7.905	4.4827
A3	1.6	22.6	9.849	4.9129
A4	6.7	39.0	24.254	7.1597
A5	48.9	137.5	124.557	12.5273
A6	154.6	177.7	168.523	4.7827
A7	153.0	178.4	171.454	4.5890
A8	94.4	141.9	133.338	7.3884
A9	97.6	140.1	128.716	6.3049
A10	97.3	127.7	117.877	5.2364
A11	99.7	122.2	112.782	4.5040

(Walk=0%)

	Minimum	Maximum	Mean	Std. Deviation
A1	1.8	33.7	15.107	7.6387
A2	1.5	21.9	9.221	5.4170
A3	3.3	23.2	12.185	4.7614
A4	10.4	54.5	30.255	8.2266
A5	122.2	144.5	135.888	5.3630
A6	160.7	176.1	169.266	4.2954
A7	137.8	175.8	153.366	8.7617
A8	133.1	147.3	140.891	4.1793
A9	126.9	144.0	136.965	4.3278
A10	116.9	136.4	127.094	4.4347
A11	108.3	128.6	118.636	4.9725

(Walk=25%)

	Minimum	Maximum	Mean	Std. Deviation
A1	1.0	25.8	10.991	5.8437
A2	2.3	18.5	10.305	4.3350
A3	8.0	29.0	16.997	5.0311
A4	22.4	46.1	33.022	6.3725
A5	113.6	145.4	129.344	6.3341
A6	154.3	173.8	166.465	4.1710
A7	153.2	178.0	171.247	4.5814
A8	123.2	145.2	134.924	4.3866
A9	118.9	142.6	130.507	4.6191
A10	107.9	134.1	120.262	4.6400
A11	104.4	127.7	114.674	4.6210

(Walk=50%)

	Minimum	Maximum	Mean	Std. Deviation
A1	3.3	35.7	17.574	7.9951
A2	2.3	24.5	11.910	5.6151
A3	.9	14.9	8.086	3.4952
A4	3.2	35.5	19.716	6.5375
A5	116.6	141.2	127.978	6.2163
A6	149.3	177.7	167.886	4.9876
A7	128.5	168.6	152.717	9.1003
A8	115.3	147.2	134.361	6.9664
A9	120.9	145.6	131.601	5.1929
A10	111.3	137.0	120.709	5.4379
A11	101.2	121.2	109.701	4.5636

(Walk=62%)

	Minimum	Maximum	Mean	Std. Deviation
A1	1.7	35.9	16.760	7.6293
A2	.4	29.4	11.503	6.1709
A3	2.1	25.3	11.270	6.1492
A4	1.4	43.9	17.281	8.6942
A5	132.6	172.2	153.137	10.7511
A6	153.9	177.5	170.130	5.0004
A7	104.8	156.4	127.372	13.0890
A8	137.7	169.1	152.136	9.1182
A9	134.2	171.0	153.949	9.9617
A10	121.0	165.6	146.161	11.2147
A11	108.5	153.1	132.524	11.0042

APPENDIX F

REGRESSION EQUATION FOR CHANGE IN ANGLE

(1) The heel height influence

Angle	P-value	Mean value			
		H0	H10	H40	H70
A1	.000	132.9491	135.9107	142.5866	149.3642
A2	.000	128.7624	132.1396	141.5204	149.9929
A3	.000	118.0553	122.4045	132.9859	142.1250
A4	.000	113.0879	115.9347	123.9261	131.5060
A5	.000	124.5057	131.8903	139.7274	148.7929
A6	.561	168.2907	169.3170	168.6735	170.7248
A7	.000	172.2494	164.5901	154.6065	145.3045
A8	.868	99.0681	98.5349	98.0028	98.4635
A9	.220	105.8735	105.0590	107.3389	109.2583
A10	.001	100.6238	98.7463	101.7798	103.6304
A11	.015	97.8319	94.6047	95.5661	94.5828
A12	.019	93.5100	93.3390	95.2165	96.1874
A13	.120	12.9147	13.0816	15.7793	15.7227
A14	.133	7.4268	8.4775	8.2953	9.5123
A15	.321	9.9780	10.1712	8.4611	9.5462
A16	.140	24.5821	23.4864	21.3012	22.4427

A1: $y = 0.2312x + 133.27$ $R^2 = 0.9986$

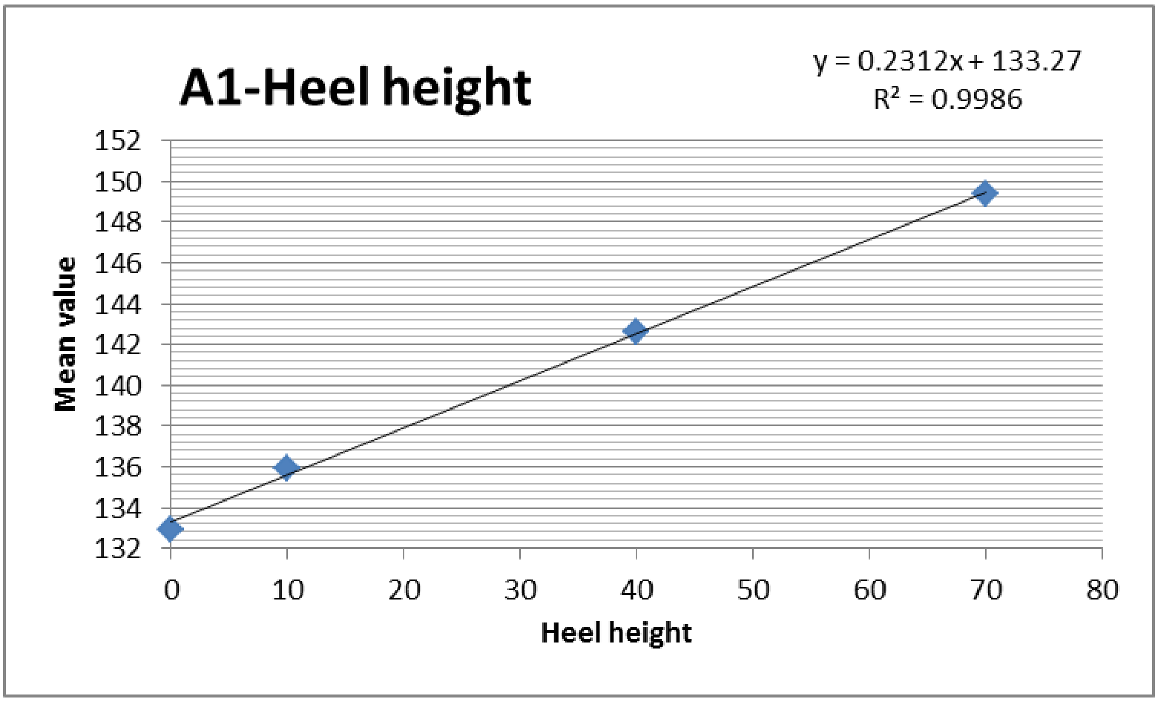

A2: $y = 0.3031x + 129.01 \quad R^2 = 0.999$

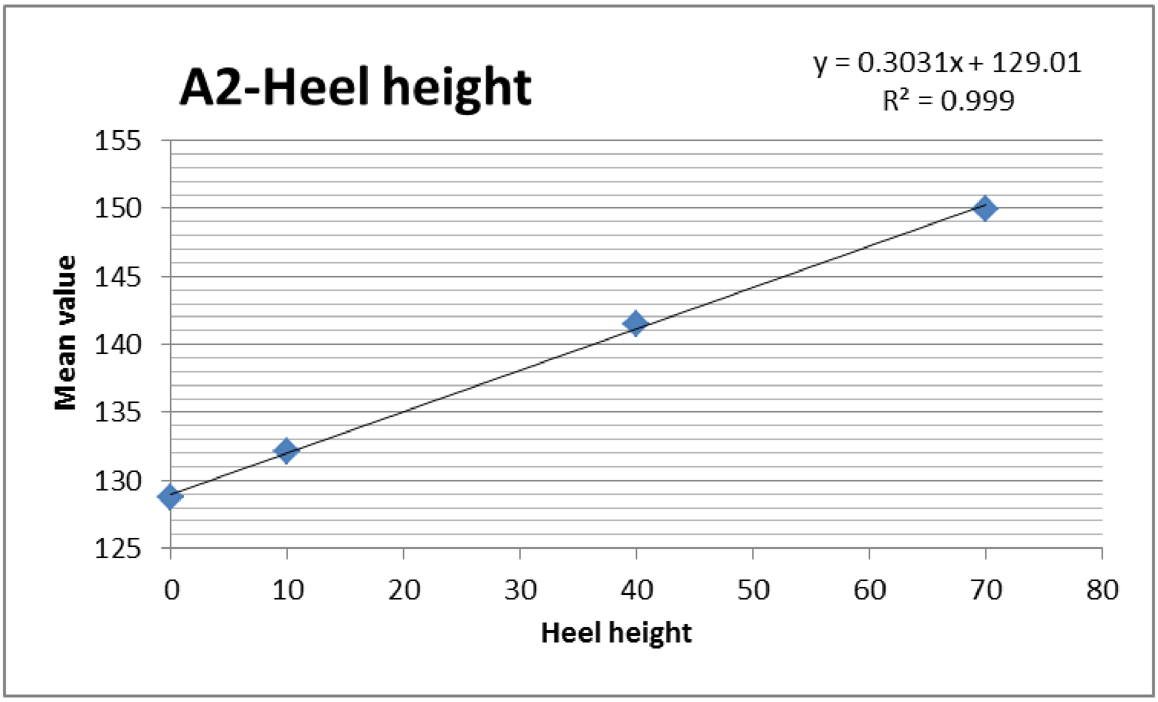

A3: $y = 0.3417x + 118.64 \quad R^2 = 0.9968$

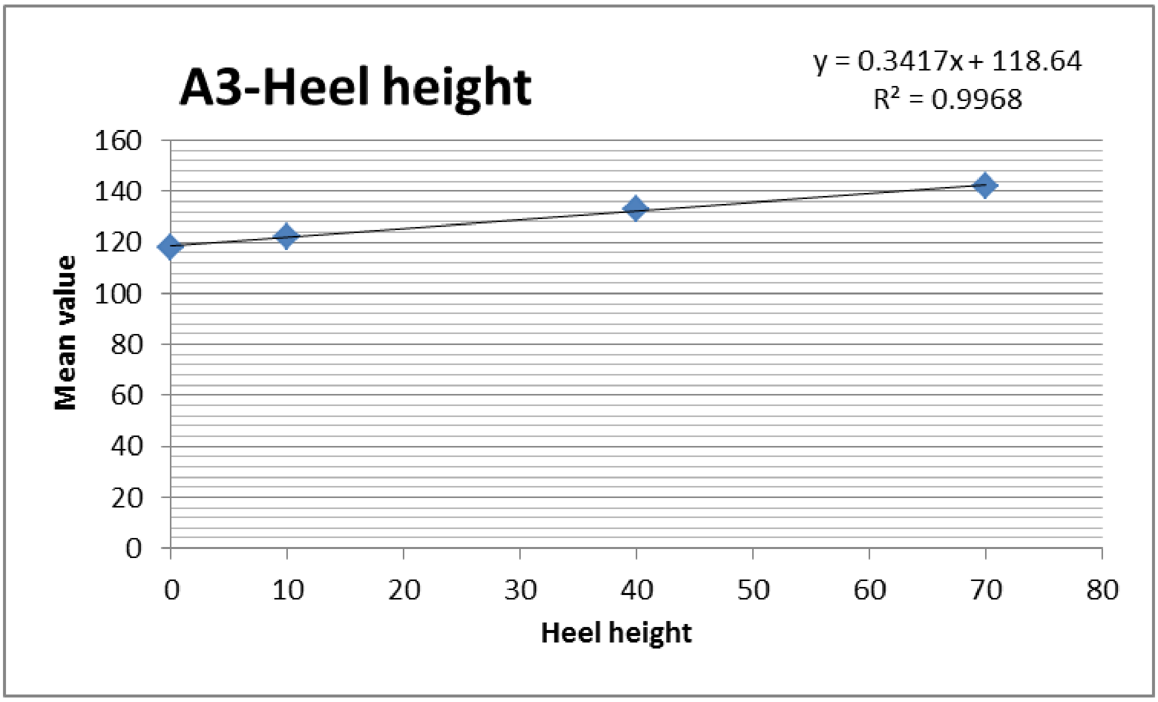

A4: $y = 0.2627x + 113.23$ $R^2 = 0.9996$

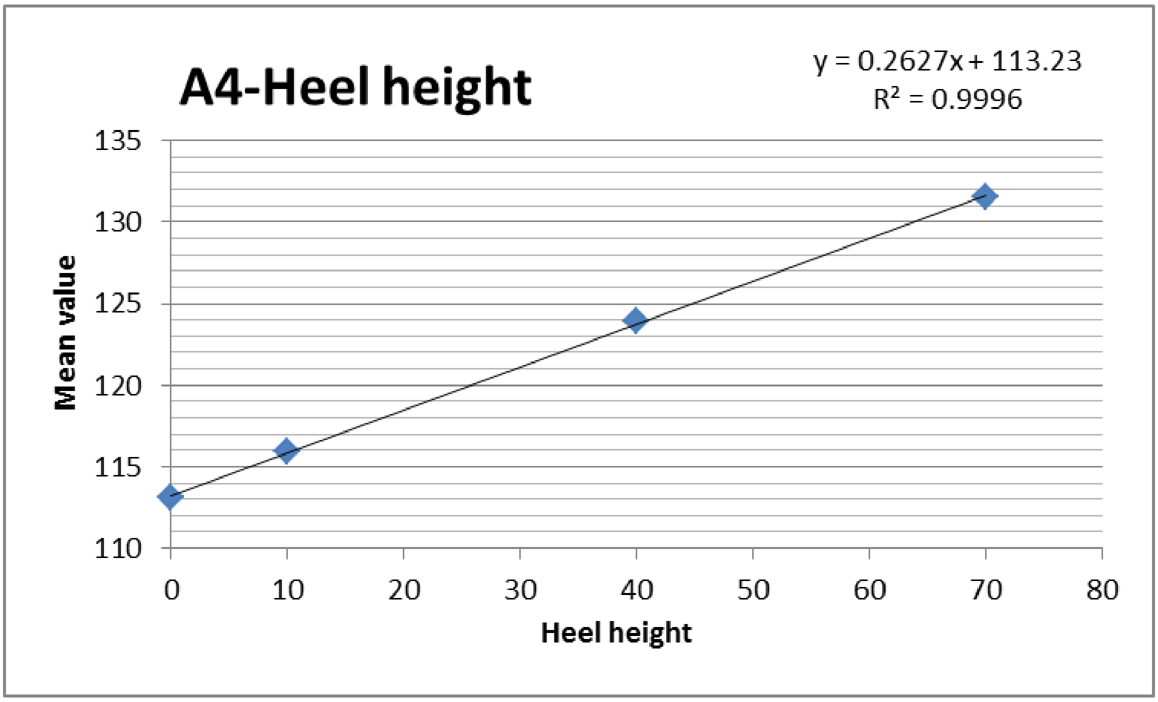

A5: $y = 0.3253x + 126.47$ $R^2 = 0.973$

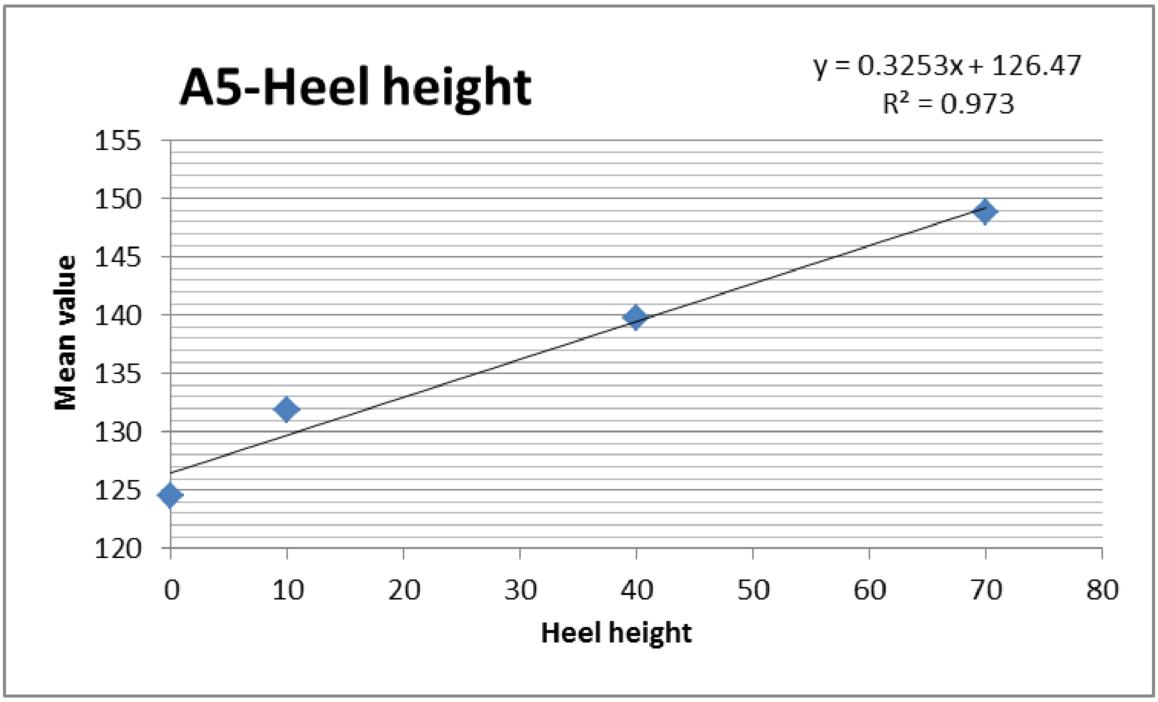

A7: $y = -0.367x + 170.2$ $R^2 = 0.9772$

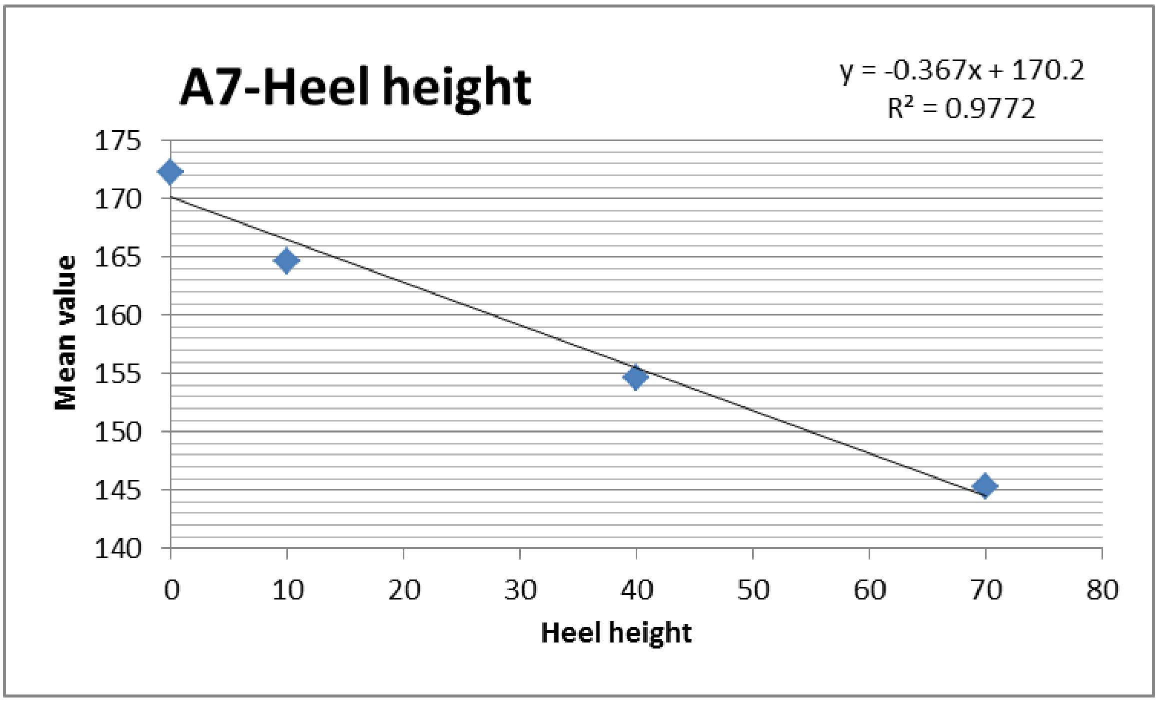

A10: $y = 0.0565x + 99.501$ $R^2 = 0.7592$

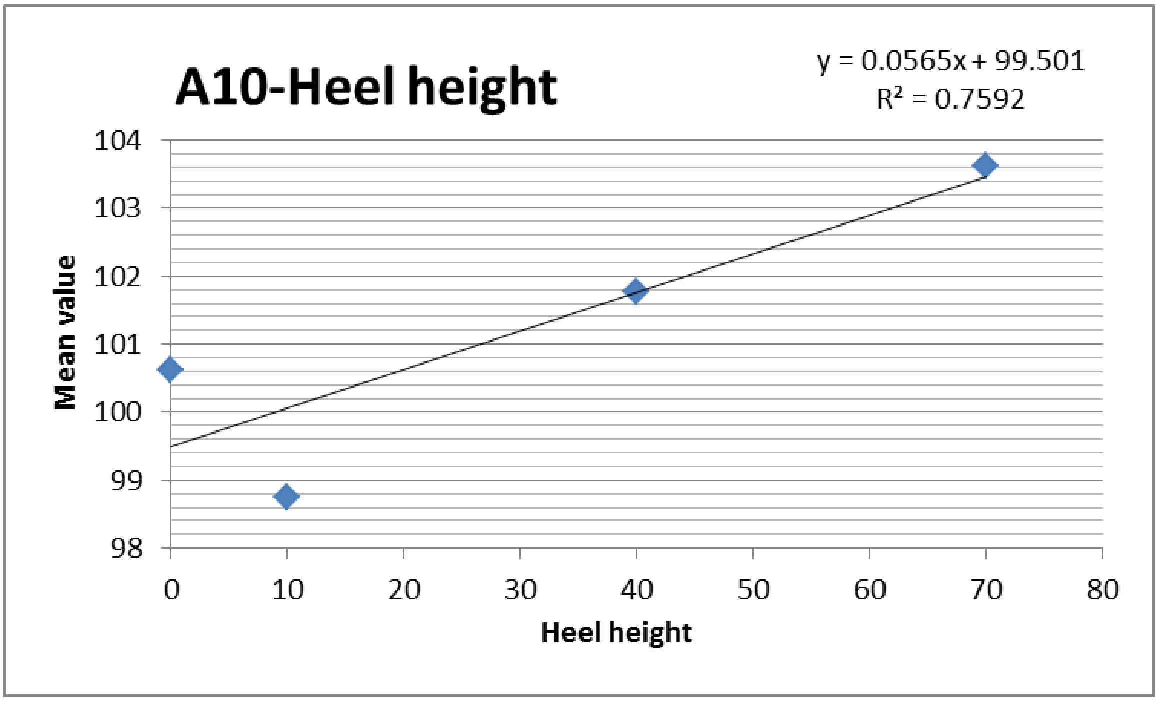

A11: $y = -0.0294x + 96.527$ $R^2 = 0.3695$

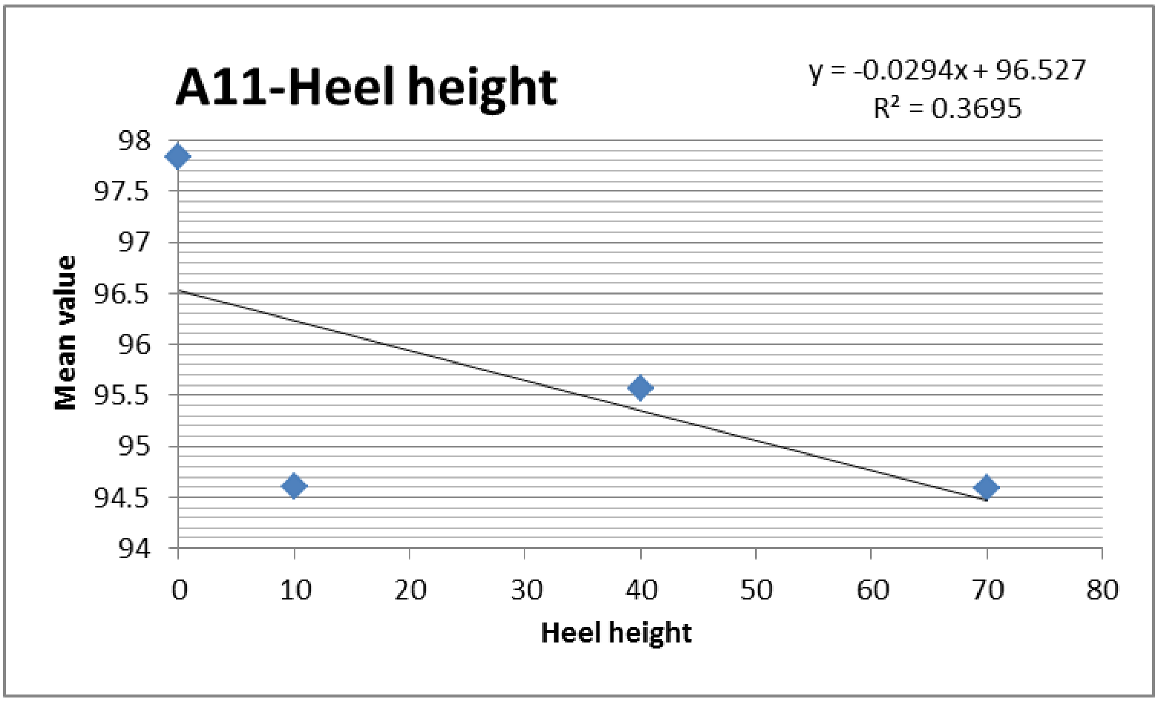

A12: $y = 0.0425x + 93.287$ $R^2 = 0.9564$

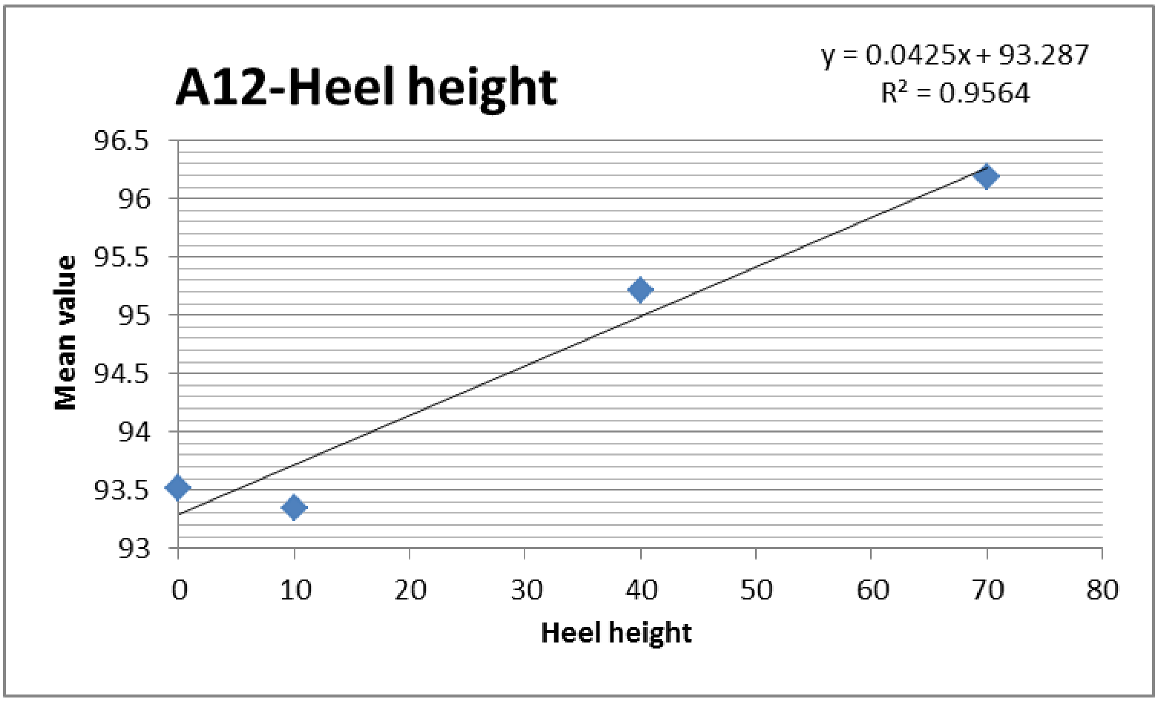

(2) The plantar flexion and dorsiflexion

Angle	P-value	Mean value				
		-25	-12.5	0	10	20
A1	.000	150.1037	144.1031	132.9491	125.4774	117.6202
A2	.000	148.3989	140.7495	128.7624	119.3850	110.3312
A3	.000	139.6641	130.8327	118.0553	107.6086	98.3403
A4	.000	135.6246	126.3356	113.0879	102.1908	92.4430
A5	.000	145.9368	138.4921	124.5057	113.9777	106.7270
A6	.001	170.7943	171.2522	168.2907	167.0106	165.0937
A7	.020	172.2224	171.2207	172.2494	170.2658	170.2438
A8	.780	98.3479	99.6463	99.0681	100.0618	99.1014
A9	.027	107.1385	108.2573	105.8735	103.5806	101.8724
A10	.826	101.0462	101.6900	100.6238	102.3660	101.4380
A11	.000	93.9083	96.6316	97.8319	101.2288	101.9480
A12	.000	83.5051	88.7098	93.5100	100.7950	104.4863
A13	.284	14.4419	14.7793	12.9147	16.1684	15.3083
A14	.001	6.8976	7.6980	7.4268	9.0682	10.0468
A15	.183	9.5084	8.4933	9.9780	7.9278	8.4466
A16	.363	24.3737	23.1250	24.5821	22.1673	22.6251

A1: $y = -0.7412x + 132.94 \quad R^2 = 0.9919$

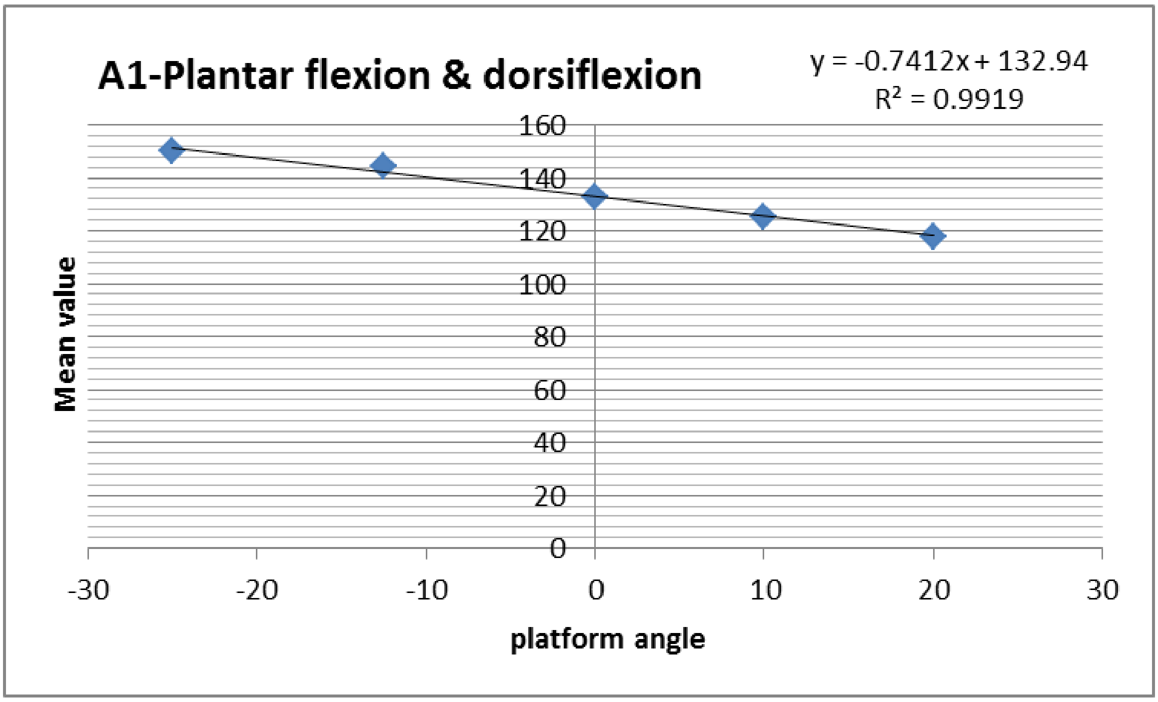

A2: $y = -0.8641x + 128.23$ $R^2 = 0.994$

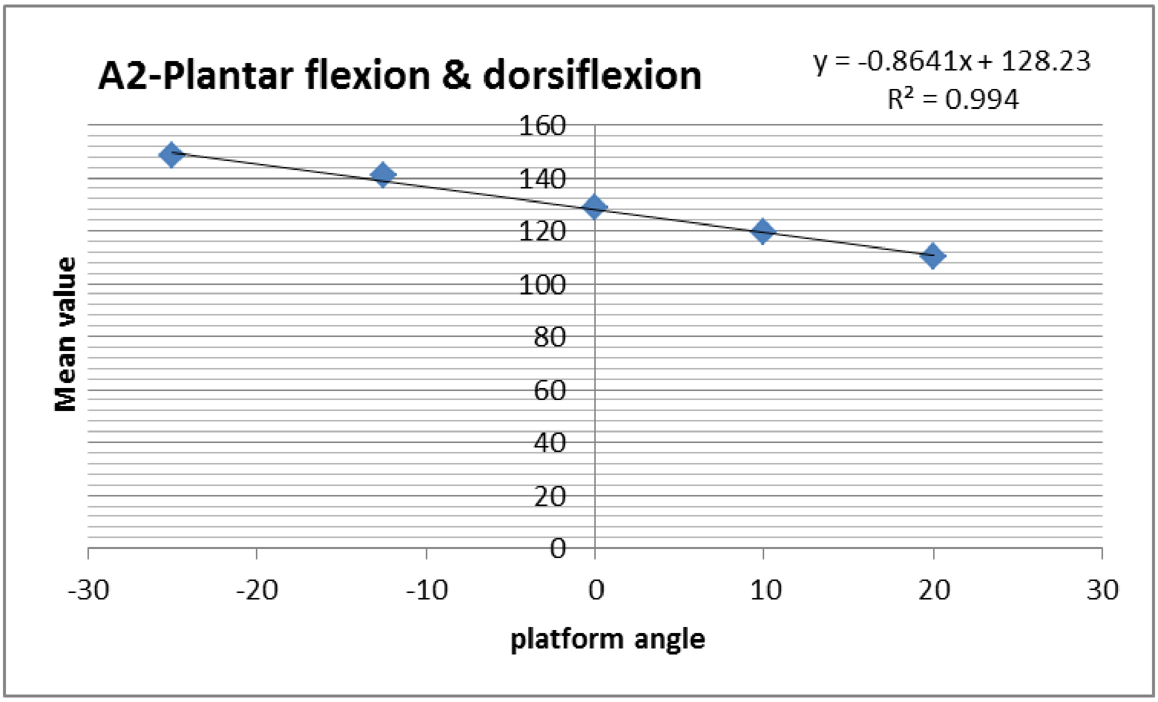

A3: $y = -0.9389x + 117.49$ $R^2 = 0.9956$

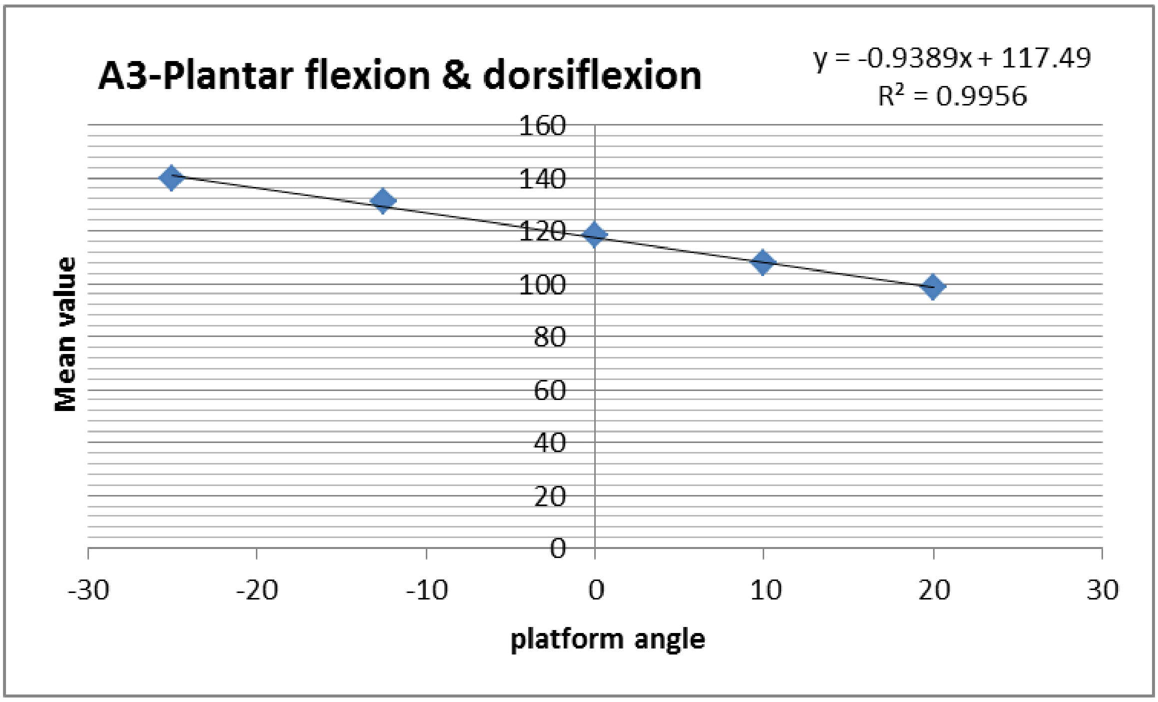

A4: $y = -0.9799x + 112.47$ $R^2 = 0.9957$

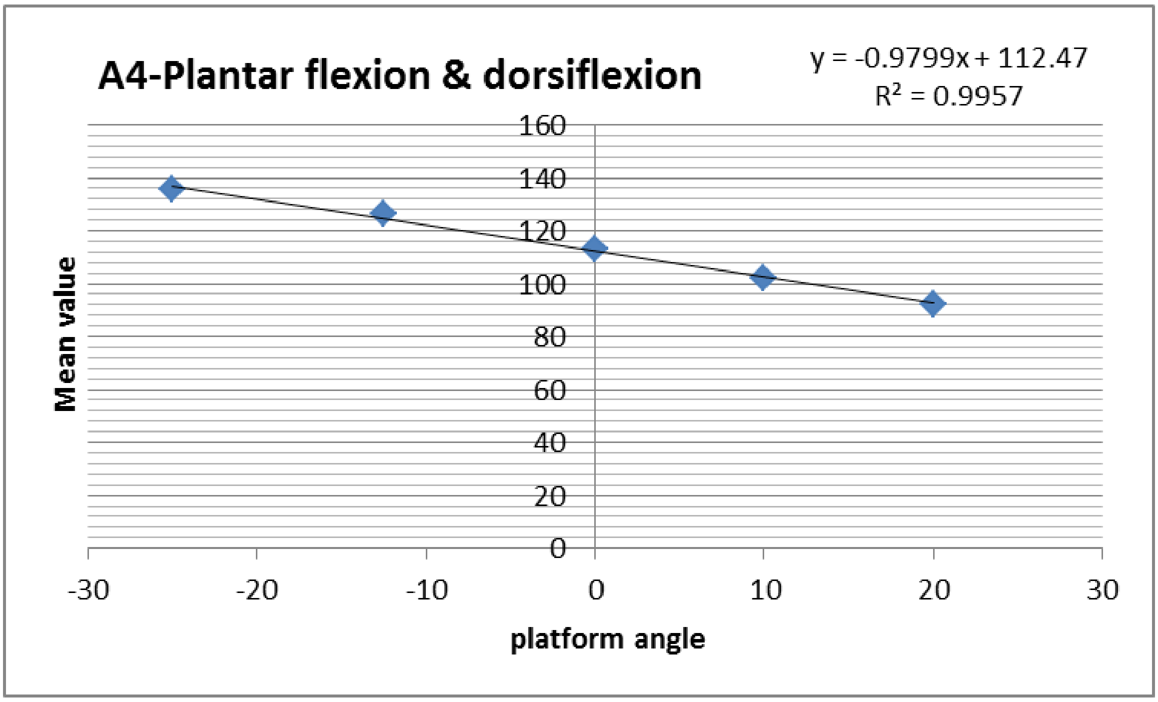

A5: $y = -0.914x + 124.56$ $R^2 = 0.99$

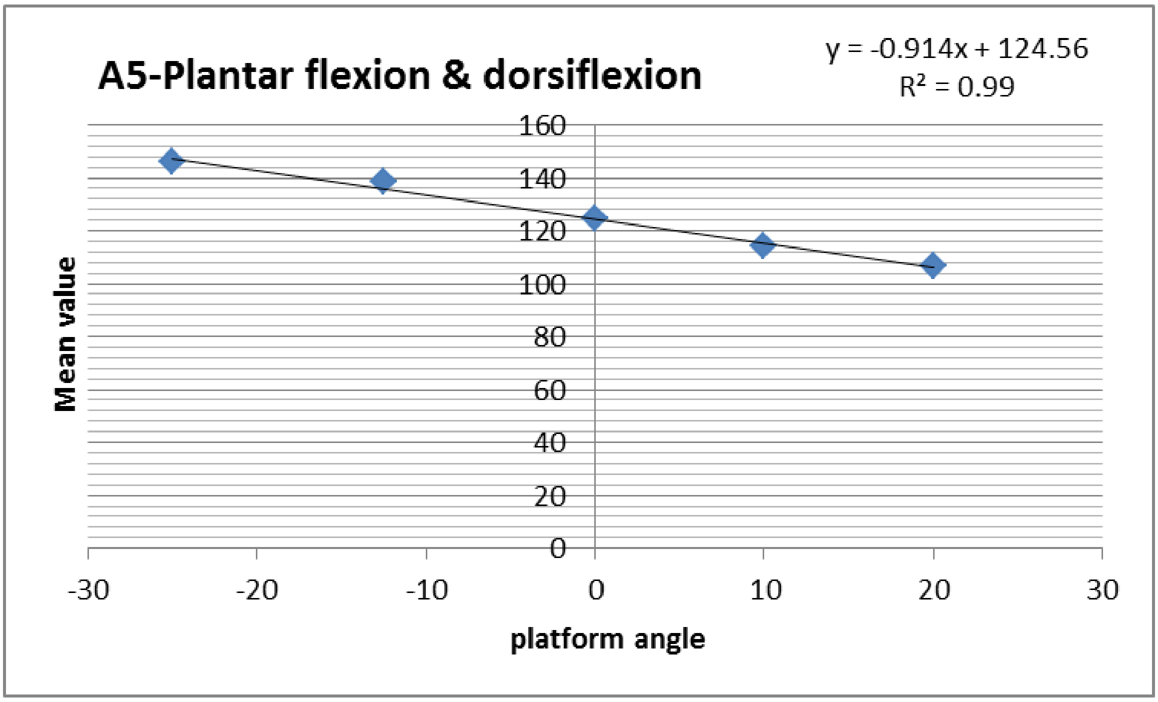

A6: $y = -0.1377x + 168.28 \quad R^2 = 0.9017$

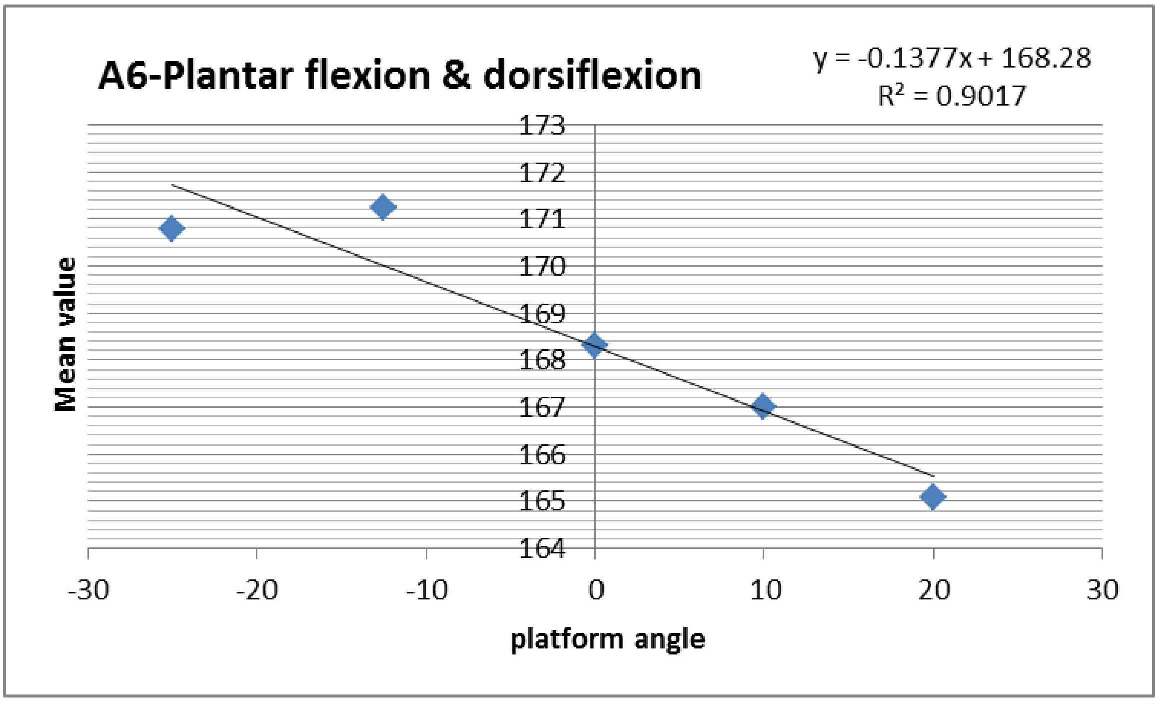

A7: $y = -0.0425x + 171.18 \quad R^2 = 0.5845$

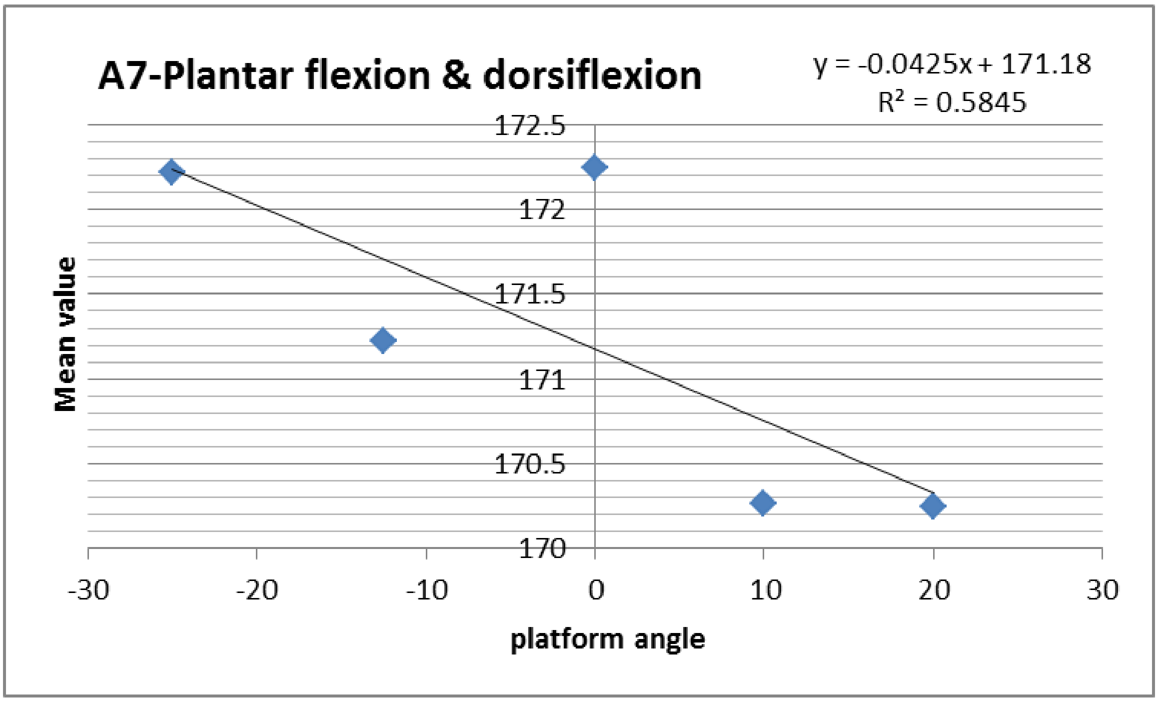

A9: $y = -0.1326x + 105.15 \quad R^2 = 0.8219$

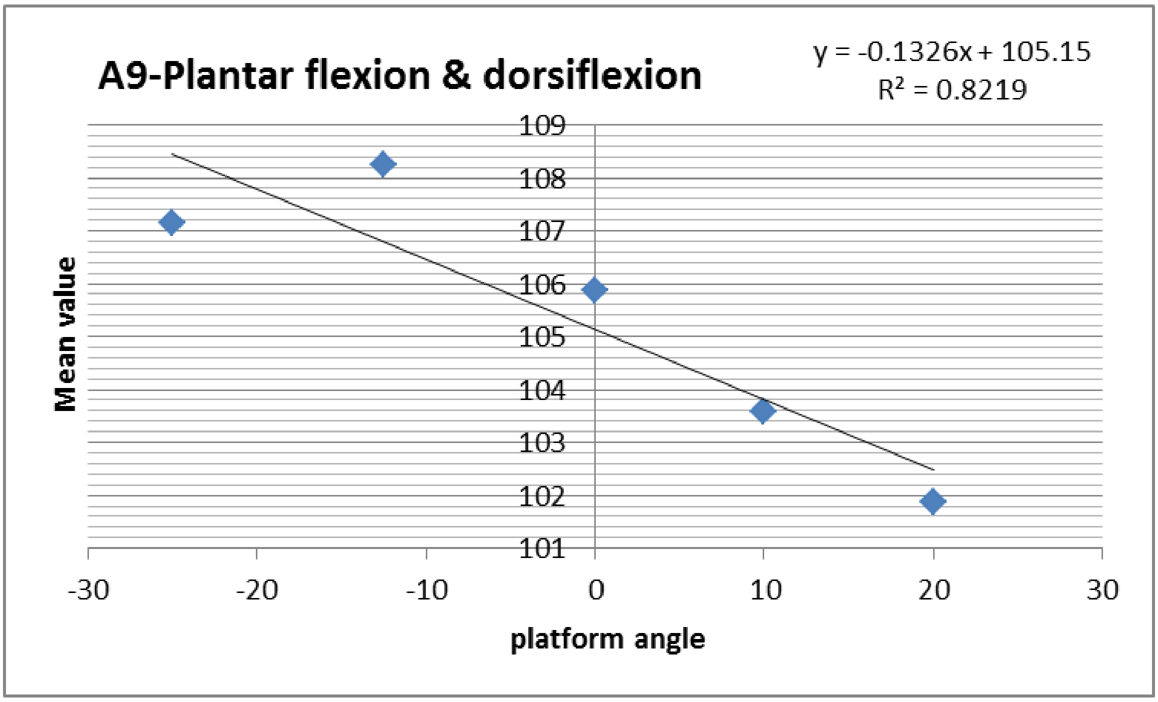

A11: $y = 0.1834x + 98.585 \quad R^2 = 0.9674$

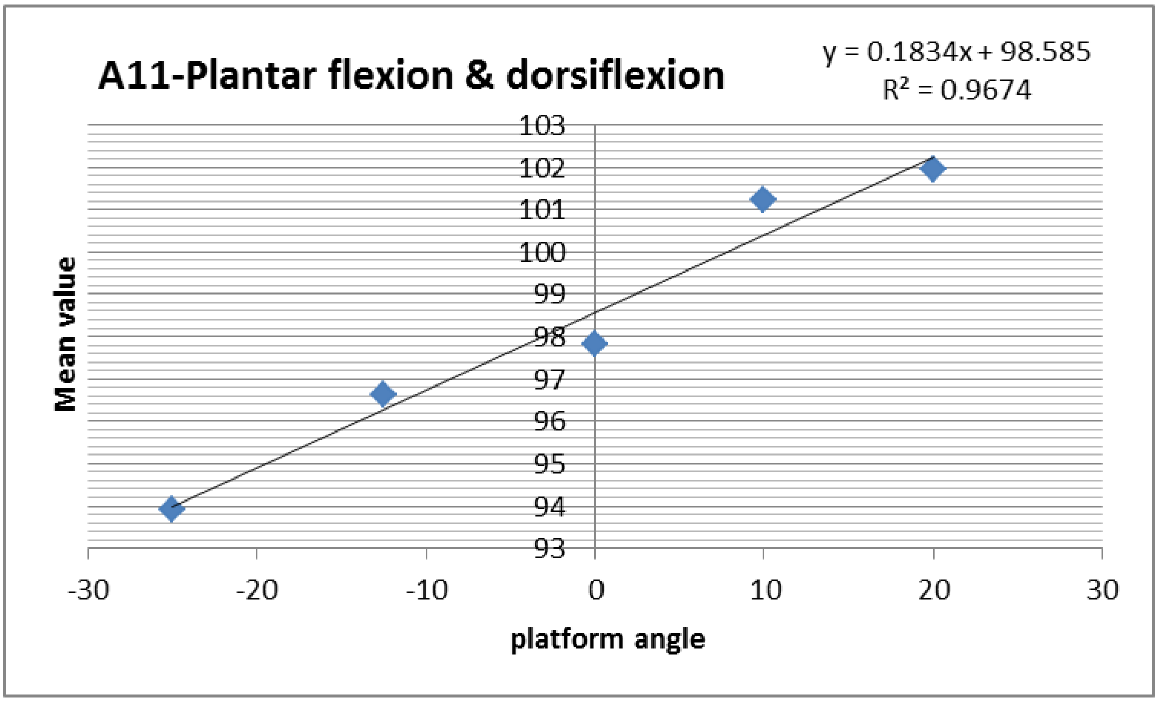

A12: $y = 0.4785x + 94.919$ $R^2 = 0.988$

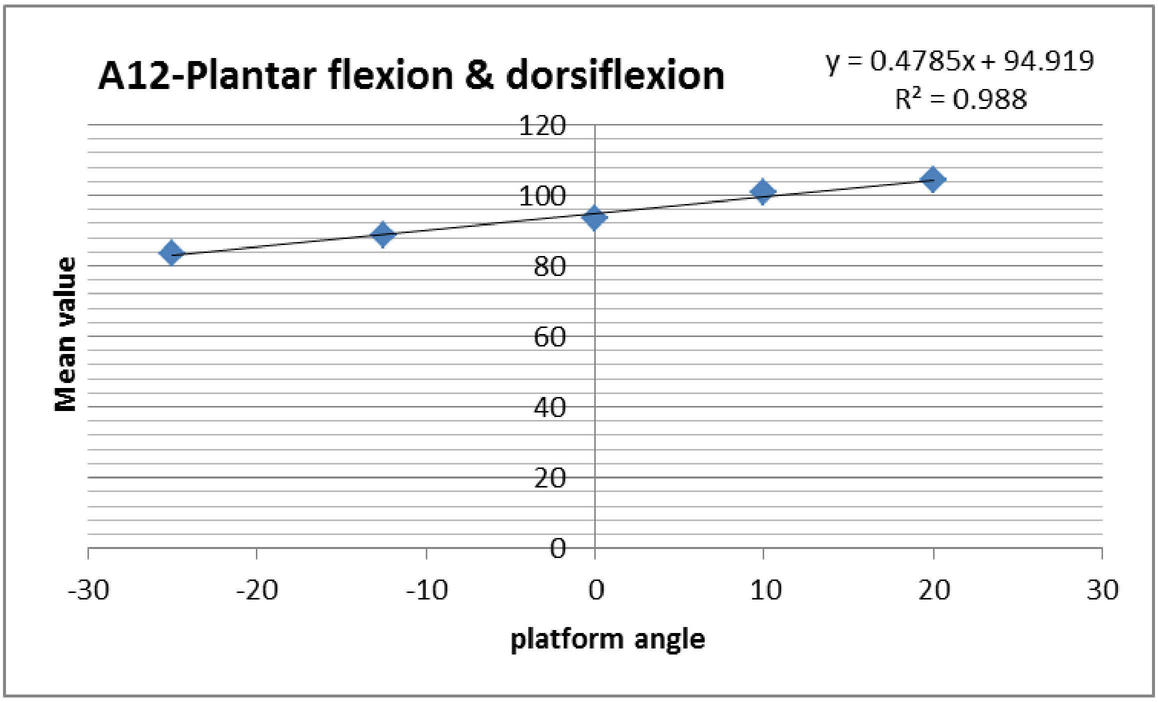

A14: $y = 0.0667x + 8.3275$ $R^2 = 0.8415$

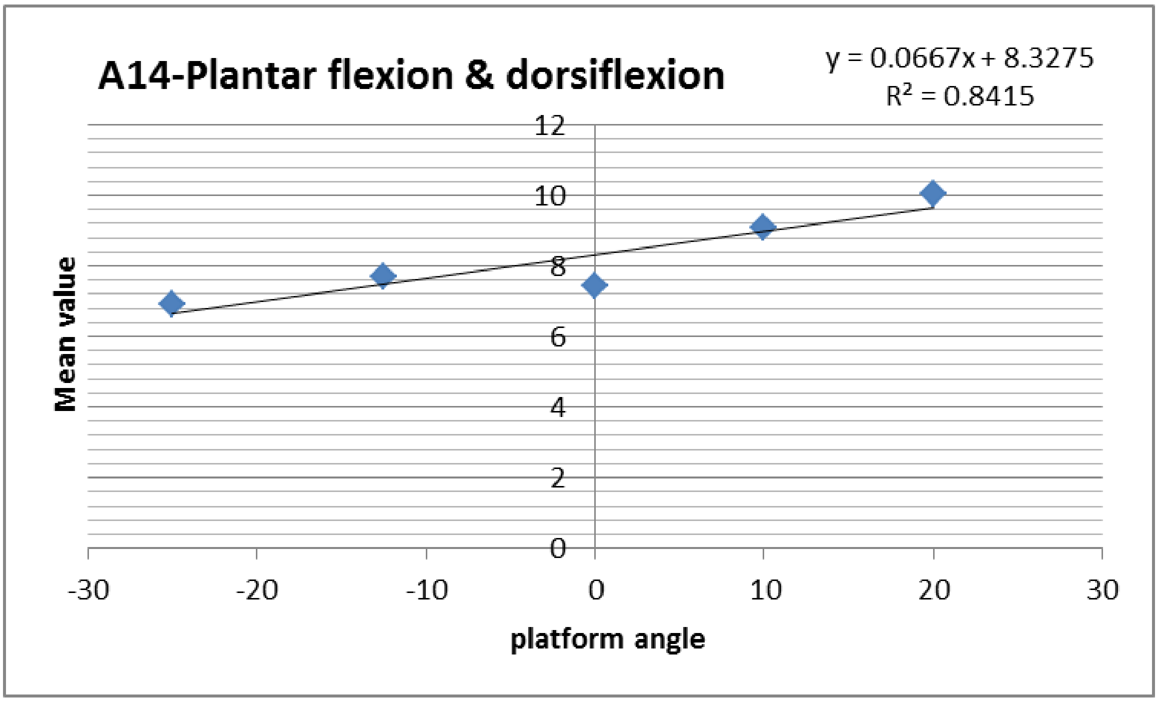

(3) The inversion and eversion

Angle	P-value	Mean value				
		10.0	5.0	0.0	-2.5	-5.0
A1	.668	134.9910	133.9689	132.9491	134.3270	133.3379
A2	.710	130.1831	129.6216	128.7624	129.9070	128.7165
A3	.835	118.8903	118.5857	118.0553	118.6876	117.8772
A4	.712	113.8001	113.8101	113.0879	113.6202	112.7820
A5	.784	126.3240	124.8848	124.5057	126.4528	124.5571
A6	.749	169.4382	168.3561	168.2907	168.1478	168.5227
A7	.821	171.7587	171.5650	172.2494	171.3047	171.4541
A8	.000	103.6262	100.9835	99.0681	99.9146	98.3982
A9	.000	115.6886	111.2115	105.8735	104.7688	102.7522
A10	.000	111.9554	107.0835	100.6238	99.9783	97.4686
A11	.000	109.7252	104.3515	97.8319	96.8269	94.9118
A12	.000	103.9034	99.4048	93.5100	92.8740	91.1269
A13	.000	18.9439	16.8098	12.9147	15.2139	13.1636
A14	.000	12.5213	10.8442	7.4268	8.0684	7.9048
A15	.413	9.2326	8.4661	9.9780	8.8727	9.8491
A16	.000	19.0547	20.9276	24.5821	23.2610	24.2535

A8: $y = 0.3201x + 99.918 \quad R^2 = 0.8862$

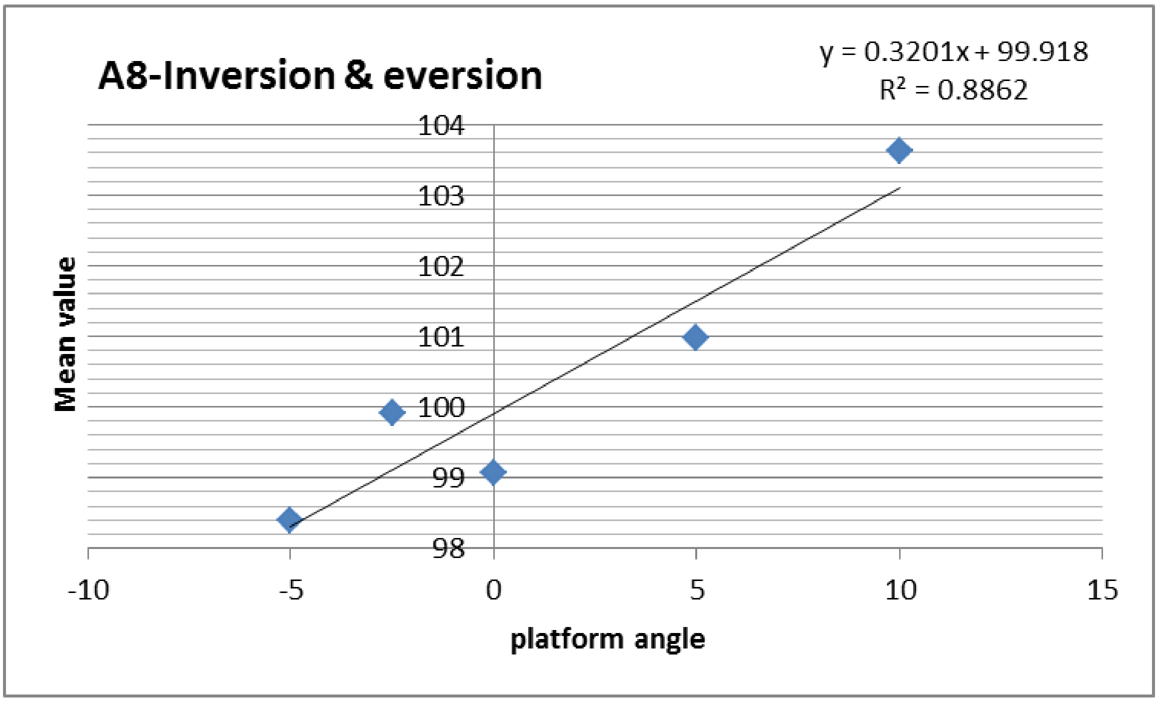

A9: $y = 0.8746x + 106.75$ $R^2 = 0.9911$

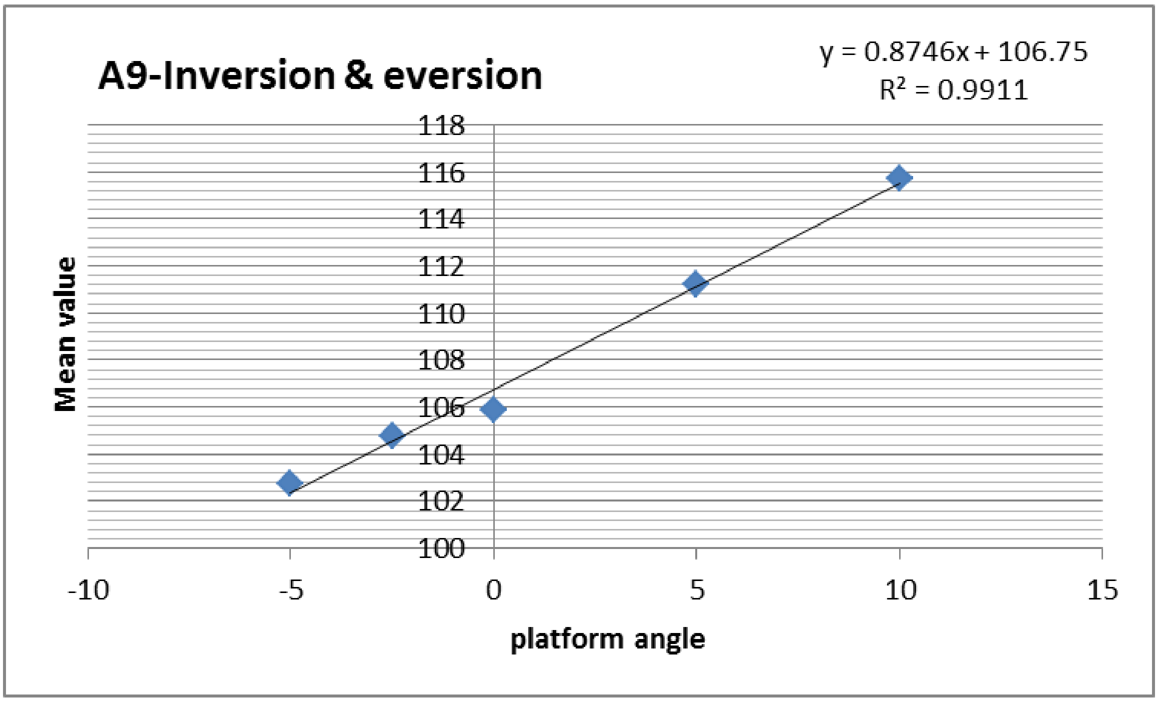

A10: $y = 0.9794x + 101.95$ $R^2 = 0.984$

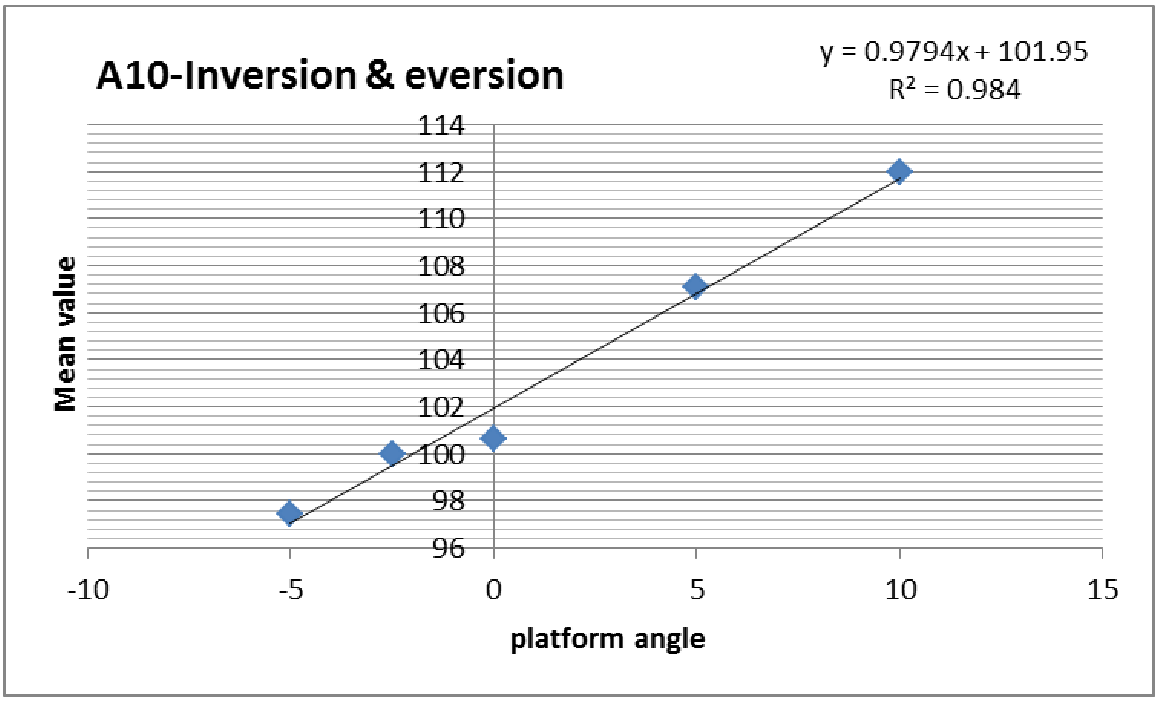

A11: $y = 1.0132x + 99.21$ $R^2 = 0.9824$

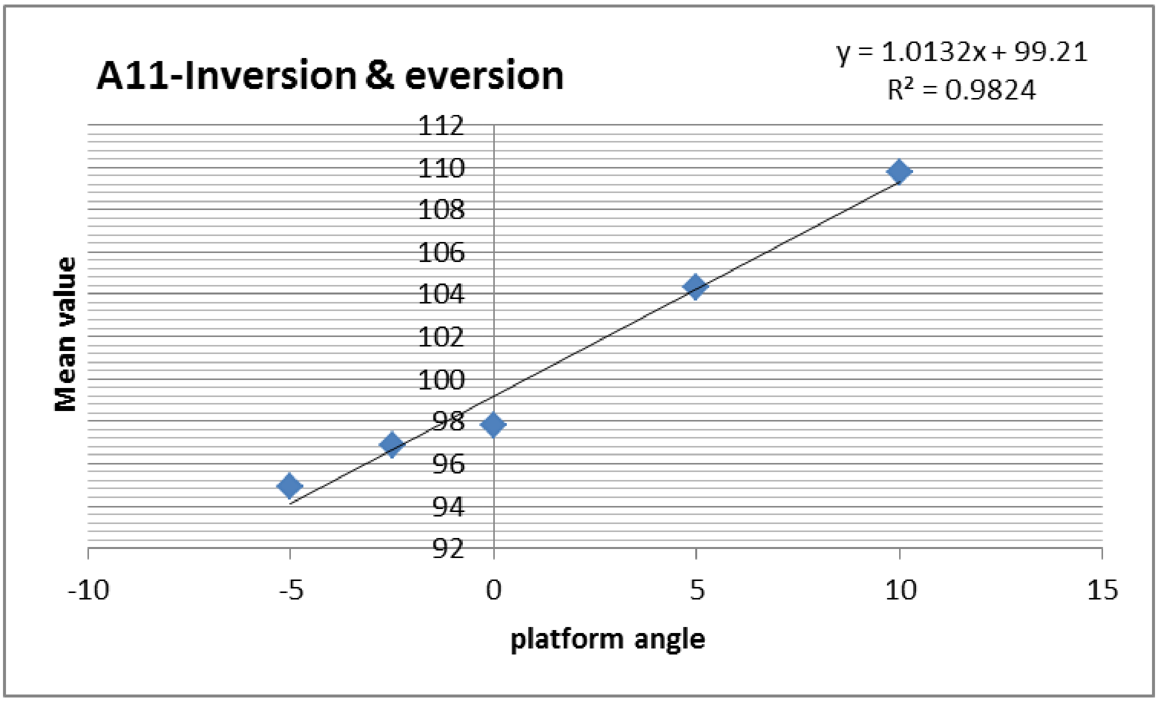

A12: $y = 0.8759x + 94.85$ $R^2 = 0.979$

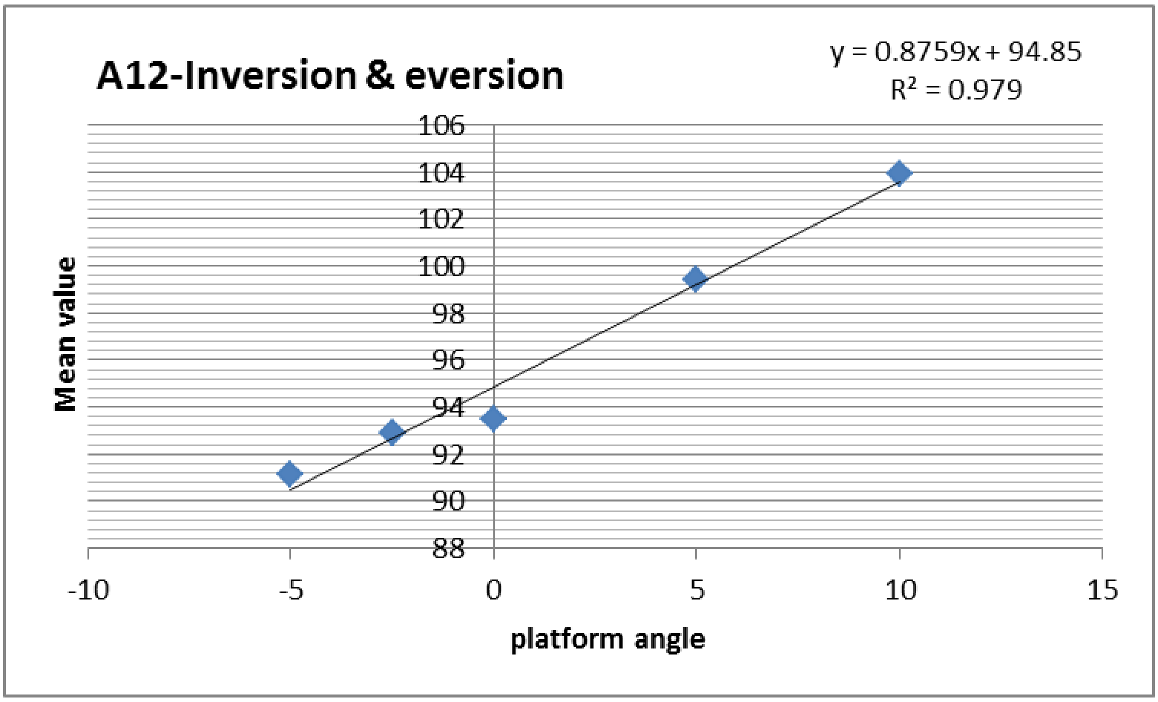

A13: $y = 0.3729x + 14.85 \quad R^2 = 0.7826$

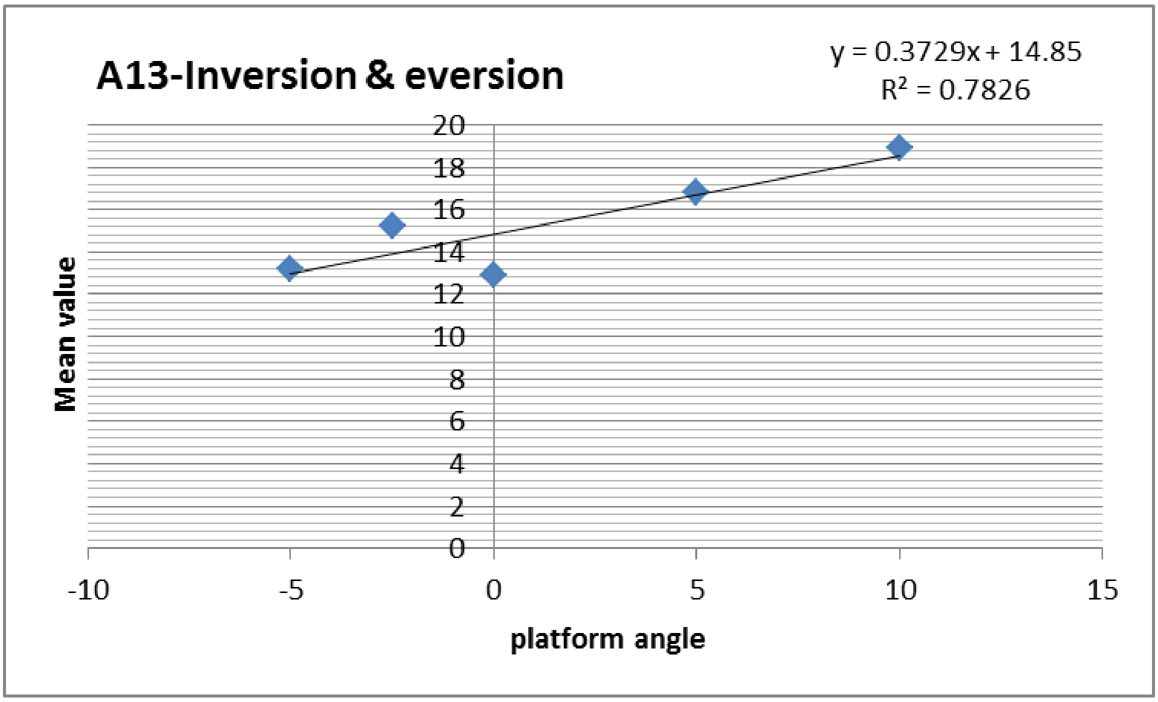

A14: $y = 0.342x + 8.8401 \quad R^2 = 0.8601$

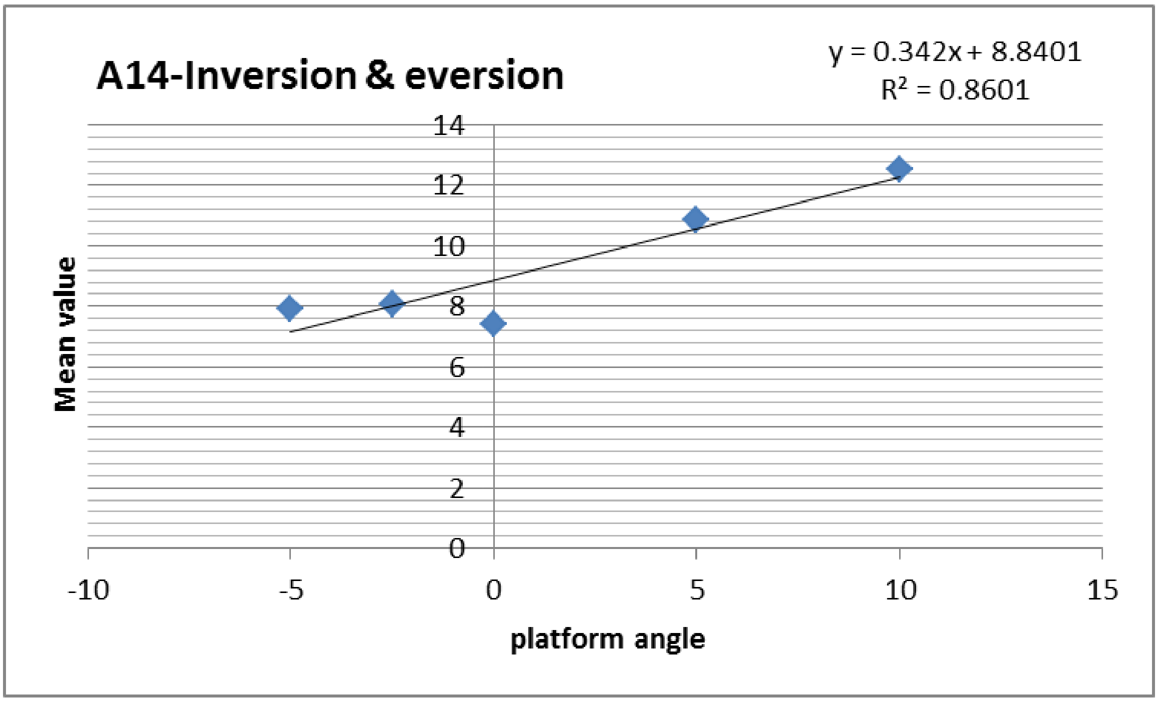

A16: $y = -0.3611x + 22.957$ $R^2 = 0.8478$

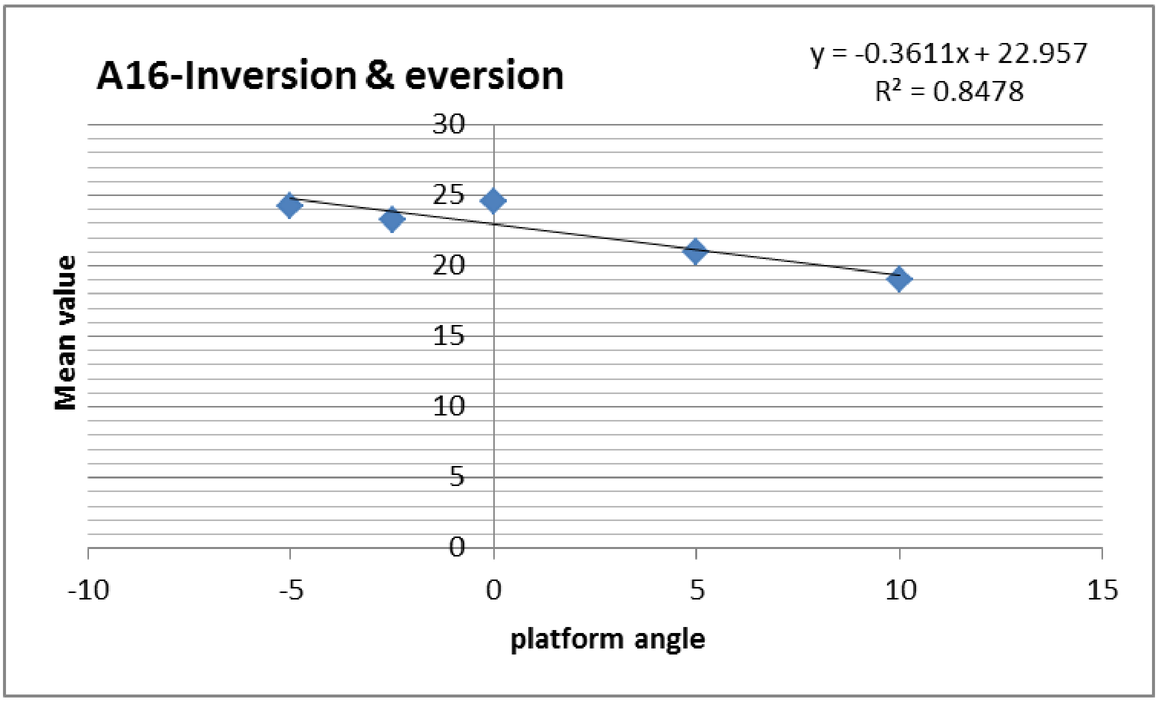

(4) The walking

Angle	P-value	Mean value			
		0%	25%	50%	62%
A1	.000	140.8909	134.9243	134.3612	152.1356
A2	.000	136.9647	130.5065	131.6009	153.9487
A3	.000	127.0938	120.2621	120.7095	146.1606
A4	.000	118.6358	114.6736	109.7011	132.5244
A5	.000	135.8883	129.3440	127.9784	153.1374
A6	.002	169.2656	166.4647	167.8858	170.1298
A7	.000	153.3656	171.2467	152.7166	127.3718
A8	.000	98.8235	94.7368	103.1079	104.1032
A9	.000	108.4110	94.8690	113.1019	116.2292
A10	.000	103.4800	87.2078	107.3683	108.7576
A11	.000	95.8633	82.2774	100.0867	97.7086
A12	.000	88.4565	78.6136	101.8615	109.8381
A13	.000	15.1074	10.9913	17.5740	16.7602
A14	.091	9.2209	10.3047	11.9100	11.5025
A15	.000	12.1851	16.9968	8.0860	11.2699
A16	.000	30.2546	33.0223	19.7160	17.2806

A1: $y = 11.613x + 136.6 \quad R^2 = 0.1503$

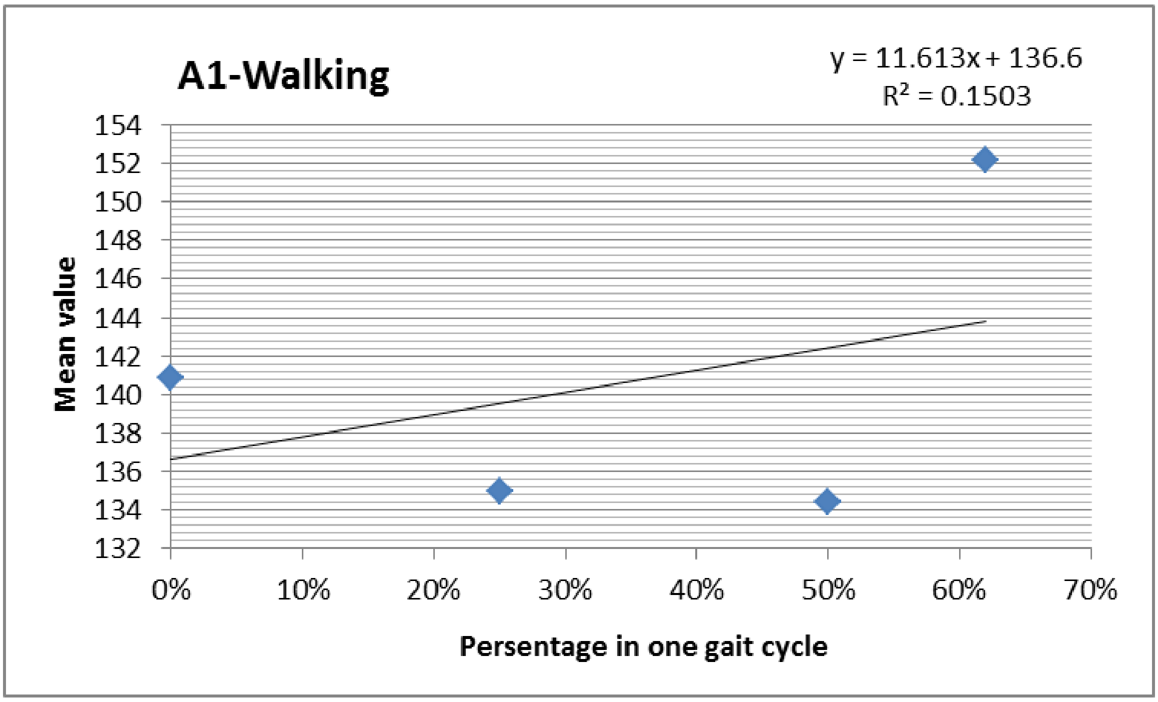

A2: $y = 19.614x + 131.54$ $R^2 = 0.2486$

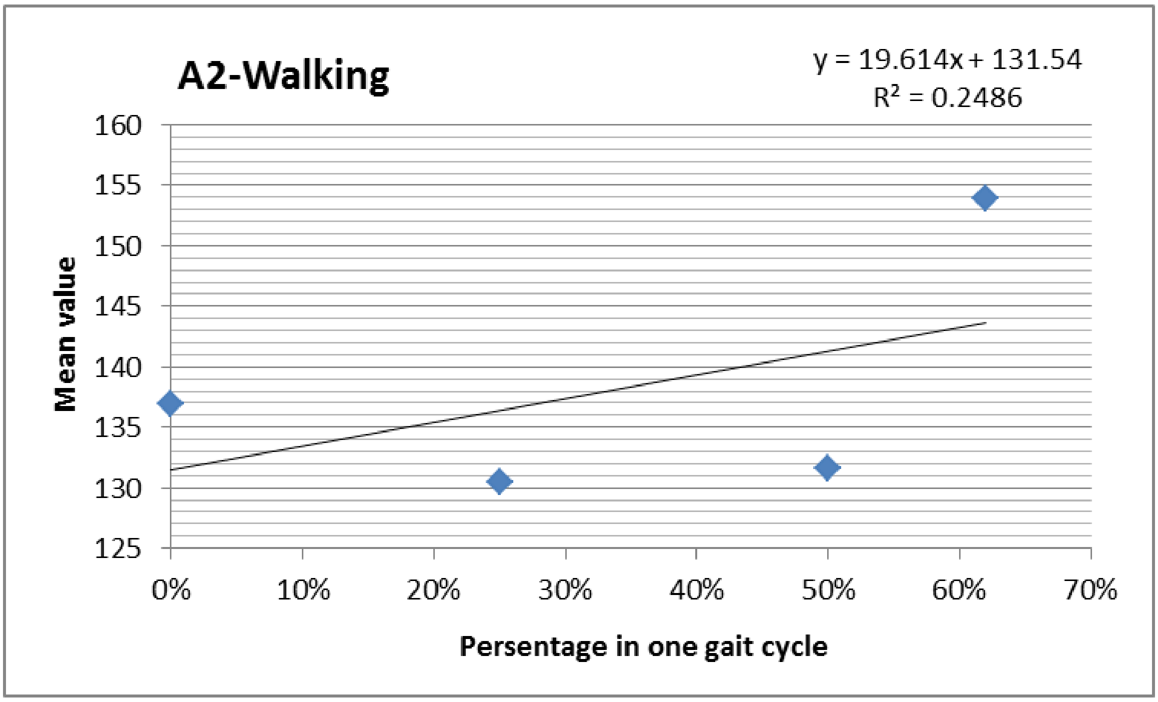

A3: $y = 21.599x + 121.16$ $R^2 = 0.2401$

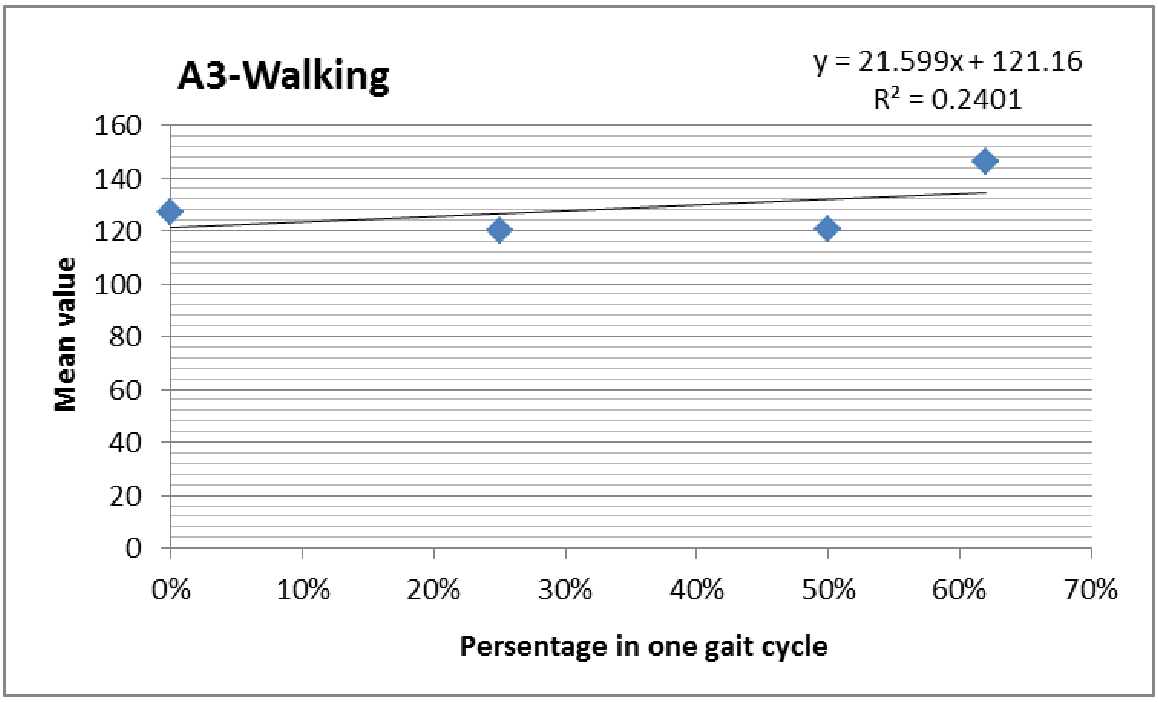

A4: $y = 12.357x + 114.65 \quad R^2 = 0.1206$

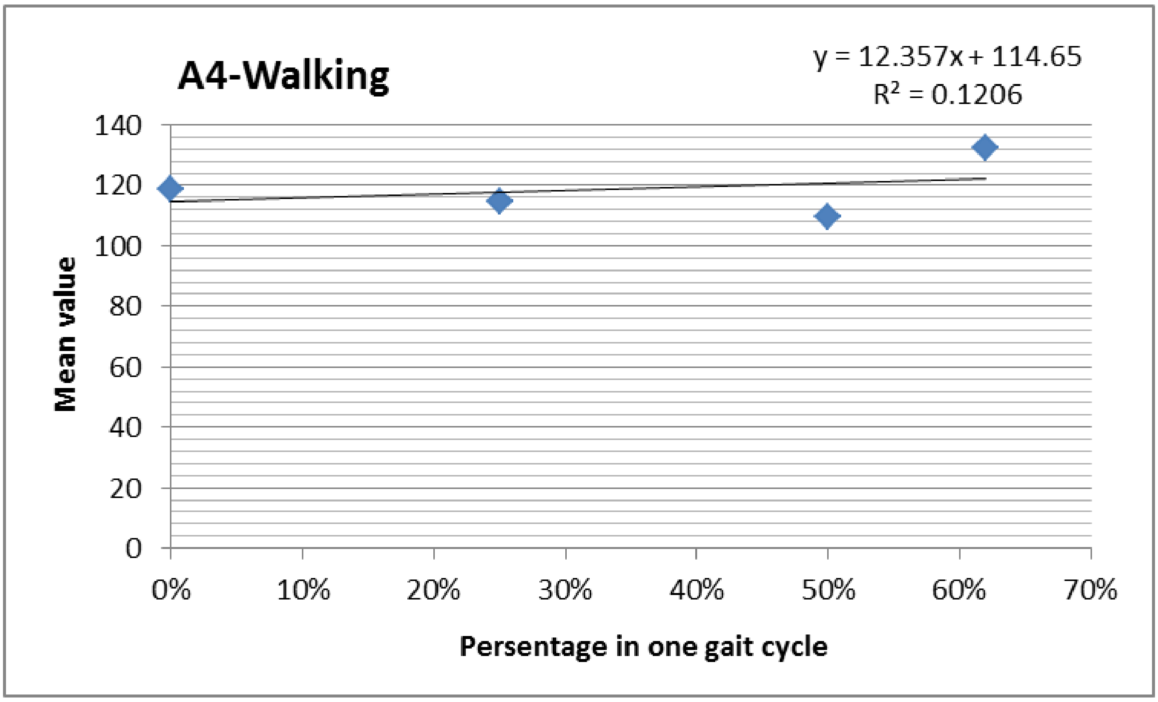

A5: $y = 18.211x + 130.35 \quad R^2 = 0.1883$

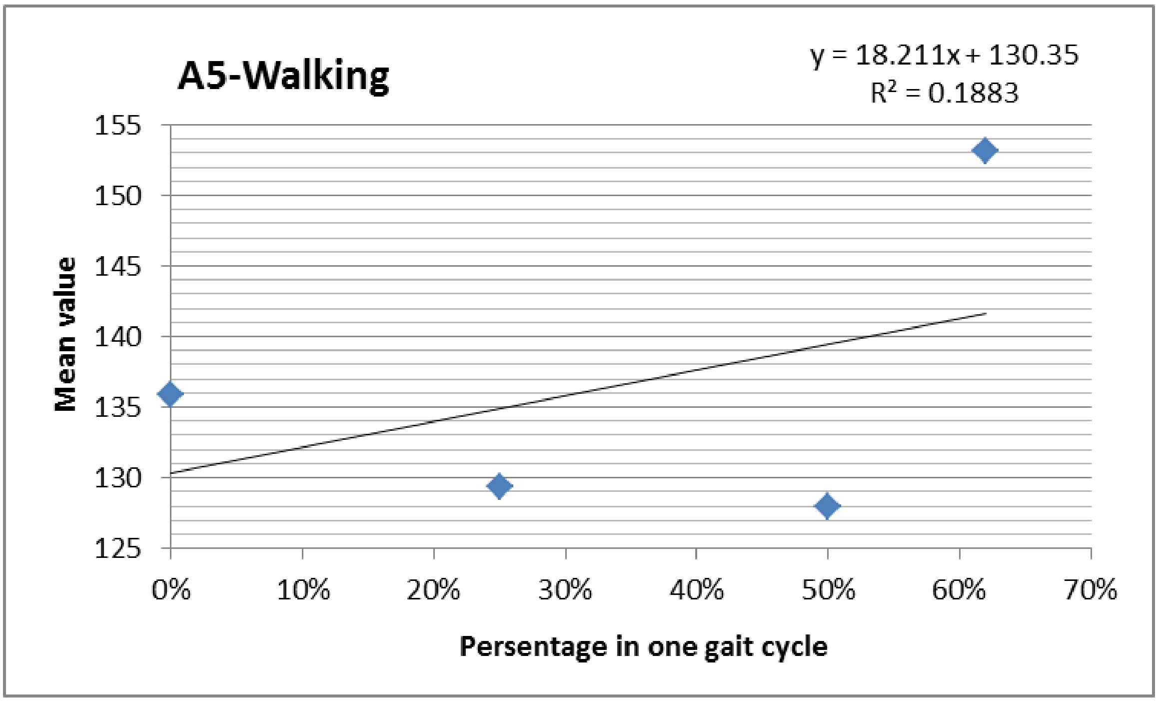

A6: $y = 1.2368x + 168.01 \quad R^2 = 0.045$

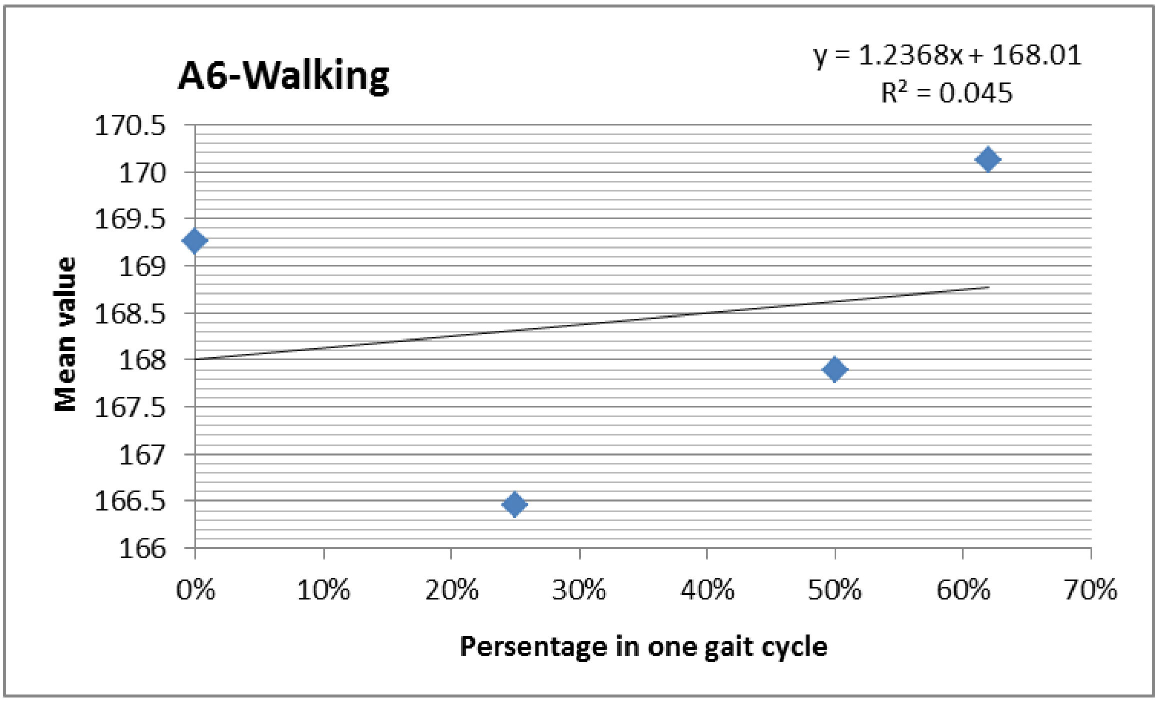

A7: $y = -39.396x + 164.67 \quad R^2 = 0.3618$

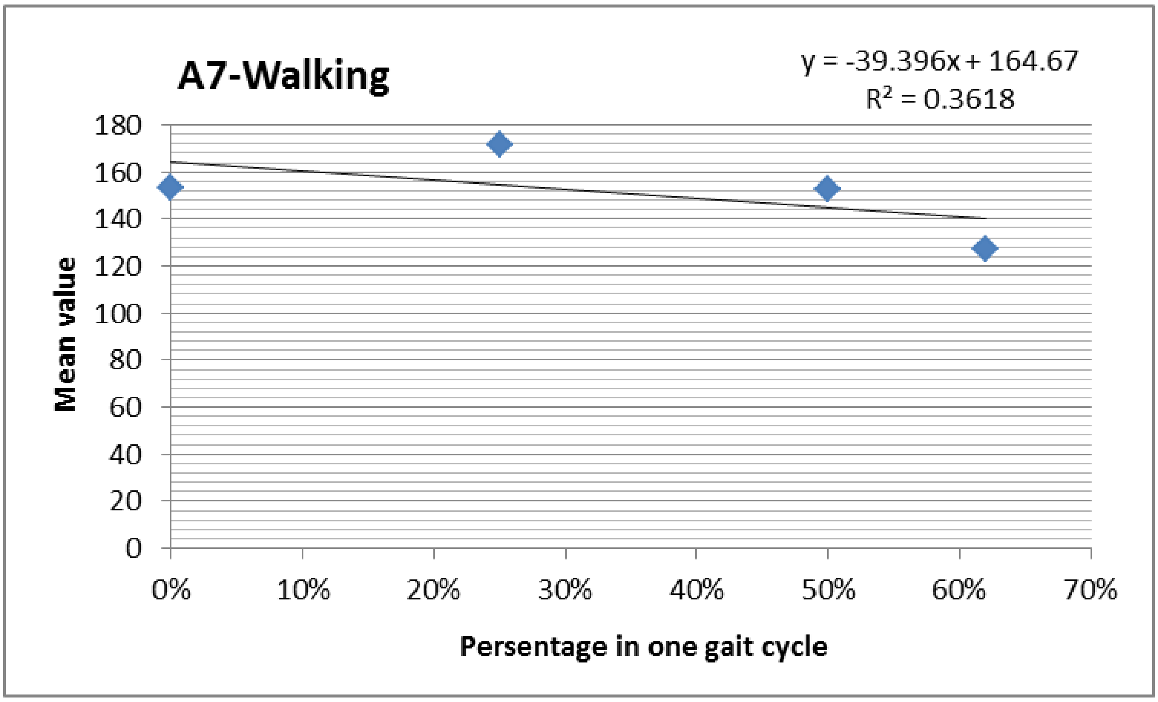

A8: $y = 11.059x + 96.405$ $R^2 = 0.5024$

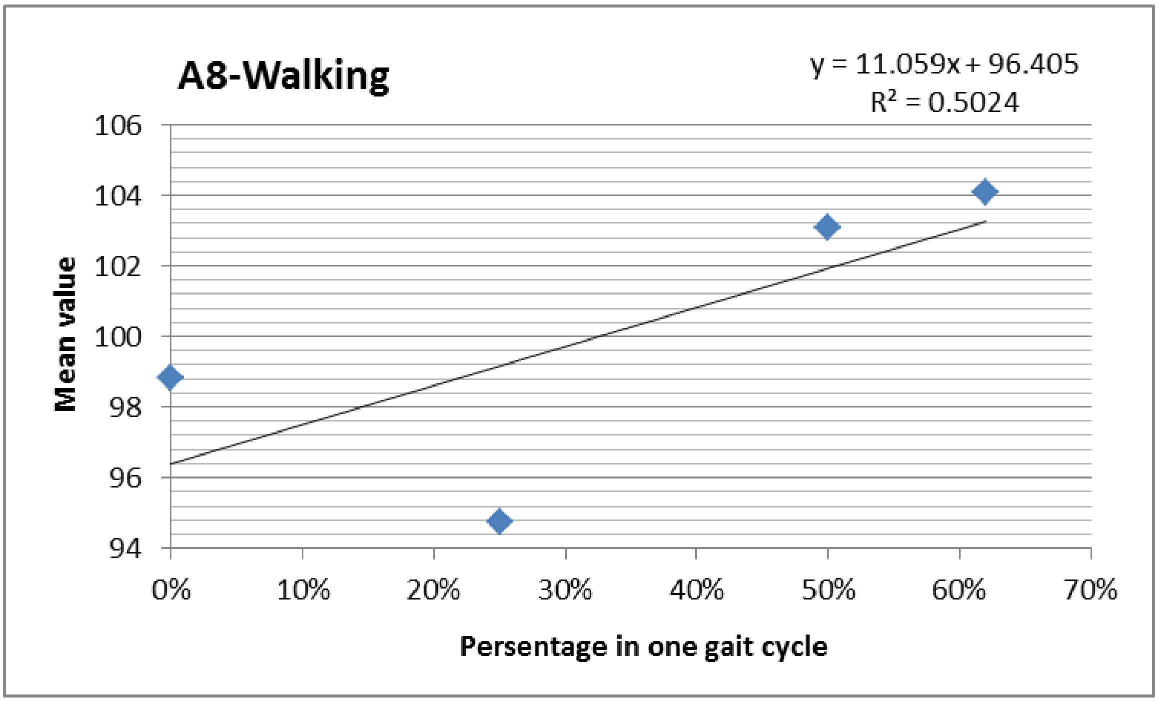

A9: $y = 18.276x + 101.89$ $R^2 = 0.2856$

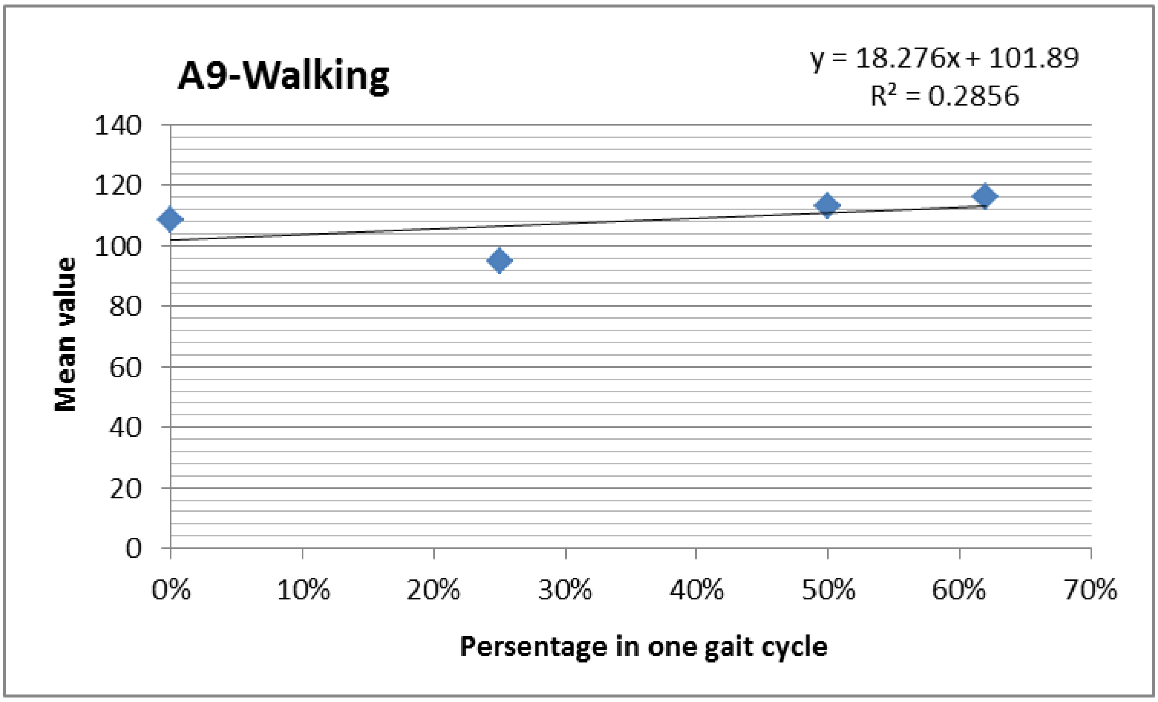

A10: $y = 15.733x + 96.315 \quad R^2 = 0.191$

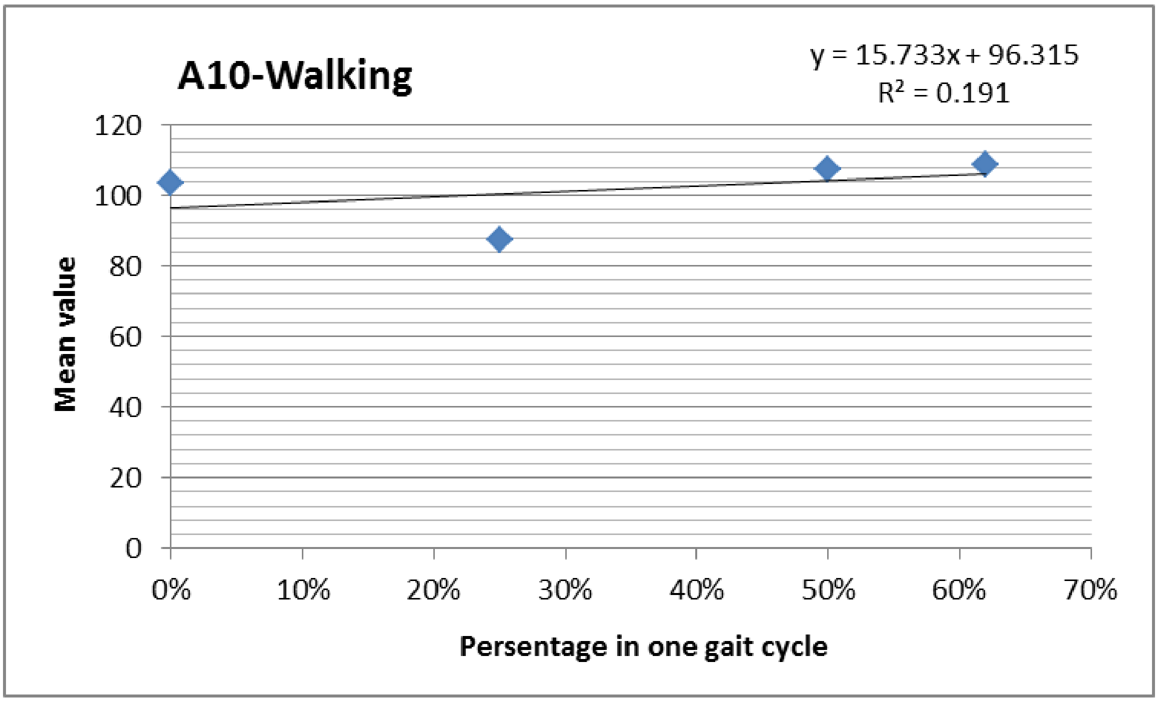

A11: $y = 10.69x + 90.323 \quad R^2 = 0.1357$

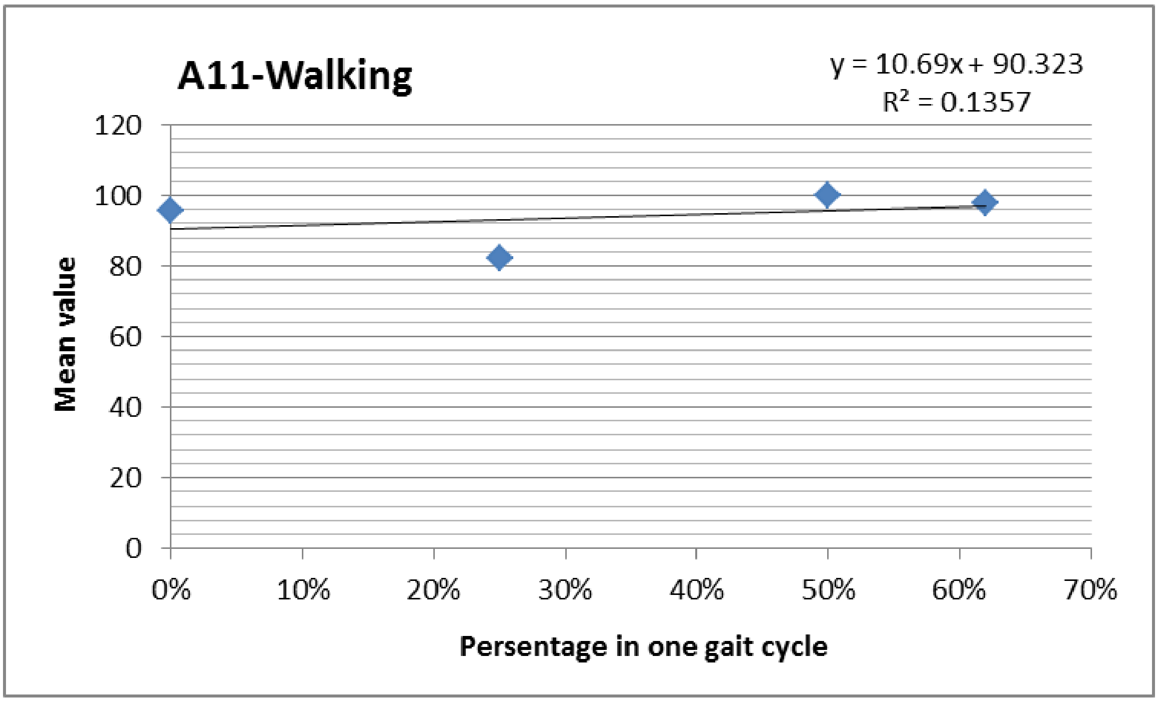

A12: $y = 39.333x + 81.221 \quad R^2 = 0.6092$

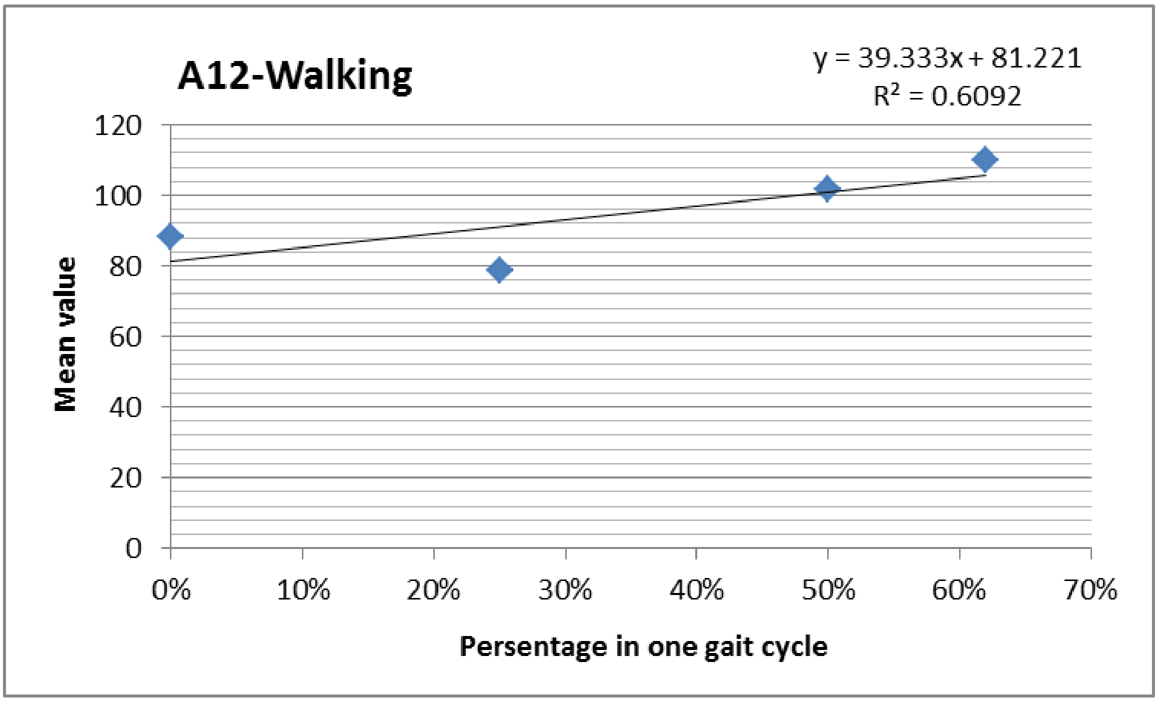

A13: $y = 5.3931x + 13.261 \quad R^2 = 0.2571$

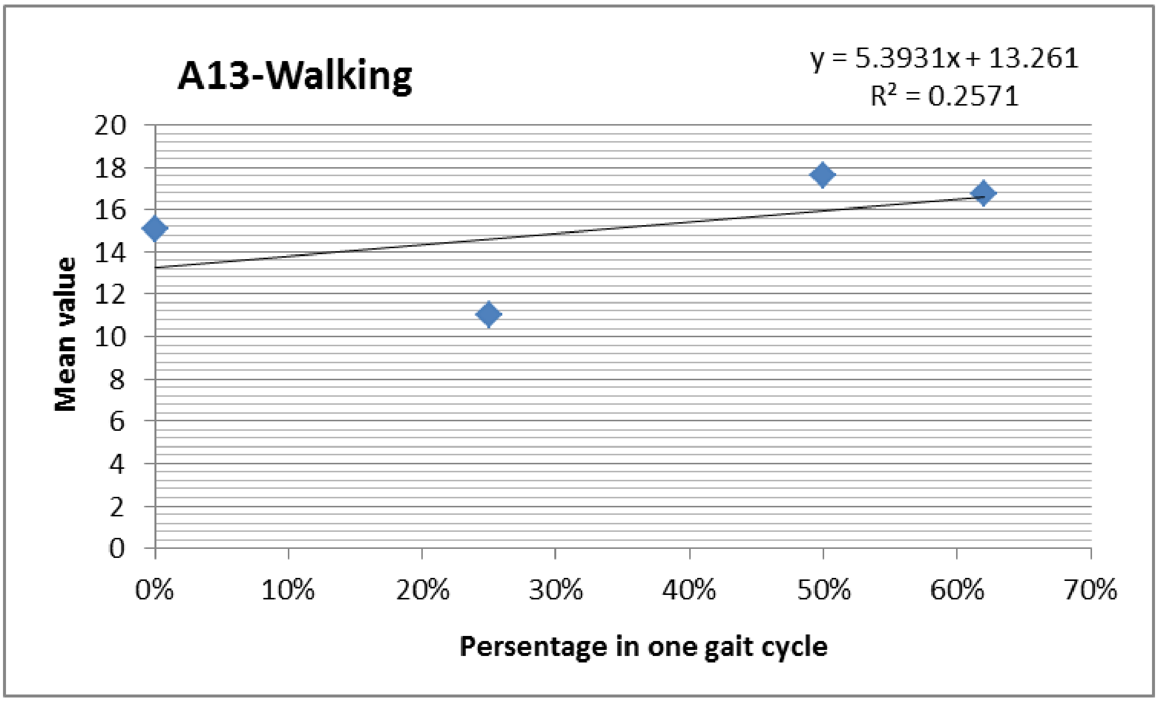

A15: $y = -5.906x + 14.157 \quad R^2 = 0.1947$

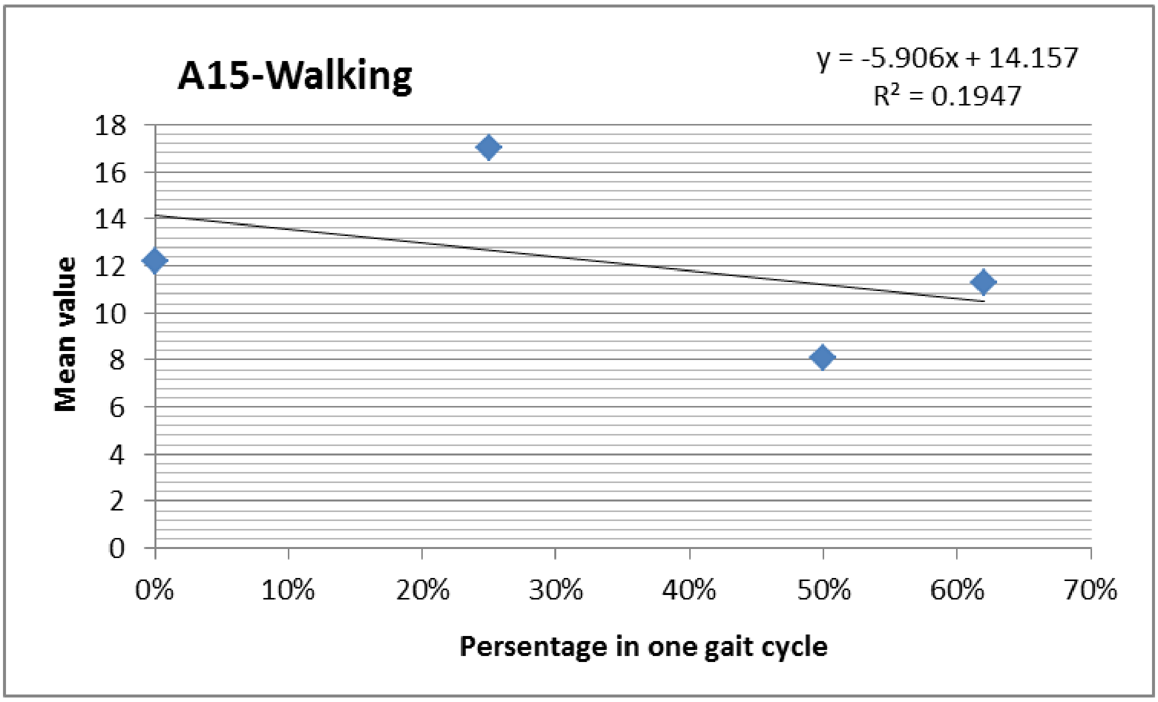

A16: $y = -24.228x + 33.366 \quad R^2 = 0.7447$

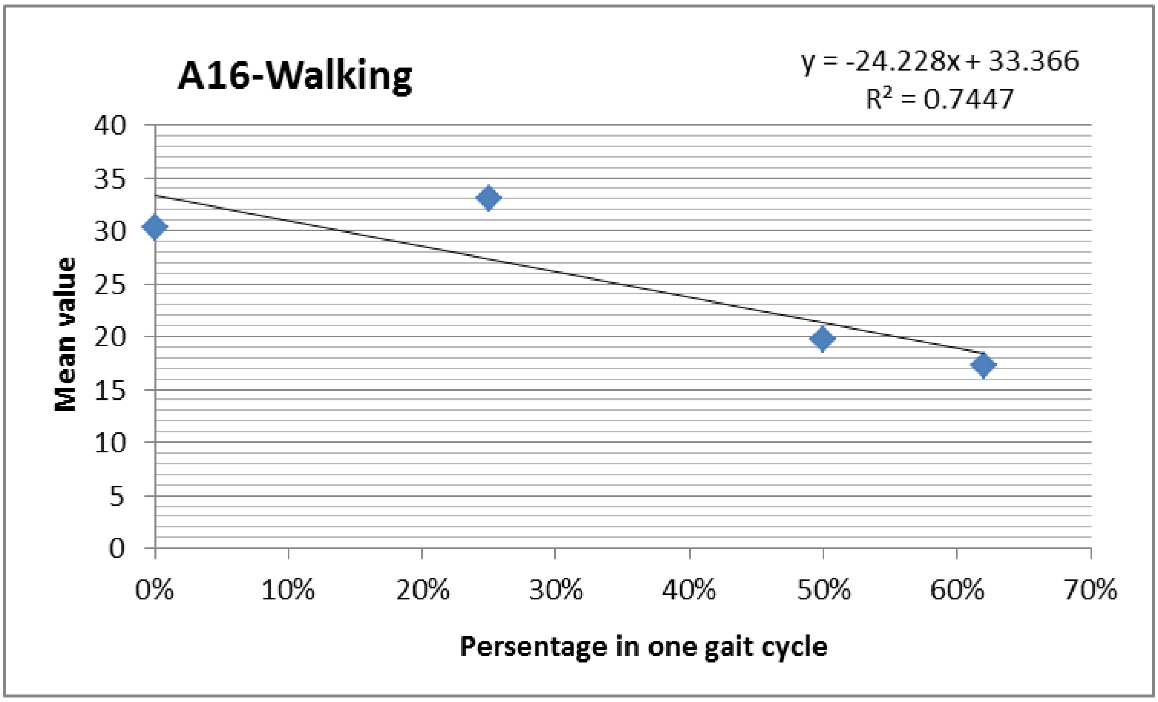

Reference

Abboud R J., (i) Relevant foot biomechanics. Current Orthopaedics, Vol.16, No.3, 2002, pp.165-179.

Almosnino S, Kajaks T, Costigan P A. The free moment in walking and its change with foot rotation angle[J]. BMC Sports Science, Medicine and Rehabilitation, Vol.1, No.1, 2009, pp.19.

Anil A., Peker T., Turgut H.B., Ulukent S.C., An examination of the relationship between foot length, foot breath, ball girth, height and weight of Turkish university students aged between 17 and 25. Anthropologischer Anzeiger, Vol.55, No.1, 1997, pp.79-87.

Åström M, Arvidson T. Alignment and joint motion in the normal foot[J]. Journal of Orthopaedic & Sports Physical Therapy, Vol.22, No.5, 1995, pp.216-222.

Blanchette A, Lambert S, Richards C L, Bouyer L.J., Walking while resisting a perturbation: effects on ankle dorsiflexor activation during swing and potential for rehabilitation, Gait & posture, Vol.34, No.3, 2011, pp.358-363.

Blenkinsopp R., Harland A., Price D., Lucas T., Roberts J., A method to measure dynamic dorsal foot surface shape deformation during linear running using digital image correlation, Procedia Engineering, Vol.34, 2012, pp. 266-271.

Boulgouris, N.V., Plataniotis, K.N., Hatzinakos, D., Gait recognition using dynamic time warping, IEEE 6th Workshop on Multimedia Signal Processing, 2004, pp. 263–266.

Bruderlin A, Calvert T W. Goal-directed, dynamic animation of human walking[C]//ACM SIGGRAPH Computer Graphics. ACM, Vol.23, No.3, 1989, pp.233-242.

Cappozzo A., Catani F.,Della Croce U., Leardini A., Position and orientation in space of bones during movement: anatomical frame definition and determination, Clinical Biomechanics, Vol. 10, 1995, pp. 171-178.

Carson M.C., Harrington M.E., Thompson N., O'Connor J.J, Theologis T.N., Kinematic analysis of a multi-segment foot model for research and clinical application: a repeatability analysis, Journal of Biomechanics, Vol. 34, 2001, pp. 1299-1307.

Cavanagh S. Content analysis: concepts, methods and applications. Nurse researcher, Vol.4, No.3, 1997, pp.5-13.

Ceseracciu E., New frontiers of markerless motion capture: application to swim biomechanics and gait analysis, 2011.

Chester V. L., E. N. Biden, M. Tingley, Gait analysis, Biomedical instrumentation and Technology, 2005, pp. 64-74.

Collins T.D., Ghoussayni S.N., Ewins D.J., Kent J.A., A six degrees-of-freedom marker set for gait analysis: Repeatability and comparison with a modified Helen Hayes set, Gait & Posture, Vol. 30, 2009, pp. 173-180.

Corazza S., M¨Undermann L., Chaudhari A. M., Demattio T., Cobelli C., Andriachii T. P., A markerless motion capture system to study musculoskeletal biomechnics: visual hull and simulated annealing approach, Annals of biomedical engineering, Vol. 34, No. 6, 2006, pp. 1019-1029.

Cong Y., Evaluationg of biomechanical environment of foot within different shoes, PhD thesis in The Hong Kong Polytechnic University, 2011.

Cong Y., Cheung J., Leung A., Zhang M., Effect of heel height on in-shoe localized triaxial stresses, Journal of Biomechanics, No. 44, 2011, pp. 2267-2272.

Davis R.B., Ounpuu S., Tyburski D., Gage J.R., A gait analysis data collection and reduction technique, Human Movement Science, Vol. 10, 1991, pp. 575-587.

Dawe E.J., Davis J., Anatomy and biomechanics of the foot and ankle, Orthopaedics and Trauma, Vol. 25, No. 4, 2011, pp. 279-286.

De Vries G, Roy K, Chester V. Using three-dimensional gait data for foot/ankle orthopaedic surgery. The open orthopaedics journal, Vol.3, No.89, 2009.

Fessler D.M.T., Haley K.J., Lal R.D., Sexual dimorphism in foot length proportionate to stature, Annuals of Human Biology, January-Feburary, Vol.32, No.1, 2005, pp.44-59.

Forner-Cordero A., Koopman, H.J.F.M., van der Helm, F.C., Describing gait as a sequence of states. Journal of Biomechanics, Vol. 39, 2006, pp. 948–957.

Freychat P., Belli A., Carret J. P., Lacour J. R., Relationship between reearfoot and forefoot orientation and ground reaction forces during running, Medicine and Science in Sports and Exercise, No. 28, 1996, pp.225-232.

Fuller J, Liu L J, Murphy M C, et al. A comparison of lower-extremity skeletal kinematics measured using skin-and pin-mounted markers, Human Movement Science, Vol.16, No.2, 1997, pp.219-242.

Gatt A., Chockalingam N., Chevalier T.L., Sagittal plane kinematics of the foot during passive ankle dorsiflexion, Prosthetics and Orthotics International, Vol.35, No. 4, 2011, pp. 425-431.

Goonetilleke R.S., Ho C.F., So R.H.Y., Foot anthropometry in Hong Kong, In Proceedings of the ASEAN 97 Conference, Louisville, KY: IEA Press, 1997, pp. 81-88.

Goonetilleke R.S., Luximon A., Foot flare and foot axis, Human factors, Vol.41, No.4, 1999, pp. 596-607.

Gu Y., Rong M. Ruan G., Outsole pressure distribution character during high-heeled walking, Procedia environmental sciences, No. 8, 2011, pp. 464-468.

Hayafune N., Hayafune Y., Jacob H.A.C., Pressure and force distribution characteristics under the normal foot during the push-off phase in gait, The Foot, No.9, 1999, pp.88-92.

Hawes M. R., Sovak D., Quantitative morphology of the human foot in a North American population, Ergonomics, Vol.37, No.7, 1994, pp.1213-1226.

Helwig N. E., Hong S.J., Hsiao-Wecksler E.T., Polk J.D., Methods to temporally align gait cycle data, Journal of Biomechanics, Vol. 44, 2011, pp. 561-566.

Herrewegen V., Cuppens K., Broeckx M., Vertommen H., Mertens M., Peeraer L., Development of a model to analyse foot biomechanics using dynamic 3D surface scanning, Computer Methods in Biomechanics and Biomedical Engineering, Vol. 15, No.S1, Sep. 2012, pp. 85-86.

Hunt A. E., Smith R.M., Torode M., Keenan A.M., Inter-segment foot motion and ground reaction forces over the stance phase of walking, Clinical Biomechanics, No.16, 2001, pp. 592-600.

Jenkyn T.R., Nicol A. C., A multi-segment kinematic model of the foot with a novel definition of forefoot motion for use in clinical gait analysis during walking, Journal of Biomechanics, Vol. 40, 2007, pp. 3271-3278.

Jezersek M., Novak B., Mozina J., Three-dimensional laser based measurement of human foot during walking, Footwear Science, Vol.3, 2011, pp. S81-S83.

Jonathan D., The foot book: a complete guide to healthy feet, Johns Hopkins University Press, 2011.

Kadaba M.P., Ramakrishnan H.K., Wotten M.E., Measurement of lower extremity kinematics during level walking, Journal of Orthopaedic Research, Vol. 8, 1990, pp. 383-392.

Kale A., Cuntoor N., Yegnanarayana B., Rajagopalan A.N., Chellappa R., Gait analysis for human identification. Lecture Notes in Computer Science, vol. 2688, 2003, pp. 706–714.

Kidder S.M., Abuzzahab F.S., Harris G.F., Johnson J.E., Asystem for the analysis of foot and ankle kinematics during gait, IEEE Transactions on Rehabilitation Engineering, Vol. 4, 1996, pp. 25-32.

Kimura M, Mochimaru M, Kouchi M, 3D cross-sectional shape measurement of the foot while walking, Proceedings of the 7th Symposium on Footwear Biomechanics, International Society of Biomechanics, 2005, pp. 34-35.

Kimura, Makoto, Masaaki Mochimaru, and Takeo Kanade. "Measurement of 3D foot shape deformation in motion." Proceedings of the 5th ACM/IEEE International Workshop on Projector camera systems. ACM, 2008.

Kitagawa M., Windsor B., MoCap for Artists: Workflow and Techniques for Motion Capture, Focal Press, Elsevier, US, 2008.

Klenerman L., The foot and its disorders, Blackwell scientific, Austria, 1991.

Klette R, Tee G. Understanding human motion: A historic review. Springer Netherlands, 2008.

Kouchi m., Kimura M., Mochinaru M., Deformation of foot cross-section shapes during walking, Gait and Posture, No. 30, 2009, pp.482-486.

Krauss I., Grau S., Mauch M., Maiwald C., Horstmann T., Sex-related differences in foot shape, Ergonomics, Vol.51, No.11, 2008, pp.1693-1709.

Kuo A.D., Stabilization of lateral motion in passive dynamic walking, The International Journal of Robotics Research, 1999, Vol.18, No. 9, pp. 917-930.

Kusumoto A., Suzuki T., Kumakura C., Ashizawa K., A comparative study of foot morphology between Filipino and Japanese women, with reference to the significance of a deformity like hallux valgus as a normal variation, Annals of human biology, Vol.23, No.5, 1996, pp.373-385.

Leardini A., Benedetti M.G., Catani F., Simoncini L., Giannini S., An anatomically based protocol for the description of foot segment kinematics during gait, Clinical Biomechanics, 1999, Vol. 14, No. 8, pp. 528-536.

Leardini A., Sawacha Z, Paolini G., Ingrosso S., Nativo R., Beneditti M.G., A new anatomically based protocol for gait analysis in children, Gait & Posture, Vol. 26, 2007, pp. 560-571.

Ledoux W., Camacho D., Ching R., Sangeorzan B., The development and validation of a computational foot and ankle model, Proceedings of the 22nd Annual EMBS International Conference, 2000.

Lewis G., Finite element analysis of a model of a therapeutic shoe: effect of material selection for the outsole, Bio-Medical Materials and Engineering, Vol. 13, 2003, pp. 75-81.

Livne M., Sigal L., Troje N.F., Fleet D.J., Human attributes from 3D pose tracking, Computer vision and image understanding, Vol. 116, 2012, pp. 648-660.

Long J.T., Wang M., Harris G. F., A model for the evaluation of lower extremity kinematics with integrated multisegmental foot motion, Journal of Experimental and Clinical Medicine, Vol. 3, No. 5, 2011, pp. 239-244.

Luo G., Houston V.L., Mussman M., Garbarini M., Beattie A.C., Thongpop C., Comparison of male and female foot shape, J Am Podiat Med Assoc, Vol.99, 2009, pp.383-390.

Lundberg A., On the use of bone and skin markers in kinematics research, Human movement science, Vol. 15, 1996, pp. 411-422.

Luximon A., Goonetilleke R.S., Foot shape modeling, Human Factors, Vol. 46, No. 2, 2004, pp. 304-315.

Luximon A., Goonetilleke R.S., Zhang M., 3D foot shape generation from 2D information, Ergonomics, Vol. 48, No. 6, 2005, pp. 625-641.

Luximon A., Goonetilleke R.S., Zhang M., 3D foot shape generation from 2D information, Ergonomics, Vol. 48, No. 6, 2007, pp. 625-641.

Luximon A, Luximon Y. Preliminary study on dynamic foot model[M]//Digital Human Modeling. Springer Berlin Heidelberg, 2011, pp.321-327.

Mann R.A., Gould J.S., The Foot book: Biomechanics of the foot, Baltimore, Williams

& Wilkins, 1988.

Manal K., McClay I., Stanhope S., Richards J., Galinat B., Comparison of surface mounted markers and attachment in estimating tibial rotations during walking: an in vivo study, Gait & Posture, Vol. 11, 2000, pp. 38-45.

Marey, E-J. Le Mouvement, Paris: Masson (Movement, Translated from French by Pritchard, E., London: William Heinemann, 1895), 1894.

Mauch M., Mickle K. J., Munro B.J., Dowling A.M., Grau S., Steele J.R., Do the feet of German and Australian children differ in structure? Implications for children's shoe design, Ergonomics, Vol.51, No.4, 2008, pp. 527-539.

McPoil, T.G., Cornwall M.W., Relationship between three static angles of the rearfoot and the pattern of rearfoot motion during walking, Journal of Rothopaedic and Sports Physical Therapy, Vol. 23, No. 6, June 1996, pp. 370-375.

McPoil T.G., Cornwall M.W., Medoff L., Vicenzino B., Forsberg K., Hilz D.. Arch height change during sit-to-stand: an alternative for the navicular drop test. Journal of Foot Ankle Res, Vol.1, No. 3, 2008.

Menache, A., Understanding motion capture for computer animation, Burlington, Mass., Morgan Kaufmann, 2011.

Montgomery D.C., Design and analysis of experiments, fifth edition, Wiley, USA, 2001, pp. 624-627.

Mochimaru M, Kouchi M. 4D measurement and analysis of plantar deforma- tion during walking and running.In: Proceedings of the 10th footwear biomechanics symposium; Footwear Sci, No.3, 2011, pp.109–12.

Morio C., Lake M. J., Gueguen N., Rao G., Baly L., The influence of footwear on foot motion during walking and running, Journal of Biomechanics, No. 42, 2009, pp.2081-2088.

Moseley L., Smith R., Hunt A., Gant R., Three-dimensional kinematics of the rearfoot during the stance phase of walking in normal young adult males, Clinical Biomechanics, Vol. 11, No. 1, 1996, pp. 39-45.

Myers K.A., Wang M., Marks R.M., Harris G.F., Validation of a multisegment foot and ankle kinematic model for pediatric gait, IEEE Transactions on Neural Systems and Rehabilitation Engineering, Vol. 12, 2004, pp. 122-130.

Nacher B., Alemany S., Gonzalez J.C., Alcantara E., Garcia-Hernandez J., Heras S., Juan A., A footwear fit classification model based on anthropometric data, Proceedings of the 8th annual digital human modeling for design and engineering symposium, 4-6th, July, 2006, Lyon, pp.2327.

Nester C., Jones R.K., Liu A., Howard D., Lundberg A., Arndt A., Lundgren P., Stacoff A., Wolf P., Foot kinematics during walking measured using bone and surface mounted markers, Journal of Biomechanics, Vol. 40, 2007, pp. 3412-3423.

Nielsen D B, Daugaard M. Comparison of angular measurements by 2D and 3D gait analysis. Jö nkö ping, School of Health Sciences, Jönköping University, 2008.

Nitin S., Stephen B., Understanding the gait cycle, as it relates to the foot, Orthopaedics and trauma, Vol. 25, No. 4, 2011, pp. 236-240.

Oatis C.A., Biomechanics of the foot and ankle under static conditions, Physical Therapy, Vol. 68, No. 12, 1988, pp. 1815-1821.

Perry, J., Gait Analysis: Normal and Pathological Function, SLACK Incorporated, Thorofare, NJ, 1992.

Pratt, E.J., Reeves M.L., van der Meulen J.M., Heller B.W., The development, preliminary validation and clinical utility of a shoe model to quantify foot and footwear kinematics in 3-D, Gait & posture Vol.36, No.3, 2012, pp.434-438.

Rattanaprasert U., Smith R., Sullivan M., Gilleard W., Three-dimensional kinematic of the forefoot, rearfoot, and leg without the function of tibialis posterior in comparison with normals during stance phase of walking, Clinical Biomechanics, Vol. 14, No. 1, 1999, pp. 14-23.

Ren L, Jones R K, Howard D. Predictive modelling of human walking over a complete gait cycle. Journal of biomechanics, Vol.40, No.7 2007, pp.1567-1574.

Roaas A., Andersson G., Normal range of motion of the hip, knee and ankle joints in male subjects, 30-40 years of age, Acta orthop. Scand, No.53, 1982, pp.205-208.

Roos, P.E., Dingwell J.B., Influence of simulated neuromuscular noise on movement variability and fall risk in a 3D dynamic walking model, Journal of Biomechanics, Vol. 43, No. 15, 2010, pp. 2929-2935.

Roos, P.E., Dingwell J.B., Influence of simulated neuromuscular noise on the dynamic stability and fall risk of a 3D dynamic walking model, Journal of Biomechanics, Vol. 44, 2011, pp. 1514-1520.

Roos P.E., Dingwell J.B., Influence of neuromuscular noise and walking speed on fall risk and dynamic stability in a 3D dynamic walking model, Journal of Biomechanics, Vol. 46, 2013, pp. 1722-1728.

Rout N., Zhang Y.F., Khandual A., Luximon A., 3D foot scan to custom shoe last, Special Issue of IJCCT, Vol.1, Issue 2,3,4, 2010 FOR International Conference.

Rosenhahn, B., Human motion: understanding, modeling, capture and animation. Dordrecht, Springer, 2008.

Rose J D, Martorana V J. The Foot Book: A Complete Guide to Healthy Feet. JHU Press, 2013.

Sadeghi, H., Allard, P., Shafie, K., Mathieu, P.A., Sadeghi, S., Prince, F., Ramsay, J., Reduction of gait data variability using curve registration, Gait and Posture, Vol. 12, 2000, pp. 257–264.

Samson W., Hamme A.V., Sanchez S., Cheze L., Jan S.V.S., Feipel V., Foot roll-over evaluation based on 3D dynamic foot scan, Gait & Posture, Vol. 39, 2014, pp. S577-582.

Simon J., Doederlein L., McIntosh A.S., Metaxiotis D., Bock H.G., Wolf S.I., The heidelberg foot measurement method: development, description and assessment, Gait and Posture, Vol. 23, 2006, pp. 411-424.

Speksnijder C.M., Munckhlf R., Moonen S., Walenkamp G., The higher the heel the higher the forefoot-pressure in ten healthy women, The Foot, No.15, 2005, pp.17-21.

Stacoff A., Kalin X., Stussi E., The effect of shoes on the torsion and rearfoot motion in running. Medicine and Science in Sports and Exercise, No. 23, 1991, pp.428-490.

Stone E E, Skubic M. Unobtrusive, continuous, in-home gait measurement using the Microsoft Kinect. 2013.

Sturmer, M., et al. "Alignment of multiple time-of-flight 3D cameras for reconstruction of walking feet." Proceedings of ISB XXIII: 3–7th July 2011 Brussels, Belgium.

Tang Y.K., Foot shape prediction from digital images, Hong Kong University of

Science and Technology, 2007.

Tang Y.M., Hui K.C., Human foot modeling towards footwear design, Computer-Aided Design, Vol. 43, 2011, pp. 1841-1848.

Telfer S, Woodburn J. The use of 3D surface scanning for the measurement and assessment of the human foot. J Foot Ankle Res, Vol.5, No.19, 2010.

Tranberg R., Analysis of body motion based on optical markers, University of Gothenburg, 2010.

Tremaine M. D., Awad E.M., The foot & ankle sourcebook: everything you need to know, Lowell house, 1998.

Tsung B.Y.S., Zhang M., Fan Y.B., Boone D.A., Quantitative comparison of plantar foot shapes under different weight-bearing conditions, Journal of Rehabilitation Research and Development, Vol. 40, No. 6, 2003, pp.517-526.

Tu H.H., Yu C.Y., An investigation on the establishment of foot surface area estimation formula using 3-D foot scanner, Journal of the Chinese Institute of Industrial Engineers, Vol. 25, No. 3, 2008, pp. 223-228.

Wang C.S., An analysis and evaluation of fitness for shoe lasts and human feet, Comput Ind, Vol.61, 2010, pp. 532-540.

Winter, D.A., The Biomechanics and Motor Control of Human Gait: Normal, Elderly, and Pathological. University of Waterloo Press, Waterloo, Ontario, 1991.

Witana C.P., Goonetilleke R.S., Feng J., Dimensional differences for evaluating the quality of footwear fit, Ergonomics, Vol.47, 2004, pp. 1301-1317.

Witana C.P., Xiong S.P., Zhao J.H., Goonetilleke R.S., Foot measurements from three-dimensional scans: A comparison and evaluation of different methods, International Journal of Industrial Ergonomics, No. 36, 2006, pp.789-807.

Wolf S., Simon J., Patikas D., Schuster W., Armbrust P., Do¨derlein L., Foot motion in children shoes—A comparison of barefoot walking with shod walking in conventional and flexible shoes, Gait and posture, Vol. 27, 2008, pp. 51-59.

Wright W.G., Ivanenko Y.P., Gurfinkel V.S., Foot anatomy specialization for postural sensation and control, Journal of neurophysiology, Vol. 107, No. 5, 2011, pp.1513-1521.

Wunderlich R.E., Cavanagh P.R., Gender differences in adult foot shape: implications for shoe design, Medicine and Science in Sports and Exercise, 2000, pp.605-61.

Xiong S.P., Goonetilleke R.S., Midfoot shape for the design of ladies' shoes, Conference on Biomedical Engineering, BME 2006, 21st-23rd September 2006, Hong Kong.

Xiong S., Goonetilleke R.S., Zhao J., Li W., Witana C.P., Foot deformations under different load-bearing conditions and their relationships to stature and body weight, Anthropological Science, Vol. 117, No.2, 2009, pp.77-88.

Yang S.M. et al., Dynamic changes of the arches of the foot during walking, Biomechanics, No.IX-A, 1985, pp.417-422.

Youshida Y., Saito S., Aoki Y., Kouchi M., Mochimaru M., Shape completion and modeling of 3D foot shape while walking, Proceedings of ISOT'12, Intl. Symposium on Optomechatronic Technologies, 2012.

Yu C.Y., Tu H.H., Foot surface area database and estimation formula, Applied ergonomics, Vol. 40, 2009, pp. 767-774.

Yu J., Cheung J.T.M., Fan Y., Zhang Y., Leung A.K.L., Zhang M., Development of a finite element model of female foot for high-heeled shoe design, Clinical Biomechanics, Vol. 23, 2008, pp. S31-S38.